2014 / Volume 52 / Number 1
ISSN 1641-4640

Folia NEUROPATHOLOGICA

www.folianeuro.termedia.pl

Official Journal of Mossakowski Research Centre Polish Academy of Sciences
and
Polish Association of Neuropathologists

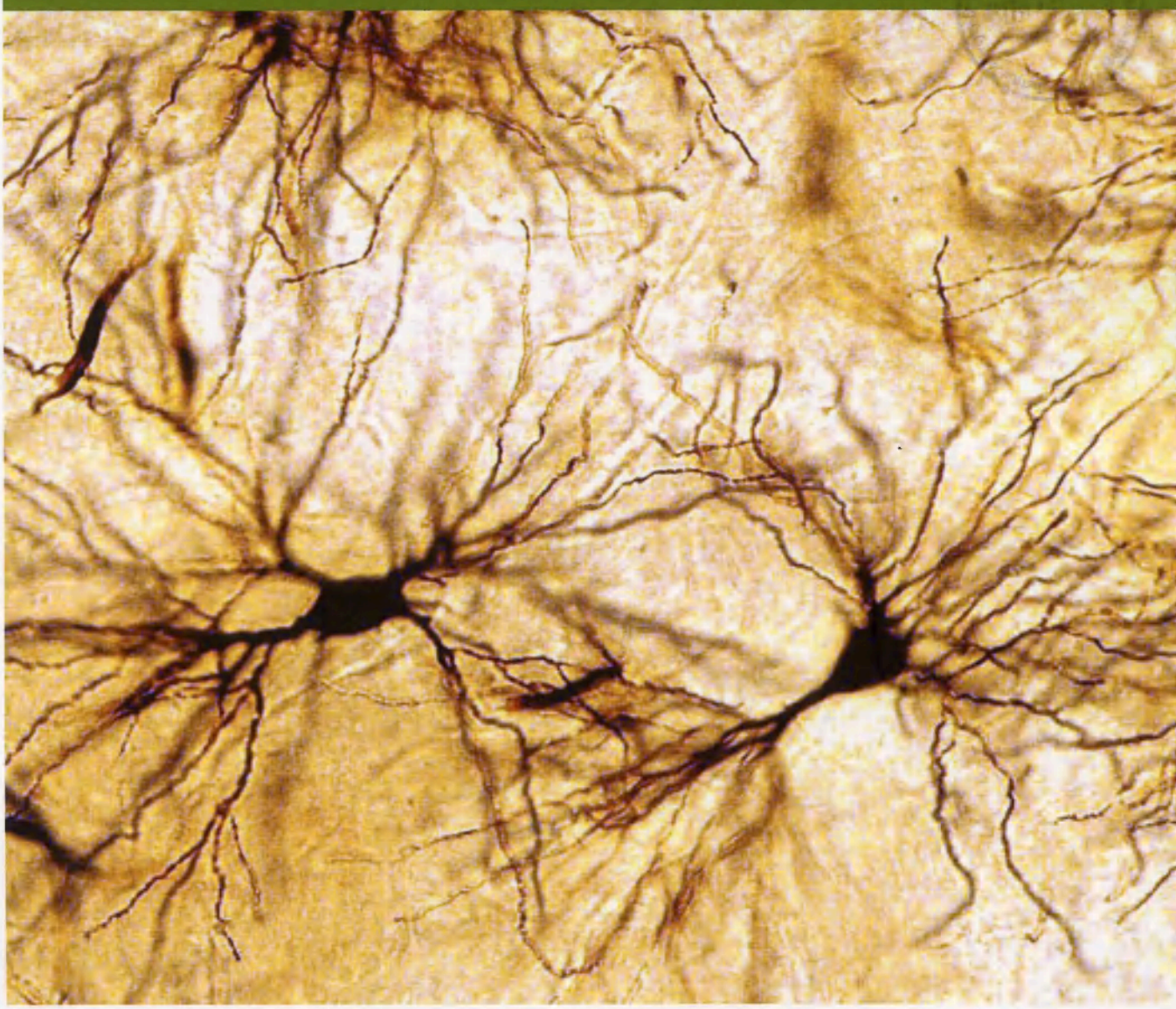

ISSN 1641-4640

Folia Neuropathologica

TERMEDIA Publishing House

Folia
Neuropathologica
former *Neuropatologia Polska*

Official Journal of Mossakowski Medical Research Centre Polish Academy of Sciences and Polish Association of Neuropathologists

The journal is partly financially supported by the Ministry of Science and Higher Education

termedia

Termedia Publishing House
Kleeberga 2, 61-615 Poznan, Poland
phone/fax: +48 61 822 77 81
e-mail: termedia@termedia.pl
www.termedia.pl
www.folianeuro.termedia.pl

Warsaw office
phone/fax: +48 22 827 75 14
e-mail: biuro.warszawa@termedia.pl

president of the management board
editor-in-chief of the Publishing House, director
Janusz Michalak
e-mail: j.michalak@termedia.pl

director of the Publishing House
Andrzej Kordas
e-mail: a.kordas@termedia.pl

Marketing and Advertising Department
Renata Dolata
phone: +48 61 822 77 81 ext. 508
e-mail: r.dolata@termedia.pl

Distribution Subscription Department
Jolanta Jankowiak
phone: +48 61 656 22 00
e-mail: prenumerata@termedia.pl

Impact Factor for Folia Neuropathologica equals 1.547
MNiSW score for Folia Neuropathologica equals 15.00
Index Copernicus score (2011) for Folia Neuropathologica equals 18.13
Position in Index Copernicus ranking systems available at http://www.indexcopernicus.pl

Abstracted and indexed in Index Medicus/MEDLINE, Neuroscience Citation Index, SciSearch, Research Alert, Chemical Abstracts, EMBASE/Excerpta Medica, Polish Medical Bibiography, Index Copernicus

The journal is financially supported by the Ministry of Sciences and Higher Education.

Print run: 450 copies

Folia
Neuropathologica
2014; 52/1: 1-110

Contents

Review paper

Folia Neuropathologica

New light on prions: putative role of co-operation of PrP^c and Aβ proteins in cognition

Adrian Andrzej Chrobak[1], Dariusz Adamek[2]

[1]Medical Faculty, Jagiellonian University Medical College, Kraków, [2]Department of Neuropathology, Chair of Pathomorphology, Jagiellonian University Medical College, Kraków, Poland

Folia Neuropathol 2014; 52 (1): 1-9 DOI: 10.5114/fn.2014.41739

Abstract

A seminal article of Takahashi et al. reporting concomitant accumulation of cellular prion protein (PrP^c) and β-amyloid (Aβ) in dystrophic neurites, within neuritic plaques raised an exciting issue that is important for our understanding of mechanisms of neurodegeneration. The mentioned authors interpreted their findings rather cautiously, however since the time of their publication, several reports representing different approaches and methods have seemed to indicate that both proteins appear to co-operate more intrinsically than it could have been imagined earlier. The goal of the review is to sum up the accruing research data with special attention to evidence pointing to the co-operative role of PrP^c and Aβ in cognitive impairment.

Key words: *prion protein, β-amyloid, cognitive impairment, Alzheimer disease, tau protein.*

Introduction

Though Alzheimer's disease (AD) and Creutzfeldt-Jakob disease (CJD) are characterized by distinct neuropathological changes, they share common pathological features. They are both conformational diseases, related to accumulation of altered proteins, which results in a loss of global cognitive functions. Alzheimer's disease is a predominant neurodegenerative disorder characterized by two major pathological changes: amyloid plaques and neurofibrillary tangles. Amyloid plaques are extracellular formations consisting of β-amyloid (Aβ) and cellular material outside and around neurons. Neurofibrillary tangles are intracellular aggregates of microtubule-associated tau protein, which has become hyperphosphorylated and misfolded. Creutzfeldt-Jakob disease is a rapidly progressive brain disease caused by infectious-like self-perpetuating mechanism leading to conversion of physiological cellular prion protein (PrP^c) to its Scrapie conformation (PrP^{Sc}) [52]. PrP^{Sc} creates extremely stable forms, which accumulate in infected tissue resulting in its spongiform degeneration [53]. There are little data concerning interactions between prion proteins and Aβ, both in their physiological and conformationally changed form with regard to cognitive functions and dementia. Takahashi *et al*. reported concomitant accumulation of PrP^c with Aβ in dystrophic neurites within one of the amyloid plaque types, called neuritic plaques [82]. Also Aβ was found to be deposited with PrP^{Sc} in CJD [26]. Due to the suspicious findings of those proteins within the same individual, speculations arise

Communicating author:
Adrian Andrzej Chrobak, Department of Pathomorphology, 16 Grzegórzecka Str., 31-531 Kraków, phone: +48 12 421 15 64, +48 12 424 72 63, fax: +48 12 411 97 25, e-mail: xchrobakx@interia.pl

around the possibility of connection between the pathophysiological processes occurring in these two neuropathological conditions [9,70]. These interactions may also have an impact on cognitive performance. Therefore, the following question arises: do prions and Aβ co-operate in cognitive impairment? Here, we review recent findings at the crossroads of cognitive neuroscience and neuropathology in order to expose the independent role of these proteins in cognition and their possible interactions, and to seek the answer to this question.

Prion protein

PrP^c is a highly conserved protein, which may be found in most of vertebrates, at every stage of their development and in all types of tissues, especially in the nervous system [79]. PrP^c is a glucolipid-anchored cell membrane sialoglycoprotein, which is localized in raft-like microdomains [57]. It is presented on the presynaptic and postsynaptic membranes [91] of neurons, of many brain areas including hippocampus and the cortex [73]. Membrane-anchored PrP^c passes internalization and recycling through the endosomal pathway [58]. It becomes internalized and degraded in lysosomes [68] or is released into the extracellular space [77]. Proposed roles in the physiology of this protein are related to its localization on the cell surface. PrP^c may act as a cellular adhesion molecule which plays a part in neurite outgrowth, neuronal differentiation and survival [54]. These functions are consistent with a finding that PrP^c can associate with surface proteins like laminin, laminin receptor precursor, and the neural cell adhesion molecule (NCAM) [6]. Animal studies have also revealed that absence of PrP^c is connected with disrupted olfactory physiology and behaviour [79], altered circadian clock, modification of sleep pattern [37], and increased sensitivity to seizures [85]. New reports bring new data indicating various potential features of this protein, making it difficult to find its one consistent function.

A growing number of works on mice models and on humans indicate a possible role of prion protein in the area of cognitive functions. The most common source of those reports comes from mice models of PrP^c gene ablation or over-expression. PrP^c null mice presented hippocampus-dependent spatial learning and memory consolidation impairment [23]. Interestingly, those changes were reversed by re-expression of PrP^c [12]. Additionally, deficiency of this protein may cause attention deficits [56]. Knockout mice were also more vulnerable to age-related decline in memory [20] and motor processes [64]. Moreover, PrP^c over-expression leads to hyperactivity, increased preference for visual, tactile and olfactory stimuli associated novelty [73]. Also it is noteworthy that a five-fold increase in PrP^c expression in comparison to wild type mice results in an increased resistance against age-related cognitive decline [72]. Due to the plenty of PrP^c functions there are many possible molecular mechanisms in which this protein affects cognitive processes. PrP^c is localized in the synaptic area, and it may interact with other proteins in this structure, playing a role in the synaptic plasticity [91]. An *in vitro* study has revealed that recombinant PrP (rPrP) induces rapid processing of both axons and dendrites as well as it increases the number of new synapses [40]. Consistently, deletion of PrP^c resulted in impaired LTP together with a decrease in fast GABA-A receptor-dependent inhibition [21,22]. Perhaps changes in LTP are associated with the ability of PrP^c to make physical interaction with receptors for the glutamate. It has been shown that PrP^c is able to co-immunoprecipitate with NR2D subunit of the NMDA, suggesting its possible direct modulation [6]. Transgenic (Tg) mice lacking PrP^c showed enhanced NMDA-induced currents, which became reversed after its over-expression [42]. PrP^c also affects kainate receptors [71] and metabotropic glutamate receptors [4] suppressing neuronal excitability through many different mechanisms. Noteworthy, it has been proved that the range of synaptic responses increased with the (higher) level of the PrP^c expression within glutamatergic synaptic transmission in the hippocampus, but the overall probability of transmitter release appeared unchanged [12]. This example shows that PrP^c-dependent modulation of glutamatergic stimulation and plasticity is more complex than just the control of the level of neurotransmitter. Regulation of glutamate signalization within synapses is important not only because of plasticity, but also due to the fact that abnormal Ca^{2+} currents, caused by aberrant activation of the NMDA receptor, results in excitotoxicity [32], which leads to neurodegeneration. Experiments mentioned above indicate that PrP^c modulates this process. This neuroprotective mechanism may be the second way in which PrP^c is involved in cognitive functions. Tg mice expressing modified PrP (with-

out its central region residues 105-125 – ΔCR PrP), resulted in massive excitotoxic degeneration of cerebellar granule neurons [15,51]. There is evidence that PrP^c also plays a role in neuroprotection through the regulation of intracellular signalling cascades, mediating cellular survival [55], and its over-expression protects cell lines from apoptosis. Protective activity has been also proved in glia cells. PrP^c acted as a radical scavenger in both ROS-rich solution and astrocytes cultures *in vitro*, and its activity was essential in their protection against oxidative stress. This feature may reflect its protective functions in conditions similar to those observed during neurodegeneration and ischemia [5]. Another defensive mechanism is associated with the ability of PrP^c to bind co-chaperon molecule, called stress-inducible protein 1 (STI1). They create a complex that acts as a survival and differentiation promoter [88]. Intriguingly, blocking the connection between PrP^c, STI1 and laminin adversely influences memory [18,19]. There are only scarce data indicating cognitive functions of PrP^c in humans, but they bring promising results. One epidemiological study of 1322 elderly participants revealed that subjects in higher serum PrP^c quintiles appeared to have lower cognitive functioning scores than those in the lowest PrP^c quintile. There are two proposed mechanisms of serum PrP^c elevation. Either there is reduced nerve cell integrity, or a higher serum PrP^c level reflects the abundance of PrP^c in neuro-cellular membranes [8].

Exploratory analysis of 335 healthy volunteers revealed that even SNP of the PrP^c gene might influence cognitive functions in humans, especially a common polymorphism at codon 129, which results in the translation of methionine or valine on a short β-sheet region in the C-terminal domain of the protein [77]. Methionine at codon 129 is associated with lower scores on several subscales of HAWIE-R subscales (German version of the Wechsler Adult Intelligence Scale Revised), especially with the Digit Symbol subtest. Interestingly, PrP-IQ association was the strongest in the less educated individuals; as opposed to other studies showing that the genetic influence on IQ is higher among higher educated families [76]. The same polymorphism is associated with the reduction of white matter in a group of healthy volunteers and patients with schizophrenia [78]. However studies on long-term memory revealed that healthy subjects presenting the same Met129 yielded the highest effect size, recalling 17 percent more words twenty four hours after the list-learning task than carriers of Val129 gene type, but there was no significant difference between those groups in short-term memory. Authors of this study hypothesize that despite the fact that Met129 allele may facilitate self-perpetuating conformational changes of the human prion protein, it may have a beneficial effect on long-term memory by hypothetical prion-based mechanism [66]. Studies mentioned above revealed that PrP^c and its gene may aspire to the role of a potential biomarker of cognitive measurements. The scarcity of investigations in humans and a plenty of possible mechanisms limit possibilities to draw a definite conclusion as for the existence of one causative relation between PrP^c and cognition. In spite of divergence of its functions, subserving somewhat unrelated processes, there is a prospect to indirectly indicate common ground of its activity. PrP^c may act as a protein, involved in global protection of the organism in a micro- and macroscopic perspective: at the microscopic (cellular) level – protecting the cell against apoptotic factors, ROS, excitotoxicity, toxins and at a macroscopic level – affecting the whole organism, by playing a significant role in cognition, especially in defensive attention, spatial and long-term memory and also olfactory physiology and behaviour (crucial for the survival chances of an animal).

β-amyloid

β-amyloid is a peptide consisting of 36-43 amino acids which originates from the cleavage of the transmembrane glycoprotein called amyloid precursor protein (APP), by the proteolytic activation of α-, β- and γ-secretase [80]. Generation of Aβ may occur in the neuronal axonal membranes and is preceded by APP-mediated axonal transport of β-secretase and presenilin-1 [39]. Amyloid precursor protein is cleaved by β-secretase, producing soluble and a cell-membrane bound fragment of APP [46], which is then cleaved by γ-secretase. This reaction produces APP intracellular domain (AICD) associated with the regulation of gene transcription and Aβ, which is released to plasma, cerebrospinal fluid and brain interstitial fluid [30,90]. It has been established that $Aβ_{39-42}$ are hydrophobic self-aggregating peptides, of which Aβ42 is a major component of senile plaques observed in AD, but it still remains controversial how those peptides are involved in the

cognitive decline observed during this disease [36]. The "Aβ cascade hypothesis" suggests the major role of amyloid plaques, especially fibrillar Aβ ones in the aetiology of AD, reporting a correlation between the amount of those formations and cognitive dysfunctions [3,24,25,35,67]. Recent studies with the use of detailed measures of Aβ pathology suggest an opposite explanation. Research on APPswe/PS1ΔE9 double transgenic mice (well-established model of AD) has revealed that hippocampal soluble $A\beta_{1-40}$ and $A\beta_{1-42}$ levels were highly correlated with spatial learning and long-term contextual memory impairments. Also, hippocampal soluble $A\beta_{1-40}$ and $A\beta_{1-42}$ levels were strongly correlated with spatial memory impairments, but no correlations were observed between mentioned cognitive functions and amyloid plaque formations such as: total Aβ plaque load, fibrillar Aβ plaque load and also insoluble Aβ levels. Authors of this study revealed that a tiny fraction of soluble peptides in the hippocampus and cortex is an independent factor in predicting cognitive impairments in this transgenic mice model, suggesting "soluble Aβ hypothesis" as a major mechanism of cognitive decline in AD [89]. Consistently with this hypothesis, experiments on young domestic chicks show that an injection of soluble Aβ 5 minutes prior to training caused memory loss, due to the consolidation failure 35 minutes later [31]. Also, reduction of soluble $A\beta_{42}$ or $A\beta_{42}$ and $A\beta_{40}$ by γ-secretase modulators (GSMs) ameliorated cognitive deficits in Tg2576 plaque-free mice model of AD. However, a later study suggests that newly synthesized soluble $A\beta_{42}$ may play a more significant role in cognitive impairments than plaque-associated soluble Aβ [61]. Injections of Aβ to rats result in rapid cognitive disruption, showing a direct interference with the cognitive functions not only through neurodegeneration, but also through interruption of their cellular mechanisms [17,50,69]. It has been shown that Aβ impairs hippocampal long-term potentiation (LTP) by deterioration of tetanus-induced activation of guanylate cyclase and increase of cGMP. Those changes prevent protein kinase G activation and phosphorylation of GluR1, finally resulting in impaired translocation of AMPA receptors to synaptic membranes [62]. Interactions of Aβ with nicotinic, insulin and glutamatergic receptors may also have an impact on synaptic plasticity and spine formation [17,50,63]. These mechanisms explain why injection of Aβ oligomers before the acquisition of new information disrupts the process of the consolidation without affecting its retrieval, when the information was properly stored [28]. Furthermore, it has been shown that Aβ may have an impact on the cognitive function through its influence on NADPH oxidase enzyme (NOX) activation. NOX is responsible for production of free radicals, and also it plays a role in neuronal physiology, particularly in hippocampal electrophysiology [43,83]. Data show a significant direct linear relationship between NOX activity, cognitive impairment and age-depended increase in $A\beta_{1-42}$. This correlation suggests that oxidative stress caused by NOX-associated redox pathway may be another possible mechanism in which Aβ is involved in cognitive decline [10]. Oxidative stress associated with membranes is a possible mechanism in which Aβ may cause synaptic dysfunction and disruption of cellular ion homeostasis [59]. Interestingly, mounting research show intraneuronal accumulation of Aβ as a possible mechanism of cognitive dysfunction, especially in the early stages of the AD [34,45,87]. This accumulation is associated with morphological alterations of synapses [81] and with a decrease in synaptophysin around the affected neurons in AD patients [38]. Studies on 3xTg-AD mice showed a correlation between the cognitive and synaptic dysfunction with the accumulation of intraneuronal Aβ which occurred before formation of amyloid plaques [7,65]. Also hypercholesterolemia accelerates intraneuronal accumulation of Aβ oligomers, resulting in synapse loss and memory impairment [84]. This view of the complexity of the mechanisms and forms by which Aβ affects cognitive functions will be helpful for proper understanding of its possible interactions with PrP^c.

Cooperation?

Tellingly, comprehensive studies have shown that out of 225 000 proteins screened in a cell model, only those with PrP^c expression were strongly binding soluble $A\beta_{42}$ [49]. It has been proposed that PrP^c exhibits receptor affinity to β-sheet-rich conformers due to its ~95-110 region and the cluster of basic residues within the *N*-terminal 23-27 segment [14]. As to the protective functions of PrP^c mentioned before, one may say that this protein will also protect the cell against Aβ, but a growing number of research comes with opposite findings and also with new controversies. Lauren et al. proposed that synthetic oligomeric forms of Aβ impair LTP through

their interactions with PrP^c [49], but other studies did not confirm this result [1,11]. However, more novel findings showed that antibodies against 94-104 domain of PrP^c blocked inhibition of LTP caused by soluble extracts of AD brain [2,29]. Also hippocampal slices lacking PrP^c were resistant to LTP inhibition by Aβ. Similar relationships can be observed in studies on Aβ-dependent neurotoxicity. Prnp 0/0 mice are more resistant to neurotoxic effects of Aβ oligomers [44] and accordingly, over-expression of PrP^c in neuronal cell lines increases vulnerability to such effects. It has been also shown that deletion of PrP^c expression in APPswe/PSen1ΔE9 rescues 5-HT axonal degeneration, loss of synaptic markers and early death, and interestingly, Tg mice containing Aβ plaques, but lacking PrP^c show no spatial learning and memory impairments [33]. APP/PS1 Tg mice, treated for 2 weeks with intraperitoneal injections of 6D11 anti-PrP antibodies, recovered in cognitive learning tasks behaving the same as wild-type mice [16]. Surprisingly, mentioned studies revealed not only that PrP^c is not neuroprotective against Aβ, but even it may be necessary for its neurotoxicity and its impact on cognitive functions. Nevertheless, some authors have reached opposite conclusions. Rial *et al.* showed that Tg-20 mice characterized by a five-fold increase in PrP^c expression was resistant to a single intracerebroventricular injection of 400 pmols/mouse of aggregated $Aβ_{1-40}$, revealing no impairments of memory and spatial learning in comparison to the wild type and PrP^c knockout mice. This resistance was accompanied with a decrease in activated caspase-3 protein and Bax/Bcl-2 ratio and reduced hippocampal cell damage [73]. Calella *et al*. [11] showed that the PrP^c level had no effect on LTP impairment in APP/PS1 mice, and those results were also confirmed by Kessels *et al*.'s studies [41]. Also participation of PrP^c in mediation of Ab neurotoxicity had been challenged by results of studies on isolated hippocampal cells from Prnp 0/0 and Prnp +/+ mice. Authors concluded that PrP^c in specific conditions may exert a relevant role in neurotoxicity because of sequestration of Aβ oligomers rather than a functional activity associated to the protein (for review [28]). A more recent study shed a light on the interactions of these proteins adding some important premise to proper understanding of the controversies and the confounding results mentioned above. Larson *et al*. revealed that AD brain-purified Aβ dimers are specifically binding PrP^c. This complex triggers Src Tyrosine Kinase Fyn, which activates the kinase and leads towards abnormal phosphorylation of Fyn and tau. This reaction occurs in neuronal dendritic spines and leads to aberrant tau missorting and hyperphosphorylation. Authors also revealed that dosage of Prnp regulates these changes. This comprehensive study made *ex vivo*, *in situ*, and *in vitro* indicates that this PrP^c-mediated process may play an important role in late stages of AD, when Aβ dimers reach their highest level [47].

Proper understanding of this finding is facilitated by Chen *et al*.'s study on human neuroblastoma cells. They found that over-expression of PrP^c downregulates tau protein transcription level through Fyn, Fyn kinase and MEK pathway. β-amyloid oligomers reverse this pathway by binding to PrP^c, probably by inducing its surface retention that interferes with caveolae-mediated PrP^c endocytosis and Fyn activation. Phosphorylated Fyn level increased in a dose-dependent manner 2 hours after Aβ oligomer treatment and interestingly it became decreased 1 day after this treatment. Surprisingly, the murine PrP^c M128V, which correspond with the high AD risk polymorphic human PrP^c M129V [74] allele was able to bind Aβ oligomers, but it was unable to reverse the tau reduction [13]. This may be another explanation why this polymorphism was associated with lower IQ and white matter reduction in the study mentioned earlier in this article.

The above authors (see ref. [13, 47], and also Larson and Lesne [48]) suggest that confounding results about PrP^c-mediated impairments, as those described previously, may be attributed only to a subset of Aβ oligomers that are mediated through PrP^c. For example, no dependence in LTP impairments in studies of Calella *et al*. [11] may be a result of low levels of Aβ dimers in young aged Tg-mice. A protective effect of PrP^c over-expression against intracerebroventricular injection of Aβ may be a result of a low concentration of its assemblies. It has been proven that picomolar concentrations of the Aβ did not trigger Fyn activation [47]. In our opinion, if PrP^c downregulates tau protein, and Aβ binds to PrP^c, reverting this process, it is quite possible that effects of Aβ will vary due to Aβ and PrP^c ratio. Noteworthy, PrP^c is not only connected in aetiology of AD by its direct interactions with Aβ, but also due to its negative modulation of BACE1 activity. PrP^c declines with age, and is decreased in sporadic AD, but there are no alterations in familial AD cases. In sporadic

AD, the PrP^c level is inversely correlated with BACE1 activity, Aβ load, soluble Aβ, and insoluble Aβ. It is also inversely correlated with the stage of disease, as indicated by Braak tangle stages, distinguished according to the distribution of the tau pathology, especially the neurofibrillary tangles. Authors of this study point out that a decreased level of PrP^c results in a decreased zinc uptake within the synapses. Such condition results in an elevated synaptic zinc level, which favours binding Aβ oligomers to the NMDA receptors, and mediates the excitotoxicity [86]. In our opinion, it is more probable that an inverse correlation with Braak stage assessed tauopathy was caused by the elevation of Aβ and PrP^c ratio, and its direct impact on tau expression. A biophysical examination of recombinant PrP revealed that this protein represents a unique intrinsic feature to form multiple non-native isoforms rich in β-sheets, which may result in a large spectrum of PrP^c *in vivo*. It has been proved that in uninfected human brains PrP is presented also in the form of oligomers, and even large aggregates, called insoluble PrP^c ($iPrP^c$) which stand for ~5-25% of total PrP. It is proposed that if soluble PrP^c can bind to soluble $A\beta_{42}$, also $iPrP^c$ will bind insoluble Aβ, modulating its deposition [91]. It is therefore consistent with Takahashi *et al.*'s findings [82] (confirming the prior report of Ferrer *et al.* [27]) indicating that PrP^c is present in amyloid deposits. Many other related issues remain seemingly untouched. For example, amyloid Aβ deposits are formed within vessels and amyloid angiopathy is not only limited to arteries, but also affects veins [60]. It is interesting whether there is also an interaction between Aβ and PrP^c in this compartment of brain tissue. To summarize, a growing number of research indicate new possible functions of PrP^c in the field of cognition, both in its physiological and pathophysiological aspects. Considering new data, we are compelled to stronger appreciate the role of soluble forms of Aβ in the pathomechanism of AD, which possibly even prevails over its insoluble deposits. This may be regarded as a "paradigm shift" in an understanding of cognitive decline in AD. Despite the remaining controversies, recent findings prompt us to consider that roads of PrP^c and Aβ meet at the point of tauopathy and moreover, formation of PrP^c-Aβ complexes may result in the consumption of PrP^c, what modulates Aβ neurotoxicity, possibly depriving nervous tissue of the neuroprotective function of PrP^c.

References

1. Balducci C, Beeg M, Stravalaci M, Bastone A, Sclip A, Biasini E, Tapella L, Colombo L, Manzoni C, Borsello T, Chiesa R, Gobbi M, Salmona M, Forloni G. Synthetic amyloid-β oligomers impair long-term memory independently of cellular prion protein. Proc Natl Acad Sci U S A 2010; 107: 2295-2300.
2. Barry AE, Klyubin I, Mc Donald JM, Mably AJ, Farrell MA, Scott M, Walsh DM, Rowan MJ. Alzheimer's disease brain-derived amyloid-β-mediated inhibition of LTP in vivo is prevented by immunotargeting cellular prion protein. J Neurosci 2011; 31: 7259-7263.
3. Bartoo GT, Nochlin D, Chang D, Kim Y, Sumi SM. The mean A beta load in the hippocampus correlates with duration and severity of dementia in subgroups of Alzheimer disease. J Neuropathol Exp Neurol 1997; 56: 531-540.
4. Beraldo FH, Arantes CP, Santos TG, Machado CF, Roffe M, Hajj GN, Lee KS, Magalhães AC, Caetano FA, Mancini GL, Lopes MH, Américo TA, Magdesian MH, Ferguson SS, Linden R, Prado MA, Martins VR. Metabotropic glutamate receptors transduce signals for neurite outgrowth after binding of the prion protein to laminin gamma1 chain. FASEB J 2011; 25: 265-279.
5. Bertuchi FR, Bourgeon DM, Landemberger MC, Martins VR, Cerchiaro G. PrPC displays an essential protective role from oxidative stress in an astrocyte cell line derived from PrPC knockout mice. Biochem Biophys Res Commun 2012; 418: 27-32.
6. Biasini E, Turnbaugh JA, Unterberger U, Harris DA. Prion protein at the crossroads of physiology and disease. Trends Neurosci 2012; 35: 92-103.
7. Billings LM, Oddo S, Green KN, McGaugh JL, LaFerla FM. Intraneuronal Aβ causes the onset of early Alzheimer's disease-related cognitive deficits in transgenic mice. Neuron 2005; 45: 675-688.
8. Breitling LP, Müller H, Stegmaier C, Kliegel M, Brenner H. Association of prion protein with cognitive functioning in humans. Exp Gerontol 2012; 47: 919-924.
9. Brown P, Jannotta F, Gibbs CJ Jr, Baron H, Guiroy DC, Gajdusek DC. Coexistence of Creutzfeldt-Jakob disease and Alzheimer's disease in the same patient. Neurology 1990; 40: 226-228.
10. Bruce-Keller AJ, Gupta S, Knight AG, Beckett TL, McMullen JM, Davis PR, Murphy MP, Van Eldik LJ, St Clair D, Keller JN. Cognitive impairment in humanized APP×PS1 mice is linked to Aβ(1-42) and NOX activation. Neurobiol Dis 2011; 44: 317-326.
11. Calella AM, Farinelli M, Nuvolone M, Mirante O, Moos R, Falsig J, Mansuy IM, Aguzzi A. Prion protein and Abeta-related synaptic toxicity impairment. EMBO Mol Med 2010; 2: 306-314.
12. Carleton A, Tremblay P, Vincent JD, Lledo PM. Dose-dependent, prion protein (PrP)-mediated facilitation of excitatory synaptic transmission in the mouse hippocampus. Pflugers Arch 2001; 442: 223-229.
13. Chen RJ, Chang WW, Lin YC, Cheng PL, Chen YR. Alzheimer's amyloid-β oligomers rescue cellular prion protein induced tau reduction via Fyn pathways. ACS Chem Neurosci 2013; 4: 1287-1296.
14. Chen S, Yadav SP, Surewicz WK. Interaction between human prion protein and amyloid-beta (Abeta) oligomers: role of N-terminal residues. J Biol Chem 2010; 285: 26377-26383.

15. Christensen HM, Dikranian K, Li A, Baysac KC, Walls KC, Olney JW, Roth KA, Harris DA. A highly toxic cellular prion protein induces a novel, nonapoptotic form of neuronal death. Am J Pathol 2010; 176: 2695-2706.
16. Chung E, Ji Y, Sun Y, Kascsak RJ, Kascsak RB, Mehta PD, Strittmatter SM, Wisniewski T. Anti-PrP C monoclonal antibody infusion as a novel treatment for cognitive deficits in an Alzheimer 's disease model mouse. BMC Neurosci 2010; 11: 130.
17. Cleary JP, Walsh DM, Hofmeister JJ, Shankar GM, Kuskowski MA, Selkoe DJ, Ashe KH. Natural oligomers of the amyloid-beta protein specifically disrupt cognitive function. Nat Neurosci 2005; 8: 79-84.
18. Coitinho AS, Freitas AR, Lopes MH, Hajj GN, Roesler R, Walz R, Rossato JI, Cammarota M, Izquierdo I, Martins VR, Brentani RR. The interaction between prion protein and laminin modulates memory consolidation. Eur J Neurosci 2006; 24: 3255-3264.
19. Coitinho AS, Lopes MH, Hajj GN, Rossato JI, Freitas AR, Castro CC, Cammarota M, Brentani RR, Izquierdo I, Martins VR. Short-term memory formation and long-term memory consolidation are enhanced by cellular prion association to stress-inducible protein 1. Neurobiol Dis 2007; 26: 282-290.
20. Coitinho AS, Roesler R, Martins VR, Brentani RR, Izquierdo I. Cellular prion protein ablation impairs behavior as a function of age. Neuroreport 2003; 14: 1375-1379.
21. Colling SB, Collinge J, Jefferys JG. Hippocampal slices from prion protein null mice: disrupted Ca(2+)-activated K+ currents. Neurosci Lett 1996; 209: 49-52.
22. Collinge J, Whittington MA, Sidle KC, Smith CJ, Palmer MS, Clarke AR, Jefferys JG. Prion protein is necessary for normal synaptic function. Nature 1994; 370: 295-297.
23. Criado JR, Sánchez-Alavez M, Conti B, Giacchino JL, Wills DN, Henriksen SJ, Race R, Manson JC, Chesebro B, Oldstone MB. Mice devoid of prion protein have cognitive deficits that are rescued by reconstitution of PrP in neurons. Neurobiol Dis 2005; 19: 255-265.
24. Cummings BJ, Cotman CW. Image analysis of beta-amyloid load in Alzheimer's disease and relation to dementia severity. Lancet 1995; 346: 1524-1528.
25. Cummings BJ, Pike CJ, Shankle R, Cotman CW. β-amyloid deposition and other measures of neuropathology predict cognitive status in Alzheimer's disease. Neurobiol Aging 1996; 17: 921-933.
26. Debatin L, Streffer J, Geissen M, Matschke J, Aguzzi A, Glatzel M. Association between deposition of beta-amyloid and pathological prion protein in sporadic Creutzfeldt-Jakob disease. Neurodegener Dis 2008; 5: 347-354.
27. Ferrer I, Blanco R, Carmona M, Puig B, Ribera R, Rey MJ, Ribalta T. Prion protein expression in senile plaques in Alzheimer's disease. Acta Neuropathol 2001; 101: 49-56.
28. Forloni G, Balducci C. β-amyloid oligomers and prion protein: Fatal attraction? Prion 2011; 5: 10-15.
29. Freir DB, Nicoll AJ, Klyubin I, Panico S, Mc Donald JM, Risse E, Asante EA, Farrow MA, Sessions RB, Saibil HR, Clarke AR, Rowan MJ, Walsh DM, Collinge J. Interaction between prion protein and toxic amyloid β assemblies can be therapeutically targeted at multiple sites. Nat Commun 2011; 2: 336.
30. Ghiso J, Frangione B. Amyloidosis and Alzheimer's disease. Adv Drug Deliv Rev 2002; 54: 1539-1551.
31. Gibbs ME, Maksel D, Gibbs Z, Hou X, Summers RJ, Small DH. Memory loss caused by β-amyloid protein is rescued by a b3-adrenoceptor agonist. Neurobiol Aging 2010; 31: 614-624.
32. Gillessen T, Budd SL, Lipton SA. Excitatory amino acid neurotoxicity. Adv Exp Med Biol 2002; 513: 3-40.
33. Gimbel DA, Nygaard HB, Coffey EE, Gunther EC, Laurén J, Gimbel ZA, Strittmatter SM. Memory impairment in transgenic Alzheimer mice requires cellular prion protein. J Neurosci 2010; 30: 6367-6374.
34. Gouras GK, Tampellini D, Takahashi RH, Capetillo-Zarate E. Intraneuronal β-amyloid accumulation and synapse pathology in Alzheimer's disease. Acta Neuropathol 2010; 119: 523-541.
35. Haroutunian V, Perl DP, Purohit DP, Marin D, Khan K, Lantz M, Davis KL, Mohs RC. Regional distribution of neuritic plaques in the nondemented elderly and subjects with very mild Alzheimer disease. Arch Neurol 1998; 55: 1185-1191.
36. Hiltunen M, van Groen T, Jolkkonen J. Functional roles of amyloid-beta protein precursor and amyloid-beta peptides: evidence from experimental studies. J Alzheimers Dis 2009; 18: 401-412.
37. Huber R, Deboer T, Tobler I. Prion protein: a role in sleep regulation? J Sleep Res 1999; 8 (Suppl 1): 30-36.
38. Ishibashi K, Tomiyama T, Nishitsuji K, Hara M, Mori H. Absence of synaptophysin near cortical neurons containing oligomer Aβ in Alzheimer's disease brain. J Neurosci Res 2006; 84: 632-636.
39. Kamal A, Almenar-Queralt A, LeBlanc JF, Roberts EA, Goldstein LS. Kinesin-mediated axonal transport of a membrane compartment containing beta-secretase and presenilin-1 requires APP. Nature 2001; 414: 643-648.
40. Kanaani J, Prusiner SB, Diacovo J, Baekkeskov S, Legname G. Recombinant prion protein induces rapid polarization and development of synapses in embryonic rat hippocampal neurons in vitro. J Neurochem 2005; 95: 1373-1386.
41. Kessels HW, Nguyen LN, Nabavi S, Malinow R. The prion protein as a receptor for amyloid-beta. Nature 2010; 466: 3-4.
42. Khosravani H, Zhang Y, Tsutsui S, Hameed S, Altier C, Hamid J, Chen L, Villemaire M, Ali Z, Jirik FR, Zamponi GW. Prion protein attenuates excitotoxicity by inhibiting NMDA receptors. J Cell Biol 2008; 181: 551-565.
43. Kishida KT, Pao M, Holland SM, Klann E. NADPH oxidase is required for NMDA receptor-dependent activation of ERK in hippocampal area CA1. J Neurochem 2005; 94: 299-306.
44. Kudo W, Lee HP, Zou WQ, Wang X, Perry G, Zhu X, Smith MA, Petersen RB, Lee HG. Cellular prion protein is essential for oligomeric amyloid-β-induced neuronal cell death. Hum Mol Genet 2012; 5: 1138-1144.
45. LaFerla FM, Green KN, Oddo S. Intracellular amyloid-β in Alzheimer's disease. Nat Rev Neurosci 2007; 8: 499-509.
46. Lahiri DK, Farlow MR, Sambamurti K, Greig NH, Giacobini E, Schneider LS. A critical analysis of new molecular targets and strategies for drug developments in Alzheimer's disease. Curr Drug Targets 2003; 4: 97-112.
47. Larson M, Sherman MA, Amar F, Nuvolone M, Schneider JA, Bennett DA, Aguzzi A, Lesné SE. The complex PrP(c)-Fyn cou-

ples human oligomeric Aβ with pathological tau changes in Alzheimer's disease. J Neurosci 2012; 32: 16857-16871a.
48. Larson ME, Lesne SE. Soluble Aβ oligomer production and toxicity. J Neurochem 2012; 120 (Suppl 1): 125-139.
49. Laurén J, Gimbel DA, Nygaard HB, Gilbert JW, Strittmatter SM. Cellular prion protein mediates impairment of synaptic plasticity by amyloid-beta oligomers. Nature 2009; 457: 1128-1132.
50. Lesné S, Koh MT, Kotilinek L, Kayed R, Glabe CG, Yang A, Gallagher M, Ashe KH. A specific amyloid-beta protein assembly in the brain impairs memory. Nature 2006; 440: 352-357.
51. Li A, Christensen HM, Stewart LR, Roth KA, Chiesa R, Harris DA. Neonatal lethality in transgenic mice expressing prion protein with a deletion of residues 105-125. EMBO J 2007; 26: 548-558.
52. Liberski PP. Historical overview of prion diseases: a view from afar. Folia Neuropathol 2012; 50: 1-12.
53. Liberski PP, Sikorska B, Wells GA, Hawkins SA, Dawson M, Simmons MM. Ultrastructural findings in pigs experimentally infected with bovine spongiform encephalopathy agent. Folia Neuropathol 2012; 50: 89-98.
54. Linden R, Martins VR, Prado MA, Izquierdo I, Brentani RR. Physiology of the prion protein. Physiol Rev 2008; 88: 673-728.
55. Lo RY, Shyu WC, Lin SZ, Wang HJ, Chen SS, Li H. New molecular insights into cellular survival and stress responses: neuroprotective role of cellular prion protein (PrPC). Mol Neurobiol 2007; 35: 236-244.
56. Lobão-Soares B, Walz R, Prediger RD, Freitas RL, Calvo F, Bianchin MM, Leite JP, Landemberger MC, Coimbra NC. Cellular prion protein modulates defensive attention and innate fear-induced behaviour evoked in transgenic mice submitted to an agonistic encounter with the tropical coral snake Oxyrhopus guibei. Behav Brain Res 2008; 194: 129-137.
57. Madore N, Smith KL, Graham CH, Jen A, Brady K, Hall S, Morris R. Functionally different GPI proteins are organized in different domains on the neuronal surface. EMBO J 1999; 18: 6917-6926.
58. Magalhães AC, Silva JA, Lee KS, Martins VR, Prado VF, Ferguson SS, Gomez MV, Brentani RR, Prado MA. Endocytic intermediates involved with the intracellular trafficking of a fluorescent cellular prion protein. J Biol Chem 2002; 277: 33311-33318.
59. Mattson MP. Pathways towards and away from Alzheimer's disease. Nature 2004; 430: 631-639.
60. Mendel T, Wierzba-Bobrowicz T, Stępień T, Szpak GM. β-amyloid deposits in veins in patients with cerebral amyloid angiopathy and intracerebral haemorrhage. Folia Neuropathol 2013; 51: 120-126.
61. Mitani Y, Yarimizu J, Akashiba H, Shitaka Y, Ni K, Matsuoka N. Amelioration of cognitive deficits in plaque-bearing Alzheimer's disease model mice through selective reduction of nascent soluble Aβ42 without affecting other Aβ pools. J Neurochem 2013; 125: 465-472.
62. Monfort P, Felipo V. Amyloid-β impairs, and ibuprofen restores, the cGMP pathway, synaptic expression of AMPA receptors and long-term potentiation in the hippocampus. J Alzheimers Dis 2010; 22: 795-809.
63. Mucke L, Masliah E, Yu GQ, Mallory M, Rockenstein EM, Tatsuno G, Hu K, Kholodenko D, Johnson-Wood K, McConlogue L. High-level neuronal expression of abeta 1–42 in wild-type human amyloid protein precursor transgenic mice: synaptotoxicity without plaque formation. J Neurosci 2000; 20: 4050-4058.
64. Nazor KE, Seward T, Telling GC. Motor behavioral and neuropathological deficits in mice deficient for normal prion protein expression. Biochim Biophys Acta 2007; 1772: 645-653.
65. Oddo S, Caccamo A, Shepherd JD, Murphy MP, Golde TE, Kayed R, Metherate R, Mattson MP, Akbari Y, LaFerla FM. Triple-transgenic model of Alzheimer's disease with plaques and tangles: intracellular Aβ and synaptic dysfunction. Neuron 2003; 39: 409-421.
66. Papassotiropoulos A, Wollmer MA, Aguzzi A, Hock C, Nitsch RM, de Quervain DJ. The prion gene is associated with human long-term memory. Hum Mol Genet 2005; 14: 2241-2246.
67. Parvathy S, Davies P, Haroutunian V, Purohit DP, Davis KL, Mohs RC, Park H, Moran TM, Chan JY, Buxbaum JD. Correlation between Abetax-40-, Abetax-42-, and Abetax-43-containing amyloid plaques and cognitive decline. Arch Neurol 2001; 58: 2025-2032.
68. Peters PJ, Mironov A Jr, Peretz D, van Donselaar E, Leclerc E, Erpel S, DeArmond SJ, Burton DR, Williamson RA, Vey M, Prusiner SB. Trafficking of prion proteins through a caveolae-mediated endosomal pathway. J Cell Biol 2003; 162: 703-717.
69. Poling A, Morgan-Paisley K, Panos JJ, Kim EM, O'Hare E, Cleary JP, Lesné S, Ashe KH, Porritt M, Baker LE. Oligomers of the amyloid-beta protein disrupt working memory: confirmation with two behavioral procedures. Behav Brain Res 2008; 193: 230-234.
70. Powers JM, Liu Y, Hair LS, Kascsack RJ, Lewis LD, Levy LA. Concomitant Creutzfeldt-Jakob and Alzheimer diseases. Acta Neuropathol 1991; 83: 95-98.
71. Rangel A, Burgaya F, Gavín R, Soriano E, Aguzzi A, Del Río JA. Enhanced susceptibility of Prnp-deficient mice to kainate-induced seizures, neuronal apoptosis, and death: role of AMPA/kainate receptors. J Neurosci Res 2007; 85: 2741-2755.
72. Rial D, Duarte FS, Xikota JC, Schmitz AE, Dafré AL, Figueiredo CP, Walz R, Prediger RD. Cellular prion protein modulates age-related behavioral and neurochemical alterations in mice. Neuroscience 2009; 164: 896-907.
73. Rial D, Piermartiri TC, Duarte FS, Tasca CI, Walz R, Prediger RD. Overexpression of cellular prion protein (PrP(C)) prevents cognitive dysfunction and apoptotic neuronal cell death induced by amyloid-β ($A\beta_{1-40}$) administration in mice. Neuroscience 2012; 215: 79-89.
74. Riemenschneider M, Klopp N, Xiang W, Wagenpfeil S, Vollmert C, Müller U, Förstl H, Illig T, Kretzschmar H, Kurz A. Prion protein codon 129 polymorphism and risk of Alzheimer disease. Neurology 2004; 63: 364-366.
75. Rodolfo K, Hässig R, Moya KL, Frobert Y, Grassi J, Di Giamberardino L. A novel cellular prion protein isoform present in rapid anterograde axonal transport. Neuroreport 1999; 10: 3639-3644.
76. Rowe DC, Jacobson KC, Van den Oord EJ. Genetic and environmental influences on vocabulary IQ: parental education level as moderator. Child Dev 1999; 70: 1151-1162.
77. Rujescu D, Hartmann AM, Gonnermann C, Möller HJ, Giegling I. M129V variation in the prion protein may influence cognitive performance. Mol Psychiatry 2003; 8: 937-941.

78. Rujescu D, Meisenzahl EM, Giegling I, Kirner A, Leinsinger G, Hegerl U, Hahn K, Möller HJ. Methionine homozygosity at codon 129 in the prion protein is associated with white matter reduction and enlargement of CSF compartments in healthy volunteers and schizophrenic patients. Neuroimage 2002; 15: 200-206.
79. Sagdullaev BT, Aguzzi A, Firestein S. Olfactory behavior and physiology are disrupted in prion protein knockout mice. Nat Neurosci 2009; 12: 60-69.
80. Šerý O, Povová J, Míšek I, Pešák L, Janout V. Molecular mechanisms of neuropathological changes in Alzheimer's disease: a review. Folia Neuropathol 2013; 1: 1-9.
81. Takahashi RH, Milner TA, Li F, Nam EE, Edgar MA, Yamaguchi H, Beal MF, Xu H, Greengard P, Gouras GK. Intraneuronal Alzheimer Aβ42 accumulates in multivesicular bodies and is associated with synaptic pathology. Am J Pathol 2002; 161: 1869-1879.
82. Takahashi RH, Tobiume M, Sato Y, Sata T, Gouras GK, Takahashi H. Accumulation of cellular prion protein within dystrophic neurites of amyloid plaques in the Alzheimer's disease brain. Neuropathology 2011; 31: 208-214.
83. Tejada-Simon MV, Serrano F, Villasana LE, Kanterewicz BI, Wu GY, Quinn MT, Klann E. Synaptic localization of a functional NADPH oxidase in the mouse hippocampus. Mol Cell Neurosci 2005; 29: 97-106.
84. Umeda T, Tomiyama T, Kitajima E, Idomoto T, Nomura S, Lambert MP, Klein WL, Mori H. Hypercholesterolemia accelerates intraneuronal accumulation of Aβ oligomers resulting in memory impairment in Alzheimer's disease model mice. Life Sci 2012; 91: 1169-1176.
85. Walz R, Amaral OB, Rockenbach IC, Roesler R, Izquierdo I, Cavalheiro EA, Martins VR, Brentani RR. Increased sensitivity to seizures in mice lacking cellular prion protein. Epilepsia 1999; 40: 1679-1682.
86. Whitehouse IJ, Miners JS, Glennon EB, Kehoe PG, Love S, Kellett KA, Hooper NM. Prion protein is decreased in Alzheimer's brain and inversely correlates with BACE1 activity, amyloid-β levels and Braak stage. PLoS One 2013; 8: e59554.
87. Wirths O, Multhaup G, Bayer TA. A modified β-amyloid hypothesis: intraneuronal accumulation of the β-amyloid peptide – the first step of a fatal cascade. J Neurochem 2004; 91: 513-520.
88. Zanata SM, Lopes MH, Mercadante AF, Hajj GN, Chiarini LB, Nomizo R, Freitas AR, Cabral AL, Lee KS, Juliano MA, de Oliveira E, Jachieri SG, Burlingame A, Huang L, Linden R, Brentani RR, Martins VR. Stress-inducible protein 1 is a cell surface ligand for cellular prion that triggers neuroprotection. EMBO J 2002; 21: 3307-3316.
89. Zhang W, Hao J, Liu R, Zhang Z, Lei G, Su C, Miao J, Li Z. Soluble Aβ levels correlate with cognitive deficits in the 12-month-old APPswe/PS1dE9 mouse model of Alzheimer's disease. Behav Brain Res 2011; 222: 342-350.
90. Zlokovic BV, Frangione B. Transport-clearance hypothesis for Alzheimer's disease and potential therapeutic implications. Landes Bioscience 2003; 114-122.
91. Zou WQ, Zhou X, Yuan J, Xiao X. Insoluble cellular prion protein and its association with prion and Alzheimer diseases. Prion 2011; 5: 172-178.

Review paper

Folia Neuropathologica

Ultrastructural alterations of human cortical capillary basement membrane in human brain oedema

Orlando José Castejón

Biological Research Institute, Faculty of Medicine, Zulia University, Maracaibo, Venezuela

Folia Neuropathol 2014; 52 (1): 10-21 DOI: 10.5114/fn.2014.41740

Abstract

The capillary basement membranes are examined in severe traumatic brain injuries, vascular malformation, congenital hydrocephalus and brain tumours. They exhibit homogeneous and nodular thickening, vacuolization, rarefaction, reduplication, and deposition of collagen fibers. Their average thickness varied according to the aetiology and severity of brain oedema. In moderate brain oedema the thickness ranged from 71.97 to 191.90 nm in width, and in patients with severe brain oedema it varied from 206.66 to 404.22 nm. The basement membrane complex appears apparently intact in moderate oedema, and shows glio-basal dissociation in severe oedema. In areas of highly increased cerebro-vascular permeability, the basement membrane shows matrix disorganization, reduplication, and bifurcations protruding toward the endothelial cells, and acting as abluminal transcapillary channels. In regions of total brain necrosis, its structural stability is lost showing loosening, dissolution and rupture. Basement membrane swelling is due to overhydration of its protein-complex glycoprotein matrix. The thickening, rarefaction and vacuolization are induced by the increased vacuolar and vesicular transendothelial transport. The degenerated basement membrane areas exhibit a finely granular precipitate interpreted as protein, proteoglycan, glycoprotein, and agrin degraded matrix.

Key words: *basement membrane, brain oedema, electron microscopy.*

Introduction

Brain oedema is an appropriate pathological condition for studying the fine ultrastructural alteration of capillary basement membrane [16]. This structure forms the second line permeability barrier of the anatomical and physiological blood-brain barrier [70]. In the animal central nervous system, the vascular basal lamina appears as a homogeneous structure with a density similar to that observed in glomerular lamina densa [25,29]. Numerous studies based on experimental and pathological conditions performed in several vertebrates, including man, have reported the following alterations of capillary basement membrane: thickening, rarefaction, vacuolization and reduplication [4,6,12,17,23,24,28,30,32,34,47-49,54-56, 58,60,61,67,78,79,83,91]. Deposition of collagen in the basement membrane after arterial hypertension was reported by Garcia *et al*. [35], in rats after 10-minute cardiac arrest [87], in cerebral hypoperfusion considered as a risk factor for Alzheimer's disease [26], and after traumatic brain injury in the rat cerebral cortex [88]. Thickening of capillary endothelial cell basement

Communicating author:

Prof. Orlando José Castejón, MD, Biological Research Institute, Faculty of Medicine, Zulia University, Maracaibo, Venezuela, fax: 58-261-7831611, e-mail: ocastejo@cantv.net

membrane has been found as the most characteristic morphologic feature of diabetic microangiopathy [12,42,50], in hypertension combined with diabetes [43], and in galactosaemic rats [31]. There also is thickening of the basement membrane covering a non-vascular cell of nerve, the perineural cells [41]. Thickening of the basement membrane of cortical capillaries has also been reported in Alzheimer's disease [57,59,68,69,72,74,93], scleroderma and Raynaud's disease [11], and in glomerular diseases [71]. In addition, age-related thickening of retinal capillary basement membrane was described earlier [64]. Berzin *et al*. [3] found that agrin is associated with heparan sulphate proteoglycans in the basement membrane, and that agrin and laminin fragmentation occurs in Alzheimer's disease. Inoue [39] and Inoue and Kisilevski [40] reported abundant microfibril-like β-amyloid in the basement membrane in the cerebrovascular amyloid angiopathy of Alzheimer's disease. Sehba *et al*. [75] demonstrated an acute loss of collagen IV from the cerebral microvasculature after aneurysmal subarachnoid haemorrhage.

Plesea *et al*. [67] found focal or circumferential capillary thickening due to densification of the type IV collagen material from the basement membrane structure in hypertensive cerebral haemorrhage. Schóller *et al*. [76] demonstrated basal lamina damage correlated with blood-brain barrier dysfunction following subarachnoid haemorrhage in rats. According to Wang *et al*. [86], damage to the basal lamina causes the dismantlement of microvascular wall structures, which in turn results in the increase of microvascular permeability, haemorrhagic transformation, brain oedema and compromise of the microcirculation. In animal models, ischaemia reperfusion (IR) injury triggers membrane lipid degradation and accumulation of lipoxidative exacerbations in the neurovascular unit, leading to blood-brain barrier damage and neurologic deficits [38]. Uranova *et al*. [81] found ultrastructural abnormalities of capillaries in schizophrenia included thickening and deformation of basal lamina. String vessels or collapsed empty basement membrane tubes devoid of endothelial cells, and considered acellular capillaries, are often associated with pathologies such as Alzheimer's disease, ischaemia, and irradiation, but are also found in normal human brains from preterm babies to the aged. This causes an age-related decline in cerebral angiogenesis and results in neuronal loss. These string capillaries can re-grow by proliferation and migration of endothelial cells into empty basement membrane tubes, which provide a structural scaffold, replete with signalling molecules [7]. Castejón [21] showed thin and fragmented basement membranes with areas of focal thickening in human congenital hydrocephalus. Castejón [22] also reported that hypertrophic pericytes induce basement membrane splitting in traumatic brain oedema.

The purpose of this review is to describe the alterations of capillary basement membrane in vascular anomaly, brain trauma, congenital hydrocephalus, and brain tumours. The following aspects are summarized: the basement membrane complex in an apparently normal basement membrane, the basement membrane thickness according to aetiology, degree of brain oedema, and age of the patients; the alterations of the basement membrane complex and the pathogenesis of glio-basal dissociation, and the transbasal membrane pathway for haematogenous oedema fluid. In addition, we have postulated a neurobiological interpretation of thickening, rarefaction and vacuolization of the basement membrane in the light of present knowledge on chemical composition of basement membrane, pathogenesis of vasogenic brain oedema, and the increased transendothelial vacuolar and vesicular transport. It is also important to make an evaluation of the structural stability of basement membrane in severe oedema and perivascular total brain necrosis, and to discuss the proliferation of collagen fibers into the basement membrane.

The normal capillary basement membrane

In human brain capillaries as observed in moderate oedematous regions of cortical biopsies of patients with vascular anomalies and congenital hydrocephalus, the basement membrane appears as a homogeneous, thin and continuous dense lamina due to its condensed filamentous pattern, embedded in a homogeneous matrix (Fig. 1).

Basal lamina splitting occurs in apparently normal areas, in which the cell body and the pericyte processes can be seen enclosed within the basal lamina compartments. This apparently normal capillary basement membrane closely resembles that observed in normal vertebrate [1,8,25,73], and invertebrate tissue [2]. In humans and in experimental animals, the basement membrane thickness varies from capillary to capillary, and even locally within a single

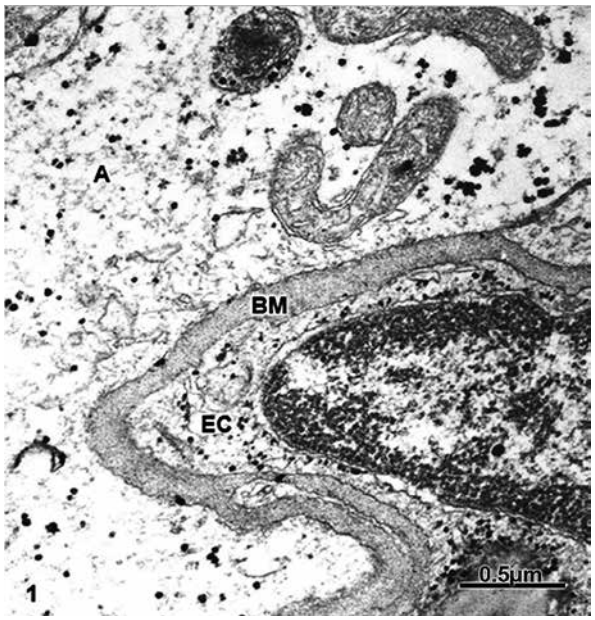

Fig. 1. Anomaly of the anterior cerebral artery. Right parietal cortex. Capillary from a moderate oedematous region showing an apparently normal basement membrane (BM) exhibiting a homogeneous dense matrix. The endothelial cell (EC) and the swollen astrocytic glial end-foot (A) plasma membranes are closely applied to the basement membrane luminal and abluminal surfaces.

capillary [73]. Furthermore, the average thickness seems to increase with the aging process [46,64]. According to Laursen and Diemer [49], the harmonic mean basement membrane thickness of normal cortical capillaries of male Wistar rats is 52.37 nm in width.

Basement membrane thickening in moderate and severe traumatic brain oedema

In patients with traumatic brain injuries, examination of moderately oedematous regions show capillaries apparently not activated by the traumatic agent. In such regions, the apparently normal capillary basement membrane width ranges from 71.97 to 191.90 nm [19] (Fig. 2).

In patients with severe traumatic brain oedema the capillary basement membrane appear thickened. The basement membrane width ranges from 206.66 to 404.22 nm [19]. In addition, the basement membrane appears vacuolated (Fig. 3).

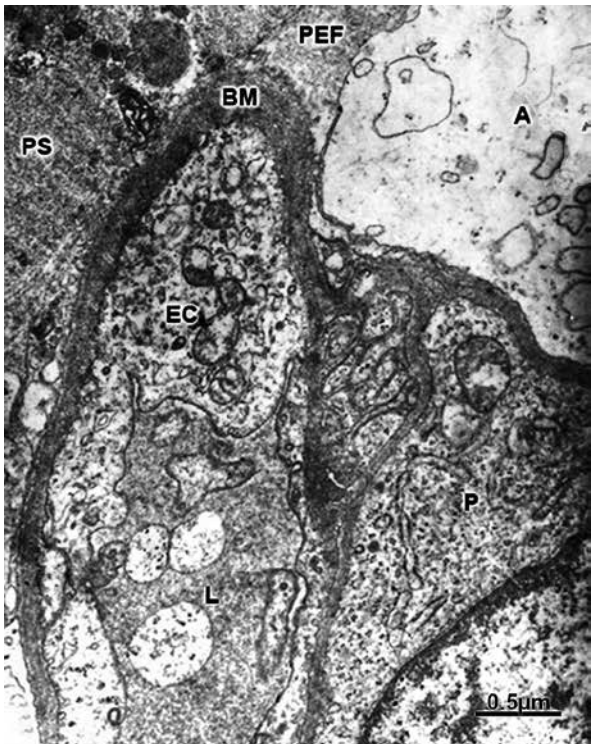

Fig. 2. Brain trauma. Right epidural haematoma. Right temporal cortex. Compact and dense capillary basement membrane (BM) showing an apparently normal structure in a moderate oedematous region. On the contrary, the clear perivascular astrocytic end-foot (A) shows a marked oedema. The pericytal cytoplasm (P) enclosed within the basement branches, the activated endothelial cell (EC), and the capillary lumen (L) are also seen. Note the presence of proteinaceous oedema fluid (PEF) in the perivascular space (PS).

Capillary basement membrane vacuolization

In patients with severe brain traumatic injuries, and loss of consciousness after alcohol ingestion, in addition to the increased vesicular and vacuolar transendothelial transport, a thickened and vacuolated basement membrane is found [14,16]. The mechanisms of increased extravasation of macromolecules across the blood-brain barrier exerted by ethanol intoxication are obscure. Theoretically, changes in vascular tones, vascular perfusion, as well as interference with blood coagulation, endothelial biogenic amine metabolism, and endothelial plasmalemma, all might contribute to this increased extravasation [66].

Endothelial vacuoles are observed discharging their content directly into the basement membrane or by means of plasmalemmal vesicles. Clathrin-coated and uncoated vesicles have also been found connected to the basement membrane surface [14,16] at the endothelial and pericytal margins. This increased vacuolar and vesicular transport induces progressive and slow alteration of the basement membrane matrix resulting in a gradual process of hydration, thickening, rarefaction, vacuolization and structural matrix disorganization. From the damaged basement, the oedema fluid penetrates into the astrocytic perivascular end-feet processes via the astrocyte cell soma [82]. The basement membrane vacuolization observed in very severe oedematous areas and in regions of brain parenchyma destruction reveals a complete loss of its diffusion-barrier function. A simultaneous vacuolization of endothelial cells, pericytes, astrocytes, and open endothelial junctions [17,23] was also encountered as the morphological substrate of enhanced transcapillary protein transport [14].

If endothelial cells, pericytes and perhaps glial cells participate in the elaboration of the normal basement membrane [25], the reverse process: the degeneration of these cells could induce basement membrane degradation and lysis. Basement membrane thickening and vacuolation also were observed by Kamyrio *et al*. [44] after gamma knife irradiation. In addition, Li *et al*. [51] have reported basement thickening in rats after simulated weightlessness.

In patients with head trauma and blood hypertension, the possibility exists that, in addition to the brain oedema, degenerative changes of capillary basement membrane should be present, as part of the degenerative changes of smaller penetrating cerebral vessels. The development of severe oedema in this case could be due in part to permeability changes to protein in penetrating vessels [27].

In several models of animal and human brain oedema, in which enhanced permeability to protein exists, loosening and swelling of the basement membrane have been earlier described [28,48,58,60,76,78].

In earlier studies [14,16,19], we have shown increased vesicular and vacuolar endothelial transport in cortical capillaries of patients with brain trauma, brain tumours, and congenital malformations. These morphological features of increased capillary permeability are closely related with the basement membrane thickening [19]. Basement membrane thickening has also been reported in different non-nervous pathological entities. Laursen and Diemer [49] reported an increase in the thickness of the brain capillary basement membrane after 30 days of portocaval anastomosis. Enlargement of the basement membrane has been described myxedema and polymyositis [84]. Basement membrane thickening in diabetes is also associated with increased capillary permeability which becomes manifest when the duration of diabetes exceeds 10 years [59]. According to these authors, the ischaemia could be a contributing factor to the basement membrane thickening. Basement membrane changes seem to be more a result than the cause of increased capillary

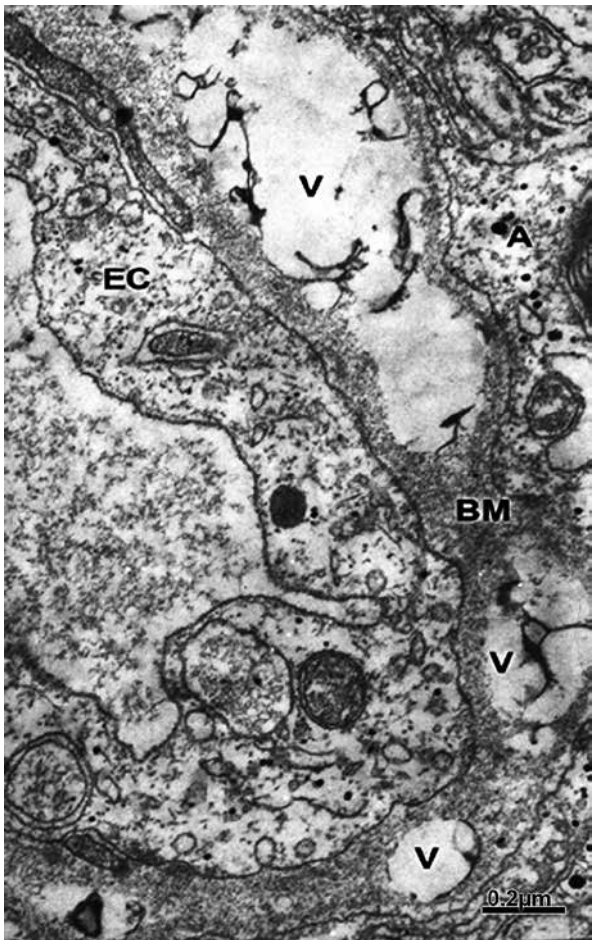

Fig. 3. Brain trauma. Right parieto-temporal subdural haematoma. Right parietal cortex. Thickened and vacuolated (V) basement membrane (BM) of a capillary localized in a severely oedematous area. The swollen and vacuolated endothelial cell (EC) and astrocytic end-foot (A) are also observed.

permeability. In addition, it has been reported that hypoxia causes oedema and disruption of endothelial basement membrane in pulmonary arteries [62]. Increased basement membrane thickness of skeletal muscle capillary in congestive heart failure has been reported by Longhurst *et al*. [54]. In congestive heart failure a high degree of local hypoxia undoubtedly occurs especially during exercise. According to these authors, an increased basement membrane thickness may be a result of local hypoxia and cell death. With the formation of new cell components, the new basement membrane material may oppose itself to the old lamina leading to significant thickening.

In an experimental model of brain oedema, such as cold injury oedema, one of the most commonly used model for traumatic vasogenic oedema [52], rarefaction and widening of the capillary basement membrane occur almost before any other vascular change. Thickening of the basement membrane has been also reported in the vasogenic brain oedema induced by intraventricular collagenase infusion [36]. The collagenase induces blood-brain barrier impairment by its action on the vascular basement membrane, not altering the structures in the brain parenchyma, and causing oedema formation and protein extravasation. Thickened capillary basement membrane is also reported in arterial hypertension [35], and diabetes [42]. Hypertension combined with diabetes also enhance basement thickening [43]. Similar findings are observed in galactosaemic rats [31], and in streptozotocin-induced diabetes [6].

Capillary basement membrane thickening in Alzheimer's disease has been widely reported by several workers [68,69,74,93]. Berzin *et al*. [3] and Salloway *et al*. [72] have implicated agrin, a synaptic organizing protein, in basement membrane damage in Alzheimer's disease.

Swollen and vacuolized capillary basement membrane in vascular anomaly and congenital hydrocephalus

In congenital malformations, such as vascular anomalies and congenital hydrocephalus, basement membrane thickening and vacuolization is also observed (Figs. 4 and 5).

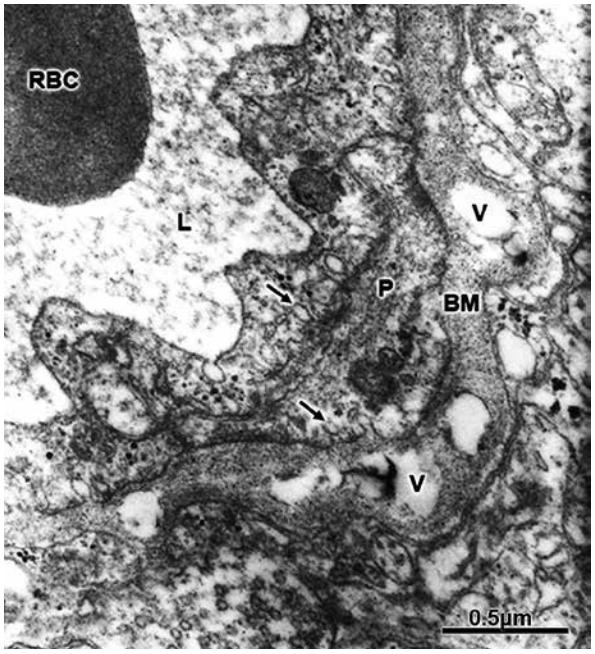

Fig. 4. Anomaly of the anterior cerebral artery. Right parietal cortex. Severe oedema. Swollen and vacuolized (V) capillary basement membrane (BM). Increased pinocytotic activity is observed in the endothelial cell and pericytal cytoplasm (P) (arrows). The capillary lumen (L) and a red blood cell (RBC) are also distinguished.

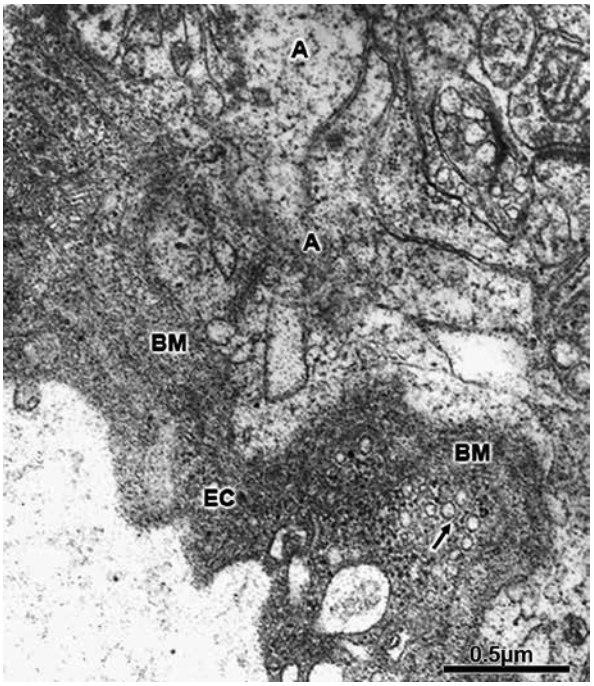

Fig. 5. Congenital hydrocephalus. Right parietal cortex. A swollen, undulated and immature capillary basement membrane (BM) is observed. Note the increased pinocytotic activity (arrow) in the dark endothelial cell (EC), and the swollen perivascular astrocytic end-feet (A).

Capillary basement membrane thickening in brain tumours

In brain tumours the capillary basement membrane also appears notably swollen, rarefacted, and exhibiting a dark and finely granular precipitate (Fig. 6).

Immunohistochemical expression of laminin 1 and 2 has been found in brain tumour vessels [80] and in breast cancer [33]. A redistribution of aquaporin-4 channels and loss of agrin has been observed by Warth *et al*. [90] in human glioblastoma.

Basement membrane bifurcations acting as abluminal channels

The basement membrane bifurcations enclosing the pericyte processes appear as irregularly dilated translucid channels, following a contoured course, approaching to the luminal endothelial plasma membrane [13,22]. These expansions originate from the basement membrane and after a short trajectory applied to the endothelial cytoplasm, converge again onto the basement membrane. These expansions lost their matrices in large segments, and appear as dilated electronlucid channels, resulting from increased capillary permeability (Fig. 7).

The swollen capillary basement membrane branches seem to function as abluminally oriented transcapillary channels for massive escape of haematogenous oedema fluid. These dilated basement membrane branches have been interpreted as basement membrane modifications in response to heightened transcapillary exchange in traumatic brain oedema [19]. Such structures, together with transendothelial, pericytal and astrocytic channels [15,17,19,23] seem to represent the basic morphological substrate for massive escape of hematogenous oedema fluid in vasogenic brain oedema.

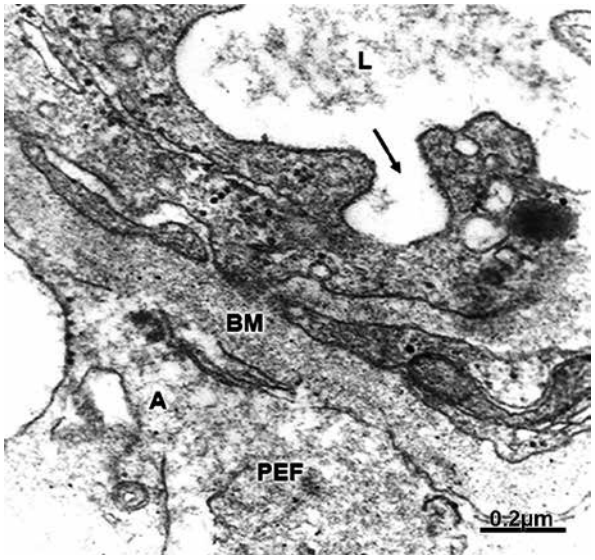

Fig. 6. Cystic craniopharyngioma. Right frontal cortex. Swollen capillary basement membrane (BM) exhibiting rarefaction and a fine and dark granular precipitate. Note the proteinaceous oedema fluid (PEF) in the perivascular astrocytic end-foot (A) similar to that observed in the capillary lumen (L). The endothelial cell shows deep invaginations (arrow) of the luminal surface to form protein containing vacuoles.

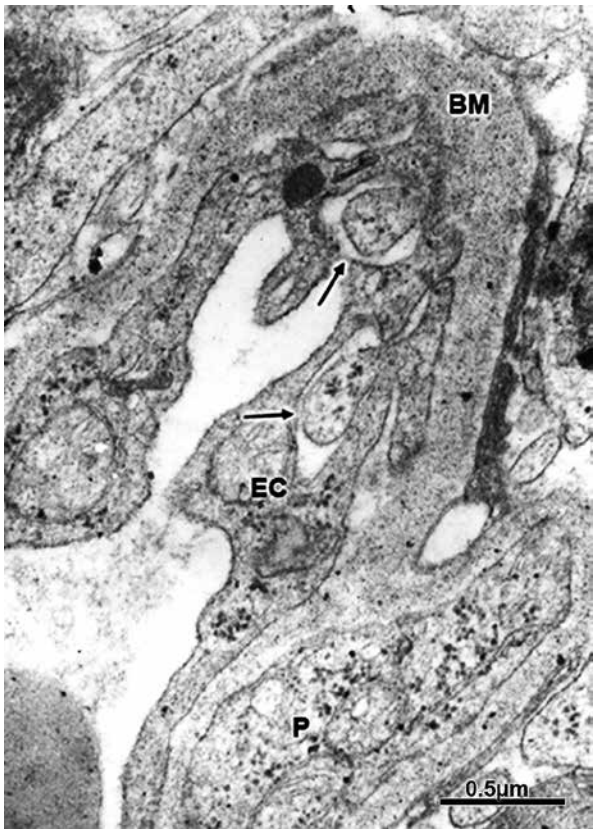

Fig. 7. Brain trauma. Contusion and fracture of the frontal region. Left frontal cortex. Dilated and contorted basement membrane branches (arrows) approaching to the endothelial cell (EC), and acting as abluminal transcapillary channels. Note the continuity with the swollen basement membrane (BM). P labels the enclosed pericytal cytoplasm (P) within the basement membrane.

The glio-basal dissociation process

In some severe brain oedema areas, the astrocytic end-feet limiting membrane appears slightly detached from the basement membrane outer surface and follow an undulated trajectory. In these areas, the astrocytic glial end-feet are extremely swollen and glial filaments are frequently absent. The lack of attached glial filaments probably induced the glio-basal dissociation process [19] (Fig. 8).

Astrocytic invaginations precede the formation of astrocytic vacuoles, by means of which the oedema fluid seems to be transported to the neighbouring neuropil [16,82]. Apparently in the severe oedema, the swollen and fragmented astrocytic processes release the already up-taken haematogenous oedema fluid in the neighbouring enlarged extracellular space which, in turn, dissects the astrocytic membrane from the basement membrane complex [19]. In areas of total brain tissue necrosis due to traumatic alteration of the blood-brain barrier, evinced by presence of extravasated erythrocytes, a severe alteration of basement membrane is observed consisting of loosening up and dissolution of its matrix.

As illustrated in Fig. 9, the denuded basement membrane tends to loosen up and shows evidence of the actual rupture not preventing the spreading of perivascular haemorrhages.

After a long evolution time of a brain trauma, the basement membrane and the perivascular glia still persist, demonstrating that these structures are the most resistant barrier elements of the vessel walls. This fact indicates the high structural stability of basement membrane in relationship to endothelial cells, pericytes and astrocytic end-feet, as it has been previously pointed out by Blinzinger *et al*. [5] in areas of cold-induced total cortical necrosis.

Proliferation of collagen fibers in the basement membrane

In some cases, the thickened basement membrane exhibits proliferation of collagen fibers (Fig. 10).

Proliferation of collagen fibers has also been reported by Long *et al*. [53] in malignant brain tumours, and by Calhoun and Mottaz [10] in experimental cerebral infarction. Nevertheless, these authors reported the presence of fibroblast in the pericapillary space. Although chemical evidence of a collagenous protein exists in the basement membrane [77], electron microscopy has not demonstrated collagen fibrils in the normal brain capillary basal lami-

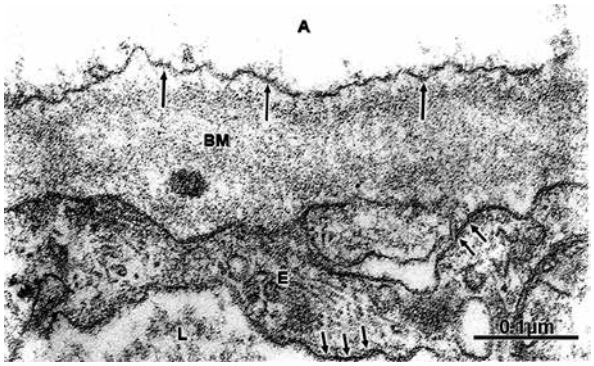

Fig. 8. Brain trauma. Left parieto-occipital subdural hygroma. Capillary of left parietal cortex. The thickened basement membrane (BM) exhibits matrix rarefaction and a finely granular appearance, corresponding to uranyl and lead staining of the swollen and degenerated basement membrane matrix. The luminal and abluminal endothelial (E) membranes are structurally intact (short arrows). The astrocytic end-foot (A) membrane follows an undulated course (long arrows) and the glio-basal dissociation process is initiated. The capillary lumen is labelled with an L.

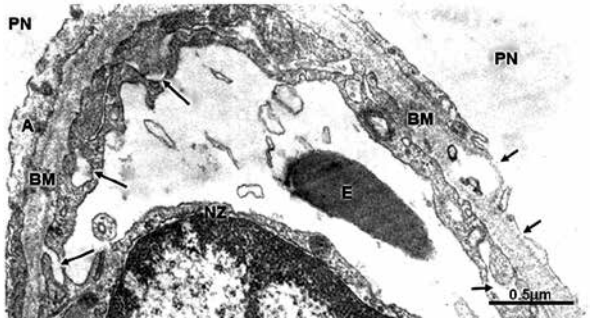

Fig. 9. Brain trauma. Subdural hygroma. Left parietal cortex. Capillary located in area of brain tissue necrosis showing a denuded and vacuolated (short arrows) basement membrane (BM). A thin layer of perivascular astrocytic end-foot (A) is still appreciated. The long arrows indicate swollen basement branches invaginating the endothelial cytoplasm, and acting as abluminal channels. Note the absence of perivascular neuropil (PN), the prominent endothelial nuclear zone (NZ), and a partial view of an intraluminal erythrocyte (E).

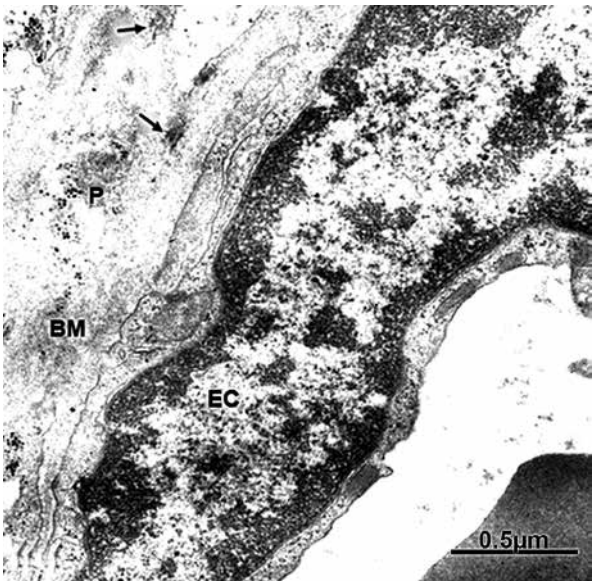

Fig. 10. Meningioma of the frontal cortex. Capillary of the right frontal cortex. Proliferations of collagen fibers (arrows) are observed within the basement membrane (BM) surrounding the pericytal cytoplasm (P). The endothelial cell (EC) is also seen.

na [25]. Proliferation of collagen fibers at the level of the basement membrane coexists with the presence of dark neuroglial cells, apparently pericytal microglia [63] attached to its outer surface, replacing the astrocytic pericapillary layer. We infer that pericytal microglia acquire fibroblastic properties and elaborate collagen properties, as an adventitial reaction. If, as considered by Bar and Wolff [1], the basement membrane plays a role in regulating the differentiation of adjacent neuroglial cells, it seems plausible that the capillary basement membrane could regulate the differentiation of this neighbouring pericytal microglia. It is also possible that this cell participates in the formation and maintenance of the reduplicated basement membrane. Collagen fibrils have been found beneath the basement membrane by García *et al*. [35] after arterial hypertension, by Walski *et al*. [87], and Walski and Gajkovska [88] after traumatic brain injury in rat cerebral cortex, and within the basement membrane in aged rats [26]. β-amyloid fibrils have been described in the capillary basement membrane in Alzheimer's disease [39,40]. Plesea *et al*. [67] encountered densification of the type IV collagen material in the basement membrane of cerebral vasculature in hypertensive intracerebral haemorrhage.

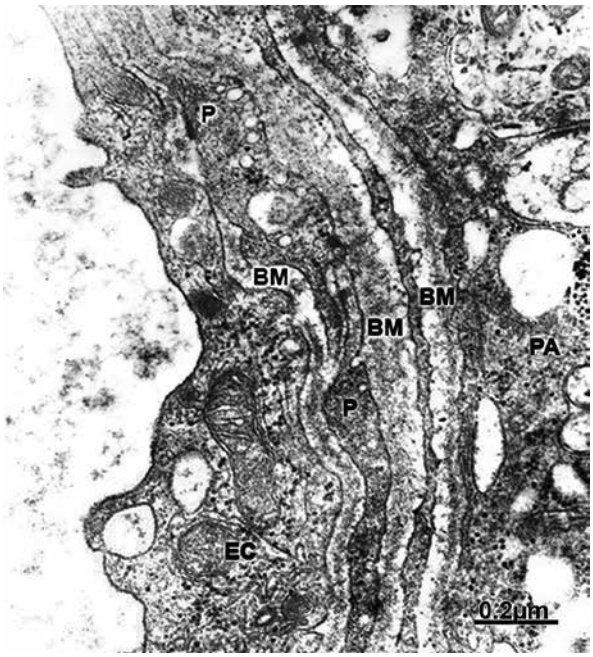

Fig. 11. Brain trauma. Right parieto-temporal subdural hematoma. Left parietal cortex. Cortical capillary showing reduplicated basement membranes (BM) which appear separated by thin bands of pericytal cytoplasm (P). The vacuolated endothelial cell (EC), and dark perivascular astrocytic end-foot (PA) are also seen.

Reduplication of capillary basement membrane

Reduplicated capillary basement membranes have been also found in our patients with brain oedema associated to brain trauma and tumours (Fig. 11).

Reduplicated capillary basement membrane has been earlier reported by Luse and McDougal [55] in allergic encephalomyelitis; by Kiser and Kending [47] in the capsule of cerebral abscesses, by Ward *et al*. [89], Ferrer and Lopez-Pousa [30], and McLone [61] in brain tumours. According to Vracko and Benditt [84], the accumulation and lamellation of basement membrane would be a result of repeated episodes of cell death and regeneration. Therefore, Vracko [85] considers that layering, splitting or lamination of basement membrane is due to cell death and cell replenishment. The individual layer has been deposited there by new cell generation and gives an indication of the number of cell generations which have occurred at that particular site. The reduplication of the basement membrane could also be

a phenomenon induced by pericyte cell hypertrophy [15]. A multilayered basement membrane has been described by Yoshida *et al*. [92] in the repair process of cerebral infarction in rats, in subarachnoid haemorrhage [56], and in capillary vessels of neurohypophysis after focal ischaemia of cerebral cortex [32].

Basement membrane thickening and the aging process

We have studied a group of patients with congenital hydrocephalus whose age ranges from several months up to ten years, which exhibit focal swelling of basement membrane [18,21], and in patients with traumatic head injuries up to 80 years of age [20]. We have tried to establish a correlation between the age of the patient and the basement membrane width, in order to elucidate if, besides the pathological basement membrane thickening associated to brain oedema, there is also an increase in basement membrane thickness due to the aging process, as earlier suggested by Kilo *et al*. [46], and Nagata [64]. An increased basement membrane thickness is found up until 60 years of age. However further changes were not detected between 60 and 80 years [19]. Bruns *et al*. [9] have earlier reported an increased basement membrane thickness of cortical capillaries with increasing age in the cerebral cortex of the aging primate, *Macaca nemestrina*. The authors reported an increased basement membrane thickness between 4 and 10 years, but no further changes between 10 and 20 years. According to these authors, a regression analysis revealed no significant increase in thickness of the basement membrane with increasing age. In our study we have considered that only 45% of the variability of basement membrane width is due to the aging process, and the remaining 55% of the variability is related to the associated brain oedema [19]. A further study should be done in normal old subjects to really evaluate the possible changes of basement membrane thickness during aging. This study is obviously limited for ethical reasons in the normal human central nervous system.

A neurobiological interpretation of capillary basement thickening

We have considered the basement membrane enlargement in brain oedema as an unspecific reaction due to overhydration of its protein polysaccharide matrix. According to Hall [37] and Spiro [77], the basement membrane can be conceived as a network of collagen molecules having positive charges, surrounded by negatively charged mucopolysaccharides. According to Pease [65] in the presence of water, polysaccharides occupy large areas or domains compared to the weight of the molecule and not only water may penetrate these polysaccharide domains, but ions and small molecules. Berzin *et al*. [3] demonstrated that agrin is associated with heparan sulphate proteoglycans in the basement membrane. These biochemical data could explain the basement membrane thickening in human brain oedema. As we have previously postulated [16,19], the increased transcapillary passage of ions and water in brain oedema would produce a high state of hydration of the basement membrane matrix. Since the fundamental alteration in vasogenic brain oedema is an increased transcapillary transfer of fluids, ions, proteins and small molecules, we infer that the enlargement of the basement membrane can be initially considered as a state of overhydration of its protein – polysaccharide matrix or anionic sites. Consequently a notable loss of the role of the basement membrane as a semipermeable filter [45] or permeability-barrier function occurs in brain oedema. A discontinuity in the distribution of anionic sites can be associated with an increased capillary permeability, as observed in scrapie-infected mice [83].

Through the effect of cerebral oedema, collagen or proteins similar to collagen, proteoglycans and glycoproteins of the basement membrane are degraded, presumably producing a selective precipitation of uranyl and lead salts in these areas, as observed in the transmission electron microscopic images stained by these electron staining techniques [19]. Fragmentation of agrin, a synaptic organizing protein, found in the basement membrane [3,72] could also be implicated as the molecular substrate for basement membrane granularity.

Concluding remarks

The capillary basement membranes are examined in severe traumatic brain injuries, vascular malformation, congenital hydrocephalus and brain tumours. The capillary basement membrane exhibits homogeneous and nodular thickening, vacuolization, rarefaction, reduplication, and deposition of collagen fibers. Their average thickness varied according to the aetiology and severity of brain oedema. In

moderate brain oedema the thickness ranged from 71.97 to 191.90 nm in width, and in patients with severe brain oedema it varied from 206.66 to 404.22 nm. The basement membrane complex appears apparently intact in moderate oedema and shows glio-basal dissociation in severe oedema. In areas of highly increased cerebro-vascular permeability, the basement membrane shows matrix disorganization, reduplication, and bifurcations protruding toward the endothelial cells, and acting as abluminal transcapillary channels. In regions of total brain necrosis, its structural stability is lost showing loosening, dissolution and rupture. Basement membrane swelling is due to an overhydration of its protein-complex glycoprotein matrix. The thickening, rarefaction and vacuolization are induced by the increased vacuolar and vesicular transendothelial transport. The degenerated basement membrane areas exhibit a finely granular precipitate interpreted as protein, proteoglycan, glycoprotein, and agrin degraded matrix.

References

1. Bär T, Wolff JR. The formation of capillary basement membranes during internal vascularization of the rat's cerebral cortex. Z Zellforsch Mikrosk Anat 1972; 133: 231-248.
2. Barber VC, Graziadei P. The fine structure of cephalopod blood vessels. I. Some smaller peripheral vessels. Z Zellforsch Mikrosk Anat 1965; 66: 765-781.
3. Berzin TM, Zipser BD, Rafii MS, Kuo-Leblanc V, Yancopoulos GD, Glass DJ, Fallon JR, Stopa EG. Agrin and microvasclar damage in Alzheimer's disease. Neurobiol Aging 2000; 21: 349-355.
4. Bi L, Li YX, He M, Huang ZM, Zhao DS, Lan JQ. Ultrastructural changes in cerebral cortex and cerebellar cortex of rats under simulated weightlessness. Space Med Med Eng 2004; 17: 180-183.
5. Blizinger K, Matsushima A, Anzil AP. High structural stability of vascular and glial basement membranes in areas of total brain tissue necrosis. Experientia 1969; 15: 976-977.
6. Bouchard P, Ghitescu LD, Bendayan M. Morpho-functional studies of the blood-brain barrier in streptozotocin-induced diabetic rats. Diabetologia 2002; 45: 1017-1025.
7. Brown WR. A review of string vessels or collapsed, empty basement membrane tubes. J Alzheimers Dis 2010; 21: 725-739.
8. Bruns RR, Palade GE. Studies on blood capillaries. I. General organization of blood capillaries in muscle. J Cell Biol 1968; 37: 244-276.
9. Bruns EM, Kruckeberg MS, Comerford LE, Buschmann MBT. Thinning of capillary walls and declining numbers of endothelial mitochondria in the cerebral cortex of the aging primate, Macaca Nemestrina. J Gerontol 1979; 34: 642-650.
10. Calhoun CC, Mottaz JA. Capillary bed of rat cerebral cortex. The fine structure in experimental cerebral infarction. Arch Neurol 1966; 15: 320-328.
11. Camilleri JP. Fine structural capillary changes and basal lamina thickening in scleroderma (progressive systemic sclerosis) and Raynaud's disease. Pathol Res Pract 1984; 178: 230-236.
12. Carson KA, Hanker JS. Basal lamina thickness and permeability to horseradish peroxidase of intraneural capillaries in diabetic mice. Microvasc Res 1980; 20: 223-232.
13. Castejón OJ. Formation of transendothelial channels in traumatic human edema. Pathol Res Pract 1984a; 179: 7-12.
14. Castejón OJ. Increased vesicular and vacuolar transport in traumatic human brain edema. A combined electron microscopy and theoretical approach. J Submicrosc Cytol 1984b; 16: 359-369.
15. Castejón OJ. Submicroscopic changes of cortical capillary pericytes in human perifocal brain edema. J Submicrosc Cytol 1984c; 16: 601-618.
16. Castejón OJ. Electron microscopic study of capillary wall in human cerebral edema. J Neuropathol. Exp Neurol 1980; 39: 296-328.
17. Castejón OJ. Electron microscopic observations of endothelial junctions in perifocal human brain edema. An interpretative study. J Submicrosc Cytol 1985; 17: 105-114.
18. Castejón OJ. Transmission electron microscope study of human hydrocephalic cerebral cortex. J Submicrosc Cytol Pathol 1994; 26: 29-39.
19. Castejón OJ. Ultrastructural alteration of human cortical capillary basement membrane in perifocal brain edema. J Submicrosc Cytol Pathol 1988; 20: 519-536.
20. Castejón OJ, Castejón HV, Diaz M, Castellano A. Consecutive light microscopy, scanning-transmission electron microscopy and transmission electron microscopy of traumatic human brain oedema and ischaemic brain damage. Histol Histopathol 2001; 16: 1117-1134.
21. Castejón OJ. Submicroscopic pathology of human and experimental hydrocephalic cerebral cortex. Folia Neuropathol 2010; 48: 159-174.
22. Castejón OJ. Ultrastructural pathology of cortical capillary pericytes in human traumatic brain oedema. Folia Neuropathol 2011; 49: 162-173.
23. Castejón OJ. Ultrastructural pathology of endothelial tight junctions in human brain oedema. Folia Neuropathol 2012; 50: 118-129.
24. Cervós-Navarro J. Brain edema due to ionizing radiation. In: Klatzo Y, Seitelberger F (eds.). Brain Edema Springer-Verlag, New York 1967; pp. 632-638.
25. Delorme P, Grignon G. An autoradiographic study on the biosynthesis of the capillary basal lamina in the chick embryo telencephalon. Cell Tissue Res 1978; 192: 299-308.
26. De Jong GI, De Vos RA, Steur EN, Luiten PG. Cerebrovascular hypoperfusion: a risk factor for Alzheimer's disease? Animal model and postmortem human studies. Ann N Y Acad Sci 1997; 26: 826-856.
27. Dinsdale HB. Hypertension and the blood-brain barrier. In: Cervos-Navarro J, Betz E, Ebhardt G, Ferst R, Wullemweber R (eds.). Advances in Neurology. Vol. 20. Raven Press, New York 1978; pp. 341-346.
28. Donahue S, Zeman W, Watanabe L. Alterations of basement membrane of cerebral capillaries. J Neuropathol Exp Neurol 1967; 26: 397-411.

29. Donahue J, Pappas GD. The fine structure of capillaries in the cerebral cortex of the rat at various stages of development. Am J Anat 1961; 108: 331-347.
30. Ferrer I, Lopez-Pousa S. Microvascularizacion de tumores cerebrales. Un estudio con bencidina y ultraestructura. Morfol Norm Patol 1980; 4: 13-24.
31. Frank RN, Dutta S, Frank SE. Cerebral cortical capillary basement membrane thickening in galactosaemic rats. Diabetologia 1987; 30: 739-744.
32. Frontczak-Baniewicz M. Focal ischemia in the cerebral cortex has an effect on the neurohypophysis. I. Ultrastructural changes in capillary vessels of the neurohypophysis after focal ischemia of the cerebral cortex. Neuro Endocrinol Lett 2001; 22: 81-86.
33. Fujita M, Khaznzon NM, Bose S, Sekiguchi K, Sasaki T, Carter WG, Ljubimov AV, Black K, Ljubimova JY. Overexpression of beta1-chain-contaning laminin in capillary basement membranes of human breast cancer and its metastases. Breast Cancer Res 2005; 7: 411-421.
34. Garcia JH, Lossinsky AS, Nishimoto K, Klatzo I, Light-Foote Jr. W. Cerebral microvasculature in ischemia. In: Cervós-Navarro J, Betz E, Ebhardt G, Ferst R, Wullemweber R (eds.). Advances in Neurology. Vol. 20. Raven Press, New York 1978; pp. 141-148.
35. Garcia JH, Ben-David E, Conger KA, Geer JC, Hollander W. Arterial hypertension injures brain capillaries. Definition of the lesions. Possible pathogenesis. Stroke 1981; 12: 410-413.
36. Gazendam J, Houthoff HJ, Huitema S, Go KG. Cerebral edema formation and blood brain barrier impairment by intraventricular collagenase infusion. In: Go KG, Baethmann A (eds.). Recent Progress in the Study and Therapy of Brain Edema. Plenum Press, New York 1982; pp. 45-54.
37. Hall BV. Renal glomerular basement membrane as a macromolecular system forming a complex multiple random-slit membrane filter. Anat Rec 1965; 151: 356-357.
38. Hoda MN, Singh I, Singh AK, Khan M. Reduction of lipoxidative load by secretory phospholipase A2 inhibition protects against neurovascular injury following experimental stroke in rat. J Neuroinflammation 2009; 13: 6-21.
39. Inoue S. Basement membrane and beta amyloid fibrillogenesis in Alzheimer's disease. Int Rev Cytol 2001; 210: 121-161.
40. Inoue S, Kisilevsky R. Beta-amyloid fibrils of Alzheimer's disease: pathologically altered, basement membrane-associated microfibrils? Ital J Anat Embryol 2001; 106: 93-102.
41. Johnson PC, Brendel K, Meezan E. Human diabetic perineural cell basement membrane thickening. Lab Invest 1981; 44: 265-270.
42. Johnson PC, Brendel K, Meezan E. Thickened cerebral cortical capillary basement membranes in diabetics. Arch Pathol Lab Med 1982; 106: 214-217.
43. Junker U, Jaggi C, Bestetti G, Rossi GL. Basement membrane of hypothalamus and cortex capillaries from normotensive and spontaneously hypertensive rats with streptozoticin-induced diabetes. Acta Neuropathol 1985; 65: 202-208.
44. Kamiryo T, López MB, Kassell NF, Steiner L, Lee KS. Radiosurgery-induced microvascular alterations precede necrosis of the brain neuropil. Neurosurgery 2001; 49: 409-414.
45. Kefalides NA, Alpert R, Clark CH. Biochemistry and metabolism of basement membrane. Int Rev Cytol 1979; 61: 167-228.
46. Kilo C, Vogler N, Williamson JR. Muscle capillary basement membrane changes related to aging and to diabetes mellitus. Diabetes 1972; 21: 881-889.
47. Kiser JL, Kending JH. Intracranial suppuration. J Neursurg 1963; 20: 494-511.
48. Lampert P, Carpenter S. Electron microscopic studies on the vascular permeability and the mechanism of demyelination in experimental allergic encephalomyelitis. J Neuropathol Exp Neurol 1965; 24: 11-24.
49. Laursen H, Diemer NH. Capillary size, density and ultrastructure in brain of rats with urease-induced hyperammonaemia. Acta Neurol Scand 1980; 62: 103-115.
50. Lazarow A, Speidel E. The chemical composition of glomerular basement membrane and its relation to the production of diabetic complications. In: Siperstein MD, Colwell AR, Meyer K (eds.). Small Blood Vessel Involvement in Diabetes Mellitus. American Institute of Biological Sciences, Washington 1966; pp. 195-198.
51. Li C, Zhang WF, Zhao YF. Pericytes may have important role in the pathogenesis of vascular malformation. Med Hypothesis 2007; 68: 808-810.
52. Long DM. Microvascular changes in cold injury edema. In: Go KG, Baethmann A (eds.). Recent Progress in Study and Therapy of Brain Edema. Plenum Press, New York 1982; pp. 45-54.
53. Long DM, Hartman JF, French L. The ultrastructure of human cerebral edema. J Neuropathol Exp Neurol 1966; 25: 373-395.
54. Longhurst J, Capone RJ, Selis R. Evaluation of skeletal muscle capillary basement membrane thickness in congestive heart failure. Chest 1975; 67: 195-198.
55. Luse SA, McDougal D. Electron microscopic observations on allergic encephalomyelitis in the rabbit. J Exp Med 1960; 112: 735-742.
56. Makhamov KE, Baïbekov IM. Ultrastructure of the hematoencephalic barrier in subarachnoid hemorrhage and effect of phenobarbital. Zh Vopr Neirokhir Im N N Burdenko 2001; 1: 19-22.
57. Mancardi GL. Thickening of the basement membrane of cortical capillaries in Alzheimer's disease. Acta Neuropathol (Berl) 1980; 49: 79-83.
58. Manz HJ, Robertson DM. Vascular permeability to horseradish peroxidase in brainstem lesions of thiamine deficient rats. Am J Pathol 1972; 66: 565-575.
59. Matikainen E, Leinonen H, Juntunen J. Capillary morphology and muscle blood flow in diabetic neuropathy. Eur Neurol 1982; 21: 22-28.
60. McDonald LW, Hayes L. The role of capillaries in the pathogenesis of delayed radionecrosis of brain. Am J Pathol 1967; 50: 745-764.
61. McLone DG. Ultrastructure of the vasculature of central nervous system of childhood. Child's Brain 1980; 6: 242-252.
62. Meyrick B, Reid L. Endothelial and subintimal changes in rat hilar pulmonary artery during recovery from hypoxia. Lab Invest 1980; 42: 603-615.
63. Mori S, Leblond CP. Identification of microglia in light and electron microscopy. J Comp Neurol 1969; 135: 57-80.

64. Nagata M. Age related thickening of retinal capillary basement membranes. Invest Ophthalmol Vis Sci 1986; 27: 437-440.
65. Pease DC. Polysaccharides associated with the exterior surface of epithelial cells: kidney, intestine, brain. J Ultrastruct Res 1966; 15: 555-558.
66. Persson L, Rosengren L. Increased blood-brain barrier permeability around cerebral stab wounds aggravated by acute ethanol intoxication. Acta Neurol Scand 1977; 56: 7-16.
67. Plesea IE, Camenita A, Georgescu CC, Enache SD, Zaharia B, Georgescu CV, Tenovici M. Study of cerebral vascular structures in hypertensive intracerebral haemorrhage. Rom J Morphol Embryol 2005; 46: 249-256.
68. Perimutter LS, Choi HC. Microgliopathy, the vascular basement membrane and Alzheimer's disease: a review. Brain Res Bull 1990; 24: 677-686.
69. Perimutter LS. Microvascular pathology and vascular basement membrane components in Alzheimer's disease. Mol Neurobiol 1994; 9: 33-40.
70. Reese TS, Karnovsky MJ. Fine structural localization of a blood-brain barrier to exogenous peroxidase. J Cell Biol 1967; 34: 207-217.
71. Rumpelt HJ. Hereditary nephropathy (Alport's syndrome): spectrum and development of glomerular lesions. In: Pathology of Glomerular Disease. Rosen S (ed.). Churchill Livingstone, New York 1983; pp. 225-238.
72. Salloway S, Gur T, Berzin T, Tavares R, Zipser B, Correia S, Hovanesian V, Fallon J, Kuo-Leblanc V, Glass D, Hulette C, Rosenberg C, Vitek M, Stopa E. Effect of APOE genotype on microvascular basement membrane in Alzheimer's disease. J Neurol Sci 2002; 204: 183-187.
73. Schwink A, Wetzstein R. Die Kapillaren im Subcommissuralorgan der Ratte. Elektronenmikroskopische Untersuchungen an Tierren verschiedenen Lebensalters. Z Zellforsch Mikrosk Anat 1966; 73: 56-88.
74. Scheibel AB, Duong TH, Jacobs R. Alzheimer's disease as a capillary dementia. Ann Med 1989; 21: 103-107.
75. Sehba FA, Mostafa G, Knopman J, Friedrich V Jr, Bederson JB. Acute alterations in microvascular basal lamina after subarachnoid hemorrhage. J Neurosurg 2004; 101: 633-640.
76. Schöller K, Trinkl A, Klopotowski M, Thal SC, Plesnila N, Trabold R, Hamann GF, Schmid-Elsaesser R, Zausinger S. Characterization of microvascular basal lamina damage and blood-brain barrier dysfunction following subarachnoid hemorrhage in rats. Brain Res 2007; 1142: 237-246.
77. Spiro RG. Biochemistry of basement membranes. In: Balazs EA (ed.). Chemistry and Molecular Biology of the Intracellular Matrix. Vol. I. Academic Press, New York 1970; pp. 511-534.
78. Tani E, Evans JP. Electron microscope studies of cerebral swelling. II. Alterations of myelinated fibers. Acta Neuropathol (Berl) 1965; 4: 604-623.
79. Torack RM. Ultrastructure of capillary reaction to brain tumors. Arch Neurol 1961; 5: 86-98.
80. Toti P, Villanova M, De Felice C, Megha T, Bartolommei S, Tosi P. Expression of laminin 1 and 2 in brain tumor vessels. An immunohistochemical study. J Submicrosc Cytol Pathol 1998; 30: 227-230.
81. Uranova NA, Zimina IS, Vikhreva OV, Krukov NO, Rachmanova VI, Orlovskaya DD. Ultrastructural damage of capillaries in the neocortex in schizophrenia. World J Biol Psychiatry 2010; 11: 567-578.
82. Vise WN, Liss L, Yashow D, Hunt WE. Astrocytic process: a route between vessels and neurons following brain barrier injury. J Neuropathol Exp Neurol 1975; 34: 324-334.
83. Vorbrodt AW, Dobrogowska DH, Lossinsky AS, Wisniewski HM. Changes in the distribution of anionic sites in brain microblood vessels with an without amyloid deposits in scrapie-infected mice. Acta Neuropathol 1990; 79: 355-363.
84. Vracko R, Benditt EP. Capillary basal lamina thickening. Its relation to endothelial cell death and replacement. J Cell Biol 1970; 47: 281-285.
85. Vracko R. Basal lamina scaffold anatomy and significance for maintenance of orderly tissue structure. Am J Pathol 1974; 77: 314-346.
86. Wang CX, Shuaib A. Critical role of microvasculature basal lamina in ischemic brain injury. Prog Neurobiol 2007; 83: 140-148.
87. Walski M, Celary-Waiska R, Borowicz J. The perivascular fibrotic reaction in rat brain in the late period after experimental clinical death. II. Precapillary vessels. J Hirnforsch 1993; 34: 503-515.
88. Walski M, Gajkowska B. The changes in the ultrastructure of the cerebrovascular junction after traumatic injury of the cerebral cortex in rats. Neuro Endocrinol Lett 2001; 22: 19-26.
89. Ward JD, Hartfield G, Becker DP, Loving ET. Endothelial fenestrations and other vascular alterations in primary melanoma of the central nervous system. Cancer 1974; 34: 1982-1991.
90. Warth A, Kröger S, Wolburg H. Redistribution of aquaporin-4 in human gioblastoma correlates with loss of agrin immunoreactivity from brain capillary basal laminae. Acta Neuropathol 2004; 107: 311-318.
91. Wechsler W, Riverson E, Schroder JM, Kleihues P, Parmeiro JF, Hossman KA. Electron microscopic observations on different models of acute experimental brain edema. In: Klatzo I, Seitelberger F (eds.). Brain Edema. Springer-Verlag, New York 1967; pp. 598-614.
92. Yoshida Y, Yamada M, Wakabayashi K, Ijuta F, Kumanishi T. Endothelial basement membrane and seamless-type endothelium in the repair process of cerebral infarction in rats. Virchows Arch A Pathol Anat Histopathol 1989; 414: 385-392.
93. Zarow C, Baron E, Chi HC, Perimutter LS. Vascular basement membrane pathology and Alzheimer's disease. Ann N Y Acad Sci 1997; 826: 147-160.

Folia Neuropathologica

Low prevalence of most frequent pathogenic variants of six PARK genes in sporadic Parkinson's disease

Silvia García[1], Luz Berenice López-Hernández[1], Juan Antonio Suarez-Cuenca[1,2], Marlene Solano-Rojas[1,3], Martha P. Gallegos-Arreola[4], Olga Gama-Moreno[1,5], Paulina Valdez-Anguiano[1,6], Patricia Canto[1], Luis Dávila-Maldonado[7], Carlos F. Cuevas-García[8], Ramón Mauricio Coral-Vázquez[6]

[1]Centro Médico Nacional "20 de Noviembre", Instituto de Seguridad y Servicios Sociales de los Trabajadores del Estado, México, D.F., [2]Hospital General de Zona No. 58, IMSS Estado de México; Mexican Group for Basic and Clinical Research in Internal Medicine, AC., México D.F., [3]Universidad Autónoma de Guerrero, U.A.C.Q.B, Guerrero, [4]Centro de Investigación Biomédica de Occidente, Jalisco, [5]Universidad Autónoma de Guadalajara, [6]Sección de Estudios de Posgrado e Investigación, Escuela Superior de Medicina, Instituto Politécnico Nacional, México, D.F., [7]Instituto de Ciencias Médicas y de la Nutrición Salvador Zubirán, México, D.F., [8]Centro Médico Nacional Siglo XXI, Instituto Mexicano del Seguro Social, México, D.F.

Folia Neuropathol 2014; 52 (1): 22-29 DOI: 10.5114/fn.2014.41741

Abstract

Genetic variants that confer susceptibility to Parkinson's disease (PD) show unbalanced distribution among different populations; genetic predisposition to either familial or sporadic forms of PD in Mexican-mestizo population has not been comprehensively studied. The aim of the present study was to analyze genetic variants in six PARK genes in PD patients. In total 381 individuals (173 patients, 208 controls) were genotyped for p.Gly2019Ser and p.Gly2385Arg variants of LRRK2. The p.Gly2019Ser variant was present in two patients and one healthy control; the p.Gly2385Arg variant was not found. In a subgroup of early-onset PD (EOPD), MLPA analysis was done for PARKIN (PARK2), PINK1 (PARK6), DJ-1 (PARK7), LRRK2 (PARK8), SNCA (PARK1/4) and ATP13A2 (PARK9). We found a heterozygous deletion of exon 2 in PARK2 in the youngest patient of the early-onset group, who showed limited response to antiparkinsonian therapy. Although the changes Gly2019Ser and Gly2385Arg of LRRK2 are associated with PD in different populations; they may be a rare cause of PD in our population. Novel population-specific variants may underlie PD susceptibility in Mexican mestizos. Our study suggests that the heterozygous deletion of exon 2 in the PARK2 gene is a risk factor for EOPD.

Key words: *Parkinson's disease, LRRK2, Mexican-mestizos, PARK2.*

Communicating authors:
Ramón M. Coral-Vázquez, Sección de Estudios de Posgrado e Investigación, Escuela Superior de Medicina del Instituto Politécnico Nacional, Plan de San Luis y Díaz Mirón s/n, Col. Casco de Santo Tomas, C.P. 11340, México, D.F., México, phone: (5255) 57296300, ext. 62820, fax: (5255) 57296300, ext. 62820, e-mail: rmcoralv@gmail.com, rcoral@ipn.mx & Luz Berenice López Hernández, División de Investigación Clínica, Subdirección de Enseñanza e Investigación, Centro Médico Nacional 20 de Noviembre, Instituto de Seguridad y Servicios Sociales de los Trabajadores del Estado, San Lorenzo 502, C.P. 03100, México, D.F., México, phone: 01 52 55 52 00 50 03, fax: 01 52 33 36 32 62 00, e-mail: lblhmedgen@gmail.com

Introduction

Parkinson's disease (PD) is a chronic progressive neurodegenerative disease that affects 1-2% of the population older than 65 years [14], diminishes quality of life and autonomy of patients [30]. Parkinson's disease is characterized by exacerbated loss of dopaminergic neurons of the *substantia nigra pars compacta*, which clinically expresses through tremor, rigidity, bradykinesia, postural instability and progressive impairment of the cognitive function [34].

Genetic factors that confer susceptibility to PD are still unclear although genetic variants in mitochondrial and nuclear genomes have been involved in this disease [17,37]; however, genetic variants in sezzzveral candidate genes (PARK genes) have been investigated in relation to both late and early onset presentations of the disease [late-onset PD (LOPD) and early-onset PD (EOPD), respectively). Among these genes, *LRRK2* and *PARK2* are the most associated to LOPD and EOPD forms, respectively [31].

LRRK2 encodes a multidomain protein, "dardarin" with kinase and GTPase activities. One of the most widely studied genetic variants within *LRRK2* is rs34637584 (c.6055G>A), (p.Gly2019Ser) located in the kinase domain [14,26]. *In vitro* studies showed an increased phosphotransferase activity due to this change [9]. It is worth noting that p.Gly2019Ser is the most common genetic variant of *LRRK2* in Caucasians; whereas another SNP, rs34778348 (p.Gly2385Arg) is considered a risk factor for PD in Asians [6,18]. The p.Gly2385Arg change in the C-terminal domain of *LRRK2* was shown to render neurons more susceptible to apoptosis under oxidative stress [35]. Thus, both variants are considered pathogenic although with different magnitude and biochemical effect.

On the other hand, *PARK2* encodes a protein named "PARKIN", a component of an enzyme complex within the ubiquitin-proteasome system, which targets proteins for degradation [39]. Mutations in *PARK2* are highly associated to familial EOPD; up to 18% of patients present mutations in this gene, and only 5% of them present in the homozygous state [21,27].

Interestingly, a skewed distribution of genetic variants of PARK genes was previously described; some authors suggested that ethnicity may play a role as a modifying factor of pathogenicity of *LRRK2* variants [13,19,36]. Interestingly, some mitochondrial variants and haplogroups are thought to modify the risk of developing PD [15,38] by decreasing or increasing the penetrance of genetic variants in nuclear disease-genes (PARK genes). In this regard, it is known that the Mexican population was a result of genetic admixture among Amerindians, Caucasian and in a lesser extent, Africans [29] and, as in other Latin American populations [1], genetic factors predisposing to PD in Mexican-mestizos remain largely unknown [23,28,40]. Therefore, the aim of this study was to analyze the possible association between variants in PARK genes and PD by multiple screening as well as the weighing of their clinical relevance in Mexican-mestizo patients with sporadic PD (sPD).

Material and methods

Study population

The study was approved by the Human Research Committees of the participating institutions and informed written consent was obtained from all individuals. This is a cross-sectional study in which two-hundred fifteen Mexican-mestizo patients with sPD were consecutively recruited from February 2009 to June 2010, from four tertiary-care level hospitals in Mexico (Neurology Departments from Centro Médico Nacional "20 de Noviembre"-ISSSTE, Centro Médico Nacional Siglo XXI-IMSS, Instituto de Ciencias Médicas y de la Nutrición "Salvador Zubirán", Mexico City; and División de Genética, Centro de Investigación Biomédica de Occidente-IMSS, Jalisco, Mexico); nevertheless, 42 patients were eliminated because of incomplete data. The diagnosis of sPD was performed by an experienced neurologist, based on the Queen Square Brain Bank criteria [16]. Early-onset PD was defined as onset at the age of 20 to 40 years. Two hundred and eight healthy individuals (controls) were analyzed; all were of Mexican-mestizo ethnic origin, and were blood bank donors and/or healthy spouses of PD patients without family history of PD or other neurological diseases. Cases with secondary parkinsonism were excluded.

Mutation analysis

Peripheral blood samples were obtained from patients and genomic DNA was isolated by the CTAB-DTAB method [11]. Real-time polymerase chain reaction (PCR) allelic discrimination TaqMan assay (AB) was used for genotyping *LRRK2* variants. Briefly, PCR reactions contained 10-20 ng of DNA, 5.0 µl of Maxima Probe qPCR Master Mix (2X), 0.25 µl of primers and probes (10X) and H_2O

to 10 µl, including the appropriate negative controls in all assays. For the p.Gly2019Ser variant, the assay was available from Applied Biosystem (assay ID: C_63498123_10), whereas for thep.Gly2385Arg polymorphism a novel hydrolysis probe assay was designed by our group. Primers sequences were as follows: forward 5'-GAAGTGTGGGATAAGAAAACTG-3' and reverse 5'-AGATGGTGCTGAGAAGCATTAC-3'. The probe for each allele was: wild-type VIC 5'-CTCTGT [G] GACTAATAGACTGCGTGCAC-3' and mutant FAM 5'-CTCTGT [A] GACTAATAGACTGCGTGCAC-3'. Real-time PCR was performed on a LightCycler 480 II (Roche Diagnostics GmbH, Switzerland). Conditions for p.Gly2019Ser and p.Gly2385Arg p.Gly2385Arg polymorphisms were 95°C for 10 min, and 40 cycles of amplification (92°C for 15 s and 60°C for 1 min). For each cycle, the software determined the fluorescent signal from the VIC or FAM-labelled probe (Roche Applied Science, Mannheim, Germany). In order to confirm results of real-time genotyping, DNA was amplified by PCR and then sequenced (conditions and sequence of primers can be found in supplementary material).

For the EOPD subgroup, Multiplex-Ligation Dependent Probe Amplification (MLPA) was used to detect genetic variants in *PARKIN* (PARK2), *PINK1* (PARK6), *DJ-1* (PARK7), *LRRK2* (PARK8), *SNCA* (PARK1/4) and *ATP13A2* (PARK9) genes. The assay also detects gross gene deletions/duplications (P051-kit MRC-Holland) by direct hybridization and ligation of exon-specific half probes to DNA, ligated probes were further amplified by fluorescent multiplex PCR and capillary electrophoresis to reveal the altered copy number in the gene of interest. Data were analyzed with GeneMarker® software (SoftGenetics).

Data analysis

Sample size was estimated according to Armitage trend test taking into account allele risk frequency in Mexican mestizo population, prevalence of PD and the risk conferred by the pathogenic variant (http://ihg.gsf.de/cgi-bin/hw/power2.pl [20/04/2013]) [32]. Age, age at onset, Hoehn & Yahr scale and drug therapy requirement were analyzed through non-paired *T*-test. Categorical variables such as gender, PD symptoms and antiparkinsonian drugs evaluation were analyzed through χ^2. Deviations from Hardy-Weinberg equilibrium (HWE) were tested using the χ^2 Pearson test (http://ihg.gsf.de/cgi-bin/hw/hwa1.pl [20/04/2013]), p value < 0.05 was considered as statistically significant. SPSS software v. 18.0 (SPSS Inc., Chicago, IL, USA) was used for statistical analyses.

Results

In total 381 individuals were included, 173 patients with sPD constituted the study group (139 males and 34 females, aged 62.8 ±11.06 [mean ± standard deviation] years old, age at onset 57.8 ±14.27), whereas 208 healthy individuals constituted the control group (87 males and 121 females, aged 68.3 ±6.75 years old; showing differences in gender proportion and age, $p < 0.0001$ vs. the study group). The screening of *LRRK2* revealed the presence of the p.Gly2019Ser variant in two male patients with sPD with the age at onset at 66 and 56 years old and in one 66-year-old male from the control group (variants submitted to the Parkinson's disease Mutation Database, http://grenada.lumc.nl/LOVD2/TPI/home.php?select_db=LRRK2 [01/06/2012]). Genotype frequency was similar to expected values, according to Hardy-Weinberg equilibrium (HWE) test in both groups (HWE *P* values $p = 0.93$ for cases, $p = 0.97$ for controls). Additionally, there was no case in our cohort carrying the p.Gly2385Arg variant, although DNA sequencing elicited the identification of a synonymous change p.Gly2385Gly in one patient (Fig. 1).

Since the prevalence of mutations in PARK genes is thought to be higher in young patients, we explored likely associations in a subgroup of 19 patients with EOPD showing particular clinical features, such as tremor 26.3%, mental impairment 5.2% ($p < 0.0002$ vs. the study group); more frequently prescribed with amantadine (89.5%), antihistamines (78%) and tricyclic acid antidepressants (78.9%) ($p < 0.002$ vs. the study group); although with similar PD progression rate and treatment response (Hoehn & Yahr scale "on-state" = 2.5 ±1.26, $p = 0.37$; "off-state" = 3.2 ±0.83, $p = 0.11$; "poor" response 10.5%, $p = 0.54$). MLPA screening of six PARK genes revealed a deletion of exon 2 in *PARK2*, the carrier was a female, and she was the youngest patient of this subgroup (30 years old with 2 years of PD symptoms), no tremor or mental impairment were found, but "poor" response to antiparkinsonian drug therapy was present in this case (L-Dopa, dopamimetics, anticholinergic and MAO inhibitors). The mutation p.Ala30Pro was also absent in all MLPA screened patients as revealed by the absence of peak signal.

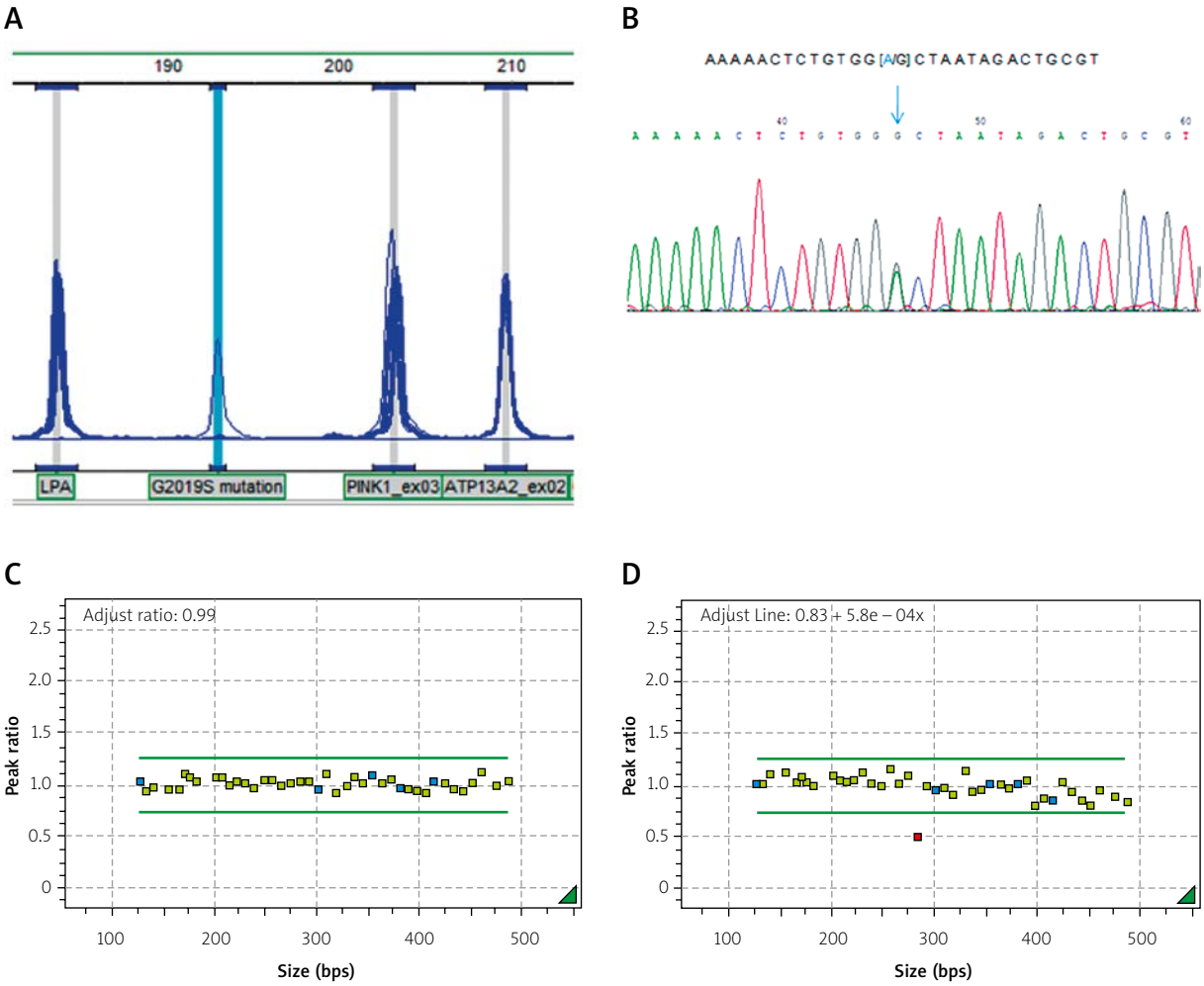

Fig. 1. A) MLPA peaks showing the p.Gly2019Ser mutation of LRRK2 as control. **B)** Sequencing of p.Gly2385Gly synonymous change. **C)** MLPA ratio analysis for PARK genes in a normal subject. **D)** MLPA ratio analysis showing a heterozygous deletion of exon 2 of PARKIN gene.

Discussion

Parkinson's disease is a complex neurodegenerative disorder in which genetic and environmental factors are involved. Ethnicity is thought to modify the effect of allelic variants associated to complex disorders; therefore, searching for prevalent mutations in PARK genes within specific populations is crucial to estimate susceptibility to PD [8]. This holds true especially for LRRK2 gene variants that have shown differential distribution among populations [18]. This also has potential in the pharmacogenetic field; since LRRK2 protein has been proposed as a therapeutic target for PD [4,41]. Nevertheless, biological mechanisms linking *LRRK2* polymorphisms to neurodegeneration are still unclear. Interestingly, LRRK2 is expressed by immune cells and up-regulated following recognition of microbial structures [12]; allelic variants in *LRRK2* and *PARK2*, have been associated to leprosy [3], celiac disease [7], Crohn's disease [20] and PD [2]; thus, there is a possible role for the immune system in the neurodegenerative process conferring population-specific susceptibility for PD.

It is worth mentioning that the highest frequency and penetrance of the *LRRK2* p.Gly2019Ser change was found in North African Arabs (NA) and Ashkenazi Jewish (AJ) [13], in which mitochondrial haplogroup H carrying the m.4336T>C change associated to PD is also common [5]. Interestingly, a high frequency of celiac disease was also described in North Africans [10]. Thus, it is likely that the combination of the

changes m.4336T>C (haplogroup H) and p.Gly2019Ser confer susceptibility LRRK2 related diseases including PD. It is worth noting that all patients (with the exception of one – see supplementary material) and controls analyzed in this study did not have the variant m.4336T>C (unpublished data), which may result in a low penetrance of the variant p.Gly2019Ser of LRRK2, and a possible reason for the presence of this variant in an individual without PD.

A prior study of *PARK2* and PD in Mexican-mestizos showed the absence of homozygous p.Arg366Trp and p.Asp394Asn polymorphisms; interestingly, two polymorphisms p.Ser167Asn and p.Val380Leu were in HWE disequilibrium; authors suggested a competing risk of death of variant carriers to explain such finding [23]. We speculate that HWE disequilibrium could be reminiscent evidence of prevalent diseases such as leprosy and tuberculosis in native populations of Mexico (http://www.salud.gob.mx/docprog/estrategia_2/salud_y_nutricion.pdf [20/04/2013]). This would further support the involvement of PARK genes in immune response, although more in-depth research on this matter is required.

Although p.Gly2019Ser and p.Gly2385Arg are commonly found in Caucasians and Asians, respectively, our study showed a low prevalence on these variants in Mexican-mestizos; similarly to other reports of p.Gly2019Ser in our population [40] and from a population of the South of Spain [24]. This is concordant with the fact that first immigrants who arrived from Europe to Mexico came from the South of Spain [29]. Regarding the p.Gly2385Arg, it remains unexplored in most Latin American populations; here we showed the absence or very low frequency of this variant in our group of patients. We also found the p.Gly2385Gly synonymous change and despite it is not linked to PD, pathogenicity could not be excluded; some apparently neutral variants may have an impact on disease development [17]. Our results indicate that p.Gly2019Ser mutation may be a rare cause of PD in patients with different ethnical origin from NA and AJ; especially in the absence of mitochondrial variants associated to PD. Indeed, a recent study in Argentina showed that approximately 5.45% (3/55) of PD patients had the p.Gly2019Ser heterozygous change and AJ ancestry, interestingly one of them presented also celiac disease [7]. Although the frequency of p.Gly2019Ser change was present in two patients and one control, it should be taken into account that the cumulative risk of PD for carriers of that variant is 51% at 69 years old [13], thus the 66-year-old individual from our control group still carries a remaining risk of developing PD. We strongly believe that genetic variants involved in the immune system and neurodegenerative diseases deserve further exploration. We speculate that the inner toxicity of dopamine production [37], exposure to pesticides that increase reactive oxygen species [33], plus increased oxidative stress caused by mitochondrial dysfunction may possibly cause protein oxidation and misfolding, and the subsequent formation of neoepitopes that trigger immune response mediated by *LRRK2* and *PARK2*. Convergent biological mechanisms and evolutive stories of populations could potentially contribute to elucidate genetic factors influencing PD susceptibility.

With regard of the analysis of the EOPD subgroup, after the screening of six PARK genes, mutation variants were rarely identified. However, our results support that *PARK2* is the most common gene mutated in the EOPD group, and also supports the notion that the lower the age at onset, the more likely a gene mutation can be found in *PARK2*, as suggested by genetic screenings [22]. We cannot rule out a potential influence of the genotype since the patient carrying the *PARK2* mutation was the youngest one affected of the EOPD subgroup, achieving a limited therapeutic response, although slow clinical progression. The mechanism responsible for this phenotype may be related to the disruption of the reading frame of *PARK2* gene, conferred by the deletion of exon 2 (c.8-?_171+?del); and although the deletion was heterozygous, this may be considered a risk factor for PD [25]. Thus, haploinsufficiency in PARKIN production could lead to a hampered turnover of damaged mitochondrion, due to inappropriate engagement of the autophagy pathway, caused by abnormal interactions between PINK1/PARKIN [39].

Conclusions

In the Mexican-mestizo population, the p.Gly2019Ser change could be a rare case of PD. The combination of variants p.Gly2019Ser and m.4336T>C was not present in any case and the p.Gly2385Arg was also absent. To our knowledge, this is the first work exploring the prevalence of pathogenic variants in various PARK genes in the Mexican-mestizo population. Our data support that *PARK2* is the most common gene involved in EOPD and deletion of

exon 2 even when heterozygous may be a risk factor. Although the most common pathogenic variants were scarce in our population, different nucleotide changes with similar biochemical properties cannot be excluded. The search for population-specific pathogenic variants in the PARK genes and in other related disease-related genes such as SNCA, MAO-B, and COMT [37] is important either to elucidate genetic unrevealed risk factors or to provide genetic counselling and discover novel therapeutic targets for PD.

Acknowledgments

We thank for the financial support from Consejo Nacional de Ciencia y Tecnología (CONACYT), México (Grant: SALUD-2009-C01-111692). We thank Z. Sánchez Mandujano for technical assistance, J.C. Zenteno and E. Pelcastre from the Instituto de Oftalmología, Fundación Conde de Valenciana for sequencing. Authors report no conflict of interest

Disclosure

Authors report no conflict of interest.

Supplementary material – A novel genotyping assay for the m.4336C>T

We designed a novel TaqMan probe for genotyping this mitochondrial change since RFLP is time consuming and sequencing is expensive compared to real time PCR.

In order to obtain a viable assay for genotyping of the mitochondrial change m.4336T>C, we searched for repetitive sequences (http://www.repeatmasker.org/). After that, appropriate conditions were chosen using Primer 3. Oligonucleotide sequences are shown below. The allele specific hydrolysis probes were:
5' (VIC)-TTCGATTCTCAT[A]GTCCTAG-3' (wild type)
and 5'(FAM)-CGATTCTCAT[G]GTCCTAG-FAM (mutant).

The expected size of the amplified fragment is 88bp. Conditions for the reaction were: 1 µl (10-20 ng) of DNA, 5.0 µl of Maxima Probe qPCR Master Mix (2X), 0.25 µl of primers and probes (40X) and water for a final volume of 10 µl, including the appropriate negative controls in all assays. Real-time PCR was performed on a LightCycler 480 II (Roche Diagnostics GmbH, Switzerland). The conditions for the reaction are 95°C for 10 min, and 40 cycles of amplification (92°C for 15 s and 62°C for 1 min). For each cycle, the software determined the fluorescent signal from VIC or FAM-labeled probes (Roche Applied Science, Germany). Only one late-onset PD patient had the 4336C allele.

References

1. Benitez BA, Forero DA, Arboleda GH, Granados LA,Yunis JJ, Fernandez W, Arboleda H. Exploration of genetic susceptibility factors for Parkinson's disease in a South American sample. J Genet 2010; 89: 229-232.
2. Buschman E, Skamene E. Linkage of leprosy susceptibility to Parkinson's disease genes. Int J Lepr Other Mycobact Dis 2004; 72: 169-170.
3. Cardoso CC, Pereira AC, de Sales Marques C, Moraes MO. Leprosy susceptibility: genetic variations regulate innate and adaptive immunity, and disease outcome. Future Microbiol 2011; 6: 533-549.
4. de Ynigo-Mojado L, Martin-Ruiz I, Sutherland JD. Efficient allele-specific targeting of LRRK2 R1441 mutations mediated by RNAi. PLoS One 2011; 6: e21352.
5. Feder J, Ovadia O, Glaser B, Mishmar D. Ashkenazi Jewish mtDNA haplogroup distribution varies among distinct subpopulations: lessons of population substructure in a closed group. Eur J Hum Genet 2007; 15: 498-500.
6. Fung HC, Chen CM, Hardy J, Singleton AB, Wu YR. A common genetic factor for Parkinson disease in ethnic Chinese population in Taiwan. BMC Neurol 2006; 6: 47.
7. Gatto EM, Parisi V, Converso DP, Poderoso JJ, Carreras MC, Marti-Masso JF, Paisan-Ruiz C. The LRRK2 G2019S mutation in a series of Argentinean patients with Parkinson's disease: clinical and demographic characteristics. Neurosci Lett 2013; 537: 1-5.
8. Gaweda-Walerych K, Safranow K, Jasinska-Myga B, Bialecka M, Klodowska-Duda G, Rudzinska M, Czyzewski K, Cobb SA, Slawek J, Styczynska M, Opala G, Drozdzik M, Nishioka K, Farrer MJ, Ross OA, Wszolek ZK, Barcikowska M, Zekanowski C. PARK2 variability in Polish Parkinson's disease patients – interaction with mitochondrial haplogroups. Parkinsonism Relat Disord 2012; 18: 520-524.
9. Gloeckner CJ, Schumacher A, Boldt K, Ueffing M. The Parkinson disease-associated protein kinase LRRK2 exhibits MAPKKK activity and phosphorylates MKK3/6 and MKK4/7, in vitro. J Neurochem 2009; 109: 959-968.
10. Gujral N, Freeman HJ, Thomson AB. Celiac disease: prevalence, diagnosis, pathogenesis and treatment. World J Gastroenterol 2012; 18: 6036-6059.
11. Gustincich S, Manfioletti G, Del Sal G, Schneider C, Carninci P. A fast method for high-quality genomic DNA extraction from whole human blood. Biotechniques 1991; 11: 298-300, 302.
12. Hakimi M, Selvanantham T, Swinton E, Padmore RF, Tong Y, Kabbach G, Venderova K, Girardin SE, Bulman DE, Scherzer CR, LaVoie MJ, Gris D, Park DS, Angel JB, Shen J, Philpott DJ, Schlossmacher MG. Parkinson's disease-linked LRRK2 is expressed in circulating and tissue immune cells and upregulated following recognition of microbial structures. J Neural Transm 2011; 118: 795-808.
13. Healy DG, Falchi M, O'Sullivan SS, Bonifati V, Durr A, Bressman S, Brice A, Aasly J, Zabetian CP, Goldwurm S, Ferreira JJ,

Tolosa E, Kay DM, Klein C, Williams DR, Marras C, Lang AE, Wszolek ZK, Berciano J, Schapira AH, Lynch T, Bhatia KP, Gasser T, Lees AJ, Wood NW. Phenotype, genotype, and worldwide genetic penetrance of LRRK2-associated Parkinson's disease: a case-control study. Lancet Neurol 2008; 7: 583-590.
14. Healy DG, Wood NW, Schapira AH. Test for LRRK2 mutations in patients with Parkinson's disease. Pract Neurol 2008; 8: 381-385.
15. Huerta C, Castro MG, Coto E, Blazquez M, Ribacoba R, Guisasola LM, Salvador C, Martinez C, Lahoz CH, Alvarez V. Mitochondrial DNA polymorphisms and risk of Parkinson's disease in Spanish population. J Neurol Sci 2005; 236: 49-54.
16. Hughes AJ, Daniel SE, Ben-Shlomo Y, Lees AJ. The accuracy of diagnosis of parkinsonian syndromes in a specialist movement disorder service. Brain 2002; 125: 861-870.
17. Kochanski A. Pathogenic mutations and non-pathogenic DNA polymorphisms in the most common neurodegenerative disorders. Folia Neuropathol 2007; 45: 164-169.
18. Kumari U, Tan EK. LRRK2 in Parkinson's disease: genetic and clinical studies from patients. FEBS J 2009; 276: 6455-6463.
19. Liu X, Cheng R, Verbitsky M, Kisselev S, Browne A, Mejia-Santana H, Louis ED, Cote LJ, Andrews H, Waters C, Ford B, Frucht S, Fahn S, Marder K, Clark LN, Lee JH. Genome-wide association study identifies candidate genes for Parkinson's disease in an Ashkenazi Jewish population. BMC Med Genet 2011; 12: 104.
20. Liu Z, Lee J, Krummey S, Lu W, Cai H, Lenardo MJ. The kinase LRRK2 is a regulator of the transcription factor NFAT that modulates the severity of inflammatory bowel disease. Nat Immunol 2011; 12: 1063-1070.
21. Lohmann E, Periquet M, Bonifati V, Wood NW, De Michele G, Bonnet AM, Fraix V, Broussolle E, Horstink MW, Vidailhet M, Verpillat P, Gasser T, Nicholl D, Teive H, Raskin S, Rascol O, Destee A, Ruberg M, Gasparini F, Meco G, Agid Y, Durr A, Brice A. How much phenotypic variation can be attributed to parkin genotype? Ann Neurol 2003; 54: 176-185.
22. Lucking CB, Abbas N, Durr A, Bonifati V, Bonnet AM, de Broucker T, De Michele G, Wood NW, Agid Y, Brice A. Homozygous deletions in parkin gene in European and North African families with autosomal recessive juvenile parkinsonism. The European Consortium on Genetic Susceptibility in Parkinson's Disease and the French Parkinson's Disease Genetics Study Group. Lancet 1998; 352: 1355-1356.
23. Martinez HR, Gonzalez-Gonzalez H, Cantu-Martinez L, Rangel-Guerra R, Hernandez-Castillo CD, Vergara-Saavedra JJ, Ramos-Gonzalez MR, Cerda-Flores RM, Morales-Garza MA, Guerrero-Munoz MJ, Montes-de-Oca-Luna R, Saucedo-Cardenas O. PARKIN-coding polymorphisms are not associated with Parkinson's disease in a population from northeastern Mexico. Neurosci Lett 2010; 468: 264-266.
24. Moran JM, Castellanos-Pinedo F, Casado-Naranjo I, Duran-Herrera C, Ramirez-Moreno JM, Gomez M, Zurdo-Hernandez JM, Fuentes E, Ortiz-Ortiz MA, Moreno AD, Gonzalez-Polo RA, Niso-Santano M, Bravo-Sanpedro JM, Perez-Tur J, Ruiz-Mesa LM, Fuentes JM. Genetic screening for the LRRK2, G2019S and R1441 codon mutations in Parkinson's disease patients from Extremadura, Spain. Rev Neurol 2010; 50: 591-594.
25. Nuytemans K, Meeus B, Crosiers D, Brouwers N, Goossens D, Engelborghs S, Pals P, Pickut B, Van den Broeck M, Corsmit E, Cras P, De Deyn PP, Del-Favero J, Van Broeckhoven C, Theuns J. Relative contribution of simple mutations vs. copy number variations in five Parkinson disease genes in the Belgian population. Hum Mutat 2009; 30: 1054-1061.
26. Paisan-Ruiz C, Lang AE, Kawarai T, Sato C, Salehi-Rad S, Fisman GK, Al-Khairallah T, St George-Hyslop P, Singleton A, Rogaeva E. LRRK2 gene in Parkinson disease: mutation analysis and case control association study. Neurology 2005; 65: 696-700.
27. Poorkaj P, Nutt JG, James D, Gancher S, Bird TD, Steinbart E, Schellenberg GD, Payami H. Parkin mutation analysis in clinic patients with early-onset Parkinson [corrected] disease. Am J Med Genet A 2004; 129A: 44-50.
28. Ramirez-Jirano LJ, Ruiz-Sandoval JL, Jimenez-Gil FJ, Ramirez--Vega J, Vargas-Frutos E, Gallegos-Arreola MP. Frequency of the IVS4+66A-G polymorphism in the alpha-synuclein gene in patients with Parkinson's disease in north-western Mexico. Rev Neurol 2007; 44: 15-17.
29. Rubi-Castellanos R, Martinez-Cortes G, Munoz-Valle JF, Gonzalez-Martin A, Cerda-Flores RM, Anaya-Palafox M, Rangel--Villalobos H. Pre-Hispanic Mesoamerican demography approximates the present-day ancestry of Mestizos throughout the territory of Mexico. Am J Phys Anthropol 2009; 139: 284-294.
30. Santos-Garcia D, Abella-Corral J, Aneiros-Diaz A, Santos--Canelles H, Llaneza-Gonzalez MA, Macias-Arribi M. Pain in Parkinson's disease: prevalence, characteristics, associated factors, and relation with other non motor symptoms, quality of life, autonomy, and caregiver burden. Rev Neurol 2011; 52: 385-393.
31. Satake W, Nakabayashi Y, Mizuta I, Hirota Y, Ito C, Kubo M, Kawaguchi T, Tsunoda T, Watanabe M, Takeda A, Tomiyama H, Nakashima K, Hasegawa K, Obata F, Yoshikawa T, Kawakami H, Sakoda S, Yamamoto M, Hattori N, Murata M, Nakamura Y, Toda T. Genome-wide association study identifies common variants at four loci as genetic risk factors for Parkinson's disease. Nat Genet 2009; 41: 1303-1307.
32. Slager SL, Schaid DJ. Case-control studies of genetic markers: power and sample size approximations for Armitage's test for trend. Hum Hered 2001; 52: 149-153.
33. Songin M, Ossowska K, Kuter K, Strosznajder JB. Alteration of GSK-3beta in the hippocampus and other brain structures after chronic paraquat administration in rats. Folia Neuropathol 2011; 49: 319-327.
34. Tabakman R, Lecht S, Lazarovici P. Neuroprotection by monoamine oxidase B inhibitors: a therapeutic strategy for Parkinson's disease? Bioessays 2004; 26: 80-90.
35. Tan EK, Zhao Y, Skipper L, Tan MG, Di Fonzo A, Sun L, Fook-Chong S, Tang S, Chua E, Yuen Y, Tan L, Pavanni R, Wong MC, Kolatkar P, Lu CS, Bonifati V, Liu JJ. The LRRK2 Gly2385Arg variant is associated with Parkinson's disease: genetic and functional evidence. Hum Genet 2007; 120: 857-863.
36. Tomiyama H, Hatano T, Hattori N. Clinical molecular genetics for PARK8 (LRRK2)]. Brain Nerve 2007; 59: 839-850.
37. Torkaman-Boutorabi A, Ali Shahidi G, Choopani S, Reza Zarrindast M. Association of monoamine oxidase B and catechol-O-methyltransferase polymorphisms with sporadic Parkinson's disease in an Iranian population. Folia Neuropathol 2012; 50: 382-389.

38. van der Walt JM, Nicodemus KK, Martin ER, Scott WK, Nance MA, Watts RL, Hubble JP, Haines JL, Koller WC, Lyons K, Pahwa R, Stern MB, Colcher A, Hiner BC, Jankovic J, Ondo WG, Allen FH Jr, Goetz CG, Small GW, Mastaglia F, Stajich JM, McLaurin AC, Middleton LT, Scott BL, Schmechel DE, Pericak-Vance MA, Vance JM. Mitochondrial polymorphisms significantly reduce the risk of Parkinson disease. Am J Hum Genet 2003; 72: 804-811.
39. Wild P, Dikic I. Mitochondria get a Parkin' ticket. Nat Cell Biol 2010; 12: 104-106.
40. Yescas P, Lopez M, Monroy N, Boll MC, Rodriguez-Violante M, Rodriguez U, Ochoa A, Alonso ME. Low frequency of common LRRK2 mutations in Mexican patients with Parkinson's disease. Neurosci Lett 2010; 485: 79-82.
41. Yun H, Heo HY, Kim HH, DooKim N, Seol W. Identification of chemicals to inhibit the kinase activity of leucine-rich repeat kinase 2 (LRRK2), a Parkinson's disease-associated protein. Bioorg Med Chem Lett 2011; 21: 2953-2957.

Original article

Folia Neuropathologica

Mutations in the exon 7 of *Trp53* gene and the level of p53 protein in double transgenic mouse model of Alzheimer's disease

Jolanta Dorszewska[1], Anna Oczkowska[1], Monika Suwalska[1], Agata Rozycka[2], Jolanta Florczak-Wyspianska[3], Mateusz Dezor[1], Margarita Lianeri[2], Pawel P. Jagodzinski[2], Michal J. Kowalczyk[4], Michal Prendecki[1], Wojciech Kozubski[3]

[1]Laboratory of Neurobiology, Department of Neurology, Poznan University of Medical Sciences, [2]Department of Biochemistry and Molecular Biology, Poznan University of Medical Sciences, [3]Chair and Department of Neurology, Poznan University of Medical Sciences, [4]Department of Dermatology and Venereology, Poznan University of Medical Sciences, Poznan, Poland

Folia Neuropathol 2014; 52 (1): 30-40 DOI: 10.5114/fn.2014.41742

Abstract

Alzheimer's disease (AD) leads to generation of β-amyloid (Aβ) in the brain. Alzheimer's disease model PS/APP mice show a markedly accelerated accumulation of Aβ, which may lead to apoptosis induction e.g. in cells expressing wild-type p53. The TP53 gene is found to be the most frequently mutated gene in human tumour cells. There is accumulating evidence pointing out to the contribution of oxidative stress and chronic inflammation in both AD and cancer. The purpose of this study was to analyze exon 7 mutations of the murine Trp53 gene and Aβ/A4 and p53 protein levels in PS/APP and control mice.

The studies were performed on female double transgenic PS/APP mice and young adults (8-12 weeks old) and age-matched control mice. The Trp53 mutation analysis was carried out with the use of PCR and DNA sequencing. The Aβ/A4 and p53 levels were analyzed by Western blotting.

The frequency of mutations was almost quadrupled in PS/APP mice (44%), compared to controls (14%). PS/APP mice with the A929T and A857G mutations had a similar p53 level. In cerebral gray matter of PS/APP mice the level of p53 positive correlated with the level of Aβ protein (R_S = +0.700, $p < 0.05$). In younger control animals, the T854G mutation was related to p53 down-regulation, while in aging ones, G859A substitution was most likely associated with over-expression of p53. In silico protein analysis revealed a possibly substantial impact of all four mutations on p53 activity. Three mutations were in close proximity to zinc-coordinating cysteine residues.

It seems that in PS/APP mice missense Trp53 exon 7 mutations may be associated with the degenerative process by changes of p53 protein function.

Key words: *Trp53 mutations, p53, Aβ/A4 proteins, PS/APP mice.*

Introduction

Alzheimer's disease (AD) is characterized both clinically by the decline of cognitive functions, such as memory, and pathologically by the presence of numerous senile plaques (SPs) and neurofibrillary tangles (NFTs) [2,3,28,40,46,51]. Neurofibrillary tangles consist of hyperphosphorylated tau protein, whereas

Communicating author:

Jolanta Dorszewska, MD, PhD, Laboratory of Neurobiology, Department of Neurology, Poznan University of Medical Sciences, 49 Przybyszewskiego Str., 60-355 Poznan, Poland, phone: +48 61 869 14 39, fax: +48 61 869 16 97, e-mail: dorszewskaj@yahoo.com

SPs are composed of amyloid β-protein (Aβ). Transgenic PS/APP mice carrying mutant amyloid precursor protein (APP) and presenilin-1 (PS1) show a markedly accelerated accumulation of the 42 amino acid long form of Aβ (Aβ42) into visible deposits [26]. Transgenic PS/APP mice can therefore be used as experimental AD models. Ohyagi *et al.* [43] have shown that intracellular Aβ42 directly activates the *TP53* promoter, resulting in p53-dependent apoptosis. Accumulation of both Aβ42 and p53 was found in degenerating neurons in transgenic simulated AD mice and in humans with AD [32,43]. Aging subjects and AD patients show an increased level of a mutant-like conformation state of the p53 protein in peripheral blood cells [33]. Lanni *et al.* [33] have shown that a conformation change of p53 may lead to a partial loss of its activity and dysfunction of cell cycle proteins. Moreover, tumour suppressive p53 is critical in preventing cancer due to its ability to trigger proliferation arrest and cell death upon the occurrence of a variety of stressful conditions [15].

Human p53 contains 393 amino acids, encoded within the *TP53* gene, located at the 17p13.1 locus [7]. The *TP53* gene is found to be the most frequently mutated in human cancers with the occurrence level of about 50%. Deletions, rearrangements, and retroviral insertional inactivations of the *Trp53* analogue gene have been found in mice. Furthermore, $p53^{+/-}$ and $p53^{-/-}$ mice have been found to develop a broad spectrum of tumours, including lymphomas, osteosarcomas, fibrosarcomas, and medulloblastomas [22,29].

There is accumulating evidence pointing out to the contribution of oxidative stress and chronic inflammation in both AD and cancer [19]. Lanni *et al.* [34] suggested that p53 protein may play a significant role in the degenerative process and cancerogenesis. The study by Serrano *et al.* [50] has shown an elevated expression of a mutant p53 in elderly AD mice. Fiorini *et al.* [18] have shown that p53 defects may alter the expression of mitochondrial proteins in murine brain. On the other hand, transgenic mice with truncated p53 exhibit enhanced resistance to spontaneous tumours, but show reduced longevity [54].

The presence of mutations in exons 4 to 8 of the *TP53* gene has been found in a variety of neoplasms, including chronic lymphocytic leukaemia (17.3%) [10], colorectal cancer (42.3%) [57], lung cancer (39.4%) [9], bladder cancer (36.2%) [24], and head and neck carcinoma (22%) [38]. Furthermore, mutations in the *TP53* gene have been found more often in higher malignancy grade scores (5.9% in grade I compared to 53.9% in grade III) in bladder tumours, while the mutation rate was sex and age independent [24].

The purpose of the study was to analyze mutations in exon 7 of the murine *Trp53* gene and estimate the levels of Aβ/A4 and p53 proteins in about 7-month-old PS/APP mice. The results were compared to control mice of similar age and to a group of younger mice (8-12 weeks old).

Material and methods

Animals

The study involved nine about 7-month-old double transgenic PS/APP female mice (B6.Cg-Tg(APP695) 3DBo Tg(PSEN1dE9)S9DBo/J strain, Jackson Laboratory, USA). PS/APP mice deposit neurotoxic Aβ at 6-8 months of age. The control group consisted of fourteen females (C57BL/6J strain, Jackson Laboratory, USA), including six young adults (8-12 weeks old) and eight moderately old mice (7 months old).

Murine brains were isolated and divided into cerebral grey matter (GM), subcortical white matter (WM) and cerebellum (C).

This study was approved by local research ethics committees and the Polish Ministry of Environment.

DNA analysis

DNA for genotyping and racial purity checks was isolated from murine blood by standard methods. Racial purity was confirmed by PCR. Doubled 20 ng genomic DNA (gDNA) samples were amplified with the use of primers targeting exon 7 (NM_011640.3, 5'-GTGAGGTAGGGAGCGACTT-3'; 5'-CCTACCACGCGCGCCTTCCT-3'), yielding a 175 bp product. The PCR was carried out in 25 µl of the mixture containing: 13.7 µl of Mili-Q water, 2.5 µl of Laemmli Sample Buffer (Bio-Rad, USA), 2 µl of primers solution, 2 µl of dNTPs (Novazym, Poland), 0.8 µl of Allegro Taq polymerase (Novazym, Poland), and 2 µl of tested DNA. The annealing temperature has been optimized to 62°C, the PCR was carried out for 30 cycles. The quality of the product was estimated by standard gel electrophoresis.

Polymerase chain reaction (PCR) product was purified and sequenced according to the standard protocol in the external unit: the Laboratory of Molecular Biology Techniques at the Faculty of Biology, Adam Mickiewicz University, Poznan, Poland. The samples

were analyzed with sequencer 3130xl Genetic Analyzer (Applied Biosystems HITACHI, USA). All samples showing the presence of mutations were re-analyzed to confirm the presence of specific changes. The sequencing results were analyzed using the BioEdit software based on a reference sequence.

Western blotting

Dissected brain tissues were lysed and homogenized with the use of a radioimmunoprotein assay (RIPA) buffer (50 mM Tris-HCl, pH 7.2; 150 mM NaCl; 1% IGEPAL CA-630; 0.05% sodium dodecyl sulfate; 1% sodium deoxycholate), supplemented with a protease inhibitor cocktail for mammalian cell extracts (Sigma, USA) [16 : 1] and phenylmethylsulfonyl fluoride (Sigma, USA) in isopropanol (10 mg/100 µl). The samples were then centrifuged and the pellet was discarded [42].

Protein aliquots (40 µg/lane) were electrophoresed in 7.5% polyacrylamide gels and transferred onto nitrocellulose filters. The filters were exposed to anti-p53 goat polyclonal antibodies (Ab) (C-19, IgG, 200 µg/ml, Santa Cruz, USA) or to anti-Aβ/A4 murine monoclonal Ab (B-4, IgG_{2a}, 200 µg/ml, Santa Cruz, USA), at dilutions of 1 : 500.

Subsequently, the filters were incubated with secondary Abs, either murine anti-goat IgG-HRP (400 µg/ml, Santa Cruz, USA) or goat anti-mouse IgG-HRP (400 µg/ml, Santa Cruz, USA) respectively, at dilutions of 1 : 2000. Peroxidase Boehringer Mannheim blocking reagent (BMB) was added (BM Blue POD Substrate, Roche-Applied Science, Germany) to stain the immunoreactive bands. The Aβ/A4 and p-53 protein levels were analyzed on separate nitrocellulose filters. The band area was registered using a Quantity One densitometer (GC-710, Bio-Rad, USA). The quantification was performed by measuring the area of registered immunoreactive bands.

Subsequently, the stripping of Aβ/A4 and p-53 filters was performed with the stripping solution (62.5 mM TRIS/HCl with 2% SDS and 0.7% 2-merkaptoethanol in Mili-Q water) to remove the primary and the secondary Abs. Then, the filters were incubated with the anti-β-actin murine monoclonal Ab (C-4, IgG, 200 µg/ml, Santa Cruz, USA), at dilution of 1 : 500. Subsequently, the processes of incubation with secondary Ab and staining were performed. The uniform β-actin bands confirmed the validity of the method.

Statistical and *in silico* analysis

Differences in protein levels were assessed with the use of the nonparametric Kruskal-Wallis test for unlinked variables. Spearman's ranked correlation test was used for correlation analysis.

BioEdit, CLC Sequence Viewer, Protein Workshop [39], and IARC TP53 R15 Database [31,45] were used for *in silico* analysis.

Results

Trp53 exon 7 sequencing showed the presence of 4 different missense mutations in blood of the mice. One mutation was found in a 7-month-old control mouse, another in an 8-12-week-old one. Two mutations were found in PS/APP mice. Both were repeated twice, thus 44% of PS/APP mice were found to carry a missense mutation, compared to only 14% of the control mice (Table I, Figs. 1A-D).

The 8-12-week-old control mouse showed the presence of a T854G mutation, resulting in Tyr233Asp substitution (Fig. 1A). The 7-month-old control mouse showed a G859A mutation, causing Met234Ile substitution (Fig. 1B). The 7-month-old PS/APP mice showed the presence of two other mutations: A929T, resulting in Ser258Cys substitution; and A857G, replacing Met to Val also at position 234 (Figs. 1C, D).

Table I. Identified *Trp53* exon 7 mutation: a summary

Mice	DNA mutation	Amino acid substitution	Mutation frequency	
			n/N	*n/N/%*
Control 8-12 week old	T854G	Tyr233Asp	1/6	2/14/ **14%**
Control about 7 month old	G859A	Met234Ile	1/8	
PS/APP about 7 month old	A929T	Ser258Cys	2/9	4/9/ **44%**
	A857G	Met234Val	2/9	

n – number of animals with mutations, N – total number of animals in the group, % mice with mutations

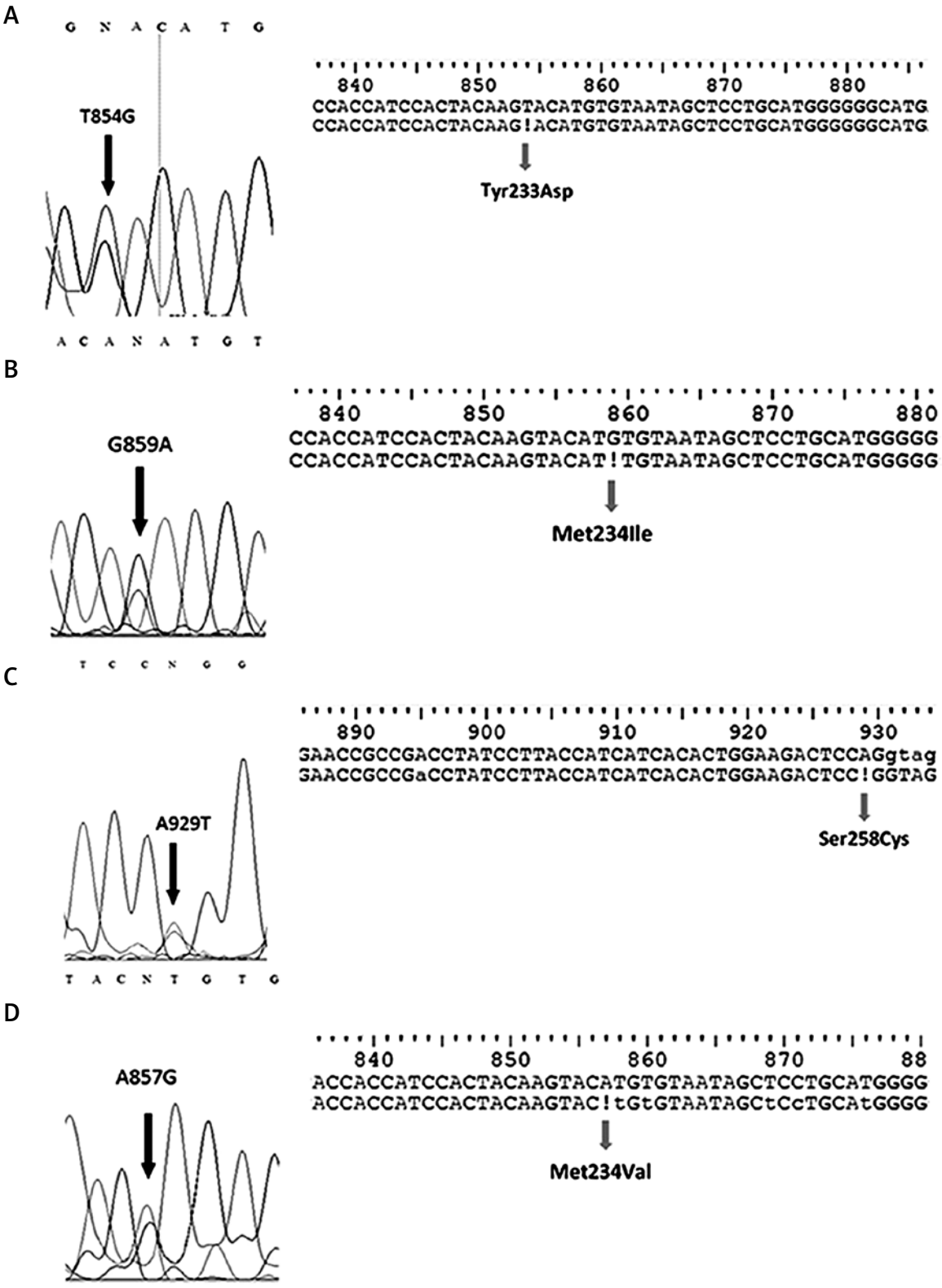

Fig. 1. Identified *Trp53* mutations. **(A)** T854G (8-12-week-old control mouse), **(B)** G859A (7-month-old control mouse), **(C)** A929T (about 7-month-old PS/APP mice), **(D)** A857G (about 7-month-old PS/APP mice).

However, analysis of p53, Aβ and Aβ/A4 proteins' level were carried out in tree structures of the mice brain: GM, WM and C (Tables II and III, Fig. 2). PS/APP mice showed tendency to a slightly lowered p53 level in GM and WM compared to controls of the same age and tendency to a greater increase in this protein level in these analyzed structures as compared to young controls (Table II). In PS/APP mice the increased level of p53 protein was shown also in C as compared to controls (Table II).

All mice stained positive for the Aβ/A4 protein precursor but only PS/APP mice were Aβ positive (Fig. 2). In GM of PS/APP mice, a positive correlation between the levels of p53 and Aβ proteins (Spearman's test, R_s = +0.7000, $p < 0.05$) was shown.

In GM of the 8-12-week-old control mouse with the *Trp53* T854G mutation we found a lower level of p53 as compared to non-mutant mice of the same age (Table III, Fig. 2). On the other hand, in the older control mouse with the *Trp53* G859A mutation, the p53 level in the GM was substantially elevated compared to respective non-mutant mice. The GM of PS/APP mice with the *Trp53* A929T and A857G mutations showed only moderate changes in p53 and Aβ levels.

The study also revealed varying band staining intensities for the Aβ/A4 precursor. In all PS/APP and control mice there were triple bands, which were more intensive in GM and/or WM than in C (Fig. 2).

Due to the overwhelming sequence similarity between human and murine p53, especially within the DNA-binding core domain, we tried to estimate the potential influence of these four mutations on the protein activity with the use of the human IARC TP53 database that compiles *TP53* variations identified in human populations and tumour samples [31,45]. Tyr233Asp, Met234Ile and Met234Val generated possibly non-functional or partially functional

Table II. P53 protein levels in cerebral structures of PS/APP and control mice

Cerebral structure	Controls 8-12 week old	Controls about 7 month old	PS/APP mice about 7 month old	*p* value
Grey matter of the cortex (GM)	27.4 ± 11.2	47.9 ± 23.7	44.5 ± 15.7	0.0804
White matter (WM)	29.6 ± 6.6	49.6 ± 21.2	44.3 ± 15.8	0.1342
Cerebellum (C)	32.5 ± 5.8	40.6 ± 16.9	45.2 ± 10.7	0.1182

Results presented as the mean percentage area of immunoreactive bands ± SD. Statistically insignificant differences in Kruskal-Wallis test ($p > 0.05$).
Spearman's test: Positive correlation found between p53 levels in GM and WM in 7-month-old control mice (R_s = +0.9762, $p < 0.001$).
Positive correlation found in GM between Aβ and p53 proteins level in PS/APP mice (R_s = +0.7000, $p < 0.05$).

Table III. β-amyloid and p53 protein levels in cerebral structures of PS/APP and control mice

	About 7 month old PS/APP mice								
	Trp53 A929T (Ser258Cys)			*Trp53* A857G (Met234Val)			No detected mutations in *Trp53*		
	GM	WM	C	GM	WB	C	GM	WM	C
Aβ	[43.2-74.1]	[64.1-64.3]	[44.6-57.9]	[64.1-67.1]	[48.6-73.4]	[43.0-44.6]	[47.2-82.8]	[53.0-72.2]	[21.4-73.7]
p53	[32.7-43.8]	[24.1-59.0]	[45.8-46.1]	[35.0-45.9]	[27.9-41.7]	[36.0-45.4]	[25.0-65.1]	[26.3-67.7]	[27.8-68.0]
	8-12 week old control mice								
	Trp53 T854G (Tyr233Asp)			No detected mutations in *Trp53*					
	GM	WM	C	GM	WM	C			
p53	[10.7]	[26.5]	[38.9]	[20.3-40.5]	[19.1-38.2]	[24.6-36.0]			
	About 7 month old control mice								
	Trp53 G859A (Met234Ile)			No detected mutations in *Trp53*					
	GM	WM	C	GM	WM	C			
p53	[97.3]	[66.7]	[34.6]	[23.9-60.5]	[21.5-83.4]	[24.2-75.1]			

Results presented as the mean percentage area of immunoreactive bands.
The range between minimum and maximum values or a single value is presented.

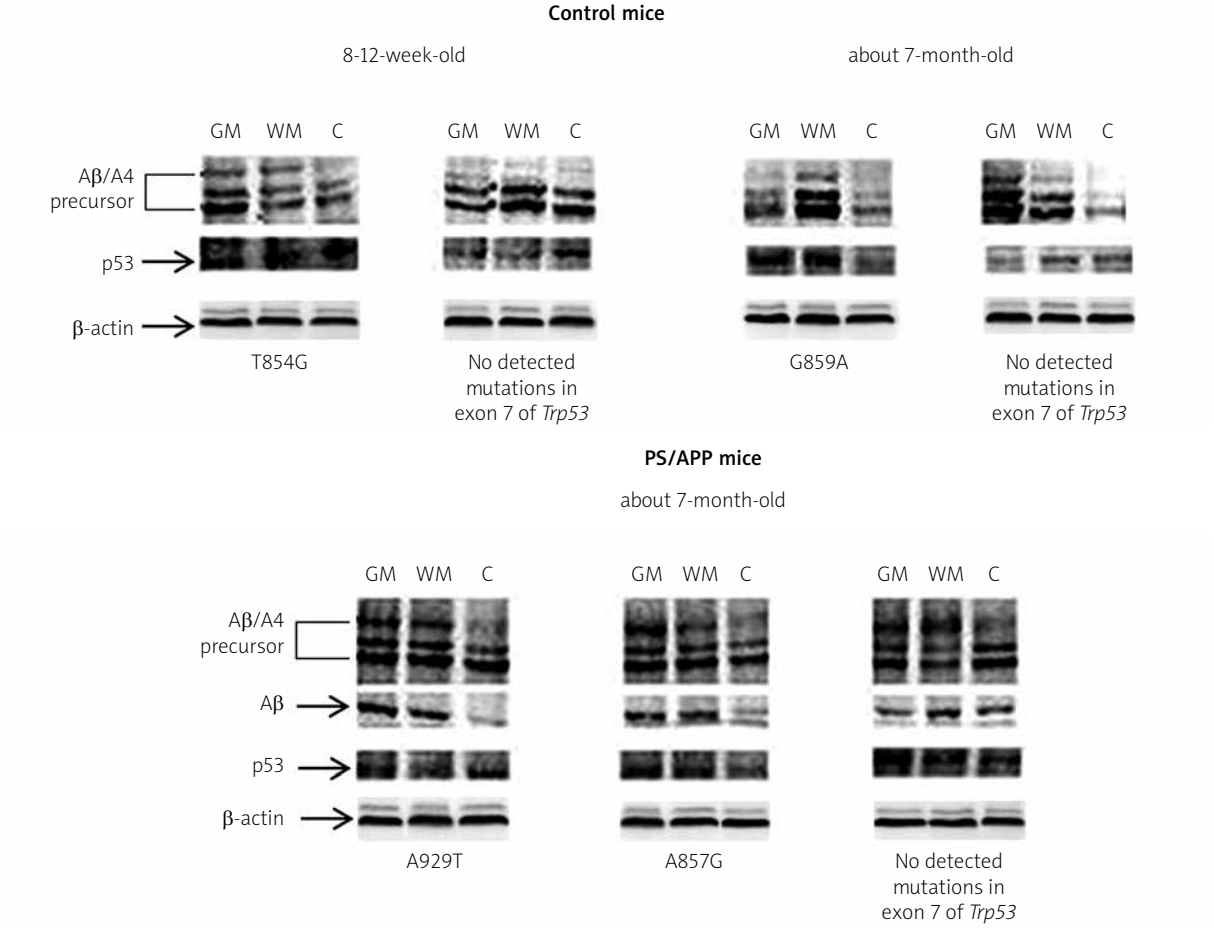

GM – grey matter of the cortex, WM – white matter, C – cerebellum, Aβ – β-amyloid, Aβ/A4 – amyloid A4 precursor

Fig. 2. Western blot analysis of p53, Aβ and Aβ/A4 protein precursor in three cerebral structures of experimental mice.

proteins. Met234Val generated a possible new donor splice site, while Ser258Cys might abrogate the exon 7-8 splice site (Table IV, Figs. 3 and 4).

Discussion

Neuronal dysfunction in AD is correlated with the deposition of fibrillar aggregates of Aβ in brain parenchyma and blood vessel walls [36,46]. Double transgenic PS/APP mice show a rapid accumulation of both fibrillar and non-fibrillar (diffuse) forms of Aβ from 12 weeks of age onwards [16,26]. In PS/APP mice, the number of fibrillar Aβ deposits increases with age, whereas the changes are less marked in terms of the deposit numbers in the diffuse forms. It has been shown that in elderly mice, Aβ is deposited in the cortex, hippocampus, thalamus and amygdala, but is additionally deposited in cerebellar cortex and WM of AD patients [16,25]. Our study performed on PS/APP mice, along with the studies of Cummings *et al.* [13] in dogs and Feng *et al.* [17] in rats, demonstrates that Aβ is deposited in the GM of the cortex but also the in C and WM. Due to its deposition in the C, Aβ may lead to learning and memory impairments [4]. The study in aged canines has shown that Aβ deposition is strongly associated with deficits of discrimination, reversal and spatial learning [13]. Cummings *et al.* [13] suggest that Aβ deposition may be a contributing factor to age-related cognitive dysfunction prior to the onset of NFTs formation.

The neurotoxic 42-43 amino acid long Aβ peptide is a breakdown product of a much larger protein, the Aβ/A4 protein precursor – APP [30]. It is known that the 4-4.5 kDa Aβ/A4 polypeptide is the major protein component of SPs [36]. The formation of Aβ/A4-containing plaque-like structures has been

Table IV. Analysis of corresponding mutations in the human IARC TP53 database

Murine mutation found	*Trp53* Tyr233Asp	*Trp53* Met234Ile	*Trp53* Met234Val	*Trp53* Ser258Cys
Corresponding human mutation	*TP53* Tyr236Asp	*TP53* Met237Ile	*TP53* Met237Val	*TP53* Ser261Cys
Mutation type	missense	missense in DNA-binding loops	missense in DNA-binding loops	missense
Assessment of transactivation capacities in yeast assays by Kato *et al.* [31]	non-functional	non-functional	partially functional	functional
Predicted effect on protein function and structure	deleterious, non-functional	deleterious, non-functional	deleterious, non-functional	neutral, functional
Predicted effect on p53 protein isoforms	all altered	all altered	all altered	all altered
Dominant negative activity	yes	yes	NA	NA
Reported mutations in human tumors	9	185	12	1
Reported germline mutations	0	1	0	0
Predicted effect on splicing	no significant change	no significant change	acceptor: no significant change donor: new site	sites broken or no significant change

NA – not applicable

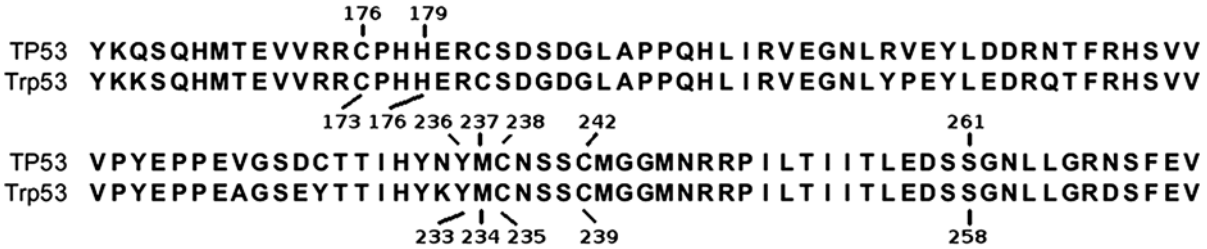

TP53 zinc-coordinating residues: Cys176, His179, Cys238, Cys242.
Trp53 zinc-coordinating residues: Cys173, His176, Cys235, Cys239.
Trp53 identified mutated residues: Tyr233, Met234, Ser258.

Fig. 3. Human and murine p53 sequence alignment. Mutant and zinc-coordinating residues are shown.

found in GM and WM [5]. It has also been shown that Aβ/A4-related peptides may occur in both AD and normal subjects, while their production is increased in familial AD, where the disease develops much earlier compared to sporadic AD [12,36]. It seems that pathological Aβ/A4 with numerous extracellular Aβ deposits, together with different levels of its precursor in GM and WM, may be included in the pathogenesis of AD [20,30]. Arendt *et al.* [5] have shown that Aβ/A4 deposition is a result of a chronic disturbance of phosphorylation balance, which may lead to a reduction of both GM and WM in the AD brain. Moreover, it has been indicated that intraneuronal Aβ may be a cause of mitochondrial [8], lysosomal [23,52] and synaptic [53] dysfunctions possibly leading to p53-dependent apoptosis [43] and reverse [18].

AD patients, p53-dependent apoptosis leads directly to neuronal loss through Aβ42 binding and activation of the p53 promoter. The accumulation of both Aβ42 and p53 is manifested in some degenerating-shape neurons in both transgenic mice and AD. Our study demonstrated the presence of Aβ in PS/APP mice, along with a high p53 level compared to younger mice, which may indicate a possible induction of apoptosis. It has been shown that p53-dependent neuronal apoptosis may also result from a decreased activity of anti-apoptotic PS1 caused by p53 protein-protein interactions or by pro-apoptotic presenilin-2 (PS2), which down-regulates PS1

expression [1,44]. It seems that the elevated p53 level influences the PS1-mediated abnormalities of intracellular calcium levels [14]. As a result, Aβ, PS1, PS2 and p53 may all increase the risk of p53-dependent apoptosis in AD.

P53 is a key regulator of multiple cellular processes, and depending on the cell type it is activated by different stressors to induce apoptosis, autophagic cell death, but is also responsible for both, reversible and irreversible cell cycle arrest, or senescence [49]. The induction of cellular aging by elevated p53 levels in response to stress is designed to prevent proliferation of damaged cells.

Two main groups of signals change p53 activation. These include DNA damage and oncogenic stress as result from cancer and/or aging and may be an effect of p53 mutation [34]. Experimental PS/APP mice have shown 44% of *Trp53* gene mutations.

Loss of heterozygosity and *TP53* mutations are commonly associated with a variety of tumours in humans and in experimental animals [6,22,27]. Mutations abrogating p53 function and allelic loss of its locus were among the first genetic lesions identified in glioblastoma multiforme [41]. *TP53* mutations are also present in all grades of human astrocytoma [55] and in the murine model of astrocytoma [48].

A *TP53* exon 7 missense mutation has been found in an adrenocortical carcinoma patient. Although the phenotype was not clinically distinct, authors suspect a hereditary background due to an early onset of the disease [56]. In this study we showed two missense mutations in PS/APP mice: A929T (Ser258Cys) and A857G (Met234Val), possibly altering p53 function as both are located within the central DNA-binding core domain (DBD). The DBD is responsible for binding LIM domain only protein 3 (LMO3), which is a confirmed human neuroblastoma oncogene [35]. Reverse Val→Met substitutions at codons 216 and 272 have also been demonstrated in brain carcinoma, and this mutation is particularly important in mediating the normal function of p53 [41]. Mineta *et al.* [38] have demonstrated a *TP53* exon 7 Ser241Cys substitution in head and neck tumours. Moreover, patients with p53 missense or nonsense mutations survived an average of only 12.5 months after diagnosis, while non-mutated subjects survived more than 160 months after diagnosis, and 43% of these examined tumours presented a low p53 level and 32% had increased p53 levels. It seems that also mutant *Trp53* tends to impact the p53 expression level in all analyzed structures of experimental PS/APP mice.

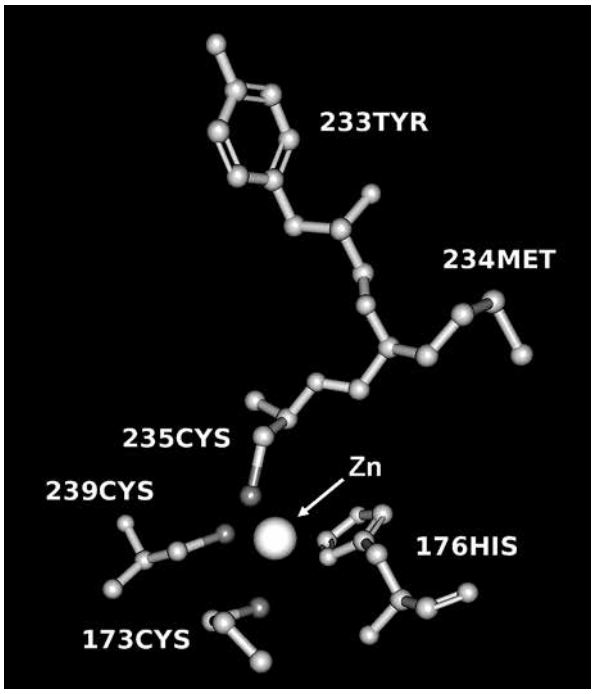

Zinc-coordination: Cys173, His176, Cys235, Cys239. Identified mutated residues: Tyr233, Met234. Zinc (Zn) atom is indicated by an arrow. Not all atoms are shown for clarity of image.

Fig. 4. Coordination of zinc in p53. Based on 1HU8 crystal structure by Zhao *et al.* [58].

Our study also demonstrated a missense mutation (T854G) in a young control mouse, resulting in a Tyr233Asp substitution, along with a tendency to a low p53 expression in the GM. Reilly *et al.* [48] have shown that the *TP53* gene is often mutated in a subset of astrocytomas that develop at a young age and progress slowly to glioblastoma [55]. Nonetheless, one of our 7-month-old control mice showed a G859A (Met244Ile) missense mutation, which seems to be related with an increased p53 level in GM. Overexpression of p53 in the process of aging has been shown by Tyner *et al.* [54], Garcia-Cao *et al.* [21] and Mendrysa *et al.* [37], and is accompanied by decreased longevity, osteoporosis, generalized organ atrophy, and diminished stress tolerance.

All of the aforementioned mutations, apart from the Tyr233Asp substitution, involve either removal or introduction of sulphur atoms into p53. Three of our mutations (Tyr233Asp, Met234Ile, Met234Val), along with the mutation found by Mineta *et al.* [55] (Ser241Cys in *TP53*, corresponding to Ser238Cys in *Trp53*), are located in or neighbour loop 3 – a region rich in

methionine and cysteine residues. It has been found that two of these residues, i.e. Cys235 and Cys239, along with Cys173 and His176, coordinate a zinc atom forming a structure crucial for DNA binding [11,47]. The Ser238Cys substitution [55] is therefore located one residue upstream of a zinc-coordinating cysteine. The identified Met234Ile and Met234Val substitutions are also located one residue upstream of such a cysteine, while the Tyr233Asp is just two residues upstream [58]. Although the Ser258Cys substitution is located downstream of the zinc-coordinating domain, not only does it disturb a double serine motif, but more importantly it spans across the exon 7-8 junction. The corresponding A929T substitution decreases the mathematical score of the 5' splice site, but its impact on the site stability remains undetermined. Although both mutations found in PS/APP mice could possibly inactivate p53, their effect on p53 and Aβ levels is not so apparent, most likely due to heterozygosity and the fact that a faulty p53 could still bind its antibody. Similarly, the reason that the Met234Ile and Tyr233Asp substitutions would impact p53 levels in the GM of control mice remains unsolved.

In conclusion, the transgenic PS/APP mice, which simulate AD, carry a missense *Trp53* exon 7 mutations about four times more frequently than controls. In PS/APP mice, the A929T (Ser258Cys) and A857G (Met234Val) mutations may alter p53 expression in a similar manner. However, in the GM of the control younger mouse, the *Trp53* T854G (Tyr233Asp) mutation may be connected with a decreased level of p53, while in the same structure of the brain of the control 7-month-old mouse, the *Trp53* G859A (Met234Ile) mutation may be associated with increased the p53 level as compared to non-mutated mice of the same age. Moreover, the GM of PS/APP mice has shown a positive correlation between levels of p53 and Aβ. *Trp53* mutations found in this study may impact the murine p53 function as shown by the *in silico* analysis and possibly also be associated with the degenerative process.

References

1. Alves da Costa C, Paitel E, Mattson MP, Amson R, Telerman A, Ancolio K, Checler F. Wild-type and mutated presenilins 2 trigger p53-dependent apoptosis and down-regulate presenilin 1 expression in HEK293 human cells and in murine neurons. Proc Natl Acad Sci U S A 2002; 99: 4043-4048.
2. Armstrong RA. On the 'classification' of neurodegenerative disorders: discrete entities, overlap or continuum? Folia Neuropathol 2012; 50: 201-218.
3. Armstrong RA. What causes Alzheimer's disease? Folia Neuropathol 2013; 51: 169-188.
4. Atkins ER, Panegyres PK. The clinical utility of gene testing for Alzheimer's disease. Neurol Int 2011; 3: e1.
5. Arendt T, Holzer M, Fruth R, Brückner MK, Gärtner U. Paired helical filament-like phosphorylation of tau, deposition of beta/A4-amyloid and memory impairment in rat induced by chronic inhibition of phosphatase 1 and 2A. Neuroscience 1995; 69: 691-698.
6. Bougeard G, Brugieres L, Chompret A, Gesta P, Charbonnier F, Valent A, Martin C, Raux G, Feunteun J, Bressac-de Paillerets B, Frébourg T. Screening for TP53 rearrangements in families with the Li-Fraumeni syndrome reveals a complete deletion of the TP53 gene. Oncogene 2003; 22: 840-846.
7. Boyd JA, Barrett JC. Tumor suppressor genes: possible functions in the negative regulation of cell proliferation. Mol Carcinog 1990; 3: 325-329.
8. Busciglio J, Pelsman A, Wong C, Pigino G, Yuan M, Mori H, Yankner BA. Altered metabolism of the amyloid beta precursor protein is associated with mitochondrial dysfunction in Down's syndrome. Neuron 2002; 33: 677-688.
9. Chen Z, An S, Xie Z, Yan H, Chen J, Su J, Zhang X, Niu F, Guo W, Wu Y. High resolution melting analysis for detecting p53 gene mutations in patients with non-small cell lung cancer. Zhongguo Fei Ai Za Zhi 2011; 14: 767-773.
10. Chiaretti S, Tavolaro S, Marinelli M, Messina M, Del Giudice I, Mauro FR, Santangelo S, Piciocchi A, Peragine N, Truong S, Patten N, Ghia EM, Torrente I, De Propris MS, Nanni M, Lawrence J, Guarini A, Foà R. Evaluation of TP53 mutations with the AmpliChip p53 research test in chronic lymphocytic leukemia: correlation with clinical outcome and gene expression profiling. Genes Chromosomes Cancer 2011; 50: 263-274.
11. Cho Y, Gorina S, Jeffrey PD, Pavletich NP. Crystal structure of a p53 tumor suppressor-DNA complex: understanding tumorigenic mutations. Science 1994; 265: 346-355.
12. Citron M, Oltersdorf T, Haass C, McConlogue L, Hung AY, Seubert P, Vigo-Pelfrey C, Lieberburg I, Selkoe DJ. Mutation of the beta-amyloid precursor protein in familial Alzheimer's disease increases beta-protein production. Nature 1992; 360: 672-674.
13. Cummings BJ, Head E, Afagh AJ, Milgram NW, Cotman CW. Beta-amyloid accumulation correlates with cognitive dysfunction in the aged canine. Neurobiol Learn Mem 1996; 66: 11-23.
14. Das HK, Tchedre K, Mueller B. Repression of transcription of presenilin-1 inhibits γ-secretase independent ER Ca(2+) leak that is impaired by FAD mutations. J Neurochem 2012; 122: 487-500.
15. Dorszewska J. Cell biology of normal brain aging: synaptic plasticity – cell death. Aging Clin Exp Res 2013; 25: 25-34.
16. Dyrks T, Dyrks E, Monning U, Urmoneit B, Turner J, Beyreuther K. Generation of beta A4 from the amyloid protein precursor and fragments thereof. FEBS Lett 1993; 335: 89-93.
17. Feng C, Zhang C, Shao X, Liu Q, Qian Y, Feng L, Chen J, Zha Y, Zhang Q, Jiang X. Enhancement of nose-to-brain delivery of basic fibroblast growth factor for improving rat memory impairments induced by co-injection of β-amyloid and ibotenic acid into the bilateral hippocampus. Int J Pharm 2012; 423: 226-234.

18. Fiorini A, Sultana R, Barone E, Cenini G, Perluigi M, Mancuso C, Cai J, Klein JB, St Clair D, Butterfield DA. Lack of p53 affects the expression of several brain mitochondrial proteins: insights from proteomics into important pathways regulated by p53. PLoS One 2012; 7: e49846.
19. Frain L, Driver J, Gaziano JM, Lu KP, Kowall N, Gagnon D, Cho K, Betensky R, Swanson D. A reduced risk of Alzheimer Disease is associated with the majority of cancers in a National cohort of Veterans. Alzheimer's Association International Conference, Boston 2013; P3-175.
20. Games D, Adams D, Alessandrini R, Barbour R, Berthelette P, Blackwell C, Carr T, Clemens J, Donaldson T, Gillespie F. Alzheimer-type neuropathology in transgenic mice overexpressing V717F beta-amyloid precursor protein. Nature 1995; 373: 523-527.
21. Garcia-Cao I, Garcia-Cao M, Martin-Caballero J, Criado LM, Klatt P, Flores JM, Weill JC, Blasco MA, Serrano M. "Super p53" mice exhibit enhanced DNA damage response, are tumor resistant and age normally. EMBO J 2002; 21: 6225-6235.
22. Gavino C, Richard S. Loss of p53 in quaking viable mice leads to Purkinje cell defects and reduced survival. Sci Rep 2011; 1: 84.
23. Glabe C. Intracellular mechanisms of amyloid accumulation and pathogenesis in Alzheimer's disease. J Mol Neurosci 2001; 17: 137-145.
24. Harano H, Wang C, Gao J, Uchida T. p53 tumor suppressor gene mutation and prognosis in 105 cases of bladder cancer-the relationship between mutation of the p53 gene with clinicopathological features and smoking. Nihon Hinyokika Gakkai Zasshi 1999; 90: 487-495.
25. Hirai S, Okamoto K. Amyloid beta/A4 peptide associated with Alzheimer's disease and cerebral amyloid angiopathy. Intern Med 1993; 32: 923-925.
26. Holcomb L, Gordon MN, McGowan E, Yu X, Benkovic S, Jantzen P, Wright K, Saad I, Mueller R, Morgan D, Sanders S, Zehr C, O'Campo K, Hardy J, Prada CM, Eckman C, Younkin S, Hsiao K, Duff K. Accelerated Alzheimer-type phenotype in transgenic mice carrying both mutant amyloid precursor protein and presenilin 1 transgenes. Nat Med 1998; 4: 97-100.
27. Hollstein M, Sidransky D, Vogelstein B, Harris CC. p53 mutations in human cancers. Science 1991; 253: 49-53.
28. Hope J, Kirby L. Amyloid and prions: some biochemical investigations of cerebral amyloidosis in mice. Folia Neuropathol 2012; 50: 13-19.
29. Jacks T, Remington L, Williams BO, Schmitt EM, Halachmi S, Bronson RT, Weinberg RA. Tumor spectrum analysis in p53-mutant mice. Curr Biol 1994; 4: 1-7.
30. Kang J, Lemaire HG, Unterbeck A, Salbaum JM, Masters CL, Grzeschik KH, Multhaup G, Beyreuther K, Müller-Hill B. The precursor of Alzheimer's disease amyloid A4 protein resembles a cell-surface receptor. Nature 1987; 325: 733-736.
31. Kato S, Han SY, Liu W, Otsuka K, Shibata H, Kanamaru R, Ishioka C. Understanding the function-structure and function-mutation relationships of p53 tumor suppressor protein by high-resolution missense mutation analysis. Proc Natl Acad Sci U S A 2003; 100: 8424-8429.
32. LaFerla FM, Hall CK, Ngo L, Jay G. Extracellular deposition of beta-amyloid upon p53-dependent neuronal cell death in transgenic mice. J Clin Invest 1996; 98: 1626-1632.
33. Lanni C, Racchi M, Uberti D, Mazzini G, Stanga S, Sinforiani E, Memo M, Govoni S. Pharmacogenetics and pharmagenomics, trends in normal and pathological aging studies: focus on p53. Curr Pharm Des 2008; 14: 2665-2671.
34. Lanni C, Racchi M, Memo M, Govoni S, Uberti D. p53 at the crossroads between cancer and neurodegeneration. Free Radic Biol Med 2012; 52: 1727-1733.
35. Larsen S, Yokochi T, Isogai E, Nakamura Y, Ozaki T, Nakagawara A. LMO3 interacts with p53 and inhibits its transcriptional activity. Biochem Biophys Res Commun 2010; 392: 252-257.
36. Matsuoka Y, Picciano M, Malester B, LaFrancois J, Zehr C, Daeschner JM, Olschowka JA, Fonseca MI, O'Banion MK, Tenner AJ, Lemere CA, Duff K. Inflammatory responses to amyloidosis in a transgenic mouse model of Alzheimer's disease. Am J Pathol 2001; 158: 1345-1354.
37. Mendrysa SM, O'Leary KA, McElwee MK, Michalowski J, Eisenman RN, Powell DA, Perry ME. Tumor suppression and normal aging in mice with constitutively high p53 activity. Genes Dev 2006; 20: 16-21.
38. Mineta H, Borg A, Dictor M, Wahlberg P, Akervall J, Wennerberg J. p53 mutation, but not p53 overexpression, correlates with survival in head and neck squamous cell carcinoma. Br J Cancer 1998; 78: 1084-1090.
39. Moreland JL, Gramada A, Buzko OV, Zhang Q, Bourne PE. The Molecular Biology Toolkit (MBT): a modular platform for developing molecular visualization applications. BMC Bioinformatics 2005; 6: 21.
40. Neve RL, Robakis NK. Alzheimer's disease: a re-examination of the amyloid hypothesis. Trends Neurosci 1998; 21: 15-19.
41. Nigro JM, Baker SJ, Preisinger AC, Jessup JM, Hostetter R, Cleary K, Bigner SH, Davidson N, Baylin S, Devilee P. Mutations in the p53 gene occur in diverse human tumour types. Nature 1989; 342: 705-708.
42. Ohnishi T, Inoue N, Matsumoto H, Omatsu T, Ohira Y, Nagaoka S. Cellular content of p53 protein in rat skin after exposure to the space environment. J Appl Physiol 1996; 81: 183-185.
43. Ohyagi Y, Asahara H, Chui DH, Tsuruta Y, Sakae N, Miyoshi K, Yamada T, Kikuchi H, Taniwaki T, Murai H, Ikezoe K, Furuya H, Kawarabayashi T, Shoji M, Checler F, Iwaki T, Makifuchi TT, Takeda K, Kira J, Tabira T. Intracellular Abeta42 activates p53 promoter: a pathway to neurodegeneration in Alzheimer's disease. FASEB J 2005; 19: 255-257.
44. Pastorcic M, Das HK. Regulation of transcription of the human presenilin-1 gene by ets transcription factors and the p53 protooncogene. J Biol Chem 2000; 275: 34938-34945.
45. Petitjean A, Mathe E, Kato S, Ishioka C, Tavtigian SV, Hainaut P, Olivier M. Impact of mutant p53 functional properties on TP53 mutation patterns and tumor phenotype: lessons from recent developments in the IARC TP53 database. Hum Mutat 2007; 28: 622-629.
46. Pluta R, Kocki J, Maciejewski R, Ułamek-Kozioł M, Jabłoński M, Bogucka-Kocka A, Czuczwar SJ. Ischemia signalling to Alzheimer-related genes. Folia Neuropathol 2012; 50: 322-329.
47. Rainwater R, Parks D, Anderson ME, Tegtmeyer P, Mann K. Role of cysteine residues in regulation of p53 function. Mol Cell Biol 1995; 15: 3892-3903.

48. Reilly KM, Loisel DA, Bronson RT, McLaughlin ME, Jacks T. Nf1;Trp53 mutant mice develop glioblastoma with evidence of strain-specific effects. Nat Genet 2000; 26: 109-113.
49. Sakamoto Y, Kato S, Takahashi M, Okada Y, Yasuda K, Watanabe G, Imai H, Sato A, Ishioka C. Contribution of autophagic cell death to p53-dependent cell death in human glioblastoma cell line SF126. Cancer Sci 2011; 102: 799-807.
50. Serrano J, Fernández AP, Martínez-Murillo R, Martínez A. High sensitivity to carcinogens in the brain of a mouse model of Alzheimer's disease. Oncogene 2010; 29: 2165-2171.
51. Šerý O, Povová J, Míšek I, Pešák L, Janout V. Molecular mechanisms of neuropathological changes in Alzheimer's disease: a review. Folia Neuropathol 2013; 51: 1-9.
52. Shie FS, LeBoeuf RC, Jin LW. Early intraneuronal Abeta deposition in the hippocampus of APP transgenic mice. Neuroreport 2003; 14: 123-129.
53. Takahashi RH, Milner TA, Li F, Nam EE, Edgar MA, Yamaguchi H, Beal MF, Xu H, Greengard P, Gouras GK. Intraneuronal Alzheimer abeta42 accumulates in multivesicular bodies and is associated with synaptic pathology. Am J Pathol 2002; 161: 1869-1879.
54. Tyner SD, Venkatachalam S, Choi J, Jones S, Ghebranious N, Igelmann H, Lu X, Soron G, Cooper B, Brayton C, Park SH, Thompson T, Karsenty G, Bradley A, Donehower LA. p53 mutant mice that display early ageing-associated phenotypes. Nature 2002; 415: 45-53.
55. Watanabe K, Sato K, Biernat W, Tachibana O, von Ammon K, Ogata N, Yonekawa Y, Kleihues P, Ohgaki H. Incidence and timing of p53 mutations during astrocytoma progression in patients with multiple biopsies. Clin Cancer Res 1997; 3: 523-530.
56. Waldmann J, Patsalis N, Fendrich V, Langer P, Saeger W, Chaloupka B, Ramaswamy A, Fassnacht M, Bartsch DK, Slater EP. Clinical impact of TP53 alterations in adrenocortical carcinomas. Langenbecks Arch Surg 2012; 397: 209-216.
57. Xu XM, Qian JC, Cai Z, Tang T, Wang P, Zhang KH, Deng ZL, Cai JP. DNA alterations of microsatellite DNA, p53, APC and K-ras in Chinese colorectal cancer patients. Eur J Clin Invest 2012; 42: 751-759.
58. Zhao K, Chai X, Johnston K, Clements A, Marmorstein R. Crystal structure of the mouse p53 core DNA-binding domain at 2.7 A resolution. J Biol Chem 2001; 276: 12120-12127.

Original article

Folia Neuropathologica

Nigrostriatal pathway degeneration in rats after intraperitoneal administration of proteasome inhibitor MG-132

Sławomir Wójcik, Jan Henryk Spodnik, Edyta Spodnik, Jerzy Dziewiątkowski, Janusz Moryś

Department of Anatomy and Neurobiology, Medical University of Gdańsk, Gdańsk, Poland

Folia Neuropathol 2014; 52 (1): 41-55 DOI: 10.5114/fn.2014.41743

Abstract

The proteins' ubiquitination and their further degradation by proteasomes are crucial for cell cycle regulation, transcription and DNA replication, inflammatory response, and apoptosis. Proteasome inhibitors have recently become considered as a promising method in cancer and inflammatory disease therapy. In this study, utilizing the rat model, we try to establish the influence of proteasome inhibitor MG-132: (1) on the basis of spontaneous and evoked locomotor activity and (2) on the condition of nigrostriatal projections eight weeks after MG-132 intraperitoneal administration. We also discuss the current status of knowledge about intraperitoneal administration of MG-132, a laboratory method that is being used more and more. Our results revealed a lack of motor abnormalities, but significant loss (20%) of substantia nigra pars compacta dopaminergic neurons after systemic MG-132 administration. This loss was accompanied by a corresponding decrease (8%) of density of dopaminergic terminals in dorsolateral striatum. Moreover, evidence of very limited but ongoing fibre degeneration within the dorsal striatum suggests that MG-132 severely disturbed the nigrostriatal pathway.

In summary, intraperitoneal application of proteasome inhibitor MG-132, despite the encouraging results of experimental treatment and prevention of many pathological processes, should be used with caution because of the potential adverse effects on the structure of the central nervous system, especially elements of the nigrostriatal pathway.

Key words: *Mg-132, proteasome inhibition, rat, striatum, substantia nigra, tyrosine hydroxylase.*

Introduction

The ubiquitin-proteasome system is the main pathway of intracellular protein degradation within eukaryotic cells. The proteins' ubiquitination and their further degradation by proteasomes are crucial for cell cycle regulation, transcription and DNA replication, inflammatory response, and apoptosis. The proteasome inhibition leads to intracellular accumulation of misfolded or unfolded proteins and, in consequence, activation of numerous cell signalling pathways resulting in heat-shock proteins expression increase, nuclear factor-κB (NFκB) and antiapoptotic cytokines decrease, mitochondrial protein expulsion into the cytoplasm, and caspase cascade activation [10,48]. Fast proliferating cells are more susceptible to ubiquitin-proteasome system disturbances. This is the reason why a new group of chemicals, called proteasome inhibitors, has recently been considered as a promising method in cancer and inflammatory disease therapy.

Communicating author:

Slawomir Wojcik, MD, PhD, Department of Anatomy and Neurobiology, Medical University of Gdańsk, 1 Dębinki Street, 80-210 Gdańsk, Poland, phone: +48 58 349 14 02, fax: +48 58 349 14 21, e-mail: swoj@gumed.edu.pl

MG-132 (Cbz-Leu-Leu-Leu-aldehyde, Z-LLL-H) is the most common and so far the most widely tested and best representative of both the peptide aldehydes and the entire group of proteasome inhibitors. It is a reversible inhibitor that gives a very quick response. MG-132 has a high degree of selective inhibition of proteasome chymotrypsin-like activity. A ten-fold higher concentration of the MG-132 inhibitor is needed to inhibit other enzymes (calpain and cathepsin), which indicates a specific inhibition of the proteasome. MG-132 properties, such as antiproliferative, anti-inflammatory, and induction of heat shock proteins, also make it the most widely used in the clinical impact of proteasome inhibition on the course of many processes at the cellular and tissue level, as well as having a link with studies of new proteasome inhibitors [15]. Literature reports indicate that under experimental conditions, intraperitoneal administration of MG-132 may play a beneficial role in the prevention and therapy of inflammatory diseases such as acute pancreatitis [9,24,50], inflammatory bowel disease [19], severe acute respiratory syndrome [28], and intestinal damage caused by ischaemia/reperfusion [1,21], and also partially prevents muscle atrophy associated with disuse [20]. However, data obtained on animal models are very controversial. Some authors [31,33] indicate that systematically administered proteasome inhibitors may penetrate the intact blood-brain barrier and cause pathological changes in the central nervous system (CNS), leading also to locomotor dysfunction and behavioural disturbances. It has also been reported that MG-132-induced hemiparkinsonism in the rat model mimics the daytime somnolence and sleep disturbance during the night observed in patients with the Parkinson's disease [26]. To date, there have been no reports describing the long-term effects of MG-132 on the CNS structures after its administration by intraperitoneal route. In this study utilizing the rat model we try to establish the influence of MG-132: (1) on the basis of spontaneous and evoked locomotor activity and (2) on the condition of nigrostriatal projections eight weeks after MG-132 intraperitoneal administration. We also discuss the current status of knowledge about intraperitoneal administration of MG-132, which is being used increasingly as a laboratory method.

Material and methods

Forty adult male Wistar rats (initial weight between 230 and 270 g) were used in the study. They were kept under standard laboratory conditions: at 22°C temperature under an artificial light/dark cycle (12/12 h), with *ad libitum* access to tap water and standard laboratory food, three animals per large cage. Handling and care of the animals were in accordance with the National Institute of Health Guidelines for the Care and Use of Laboratory Animals. For all procedures prior approval from the local Bioethics Commission was obtained. All efforts were made to reduce the number of animals and to minimize their suffering.

In the first stage of the experiment, selection of the animals on the basis of their spontaneous locomotor activity was performed.

A. Spontaneous activity – open field (automated)

Measurements of spontaneous activity was performed in accordance with well-established protocols [12]. For assessing both exploratory and locomotor activity of the rats, the Video Track v.2.5 Automated Behavioural Analysis System (View Point Life Sciences Inc, Canada) was used. For open-field study, a quiet room with controlled ventilation and temperature was used. The animals were placed in the centre of white experimental boxes of adequate size – square arena (50 × 50 cm) – surrounded by walls to prevent the animal from escaping. For ease of cleaning and to reduce behavioural response related to olfactory stimuli the experimental boxes were composed of plastic. At the same time, the activity of eight animals was video monitored. Initially, the rats were habituated to the apparatus during three sessions (10 minutes each) to reduce baseline activity. Then, spontaneous activity during light (with dimmed lighting) and dark phase (no lighting) – each one lasting 60 minutes, was recorded by the computer application Video Track VID 282 (View Point Life Sciences Inc, Canada). Image acquisition began 1 minute after the rats were placed in the box. Data were collected continuously and recorded each 30 seconds. The following parameters were evaluated:

– summary distance of exploratory movements [cm],
– summary duration of exploratory movements [s],
– summary distance of locomotor movements [cm],
– summary duration of locomotor movements [s],
– average velocity of locomotor movements [cm/s].

Due to the fact that differences in behaviour naturally occurring among animals divide them into those that exhibit greater motor activity in a novel environment (high responders – HR) and those that are less reactive (low responders – LR) [46], for further study only animals with a comparable activity

as an average were selected, animals with high and low locomotor activity were excluded.

B. Evoked motor activity – Rotarod test

Selected animals (n = 30) underwent the Rotarod tests for balance and coordination assessed pre-operatively at five speeds of rotation: 10, 12, 14, 16 and 18 rpm, to establish a baseline performance. For this test, the apparatus comprised of a rotating drum (Ugo Basile, Italy) was used. Four rats were placed on the revolving drum, one per testing station, and once they were balanced the stepper motor was started. The speed of the motor was increased to 10 rpm for 10 seconds and then progressively to 12, 14, and 16 rpm for 10 seconds each. The highest speed, 18 rpm, was maintained for 300 seconds until the 5-minute test period elapsed. To evaluate motor function the measurement of latency (time in seconds) to fall from the rotating drum was taken. The timer began automatically when the motor was switched on and stopped when the animal fell down to the floor of the apparatus. Each animal had three consecutive trials, the longest time on the drum being used for analysis. The animals were exposed to the Rotarod each day for 3 days to adapt the rats to the apparatus. The rats were then intraperitoneally injected with 10% DMSO or MG-132 solution according to the protocol described below and tested once per week during eight weeks of observation on the Rotarod for periods of 300 seconds. The means of the test results were used for statistical analysis.

C. MG-132 administration

The animals were randomly divided into three groups: control (n = 10), which received an intraperitoneal injection of 10% DMSO solution and two groups of rats that received a reversible proteasome inhibitor – MG-132 (lot # 3570428, Boston Biochem Inc., USA) dissolved in 10% DMSO. Protocol applications for both groups were based on the protocol proposed by McNaught *et al*. [33] for the application of other compounds from the group of proteasome inhibitors. Briefly, the rats received intraperitoneal injections of MG-132 every other day (total of 7 doses) for a period of two weeks. The first group of MG-132 rats (n = 10) received a higher dose (10 µg/g of body weight) of the inhibitor, while the second group (n = 10) received a lower dose (0.5 µg/g of body weight). Both doses administered to the animals were based on the those previously reported in the literature. The higher dose was used in the studies of [9,24,50], and the lower dose in the studies of [1,21].

Tissue collection and preparation

Eight weeks after first MG-132 administration the rats were deeply anaesthetized intraperitoneally with lethal doses of Nembutal (80 mg/kg of body weight), and then they were transcardially perfused with 0.9% saline containing 10,000 units of Heparin, followed by 4% solution of paraformaldehyde in 0.1 M phosphate buffer (pH 7.4; 4°C). Directly after perfusion, the brains were taken out of the skulls, postfixed in 4% paraformaldehyde for 3-4 hours, and then cryoprotected initially in 10% (overnight at 4°C) and subsequently in 30% sucrose phosphate buffer solution (pH 7.4; 4°C). After the brains soaked in the solution (1-3 days), each left hemisphere was marked by slight damage of the neocortex, and then the brains were cut on a cryostat (Microm HM 525, Thermo Scientific) into 40 µm thick coronal sections. For further studies, sections were collected and preserved in a cryoprotective solution containing glycerol.

Immunohistochemistry

To evaluate the possible changes made by MG-132 administration in the population of dopaminergic neurons in substantia nigra pars compacta (SNc), immunohistochemical staining with primary antibody against tyrosine hydroxylase (TH), a well-established marker of dopaminergic neurons, was performed. To evaluate all populations of SNc neurons double staining with anti-TH antibody and Neuro Trace 500/525 green fluorescent Nissl Stain (lot # 649182, Invitrogen, Molecular probes, USA) was performed.

Briefly, free-floating sections were blocked in a 3% normal goat serum (NGS) and 0.3% Triton X-100 in 0.01 M PBS (pH 7.2) for 1 hour at room temperature. Next, they were incubated with primary antibodies: mouse monoclonal anti-TH (Chemicon, USA; 1 : 500) in 0.01 M PBS (pH 7.2) containing NGS and 0.1% Triton X-100 at 4°C. After 48 hours the sections were washed with PBS and incubated (2 hours, room temperature) with secondary goat anti-mouse antibody coupled with Cy3 (Jackson, USA; 1 : 800). Finally, they were washed with PBS, mounted onto gelatine-coated slides, air-dried and coverslipped with Keiser Gelatin (Merck, Germany). Omission of the primary antibodies during control experiments resulted in a lack of signal.

For the unequivocal qualitative detection of both gross and fine scale neuronal degeneration, staining with Fluoro-Jade® B (Chemicon; Millipore) was used.

The manufacturer's "Protocol for using Fluoro-Jade® B" was applied for the single and double (with anti-TH antibodies) sections staining.

Qualitative analysis

The low-magnification images and initial analysis of immunostained sections were performed on an MVX10 MacroView research Macro Zoom Fluorescence Microscope (Olympus, Japan) equipped with a XC50 digital camera (Olympus, Japan). The high-magnification images and co-localization study were performed using a confocal laser scanning microscopy (CLSM) system (Radiance 2100, Bio-Rad UK) mounted on a microscope (Eclipse 600, Nikon, Japan). The CLSM images were obtained with 40× and 60× oil immersion objective lenses of N.A. = 1.3 and 1.4, respectively. The optimal iris diameter was used for each magnification. The CLSM images were analysed with LaserSharp 2000 and LaserPix v. 2.0 software (both Bio-Rad, UK).

Quantitative analysis

The CellSense Dimension 1.5 (Olympus, Japan) image analysis system was employed to assess the density of TH-ir positive cells in the substantia nigra pars compacta. The area of interest was outlined and computer-aided estimation was used to calculate the amount of TH-ir cells in the SNc. The number of TH-ir positive cells counted for both SNc on a separate slice was estimated individually for each animal. Representative sections of SNc were selected (between Bregma –4.80 and Bregma –6.04) [35]. All cells visible on the outlined area of a given section were analysed. Quantification of intensity of TH-staining within the striatum was performed according to the following method. The micrographs obtained with the aid of an image analysis system, CellSense Dimension 1.5 (Olympus, Japan), were converted into greyscale images (256 shades of grey) for measurement of TH fluorescence intensity. For morphometric analysis, greyscale intensity (GI; range 0-255: black = 0, white = 255) of TH-ir and background area were simultaneously measured using ImageJ 1.46R analysis software (NIH, USA) on a personal computer. The intensity of proportional TH-stained areas within dorsomedial, dorsolateral, and ventral striatum were measured through the rostrocaudal axis of the striatum. To compare the intensity of the sections the data are presented as proportional values of staging intensity (measured from 0 to 255) of a given area versus intensity of TH-ir-negative background. Calculation of the density of SNc dopaminergic and non-dopaminergic neurons, as well as total number of SNc neurons, was also performed by analysis with LaserPix v. 2.0 (Bio-Rad, UK) CSLM images obtained with a 40X lens and zoom set to 1.9 from double stained sections. The size of the testing area was 165 × 165 µm. At least ten areas from each animal were studied. The first test area within SNc was chosen randomly and the remaining ones were selected by systematic random sampling.

Measurements were carried out in 5 animals from each studied group (at least 3 sections/animal).

Statistical analysis

Data are expressed as mean ± standard errors of mean (SEM). To test the results for statistical significance, the following were used: (a) for data obtained from open field test – a nonparametric test Steel-Dwass: Pairwise Comparisons for One-Way Layout Design; (b) for data obtained from Rotarod test – 2 × 2 contingency table and Fisher test; (c) for TH-ir profiles distribution comparison – χ^2 test for normality; (d) for the rest of the parameters – statistics were performed with original data via unpaired *t*-test. Differences were considered significant when $p < 0.05$.

Results

In the group of rats after intraperitoneal administration of MG-132 at a dose of 10 µg/g of body weight, the mortality was 40% during 24 hours after the first dose, and then an additional 40% during the next 24 hours. Therefore, we did not pursue further experiments in this trial group.

In the group of rats that were given an intraperitoneal injection of MG-132 at a dose 0.5 µg/g of body weight and in the control group, mortality was not observed. There were no significant differences between the control group and MG-132 group in the changes of body weight during eight weeks of observation.

Intraperitoneal injection of MG-132 does not affect exploratory activities and locomotor activity adequate to the circadian rhythm

A week after the last administration of 0.5 µg/g MG-132 dose, the first evaluation of spontaneous activity in an open field test was performed (Fig. 1).

We found that in the control group and in the group treated with MG-132 adequate to the circadian rhythm, locomotor activity was maintained. There were no significant differences between the groups in the studied parameters of locomotor activity. During the light phase of open field test, the average summary distance of locomotor movements in the control group was 93.2 ± 26.4 cm while in the MG-132 group it was 148.9 ± 90.6 cm. In both groups, the value of this parameter was significantly higher ($p < 0.05$) during the dark phase of the open field test: 779.7 ± 200.0 cm and 774.7 ± 82.3 cm, respectively. The summary duration of locomotor movements during the light phase in the control group was 12.4 ± 2.3 seconds while in the MG-132 group it was 17.3 ± 11.1 seconds, and during the dark phase it was 91.6 ± 23.6 and 88.8 ± 8.9 seconds, respectively. The average velocity of locomotor movements did not differ significantly in both groups between the light and dark phases. In the control group, the values of this parameter were (light phase) 8.3 ± 0.2 cm/s and (dark phase) 8.2 ± 0.2 cm/s, while in the MG-132 group they were 8.5 ± 0.1 cm/s and 8.8 ± 0.1 cm/s, respectively.

There were also no significant differences between the control group and MG-132 group in the studied parameters of exploratory movement. During the light phase of the open field test, the average summary distance of exploratory movements in the control group was 183.3 ± 26.4 cm while in the MG-132 group it was 494.8 ± 192.3 cm. The value of this parameter was higher during the dark phase of the open field test: 843.4 ± 217.2 cm and 1300.2 ± 249.7 cm, respectively. The summary duration of exploratory movements during the light phase in the control group was 48.8 ± 11.1 seconds while in the MG-132 group it was 129.3 ± 21.3 seconds, and during the dark phase it was 200.2 ± 51.6 and 319.3 ± 70.1 seconds, respectively.

Very similar results were obtained during a second open field test performed eight weeks after the start of the experiment (after the first dose, MG-132 intraperitoneal administration).

Intraperitoneal injection of MG-132 does not influence motor activity and coordination

Evaluation of forced motor activity and coordination of animals was performed at the end of each eight consecutive weeks of observation. Only in the third week were there any observed differences between the control group and MG-132 group. Whereas all control rats could remain on the rotating

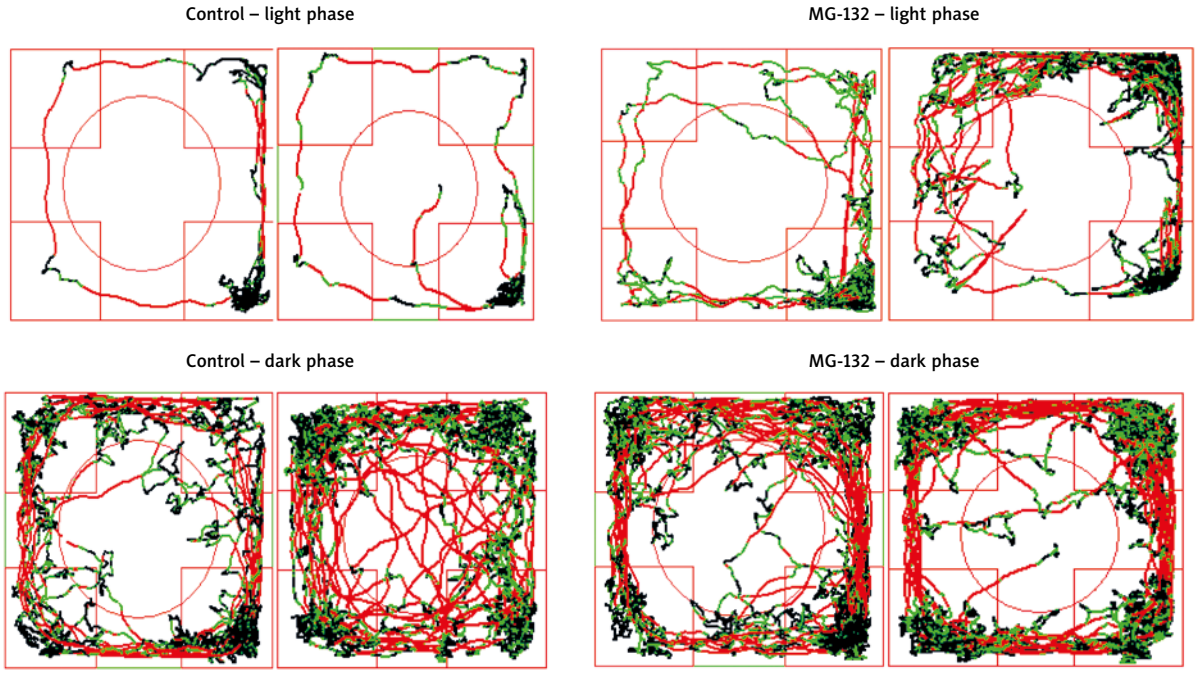

Fig. 1. Representative graphs of spontaneous activity recorded during light (with dimmed lighting) and dark phase (no lighting) of the experiment in control and MG-132 i.p. administered rats. Red colour represents locomotor movement, green colour represents exploratory movement.

rod for close to the full 300 seconds duration of the test, 40% of the rats from the MG-132 group fell off the rod sooner, but it was not statistically significant. During the remaining Rotarod tests the average results obtained in both groups were almost equal.

Intraperitoneal injection of MG-132 causes quantitative and qualitative changes in the population of rats substantia nigra pars compacta TH-ir neurons

The rats were sacrificed eight weeks after the beginning of the experiment – first intraperitoneal administration of MG-132 in DMSO or 10% DMSO (for control). Dual immunohistochemical staining followed by image analysis and cell counting revealed that the number of neuronal profiles within the SNc of the rats administered with MG-132 was significantly decreased by 17.1% ($p < 0.01$) as compared to the control animals (Fig. 2). A similar significant loss – of 20.1% ($p < 0.01$), of TH-positive neurons within the SNc of the rats administered with MG-132 as compared to control animals was also observed. There were no significant changes between the number of non-TH-ir nigral neurons between the studied groups of rats (Fig. 2). These results indicate that dopaminergic neurons within the SNc undergo degeneration, not just the loss of possibility for TH expression. It also shows that populations of SNc non-dopaminergic neurons were not as susceptible to MG-132 as dopaminergic ones were.

Within the population of SNc TH-ir neurons, in addition to quantitative, qualitative changes were also observed. Image analysis of SNc TH-ir cell profiles from controls ($n = 952$) and MG-132 administered rats ($n = 839$) revealed that distribution of those cells profiles differed significantly ($\chi^2 = 115.116$, $p < 0.0001$) between the studied groups. As is shown on the comparative distribution graph (Fig. 2), within the SNc of MG-132 administered rats there was a marked decrease of large (bigger than 200 μm^2) TH-ir neurons.

Intraperitoneal injection of MG-132 induces TH-ir elements loss in rat striatum

In the rat striatum, the immunohistochemical study revealed the presence of TH-ir fibres located predominantly within the matrix (Fig. 3A). Their diverse morphology closely corresponded to that reported by Gerfen and colleagues [16]. The most frequently observed were relatively thin (0.1-0.4 µm), smooth fibres with small varicosities (0.25-0.65 µm). These fibres were present within the matrix. They correspond to Gerfen's type A fibres, being axon terminal dopaminergic cells from the dorsal tier of SNc (dorsal A9 cell group). Much less frequently, thicker fibres (0.2-0.65 µm) with larger varicosities (0.4-1.0 µm) were present. They were predominantly located in the proximity of striosomes. Their morphology and localization corresponded to type B fibres, being axon terminals dopaminergic cells from the ventral tier of SNc (ventral A9 cell group) and the ventral tier of substantia nigra reticulata (displaced A9 cell group).

The intensity of TH-staining in the striatum of the rats after intraperitoneal administration of MG-132 compared to the density of TH-ir fibres in the control animals (Fig. 4) revealed that in the dorsomedial part of the striatum and ventral striatum no significant differences were observed (values of calculated intensity factors were 1.57 vs. 1.63 and 1.53 vs. 1.55, respectively). A significant, 8% decrease ($p < 0.05$) of TH-ir in the dorsolateral part of the striatum (1.28 in the MG-132 group vs. 1.39 in the control group, Fig. 4) was observed. A decrease in TH staining due to the loss of dopaminergic fibres was similar along the rostrocaudal axis of the striatum. This localization of TH-ir loss may indicate that while limbic and associative areas of the striatum are relatively resistant, the sensorimotor areas are more susceptible to damage caused by MG-132 administration. Fluoro-Jade B staining, detecting both gross and fine-scale neuronal degeneration, showed the presence of degenerating fibres in the dorsal striatum (Fig. 3B). Those fibres were present in both striatal compartments, within the matrix and striosomes, but only on brain sections from animals after MG-132 administration. Features of degenerating fibres morphology were very similar to those present on TH-containing axons innervating the striatum (Fig. 3). In addition to the fibres corresponding to type A and type B, occasionally (1-2 per section), a third category of fibres in the matrix were observed. They were thicker (0.45-1.05 µm), and possessed vesicular, much larger varicosities (1.5-2.9 µm). Their morphology and localization corresponded to type C fibres, being axon terminals of non-dopaminergic cells from SN. Double-labelling Fluoro-Jade B/tyrosine hydro-

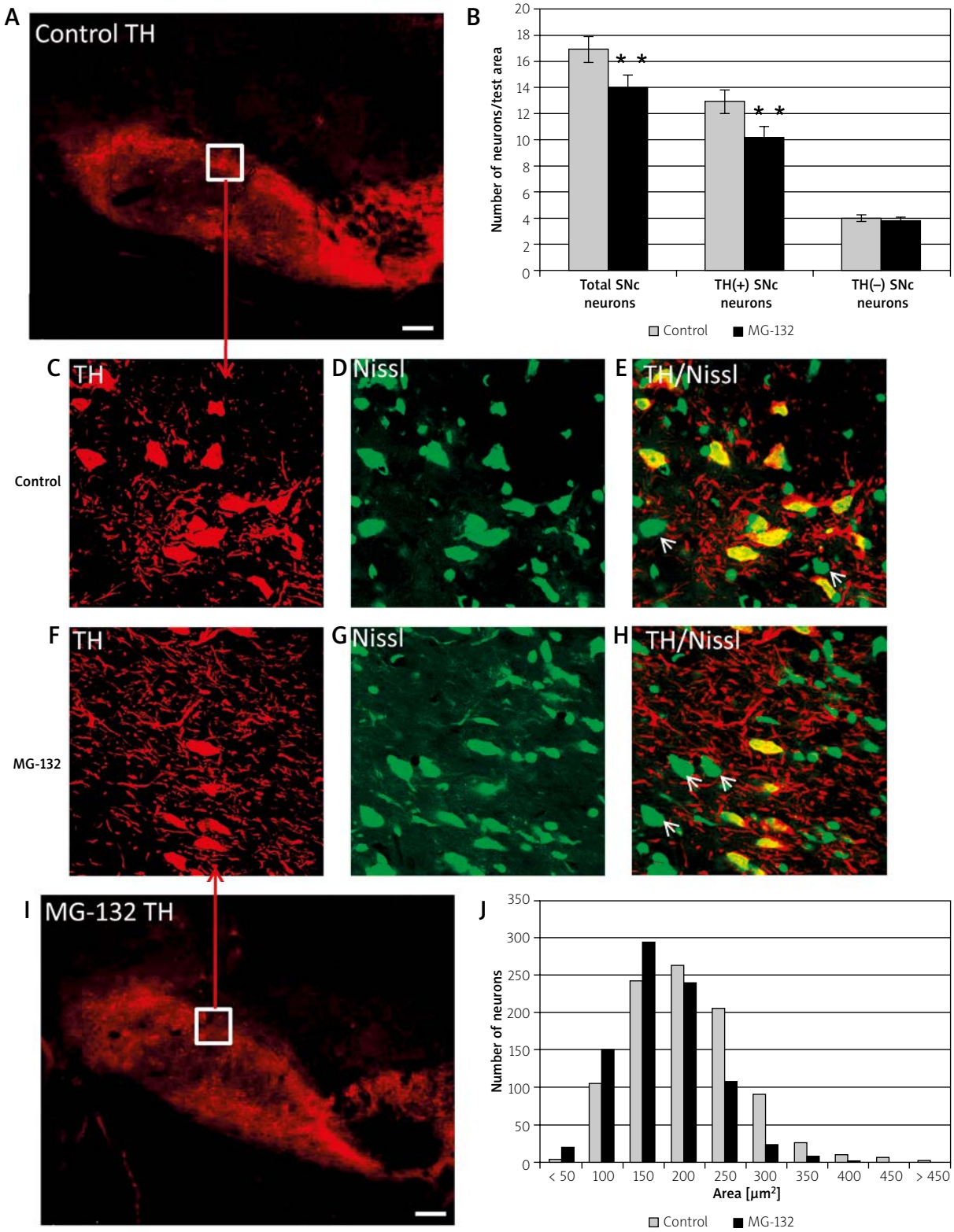

Fig. 2. Loss of TH-ir neurons in SNc in response to MG-132 administration. Normal density of TH-ir **A, C** (red), **E** (yellow) and non TH-ir **E** (green, marked with arrows) neurons in SNc in control animals. Loss of TH-ir **F, I** (red), **H** (yellow) and non TH-ir **H** (green, marked with arrows) neurons in SNc in MG-132 animals. Graph **B** shows a significant loss of all neurons and TH(+) neurons, but not TH(–) in SNc of rats administered with MG-132. Graph **J** shows distribution of TH(+) profiles according to their size within SNc of studied groups. Scale bar 200 µm.

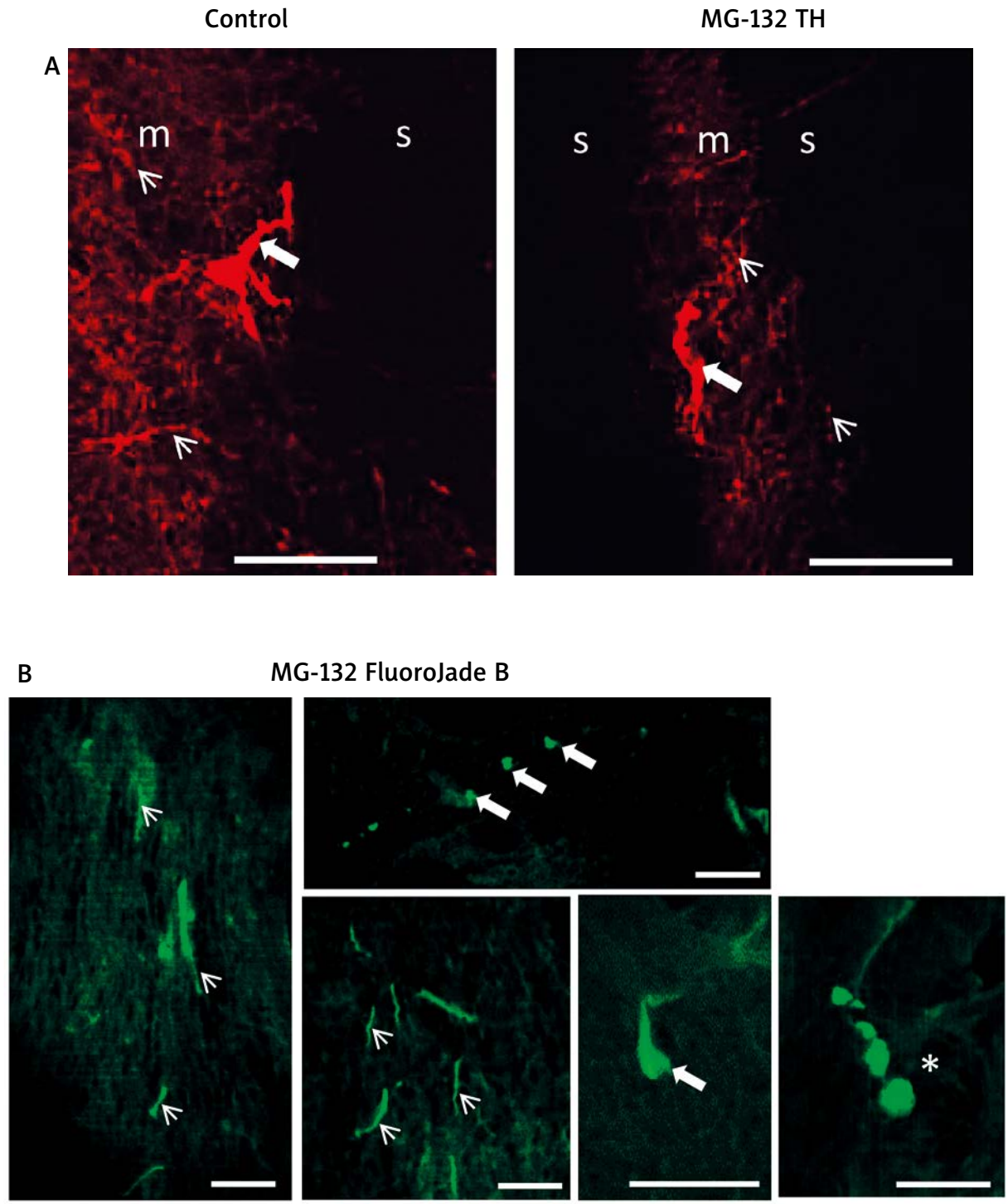

Fig. 3. Morphology of the fibres within the striatum. **A)** Distribution and morphology of TH-ir type A fibres (small arrows) and type B fibres (large arrows) within the striatum of studied groups. **B)** Morphology of degenerating fibres revealed by Fluoro-Jade B staining. Type A fibres (small arrows), type B fibres (large arrows), type C fibres (asterisk) within the striatum of MG-132 rats – detailed description in the text. (s) – striosome; (m) – matrix. Scale bar 10 µm.

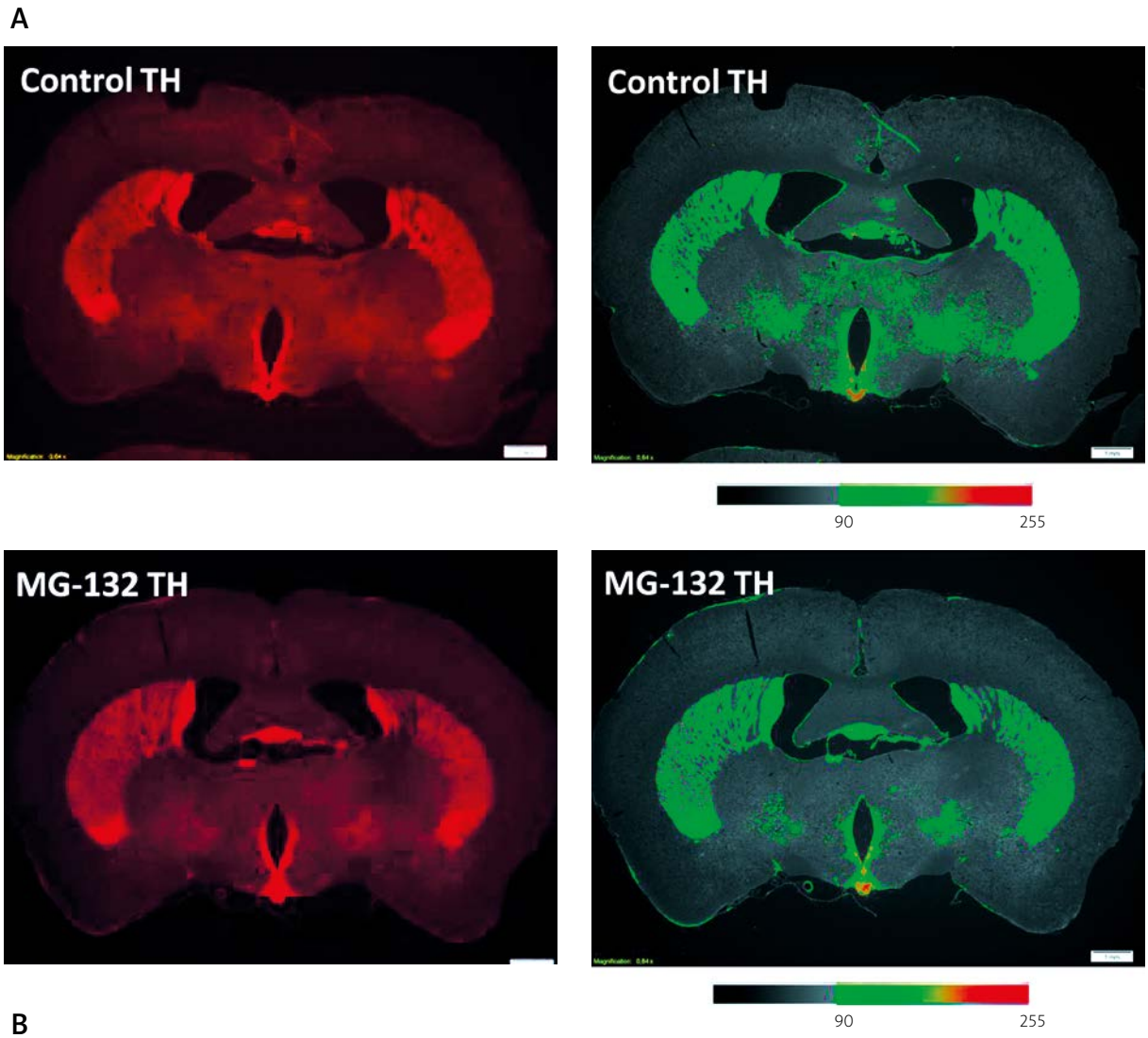

Fig. 4. Loss of TH-ir fibres in the striatum in response to MG-132 administration. **A)** The upper panel shows normal density of TH-ir fibres (red) and pseudo colour intensity (scale included) in the striatum of control animals. The lower panel shows a small loss of TH-ir fibres (red) and pseudo colour intensity (scale included) in the striatum of MG-132 animals. **B)** The graph shows a significant loss of TH(+) fibres in dorso-lateral striatum but not in dorsomedial striatum and ventral striatum of rats administered with MG-132. Scale bar 1 mm.

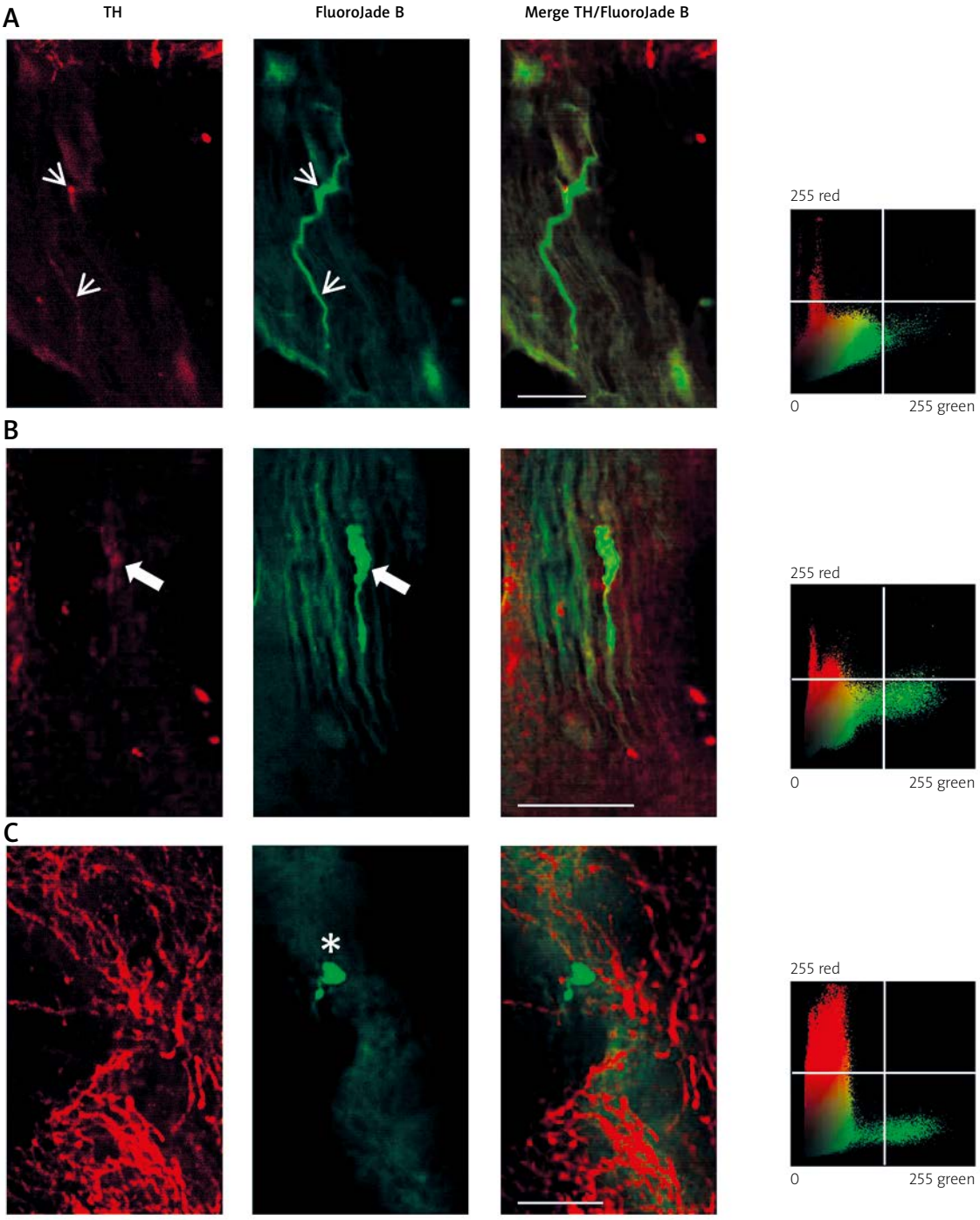

Fig. 5. Fluoro-Jade B/tyrosine hydroxylase (TH) double-labelling in the dorsal striatum of MG-132 administered rats. Degenerating fibres, Fluoro-Jade B positive, showed various morphologies – corresponding to type A of normal TH-fibres **(A)**, fibres with large varicosities, type B of normal TH-fibres **(B)** up to the type C fibres with a collection of vesicular varicosities **(C)**. Very low intensity of TH immunoreactivity (indicated by arrows) were detected in degenerating fibres with type A and B morphology **(A, B)**. At the type C fibres **(C)** Fluoro-Jade B and TH positive elements comprised two separate populations. It is also visible on the 2D colocalization plots (with intensities of red colour plotted against intensities of green colour) corresponding to the confocal images **(A-C)**. Scale bar 10 µm.

xylase (TH) revealed that in the dorsal striatum of MG-132 administered rats' degenerating fibres, very low intensity of TH immunoreactivity (Fig. 5) was detected in degenerating fibres with type A and B morphology. In the type C fibres, Fluoro-Jade B and TH positive elements comprised two separate populations. This has also been confirmed by co-localization studies.

Discussion

After Alzheimer's disease, Parkinson's disease is the second most common neurodegenerative disorder. It affects more than 1% of the world population aged 65 years. Clinical symptoms of Parkinson's disease (PD) include non-motor signs: olfactory deficits, sleep disturbances, depression, psychosis, and cognitive impairment as well as more spectacular motor signs: muscular rigidity, bradykinesia, resting tremor, and postural instability. The latter result from the destruction of the substantia nigra dopaminergic neurons projecting to the striatum, and loss of dopamine transmission in the motor loops of the basal ganglia. To date pathogenesis of PD has remained largely elusive and the general consensus is that PD is a multifactorial disease: a combination of genetic inheritance, aging and some unknown environmental factors. A growing number of reports provide evidence that inhibition of the ubiquitin-proteasome system (UPS) plays a role in the pathogenesis of PD [49]. Confirmation of UPS impairment in the brains of PD patients given by findings of accumulation of UPS components and its substrates in Lewy bodies, reduced proteasome activity in substantia nigra, and the presence of PD in patients with mutations in gene encoding for several UPS-related key molecules.

A great deal of possible information about the pathogenesis of PD has been obtained due to *in vivo* results from various animal models of this disease [3,5,40,44]. Among them, degenerative models with MPTP and rotenone are the most commonly used. However, recently it has been postulated that direct administration into elements of the nigrostriatal system [14,25,45] or systemic administration of proteasome inhibitors may serve as a new animal model of PD. The basis of this theory was the results of animal studies indicating that systemically administered (intraperitoneally) proteasome inhibitors like PSI and epoxomicin may, after absorption into the bloodstream, penetrate the intact blood-brain barrier and cause lesions at the substantia nigra, locus coeruleus, and the Meynert nucleus, and in consequence, lead to an impairment of the motor function [32,33,38]. This allowed the researches to hypothesize that the use of proteasome inhibitors could be used to obtain a new animal model of Parkinson's disease. It should be noted that not all groups of researchers were able to obtain the same results [6,23].

However, there are two previous reports describing the influence of MG-132 on the nigrostriatal pathway [41,49]. According to our knowledge, the current report is the first to estimate the influence of systemic administration of MG-132. The results we have shown in this report reveal a significant loss of SNc dopaminergic neurons in rats six weeks after the end of systemic, intraperitoneal MG-132 administration. This loss was accompanied by a corresponding decrease in density of dopaminergic fibres within the dorsolateral striatum. Moreover, evidence of very limited but ongoing TH-ir fibre degeneration within the dorsal striatum suggests that MG-132 severely disturbed the nigrostriatal pathway. Our observation that the number of SNc TH-ir cells in the rats intraperitoneally injected with small doses of MG-132 decreased by 20.1% corresponds to the results shown by Xie *et al*. [49]. They found that injection of 0.4 mg of MG-132 into the medial forebrain bundle in mice decreased the number of nigral TH-ir cells by 24.5%. The degree of SNc dopaminergic neuron loss observed by us is smaller than that produced by direct injection of 0.4 µg MG-132 in 4 µl 1% DMSO into the substantia nigra reported by Sun *et al*., which was approximately 40% [41]. Those discrepancies suggest that the different administration routes of the same proteasome inhibitor may lead to different consequences. This was also recently shown for another proteasome inhibitor – lactacystin. A unilateral, intranigral injection of lactacystin at doses of 0.5, 1, 2.5, and 5 µg/2 µl produced after 7 days, distinct decreases in the concentrations of dopamine (DA) and its metabolites (DOPAC, 3-MT, HVA) in the ipsilateral striatum. Such alterations were not observed in the striatal DA content and catabolism either 7, 14, or 21 days after a unilateral, intrastriatal high-dose lactacystin injection (5 and 10 µg/2 µl) [25].

The results of a previous study evaluating the influence of systemic administration of proteasome inhibitors on behavioural and neuropathological features of Parkinson's disease are ambiguous. In

some experimental conditions, mainly after subcutaneous administration of PSI, a loss of SN dopaminergic neurons was observed and varied between 40% [38] and 50% [51], and even exceeded 50% [33]. Four other groups of researchers, despite the fact that they tried faithfully to follow the experimental protocol proposed by McNaught *et al.*, failed to replicate the results described earlier [6,22,23,30]. Our results support the theory of McNaught *et al*.

The striatum is responsible for integrating incoming information from all areas of the cerebral cortex and creating motor patterns based on past knowledge (procedural memory) and on the recent environment and desires [11]. The striosome/matrix cytoarchitectonic structures of the striatum play a crucial role in its functional organization. Afferent connections present in the matrix, especially in the lateral part of the dorsal striatum, are related to sensomotor areas of the cerebral cortex. Matrix located more medially and striosomes have predominant associative- and limbic-related connections, respectively [11]. Similarly to data from previous successful demonstration of systemic proteasome inhibitors' effect on damage of nigrostriatal connections [32,33,38,51], we observed a loss of dopaminergic terminals within the striatum. Previous reports indicated a decrease in dopaminergic innervations of the striatum by 30 to 40%. We observed that after intraperitoneal MG-132 administration the decrease of TH staining, due to the loss of dopaminergic fibres, was similar along the rostrocaudal axis of the striatum, but significant by 8% only in the lateral part of the dorsal striatum. The changes observed by us in the distribution of the striatal TH-ir fibres correspond to previous data obtained under other experimental conditions [39]. After MPTP administration in monkeys the smallest loss of striatal TH-ir fibres named as "mild stage" was observed in the dorsolateral striatum. It suggests that the sensorimotor areas of the striatum in the rat are more susceptible to damage, including damage caused by MG-132 administration, while limbic and associative areas are relatively resistant.

Under our experimental conditions, the loss of nigral TH-ir neurons in the SNc and dopaminergic terminals in the dorsolateral striatum was not accompanied by the presence of motor abnormalities, as shown by a series of behavioural tests of spontaneous and forced locomotion. The lack of significant differences in spontaneous and forced locomotor activity observed by us appears to result from a relatively high amount (80%) of dopaminergic neurons (TH-ir), which remained in substantia nigra pars compacta and 92% of dopaminergic terminals in striatum. According to earlier reports, during Parkinson's disease at the onset of symptoms, putamenal dopamine is depleted by approximately ≈80%, and approximately ≈60% of SNc dopaminergic neurons have already been lost [13]. The results of other studies showed that motor signs of PD manifest after the loss of approximately 50% of nigral neurons and 80% of striatal dopamine [4,47]. Two postmortem studies using more rigorous quantitative methods, such as using a tessellation method [17] and dissector-based neuromorphometry [27], found that about 30% of nigral neuronal loss appeared sufficient to cause motor symptoms in PD [2]. However, recent research suggests that the first symptoms of Parkinson's disease may manifest after just a 20% decrease in the number of dopaminergic neurons SNc, which has been shown in animal models where a reduction of about 14 to 23% of nigral neuron count or 14% to 37% of striatal dopamine was sufficient to induce mild parkinsonism [43].

Systemic administration of proteasome inhibition

In rats with 50% loss of SNc dopaminergic neurons after systemic PSI administration no bradykinesia or akinesia was observed, but they did exhibit a reduction by 30 to 40% of exploratory behaviour. The 20% loss of dopaminergic cells in SNc and 8% loss of dopaminergic terminals in striatum, as observed by us, may not be sufficient to produce motor symptoms of PD.

Intraperitoneal administration of proteasome inhibitor Mg-132 is a method known for almost ten years; however, it is not applied universally. It is worth noting that attempts were made to use MG-132 for the treatment and prevention of a wide range of pathologies in animal models. The influence of intraperitoneal injection MG-132 has been studied in two aspects: (1) its immediate influence, evaluated in hours after administration and (2) its delayed influence, evaluated in days and weeks (up to 12) after administration.

Injected intraperitoneally, a single dose of MG-132, varying from 0.5 to 10 mg/kg b.w., was able to successfully act on the elements of the digestive

system. Observations made after intraperitoneal MG-132 administration have become the basis for a theory of the beneficial role of proteasome inhibitors not only in prevention, but also in the therapy of acute pancreatitis [9,24,50]. This beneficial effect is dependent on the induction of the expression of cell-protective heat shock proteins (Hsp72), modulation of DNA-binding of nuclear NFκB, suppression of the elevation of pancreatic myeloperoxidase activity, tumor necrosis factor α (TNF-α), and intracellular adhesion of molecule-1 and serum amylase. Intraperitoneal administration of MG-132 also decreases inflammatory response, by lowering the increase in interleukin 1 (IL-1), TNF-α, and IL-10 levels in the caecal ligation and puncture model of sepsis [36]. Studies by Alexandrova *et al*. showed that intraperitoneal MG-132 treatment activates the liver antioxidant enzyme system e.g. superoxide dismutase, catalase and glutathione peroxidase [1]. They postulated that MG-132 might play a preventive role in the development of cell and tissue injury. It was recently confirmed [21] in the rat model that intraperitoneal administration of MG-132 has a significant effect in protection against liver injury induced by intestinal ischaemia/reperfusion, most probably due to modulation of NFκB and Aryl hydrocarbon receptor pathways. A single intraperitoneal dose of MG-132 appears also to act effectively on the structures belonging to systems other than the gastrointestinal. According to Chen *et al*., intraperitoneal administration of MG-132 shows a protective effect on lung injury in rats by significantly decreasing pulmonary myeloperoxidase activity [9]. However, the most comprehensive study of immediate response to intraperitoneal MG-132 administration was published by Holecek *et al*. [18]. They reported a significant increase in protein synthesis not only in the digestive system (liver), but also in the kidney and skeletal muscle. In addition, they observed a significant decrease in proteasome-dependent proteolysis in skeletal muscle and the increase in protein turnover associated with a significant increase in proteasome-dependent proteolysis in the liver and kidney.

Authors more often indicate a possible systemic toxic effect and even an increase in the mortality risk in the reports where there were late effects of MG-132 and the effects of multiple doses of the MG-132 studied [29,37]. A dose of 10 mg/kg of body weight (cumulative dose of above 30 mg/kg) provided intraperitoneally seems to lead to high mortality, although rats can survive a cumulative dose of 105 mg/kg [7] delivered in 14 doses during seven days subcutaneously. After prolonged MG-132 administration, its delayed influence has been reported on more numerous structures from many systems. It has been reported that [19] in experimental inflammatory bowel disease MG-132 *in vivo* reduced T cell-mediated intestinal inflammation but significantly suppressed cell migration and epithelial cell proliferation. MG-132 also has an influence on the cardiovascular system [8,29,34]. In a low dose (0.1 mg/kg) MG-132 administered intraperitoneally once per day even for 2 or 8 weeks may effectively prevent cardiac remodelling and dysfunction in pressure-overloaded hearts without marked drug toxicity [29]. The effects of intraperitoneal injection of MG-132 was also studied on urinary [37], musculoskeletal [20,42], and respiratory systems [28]. The study revealed that MG-132 is not an adequate treatment to prevent endotoxin-induced diaphragmatic dysfunction [20,42] but partially prevents muscle atrophy associated with disuse [20]. MG-132 administered in relatively large doses (4 mg/kg, repeated seven times) did not ameliorate tubulointerstitial fibrosis in rat unilateral ureteral obstruction [37]. Positive effects of MG-132, namely attenuation pneumonitis and cytokine gene expression *in vivo* by reducing coronavirus were observed [28].

In summary, intraperitoneal application of proteasome inhibitor MG-132, despite the encouraging results of the experimental treatment and prevention of many pathological processes, should be used with caution because of the potential adverse effects on the structure of the central nervous system, especially elements of the nigrostriatal pathway.

Acknowledgement

Supported by Grant Funds from National Scientific Committee – N N401 005735.

References

1. Alexandrova A, Petrov L, Georgieva A, Kirkova M, Kukan M. Effects of proteasome inhibitor, MG132, on proteasome activity and oxidative status of rat liver. Cell Biochem Funct 2008; 26: 392-398.
2. Beach TG, Adler CH, Sue LI, Peirce JB, Bachalakuri J, Dalsing-Hernandez JE, Lue LF, Caviness JN, Connor DJ, Sabbagh MN, Walker DG. Reduced striatal tyrosine hydroxylase in incidental Lewy body disease. Acta Neuropathol 2008; 115: 445-451.

3. Betarbet R, Sherer TB, Greenamyre JT. Animal models of Parkinson's disease. Bioessays 2002; 24: 308-318.
4. Bezard E, Dovero S, Prunier C, Ravenscroft P, Chalon S, Guilloteau D, Crossman AR, Bioulac B, Brotchie JM, Gross CE. Relationship between the appearance of symptoms and the level of nigrostriatal degeneration in a progressive 1-methyl-4-phenyl-1,2,3,6-tetrahydropyridine-lesioned macaque model of Parkinson's disease. J Neurosci 2001; 21: 6853-6861.
5. Blesa J, Phani S, Jackson-Lewis V, Przedborski S. Classic and new animal models of Parkinson's disease. J Biomed Biotechnol 2012; 2012: 845618.
6. Bove J, Zhou C, Jackson-Lewis V, Taylor J, Chu Y, Rideout HJ, Wu DC, Kordower JH, Petrucelli L, Przedborski S. Proteasome inhibition and Parkinson's disease modeling. Ann Neurol 2006; 60: 260-264.
7. Caron AZ, Haroun S, Leblanc E, Trensz F, Guindi C, Amrani A, Grenier G. The proteasome inhibitor MG132 reduces immobilization-induced skeletal muscle atrophy in mice. BMC Musculoskelet Disord 2011; 12: 185.
8. Chen B, Ma Y, Meng R, Xiong Z, Zhang C, Chen G, Zhang A, Dong Y. MG132, a proteasome inhibitor, attenuates pressure-overload-induced cardiac hypertrophy in rats by modulation of mitogen-activated protein kinase signals. Acta Biochim Biophys Sin (Shanghai) 2010; 42: 253-258.
9. Chen X, Li SL, Wu T, Liu JD. Proteasome inhibitor ameliorates severe acute pancreatitis and associated lung injury of rats. World J Gastroenterol 2008; 14: 3249-3253.
10. Ciechanover A. Intracellular protein degradation: from a vague idea thru the lysosome and the ubiquitin-proteasome system and onto human diseases and drug targeting. Biochim Biophys Acta 2012; 1824: 3-13.
11. Crittenden JR, Graybiel AM. Basal Ganglia disorders associated with imbalances in the striatal striosome and matrix compartments. Front Neuroanat 2011; 5: 59.
12. Curzon P, Zhang M, Radek RJ, Fox GB. The Behavioral Assessment of Sensorimotor Processes in the Mouse: Acoustic Startle, Sensory Gating, Locomotor Activity, Rotarod, and Beam Walking. 2009.
13. Dauer W, Przedborski S. Parkinson's disease: mechanisms and models. Neuron 2003; 39: 889-909.
14. Duty S, Jenner P. Animal models of Parkinson's disease: a source of novel treatments and clues to the cause of the disease. Br J Pharmacol 2011; 164: 1357-1391.
15. Fritsch Fredin M, Vidal A, Utkovic H, Gotlind YY, Willen R, Jansson L, Hultgren Hornquist E, Melgar S. The application and relevance of ex vivo culture systems for assessment of IBD treatment in murine models of colitis. Pharmacol Res 2008; 58: 222-231.
16. Gerfen CR, Herkenham M, Thibault J. The neostriatal mosaic: II. Patch- and matrix-directed mesostriatal dopaminergic and non-dopaminergic systems. J Neurosci 1987; 7: 3915-3934.
17. Greffard S, Verny M, Bonnet AM, Beinis JY, Gallinari C, Meaume S, Piette F, Hauw JJ, Duyckaerts C. Motor score of the Unified Parkinson Disease Rating Scale as a good predictor of Lewy body-associated neuronal loss in the substantia nigra. Arch Neurol 2006; 63: 584-588.
18. Holecek M, Muthny T, Kovarik M, Sispera L. Proteasome inhibitor MG-132 enhances whole-body protein turnover in rat. Biochem Biophys Res Commun 2006; 345: 38-42.
19. Inoue S, Nakase H, Matsuura M, Mikami S, Ueno S, Uza N, Chiba T. The effect of proteasome inhibitor MG132 on experimental inflammatory bowel disease. Clin Exp Immunol 2009; 156: 172-182.
20. Jamart C, Raymackers JM, Li An G, Deldicque L, Francaux M. Prevention of muscle disuse atrophy by MG132 proteasome inhibitor. Muscle Nerve 2011; 43: 708-716.
21. Jing H, Shen G, Wang G, Zhang F, Li Y, Luo F, Yao J, Tian XF. MG132 Alleviates liver injury induced by intestinal ischemia/reperfusion in rats: involvement of the AhR and NFkappaB pathways. J Surg Res 2012; 176: 63-73.
22. Kadoguchi N, Kimoto H, Yano R, Kato H, Araki T. Failure of acute administration with proteasome inhibitor to provide a model of Parkinson's disease in mice. Metab Brain Dis 2008; 23: 147-154.
23. Kordower JH, Kanaan NM, Chu Y, Suresh Babu R, Stansell J, 3rd, Terpstra BT, Sortwell CE, Steece-Collier K, Collier TJ. Failure of proteasome inhibitor administration to provide a model of Parkinson's disease in rats and monkeys. Ann Neurol 2006; 60: 264-268.
24. Letoha T, Feher LZ, Pecze L, Somlai C, Varga I, Kaszaki J, Toth G, Vizler C, Tiszlavicz L, Takacs T. Therapeutic proteasome inhibition in experimental acute pancreatitis. World J Gastroenterol 2007; 13: 4452-4457.
25. Lorenc-Koci E, Lenda T, Antkiewicz-Michaluk L, Wardas J, Domin H, Smialowska M, Konieczny J. Different effects of intranigral and intrastriatal administration of the proteasome inhibitor lactacystin on typical neurochemical and histological markers of Parkinson's disease in rats. Neurochem Int 2011; 58: 839-849.
26. Lu CY, Yi PL, Tsai CH, Cheng CH, Chang HH, Hsiao YT, Chang FC. TNF-NF-kappaB signaling mediates excessive somnolence in hemiparkinsonian rats. Behav Brain Res 2010; 208: 484-496.
27. Ma SY, Roytta M, Rinne JO, Collan Y, Rinne UK. Correlation between neuromorphometry in the substantia nigra and clinical features in Parkinson's disease using disector counts. J Neurol Sci 1997; 151: 83-87.
28. Ma XZ, Bartczak A, Zhang J, Khattar R, Chen L, Liu MF, Edwards A, Levy G, McGilvray ID. Proteasome inhibition in vivo promotes survival in a lethal murine model of severe acute respiratory syndrome. J Virol 2010; 84: 12419-12428.
29. Ma Y, Chen B, Liu D, Yang Y, Xiong Z, Zeng J, Dong Y. MG132 treatment attenuates cardiac remodeling and dysfunction following aortic banding in rats via the NF-kappaB/TGFbeta1 pathway. Biochem Pharmacol 2011; 81: 1228-1236.
30. Manning-Bog AB, Reaney SH, Chou VP, Johnston LC, McCormack AL, Johnston J, Langston JW, Di Monte DA. Lack of nigrostriatal pathology in a rat model of proteasome inhibition. Ann Neurol 2006; 60: 256-260.
31. Matsui H, Ito H, Taniguchi Y, Inoue H, Takeda S, Takahashi R. Proteasome inhibition in medaka brain induces the features of Parkinson's disease. J Neurochem 2010; 115: 178-187.
32. McNaught KS, Olanow CW. Proteasome inhibitor-induced model of Parkinson's disease. Ann Neurol 2006; 60: 243-247.
33. McNaught KS, Perl DP, Brownell AL, Olanow CW. Systemic exposure to proteasome inhibitors causes a progressive model of Parkinson's disease. Ann Neurol 2004; 56: 149-162.

34. Meiners S, Hocher B, Weller A, Laule M, Stangl V, Guenther C, Godes M, Mrozikiewicz A, Baumann G, Stangl K. Downregulation of matrix metalloproteinases and collagens and suppression of cardiac fibrosis by inhibition of the proteasome. Hypertension 2004; 44: 471-477.
35. Paxinos G, Watson C. The rat brain in stereotaxic coordinates. 4th ed. Academic Press, San Diego, London 1998.
36. Safranek R, Ishibashi N, Oka Y, Ozasa H, Shirouzu K, Holecek M. Modulation of inflammatory response in sepsis by proteasome inhibition. Int J Exp Pathol 2006; 87: 369-372.
37. Sakairi T, Hiromura K, Takahashi S, Hamatani H, Takeuchi S, Tomioka M, Maeshima A, Kuroiwa T, Nojima Y. Effects of proteasome inhibitors on rat renal fibrosis in vitro and in vivo. Nephrology (Carlton) 2011; 16: 76-86.
38. Schapira AH, Cleeter MW, Muddle JR, Workman JM, Cooper JM, King RH. Proteasomal inhibition causes loss of nigral tyrosine hydroxylase neurons. Ann Neurol 2006; 60: 253-255.
39. Song DD, Haber SN. Striatal responses to partial dopaminergic lesion: evidence for compensatory sprouting. J Neurosci 2000; 20: 5102-5114.
40. Stoica G, Lungu G, Bjorklund NL, Taglialatela G, Zhang X, Chiu V, Hill HH, Schenk JO, Murray I. Potential role of alpha-synuclein in neurodegeneration: studies in a rat animal model. J Neurochem 2012; 122: 812-822.
41. Sun F, Anantharam V, Zhang D, Latchoumycandane C, Kanthasamy A, Kanthasamy AG. Proteasome inhibitor MG-132 induces dopaminergic degeneration in cell culture and animal models. Neurotoxicology 2006; 27: 807-815.
42. Supinski GS, Vanags J, Callahan LA. Effect of proteasome inhibitors on endotoxin-induced diaphragm dysfunction. Am J Physiol Lung Cell Mol Physiol 2009; 296: L994-L1001.
43. Tabbal SD, Tian L, Karimi M, Brown CA, Loftin SK, Perlmutter JS. Low nigrostriatal reserve for motor parkinsonism in nonhuman primates. Exp Neurol 2012; 237: 355-362.
44. Valastro B, Dekundy A, Krogh M, Lundblad M, James P, Danysz W, Quack G, Cenci MA. Proteomic analysis of striatal proteins in the rat model of L-DOPA-induced dyskinesia. J Neurochem 2007; 102: 1395-1409.
45. Vernon AC, Johansson SM, Modo MM. Non-invasive evaluation of nigrostriatal neuropathology in a proteasome inhibitor rodent model of Parkinson's disease. BMC Neurosci 2010; 11: 1.
46. White DA, Kalinichev M, Holtzman SG. Locomotor response to novelty as a predictor of reactivity to aversive stimuli in the rat. Brain Res 2007; 1149: 141-148.
47. Wolters E. Non-motor extranigral signs and symptoms in Parkinson's disease. Parkinsonism Relat Disord 2009; 15 Suppl 3: S6-12.
48. Wu WK, Cho CH, Lee CW, Wu K, Fan D, Yu J, Sung JJ. Proteasome inhibition: a new therapeutic strategy to cancer treatment. Cancer Lett 2010; 293: 15-22.
49. Xie W, Li X, Li C, Zhu W, Jankovic J, Le W. Proteasome inhibition modeling nigral neuron degeneration in Parkinson's disease. J Neurochem 2010; 115: 188-199.
50. Xu CF, Xia SJ. Effect of MG-132 upon the expression of intercellular adhesion molecule-1 in cerulein-induced acute pancreatitis in mice. Zhonghua Yi Xue Za Zhi 2010; 90: 853-856.
51. Zeng BY, Bukhatwa S, Hikima A, Rose S, Jenner P. Reproducible nigral cell loss after systemic proteasomal inhibitor administration to rats. Ann Neurol 2006; 60: 248-252.

Original article

Folia Neuropathologica

Electrospun nanofiber mat as a protector against the consequences of brain injury

Dorota Sulejczak[1], Jarosław Andrychowski[2,3], Tomasz Kowalczyk[4], Paweł Nakielski[4], Małgorzata Frontczak-Baniewicz[5], Tomasz Kowalewski[4]

[1]Department of Experimental Pharmacology, Mossakowski Medical Research Centre, Polish Academy of Sciences, Warsaw, [2]Department of Neurosurgery, Medical University of Warsaw, Bielanski Hospital, Warsaw, [3]Department of Neurosurgery, Mossakowski Medical Research Centre, Polish Academy of Sciences, Warsaw, [4]Institute of Fundamental Technological Research, Polish Academy of Sciences, Warsaw, [5]Electron Microscopy Platform, Mossakowski Medical Research Centre, Polish Academy of Sciences, Warsaw, Poland

Folia Neuropathol 2014; 52 (1): 56-69 DOI: 10.5114/fn.2014.41744

Abstract

Traumatic/surgical brain injury can initiate a cascade of pathological changes that result, in the long run, in severe damage of brain parenchyma and encephalopathy. Excessive scarring can also interfere with brain function and the glial scar formed may hamper the restoration of damaged brain neural pathways. In this preliminary study we aimed to investigate the effect of dressing with an L-lactide-caprolactone copolymer nanofiber net on brain wound healing and the fate of the formed glial scar. Our rat model of surgical brain injury (SBI) of the fronto-temporal region of the sensorimotor cortex imitates well the respective human neurosurgery situation. Brains derived from SBI rats with net-undressed wound showed massive neurodegeneration, entry of systemic inflammatory cells into the brain parenchyma and the astrogliosis due to massive glial scar formation. Dressing of the wound with the nanofiber net delayed and reduced the destructive phenomena. We observed also a reduction in the scar thickness. The observed modification of local inflammation and cicatrization suggest that nanofiber nets could be useful in human neurosurgery.

Key words: *brain injury, L-lactide-caprolactone copolymer nanofiber net, glial scar, neurodegeneration.*

Introduction

Traumatic brain injury (TBI) and its sequels constitute a serious, critical public health and socioeconomic problem throughout the world. It is the most important cause of mortality and disability mostly among young population in the world because of different causes of trauma, i.e. the rising number of motor vehicle accidents [4,5,14,18,21]. This is the problem not only in the highly developed countries, but in other countries, too. There are short- and long-term aspects of clinically visible consequences of TBI. The instant or early posttraumatic consequences are monitored and treated after hospital admission; many of them are caused by neurosurgical interventions. Long-term consequences of TBI, or so-called posttraumatic syndrome, was divided to three major categories, physical, cognitive and psychological [17]. The progress of posttraumatic long-term consequences of the above mentioned diseases is unpredictable. It is known that even very minor brain damages can

Communicating author:
Dorota Sulejczak, Department of Experimental Pharmacology, Mossakowski Medical Research Centre, Polish Academy of Sciences, 5 Pawinskiego Str., 02-106 Warsaw, Poland, phone: +48 22 608 65 81, fax: +48 22 608 65 90, e-mail: dsulejczak@imdik.pan.pl

result in the most severe symptoms, conditions and consequences [13,23,31,33,34].

Another aspect to discuss is the potential trauma of post-surgical interventions due to the changes in the region of preparation, described as an oedematous or vascular lesion. Obviously, the neurosurgical interventions to the brain should be minimally invasive, which means avoiding additional brain trauma, using safety entrance region to the lesions, avoiding inappropriate microsurgical manoeuvres. However, the posttraumatic brain injury and micro trauma after surgery can induce and initiate pathological machinery into parenchyma and possible potential cascade of changes that result, in the long run, in progressive tissue damage [24]. After trauma, unfortunately there is no efficient neuroprotective treatment avoiding inflammatory response and this information is crucial for developing preventive and new treatment strategies.

It is known that the scar tissue can be formed as a consequence of injuries or damages such as tumour or traumatic brain injury. Brain scar tissue can obstruct proper healing and brain function and may slow the nerve regeneration in the brain. It is known that disrupted nerve growth results in neural dysfunctions. This is the cause of symptoms in patients with brain damage involving the scar. Additionally, untreated scar can further worsen the brain function.

One of the possibilities to remove brain scar tissue is to eliminate it by surgery. However, depending on where the scar tissue is located and how much it is, not all of it may be removed. New technologies, such as nanotechnology, provide a variety of different treatment options of getting rid of the brain scar tissue as well as encouraging brain nerve regrowth.

In our earlier studies we used a rat model of surgical brain injury (SBI) for investigating the consequences of brain damage and scar formation [9]. In this animal model, the SBI is done by excising a moderate-sized piece of sensorimotor cerebral cortex. This model imitates well the respective human neurosurgery situation in that it involves the most typical early consequences of TBI, such as brain oedema and neuronal death. The changes are very similar to those observed following brain ischemia [15,35].

The electrospinning has been known since the 1930s. It is a comparably cheap and versatile method of production of micro- and nanofibers of a diameter ranging from a few micrometers to a few nanometres. In the process, a fluid filament is stretched in a strong electric field and produces material that is collected as a nonwoven mat of micro- and nanofibers. Biomedical applications of nanofibers are concentrating on a unique property of micro- and nanofibers – they can mimic extracellular collagen matrix (fibrils size of 50-500 µm) [1]. The membranes are colonized by cells and nativized. If nanofibers are produced from biodegradable material they can serve as a temporary scaffold for externally produced implants seeded by cells. In such case, artificial nanofibrous scaffold is gradually digested by the cells and replaced by a native collagen matrix.

Implantable devices made of micro-nanofibers are supporting guided cells growth for the use in regenerative medicine to rebuild damaged, worn or aged tissue. For such types of applications, electrospun nanofibers have been tested for the urinary bladder wall regeneration, bone scaffold coatings, scaffolds for skin regeneration, post-surgery barrier material [e.g. 3]. Nanofibers are manufactured at a room temperature that enables to produce membranes made of temperature-sensitive materials (e.g. polyhydroxyesters or proteins) [19]. Different types of drugs or even living cells can be incorporated into the material. Materials of biological significance are produced by the electrospinning process [11,25].

The aim of our present study was to examine the influence of the wound dressing material made of electrospun nanofiber membrane (nanofiber mat/net) on injured brain parenchyma in an SBI rat model.

Material and methods

All applied routines involving animals were authorized by the 4th Local Animal Experimentation Ethics Committee and were compatible with European Union regulations governing the care and use of laboratory animals. Animals were kept in precisely specified and controlled conditions: in 60-70% relative humidity and temperature 20°C at 12 h/12 h light/dark cycle (lights on at 7 a.m.), and were fed on standard food for laboratory rodents (Ssniff M-Z, ssniff Spezialdiäten GmbH, Soest, Germany) and purified tap water *ad libitum*. Experiments were carried out on adult Wistar male rats, weighing at the beginning of the experiment 200-250 g. Animals were divided into five experimental groups:

1) control, intact animals (sacrificed in the following time points: 4, 7, 14 and 30 day of the experiment; 7 animals for each investigated time point),
2) animals with applied biodegradable nanofiber dressings on the surface of undamaged cerebral cortex (sacrificed in the following time points: 4, 7, 14 and 30 day of the experiment; 7 animals for each investigated time point),
3) animals with the surgical injury of the cerebral cortex made (sacrificed in the following time points: 4, 7, 14 and 30 day of the experiment; 7 animals for each investigated time point),
4) sham-operated animals (full procedure of the scull trepanation was conducted) sacrificed in the following time points: 4, 7, 14 and 30 day of the experiment; 7 animals for each investigated time point,
5) animals with the surgical injury made with applied biodegradable nanofiber dressings on the surface of postoperative wound (sacrificed in the following time points: 4, 7, 14 and 30 day of the experiment; 7 animals for each investigated time point).

Nanomaterials used in our study were produced by electrospinning of poly (L-lactide-*co*-caprolactone) (PLCL, containing 70% L-lactide and 30% caprolactone units) purchased from Purac Biochem BV, Gorinchem, the Netherlands, and dimethylformamide (DMF) purchased from POCH, Poland. All of the materials were used without any further purification. The electrospinning process was performed according to the procedure described in detail earlier [19]. Briefly, the electrospinning solution was made of 9% of PLCL dissolved in 1:9 (wt/wt) mixture of DMF and $CHCl_3$. The solution flow rate was fixed at 500 µl/h, positive electric potential of the 0.75 kV/cm was applied to the needle and spinning distance was 20 cm. The resulting polymer nanofibers were collected on a rotating drum (3000 rpm) covered with aluminium foil. The structure of the mat was examined by the Scanning Electron Microscopy (SEM, Jeol, JSM 6390 LV, Japan). Fibers were sputtered with a gold (mini sputter coater SC 7620, Polaron, United Kingdom) and the thickness of fibers and whole mats were analyzed. The thickness of fibers was 0.5-2.3 µm and the size of investigated mats was 80-120 µm. Porosity of the material was calculated by dividing the density of the nanofibrous mat (net) by PLCL density (1.17 g/cm^3), according to the method presented by Lee, it was 69% [22].

Neurosurgical damage of some part of the somatosensory cerebral cortex was performed according to the procedure described previously [7]. In short, the operation of surgical injury of the cerebral cortex was performed under deep anaesthesia (20 mg/kg ketamine hydrochloride). After the skin was incised, the frontal bone was trepanned 2 mm laterally from the bregma and 2 mm anteriorly to the coronal suture and the meninges was incised. The operated cortex (a 2 × 2 × 2 mm region of the somatosensory cortex) was hemisected with a small scalpel and the wound was closed. The skin wound was sutured. After the operation, the animals were placed in standard animal house conditions under the experimenter's care. After the above specified survival times the animals were perfused and material collected from their brains was evaluated using techniques of light and electron microscopy (see below).

All animals were deeply anesthetized using Nembutal (80 mg/kg b.w., i.p.) and perfused by the ascending aorta, initially applying 0.9% NaCl in 0.01 M sodium-potassium phosphate buffer pH 7.4 (PBS), and afterwards with 'regular' ice-cold fixative (with 4% formaldehyde in 0.1 M phosphate buffer pH 7.4 for light microscopy or with 2% paraformaldehyde and 2.5% glutaraldehyde in 0.1 M cacodylate buffer, pH 7.4 for transmission electron microscopy), as described earlier [7]. Following the perfusion, the brains were taken away from the sculls to be immersed for 2 h in the same fixing agent. Afterwards, the brains were saturated with sucrose through immersing in 10, 20 and 30% (w/v) sucrose solutions in PBS and cut to 40 µm-thick free-floating coronal sections applying a cryostat (CM 1850 UV, Leica, Germany). In the next step, the sections were prepared for immunohistochemical (IHC) studies.

Free-floating brain sections were preincubated with 3% normal goat serum solution in PBS supplemented with 0.2% Triton X-100 (PBS+T). Subsequently, the sections were incubated for 1 h at 37°C with PBS+T containing 1% normal goat serum and following primary antibodies (Abs): 1) murine monoclonal Ab against NeuN (Chemicon, USA, dil. 1 : 1000); 2) murine monoclonal Ab against GFAP (Chemicon, USA, dil. 1 : 1000); 3) murine monoclonal Ab against Vimentin (Santa Cruz, USA, dil. 1 : 400) and 4) murine monoclonal Ab against macrophages (Santa Cruz, USA, dil. 1 : 400). The reaction was terminated by washing the sections with PBS+T. Next, the sections were incubated for 1 h at 37°C with the respective secondary Abs. The secondary Abs used were as follows: 1) goat anti-mouse antibody

conjugated with Alexa Fluor 594 (Invitrogen, USA, dil. 1 : 100) or 2) goat anti-mouse antibody conjugated with HRP (Bio Rad, USA, cat. no. 170-5047, dil. 1 : 1000; and the reaction was visualized using DAB as a chromogen). Finally, the sections were rinsed with PBS+T, mounted on silanized glass slides (Sigma) and covered with Vectashield mounting medium for fluorescence microscopy (Vector Labs Inc., Burlingame, CA, USA).

Immunostaining was detected with a model Optiphot-2 Nikon fluorescent microscope (Japan) equipped with the appropriate filters, and recorded with a model DS-L1 Nikon camera (Japan). Specificity of the immunostaining was verified by performing a control ("blank") staining procedure with primary antibodies omitted in the incubation mixture. No staining was observed in these control sections.

Morphology of cell nuclei was examined on brain sections mounted on microscope slides. Sections were washed in PBS and incubated in a 1 µg/ml solution of Hoechst stain (bisbenzimide dye, No 33258, B-2883, Sigma; prepared in PBS) for 2 min at room temperature. The stain was then drained off and cover slipped with PBS for visualization.

Tissue specimens for electron microscopy analyses were collected from rats anesthetized and perfused as above. The tissue specimens for electron microscopy analyses were collected from the cerebral cortex bordering the surgical cortical injury in the operated rats and from the related cortex part in the control rats. The specimens were handled with the typical ice-cold fixative (see above) post-fixed in 1% (w/v) OsO_4 solution in deionized water, dehydrated in an ethanol gradient, and at last encased

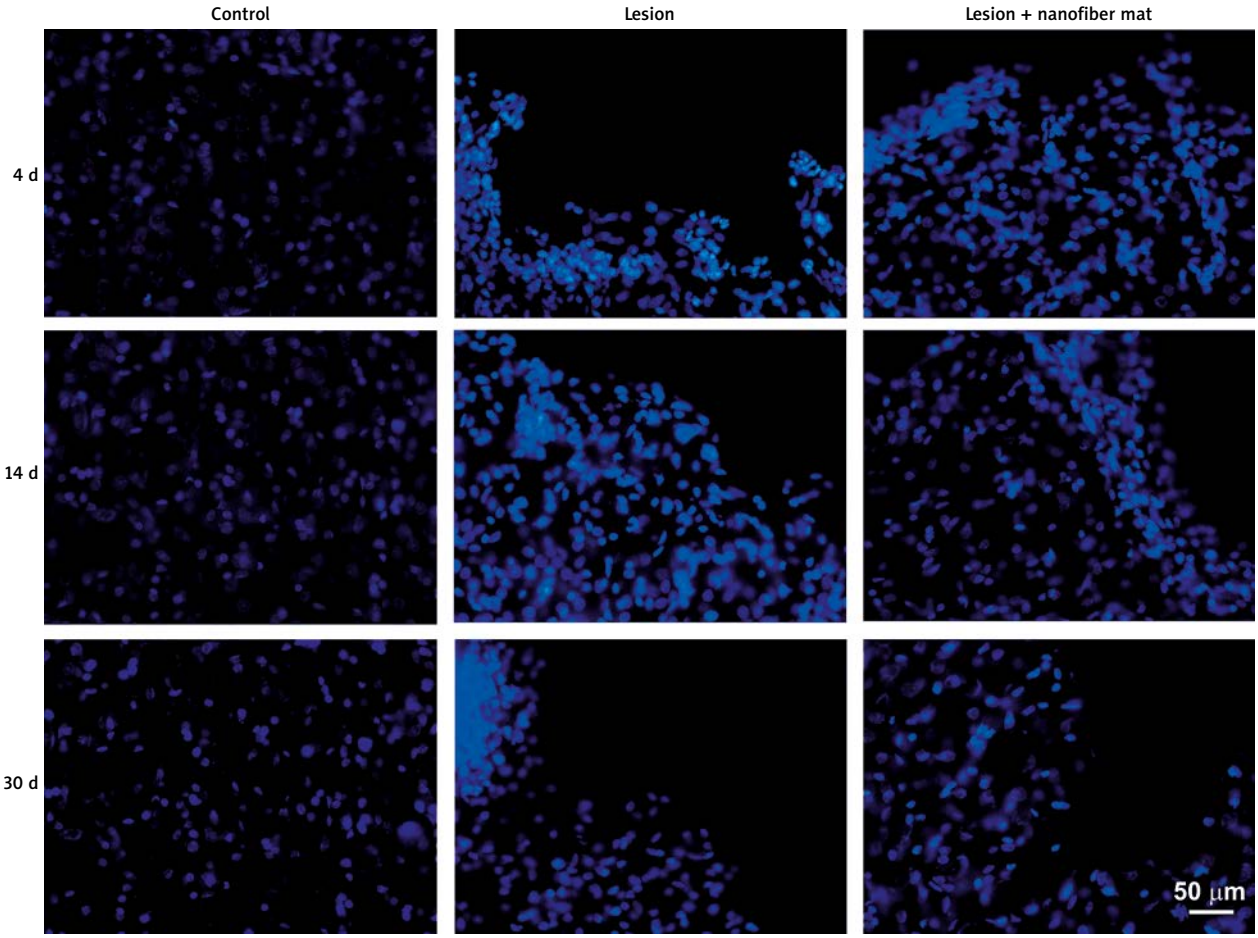

Fig. 1. Hoechst labelling of cell nuclei. The control cortex shows the presence of numerous nuclei with unchanged morphology (left panel). The lesioned cortex shows many cells with pyknotic nuclei revealed by intense fluorescence (middle panel). Application of the poly-caprolactone nanofiber mat at the time of the lesion (right panel) hampers the changes in the nuclear morphology.

in epoxy resin (Epon 812). Ultrathin (60 nm) sections were prepared as described earlier [8]. Material was examined in a transmission electron microscope (JEM-1200EX, Jeol, Japan).

GFAP-positive structures (processes and somata) forming the glial scar on the wound were examined using the Scion Image software (Scion Corp.). The GFAP-positive structures are reduced to a single pixel in width.

Results

Brain sections of intact control animals (experimental group 1) from all investigated time points revealed a proper morphological structure of all composing elements of the neurovascular unit: neurons, astrocytes and capillary blood vessels (Figs. 1-5). Similar results were obtained in the respective samples from sham-operated animals – experimental group 4 (data not shown).

Analysis of samples from the rats with nanofiber net dressing placed on the surface of intact neocortex (experimental group 2) has demonstrated no major changes in the examined structures (data not shown). In particular, there were neither neurodegeneration nor inflammatory reaction in the brain cortex as evidenced by the absence of macrophages. We also did not detect any activated astro- and microglial cells, only a slight increase in the number of GFAP-positive astrocytes was found in the vicinity of the dressing, but the cells showed no signs of hypertrophy (data not shown).

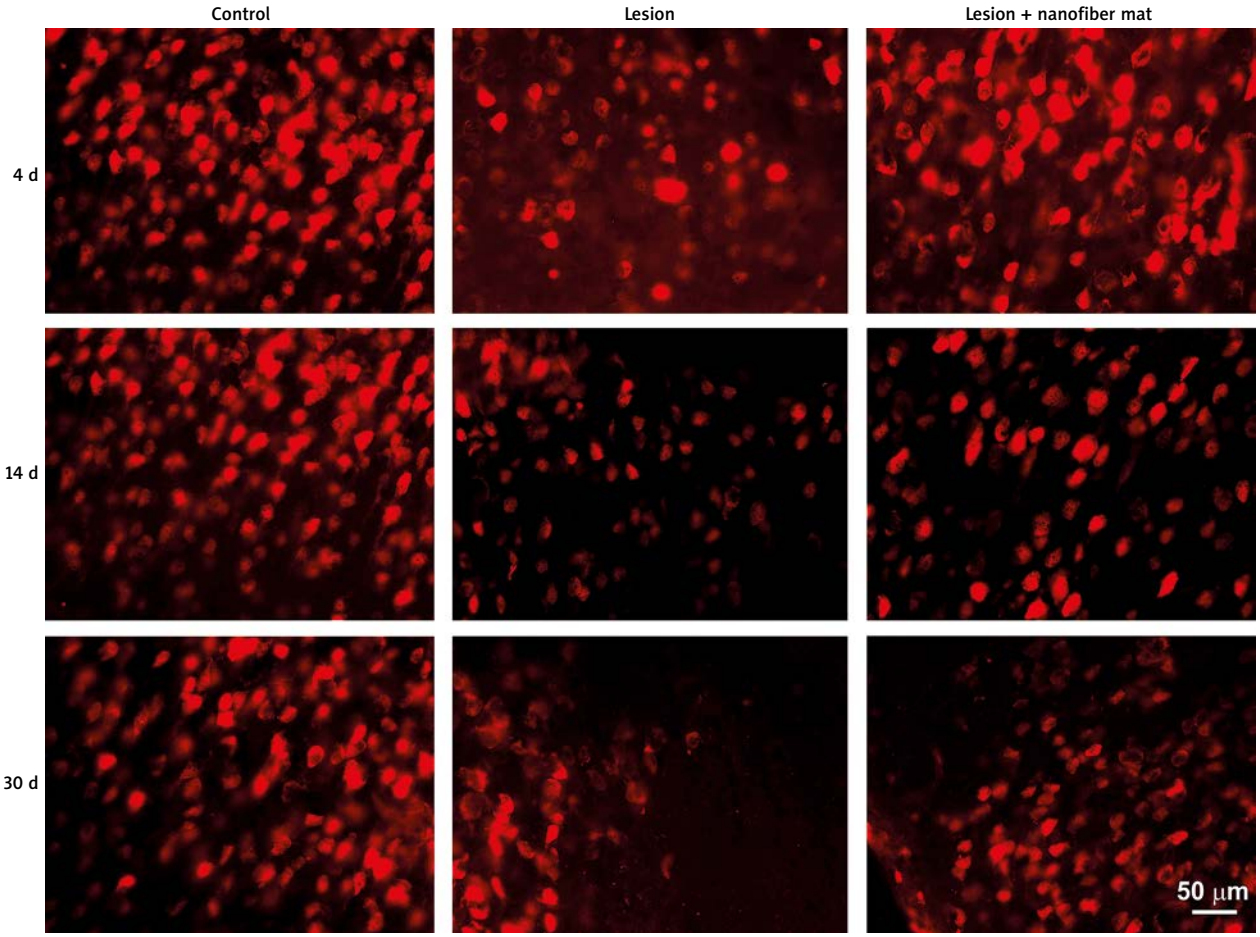

Fig. 2. NeuN immunostaining of rat cerebral cortex. Cortical sections derived from control animals (left panel) show the presence of numerous intensively stained neurons. Material from the damaged cortex (middle panel) shows a major decrease in staining intensity and in the number of labelling cells. Sections from brains dressed with nanofiber nets (right panel) show many neurons revealing intense immunosignal in all investigated time points.

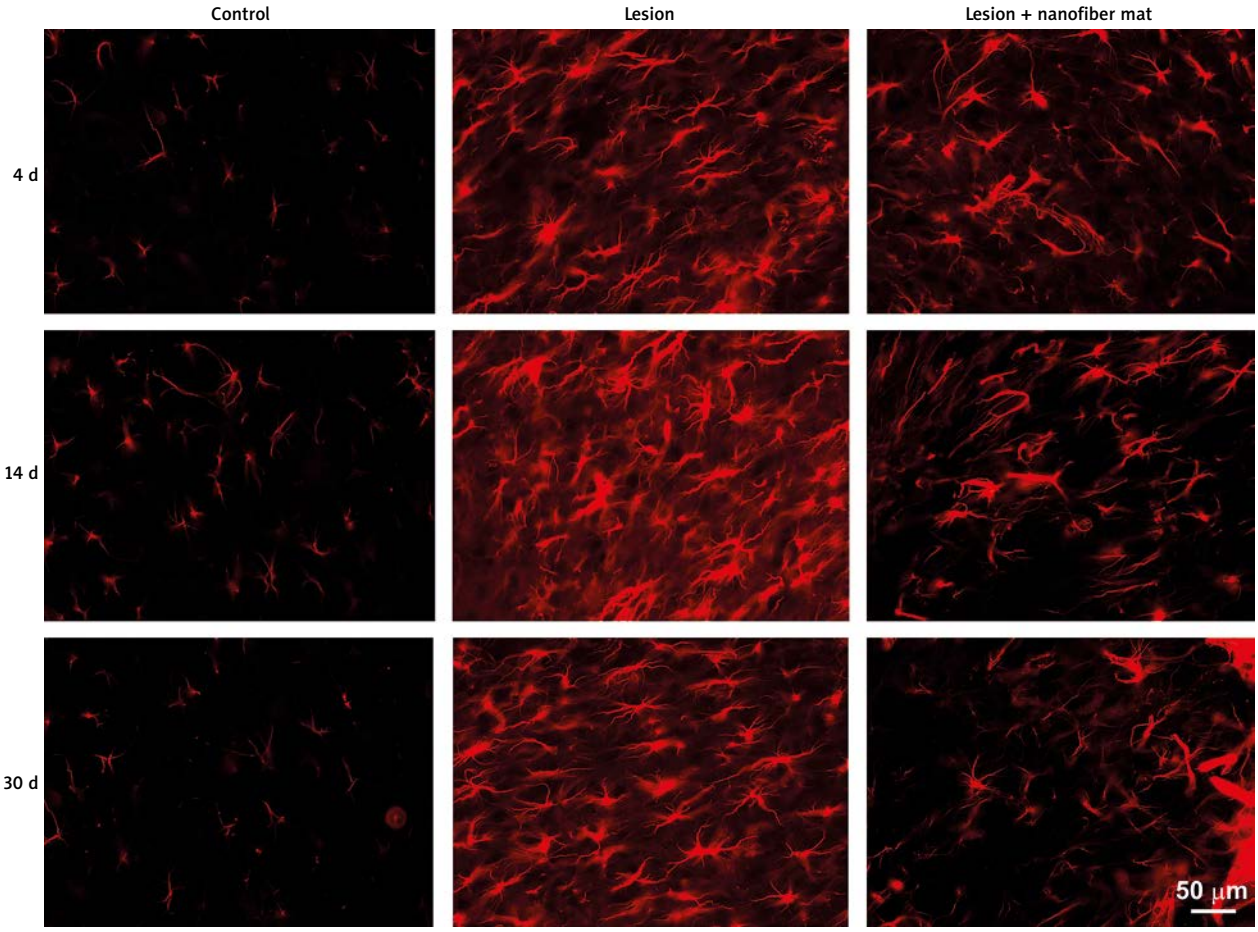

Fig. 3. GFAP immunostaining within the cerebral cortex area located distant to the lesion. Sections from the control cortex show scanty GFAP immunoreactivity (left panel). In the lesioned cortex, a massive increase in GFAP signal and astrocyte activation is visible (middle panel). Following the application of the nanofiber mat, the number of astrocytes and the intensity of GFAP signal were smaller than those observed in the injured animals (right panel).

Brain sections from rats subjected to the surgical lesion of the cerebral cortex (experimental group 3) showed massive death of neuronal cells (Figs. 1 and 2), which was most intense between 4 and 14 days post-surgery, and were associated with macrophage influx from the site of the trauma (Figs. 5C and 6). Electron microscopic data confirmed and extended that result. We found many macrophages localized in the vicinity of the lesion. We also detected numerous neurons dying *via* apoptosis and only few apoptotic astrocytes (data not shown).

Starting from the early post-surgery times (4 days post-lesion) a massive hypertrophy of astrocytes was seen in the perilesional cortical area (Fig. 7). The same phenomenon was observed in the area located at some distance to the injured tissue (Fig. 3). The scar-forming GFAP-immunoreactive (GFAP-IR) cells observed in the later post-operative time points were highly hypertrophied (Fig. 7), and some of the scar-forming astrocytes were vimentin-positive (Fig. 8). Some of the astrocytes located in the distance to the damaged cortical region were vimentin-positive too (Fig. 4). The activation of astroglial cells and glial scarring were associated with the formation of new capillary blood vessels in the perilesional area (Fig. 9). Thirty days post-lesion the scar formed at the site of the trauma showed signs of destabilization and secondary degeneration (Fig. 9B).

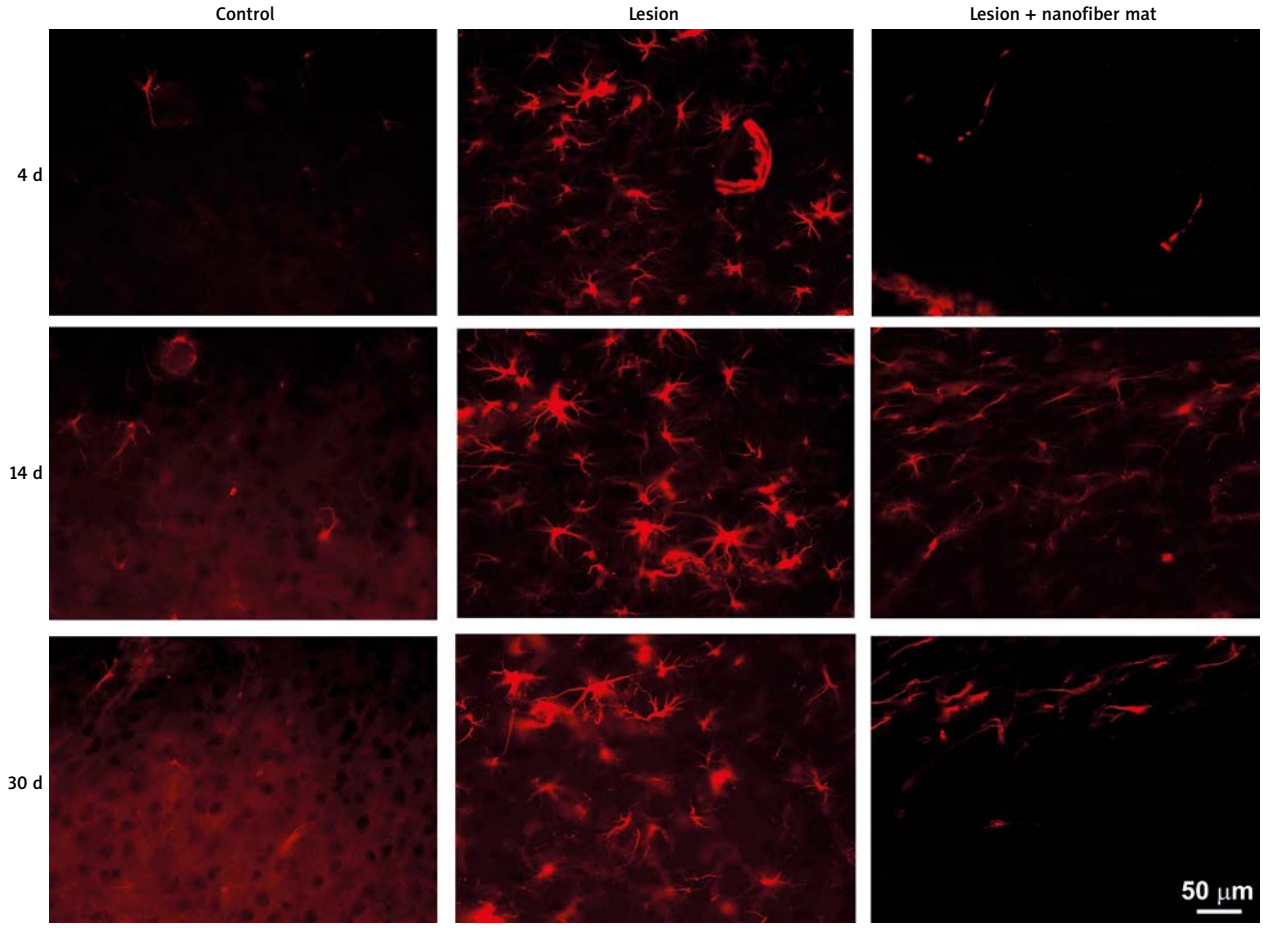

Fig. 4. Vimentin immunostaining within the cerebral cortex area located distant to the lesion. In the control cortex, negligible vimentin immunoreactivity was observed (left panel). The injured cortex revealed increase in the staining intensity (middle panel). Application of the nanofiber mat (right panel) counteracts the change.

The analysis of brain sections from the rats subject to surgical neocortex lesion that has been dressed with the nanofiber net (experimental group 5) showed only weak inflammatory signs. In particular, no macrophage infiltration or only single macrophages were found in the investigated brain area (Figs. 5D and 6).

There was also no formation of new blood vessels and no massive glial scarring (Fig. 5D). Several induction of astroglia (GFAP- or vimentin-positive cells) (Figs. 3, 4 and 7, 8) and formation of a subtle, barely visible glial scar on the surface of the lesioned neocortex were observed. Additionally, the glial scar was much thinner than that observed in the lesioned brains without dressing with nanofiber mat. Its structure was also much more "orderly" (see Figs. 5D, 7 and 8).

The GFAP immunoreactive structures (perikarya and cell processes) were analyzed with use of the Scion Image software, where these structures were reduced to a single pixel in thickness (Fig. 10).

Discussion

Membranes manufactured using the electrospinning method have bounded permeability, particularly for cells, however, permanent drainage of their decomposition products is kept. Besides, nutrient, oxygen and metabolites diffuse with ease through the membrane. The above membranes were made of micro- and nanofibers, which – because of their similarity to the Extracellular Collage Matrix – are treated as a natural environment by cells. The electrospun membranes are composed of polyester which gained medical approval: poly(L-lactide-*co*-caprolac-

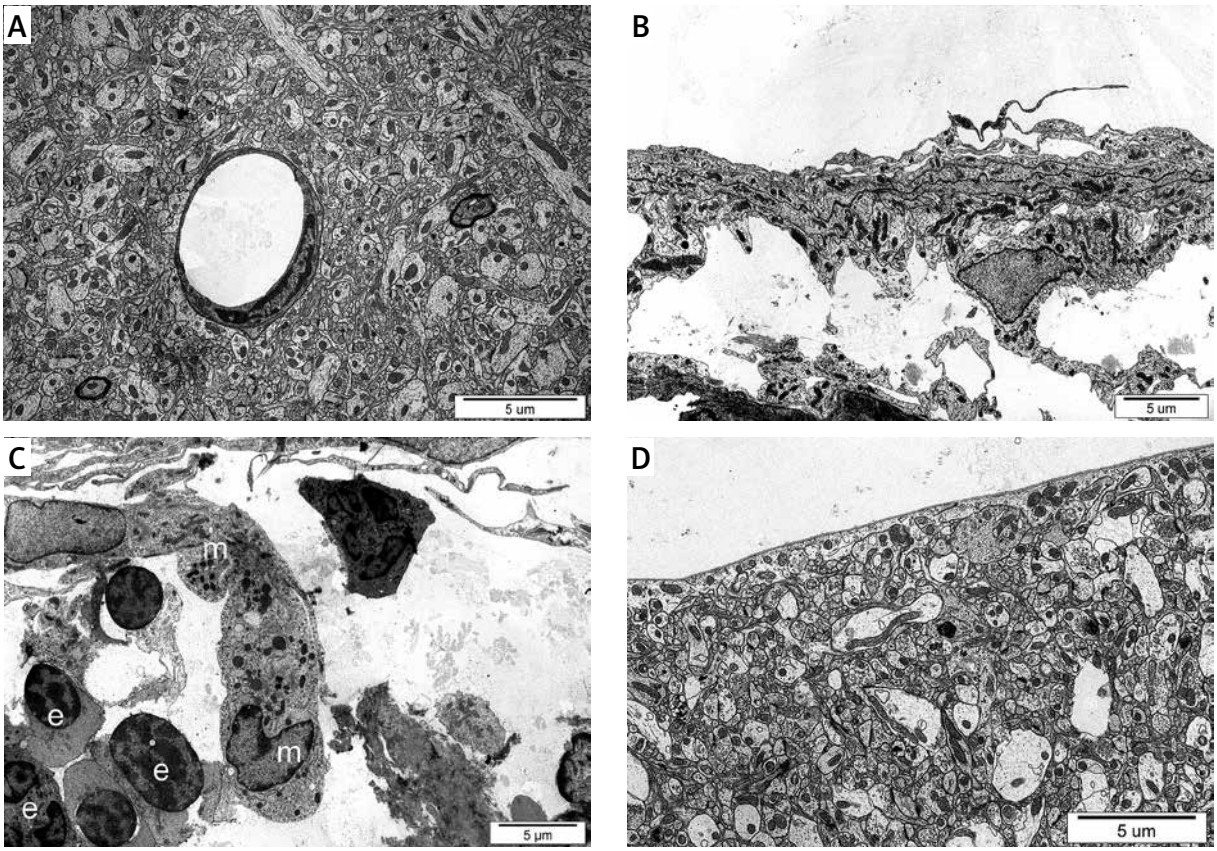

Fig. 5. Electronograms of the control (sham-operated, **A)** and lesioned cerebral cortex **(B-D)**; 4 days post-lesion. Electronogram B reveals massive glial scarring observed in the absence of the nanofiber net in the cortical molecular layer. The zone above the lesion **(C)** shows the presence of macrophages (m) and probably lymphocytes (e). Nanofiber net application at the time of the lesion attenuates the scarring and prevents infiltration of morphotic blood elements **(D)**. Electronogram D shows a part of the cortical molecular layer.

tone) (PLCL). PLCL is a copolymer of lactic acid and 6-hydroxyhexanoic acid. The electrospun mat was used to protect damage brain tissue from further progressing injury in the SBI rat model. Gradual biodegradation (12-24 months) of the mat was supposed to promote the correct healing process.

There are two kinds of products of membrane degradation: natural metabolite (lactic acid) and its analogue (6-hydroxyhexanoic acid). By reason of chemical character, both of acids in high concentrations have an irritating action to tissue. Lactic acid (pKa = 3.83) is eight times stronger than its non-toxic analogue – 6-hydroxyhexanoic acid (pKa = 4.75). Although the fibrous mat maintained strength comparing to the solvent-cast membrane, it was created from far less material. Thanks to contact of the damaged tissue with far less irritating hydroxy acids (produced during hydrolysis), inflammation is presumed to be much lower. Solvent-cast polymeric membranes accumulate hydroxy acids which were formed during the *in vivo* hydrolytic degradation of polyhydroxy acid (PHA), monomeric hydroxy acids. These acids play an autocatalytic role, that is they accelerate the process of hydrolytic degradation what in consequence causes faster degradation of thicker materials. The fibrous structure is also a key issue for the stability of the membrane. The nanofibrous mat is easily emptied by biological fluids and do not accumulate hydroxy acids. A class of biopolymers, aliphatic polycarbonates, which was widely studied by the authors before [26-29], creates a very weak carbonic acid during the hydrolytic degradation and therefore is free from the problem of autocatalytic hydrolysis.

Nanomaterials have a huge potential for the new techniques in the tissue engineering. The aim of tis-

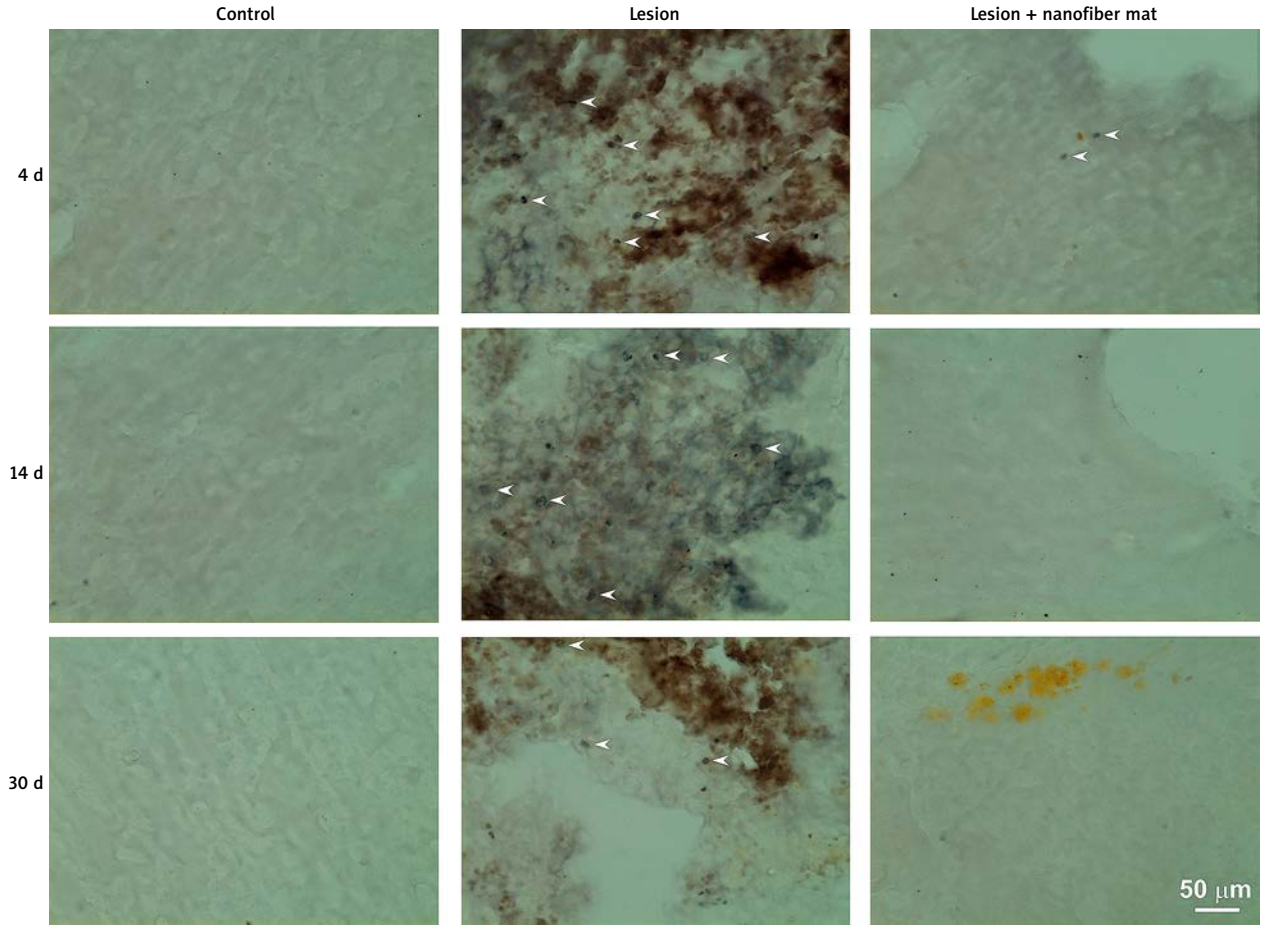

Fig. 6. Macrophages immunostaining. Macrophages in the cerebral cortex. In the control cortex we did not find any macrophages (left panel), but numerous macrophages were detected in the lesioned cortex (middle panel). Tissue dressed with the nanofiber mat (right panel) show only few macrophages at the early experimental time point.

sue engineering and regenerative medicine is to produce a biological substitute in order to restore, maintain or repair damaged tissue and organ functionality.

Our preliminary research employs the electrospun nanofiber mat in order to prevent nervous tissue from cicatrization after surgical injury. Glial scar formed after brain injury is an effective barrier preventing regeneration of the damaged area of the brain. Moreover, delayed consequences of such injuries are reported [31]. Prevention of nervous tissue from cicatrization leads to its better post-damage condition.

Our model imitates well the respective human neurosurgery situation and involves the most typical consequences of SBI, such as brain oedema and neuronal death. The model makes it possible to study various processes accompanying the course of repairing and rebuilding the damaged area of the brain at different time intervals after the injury.

The results obtained from intact animals (experimental group 1) analyzed at all experimental time points show proper morphology of all neurovascular unit components. Similar data were obtained from the brains derived from animals of experimental group 2 (animals with the nanofibrous mat applied on the undamaged cerebral cortex). These data let us to suppose that the nanofiber nets did not evoke inflammation, e.g. they meet the first criterion to be used as a material for medical applications.

Results of analysis of material harvested from animals of experimental group 4 (sham-operated rats) were similar to results of the control group.

Results of experimental group 3 (animals with performed surgery) revealed that surgical injury

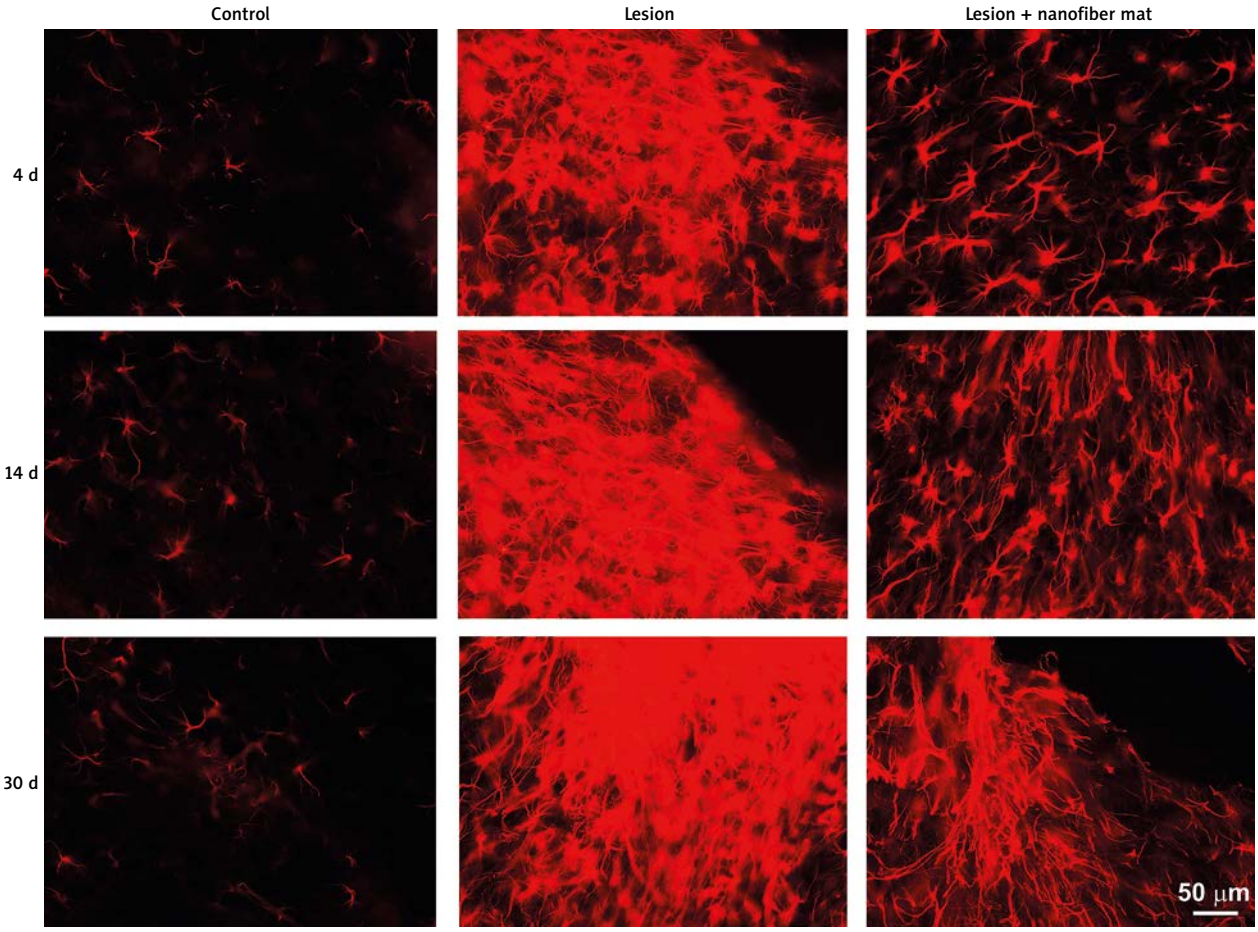

Fig. 7. GFAP immunostaining of the cortical region adjacent to the lesion. The control cortex shows scanty GFAP immunoreactivity (left panel). The cortical lesion induces massive increases in the staining and astrocyte activation (middle panel). Application of the nanofiber mat (right panel) counteracts the changes.

of the cerebral cortex leads to degeneration and death of cells close to the wound. Afterwards, it also affects areas distant to the lesion [32]. In the cortex of animals of this group we detected numerous dying neurons with features indicating apoptosis (highly condensed nuclear chromatin, the presence of apoptotic cells) as well as necrosis (cells bloating, defecting of cell organelles). Our data confirmed the results of other investigators [6].

The trauma also disrupted the blood-brain barrier (BBB), which enabled massive migration of blood cells and serum into the wound area. Disruption of the BBB was an early feature of lesion formation leading to oedema, excitotoxicity and entry of serum proteins and inflammatory cells [11]. It is known that damage to the endothelium of blood vessels is a known pathway for initiation of inflammation. Monocytes from the bloodstream enter peripheral tissue and transform into macrophages, which are the primary phagocytes of the immune system [12].

At four days after the surgery we registered a considerable number of macrophages on the analyzed area of the cerebral cortex.

Astrocytes take part in all forms of CNS insults (e.g. trauma or ischemia) by a process commonly referred to as reactive astrogliosis. This process results in scar formation [30]. Reactive astrogliosis plays an essential role in orchestrating the (brain) injury response as well as in regulating inflammation and repair. In the analyzed model of brain damage as early as 4 days after injury, a massive astrogliosis appears and at later post-lesion time points, glial scar formation starts at the place of damage [7].

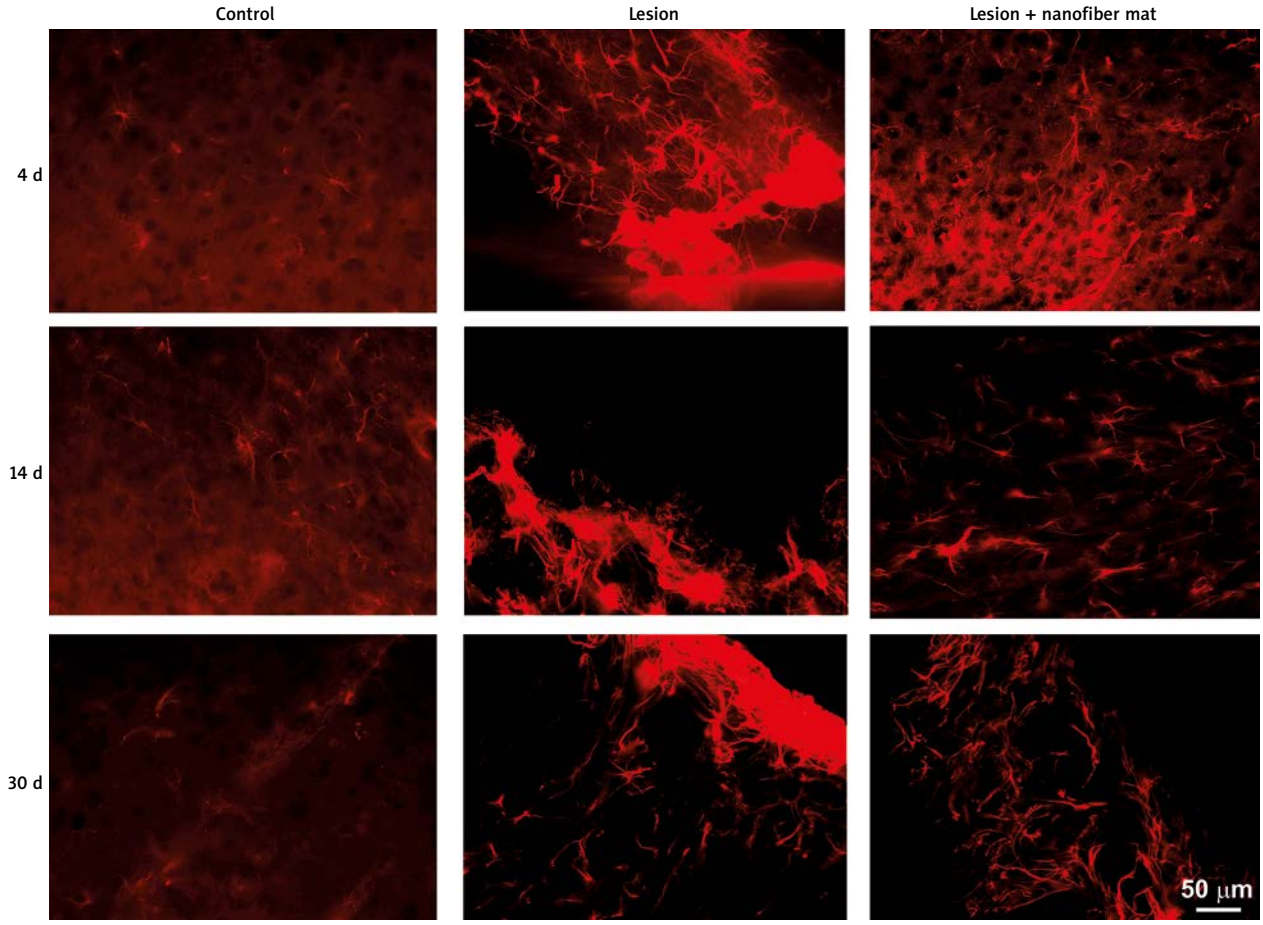

Fig. 8. Vimentin immunostaining of the cortical region adjacent to the lesion. The left panel shows sections from the control cortex with only weak vimentin immunoreactivity, opposite to the heavy immunoreaction visible in the injured cortical area (middle panel). Application of the nanofiber membrane (right panel) counteracts the changes.

Electron-microscopic (TEM) observations confirmed the light microscopic findings.

Numerous active astrocytes were part of the glial scar (GFAP- positive and Vim-positive) and possessed distinct attributes of hypertrophy. Astrocytes were arranged randomly and form a thick multilayer structure on the surface of the damaged cerebral cortex. Recent studies indicate the ambiguous role of reactive astrocytes in the formation of glial scars after the injury. On the one hand, it forms an effective barrier precluding the regeneration of nerve fibers on the damaged area, but on the other hand, it also precludes penetration of blood elements, which could additionally deepen the processes of degeneration through intensification of inflammatory processes in the tissue [16]. The contribution of immature (Vim-positive) astrocytes, occurring in the scar, in the promotion of regeneration after damage is also postulated. Nevertheless, our experiments conducted for an extended time after injury demonstrated that the glial scar is not a stable structure at this scale of time. Just 30 days after the operation, the initiation of scar decomposition and delayed degeneration in the area adjacent to the scar was observed. Considering these results we believe that the inhibition of reactive astrogliosis may be a useful therapeutic target in some situations.

At early postoperative time (4 days), the formation of new blood vessels in the area adjacent to the damage was observed. Nascent blood vessels, however, were morphologically anomalous to a high degree, which indicates its dysfunctionality. Most of them showed no pericytes in the vessel wall.

The main target of current research was to examine if the electrospun nanofiber mat may be useful as

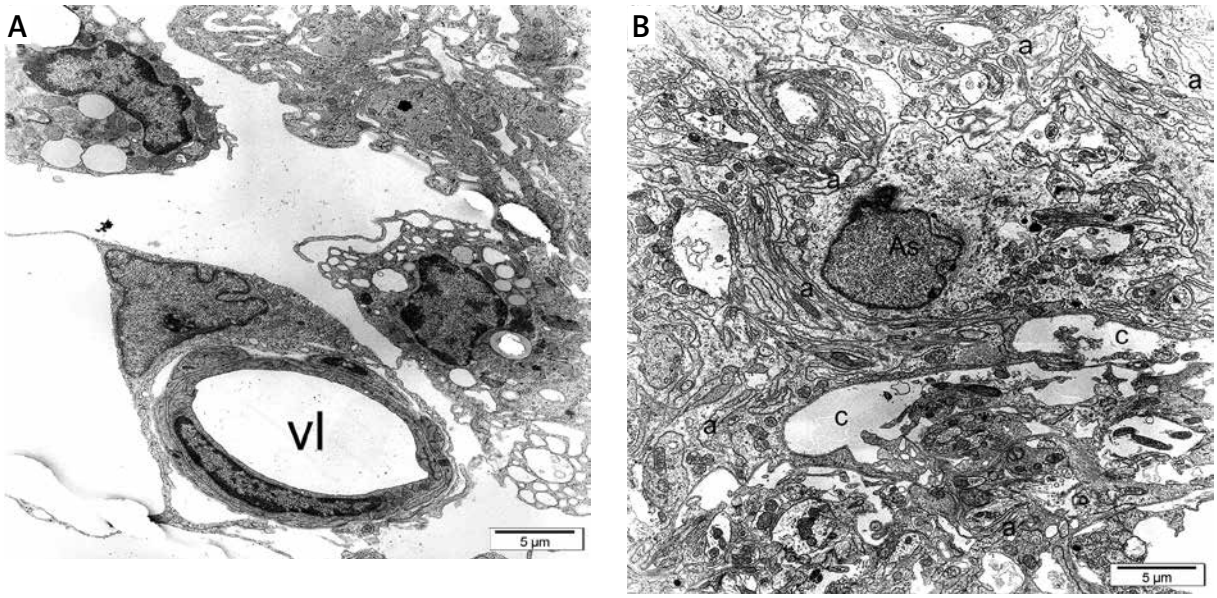

Fig. 9. Electronograms of the lesioned cerebral cortex. Electronogram **A** shows a new blood vessel formed in the peri-lesion zone, 14 days post-lesion; "vl" denotes vessel lumen. Electronogram **B** shows the glial scar region, 30 days post-lesion. Note signs of scar destabilization: astrocyte (As) and astrocytic processes (a) with signs of swelling, "c"s denote cavities formed due to glial scar decay.

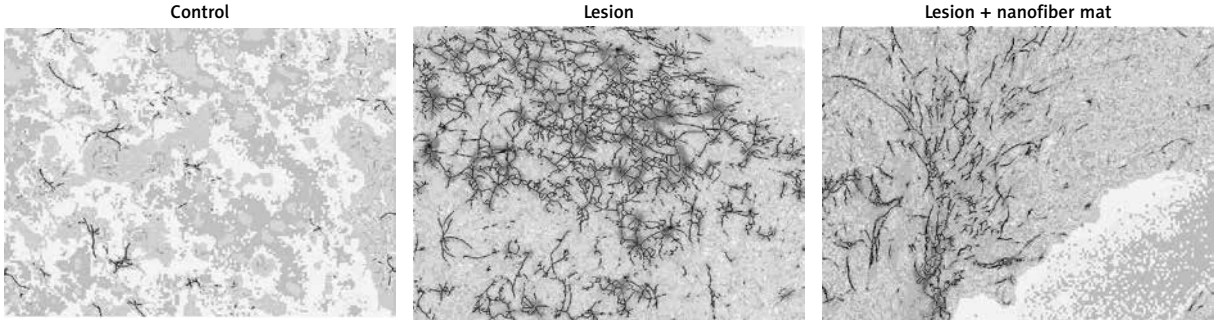

Fig. 10. Skeletonization of GFAP immunoreactive processes and somata. Note the highest density of GFAP-positive structures in the lesioned cortex with no nanofiber net application.

a barrier material preventing from cicatrization of the brain parenchyma. A massive astrogliosis observed in the experimental group 3 was not detected in the brains derived from animals with the nanofiber mat applied on the injured cortex (experimental group 5). Observed astrocytes did not show any signs of hypertrophy. Interestingly, a glial scar was formed by astrocytes organized in a more "orderly" manner than that observed in experimental group 3. The scar was also much thinner and had an ordered character. No influx of macrophages was observed in the area of damaged tissue. It suggests that the nanofiber net may protect tissue against the cascade of uncontrolled damage resulting from excessive proliferation of astrocytes and inflammation initiated. We suppose that the structure of the nanofiber mat can also simulate the structure of extracellular collagen matrix for the damaged tissue and have an influence on the lesion to particular components of the neurovascular unit. This would mean that the material simulating regular environment of extracellular matrix may modify the response of cells to the surgical injury. Furthermore, the main product of the nanofiber mat degradation, lactic acid, is postulated as a neuroprotective factor [2].

Conclusions

The nanofiber net used in this study is biocompatible and favourably modifies local inflammation

and cicatrization. Our results suggest that such nanofibers could be useful in neurosurgery.

Acknowledgements

This study was supported by the National Centre for Research and Development Project #NR13-0081-10-2010.

References

1. Barnes CP, Sell SA, Boland ED, Simpson DG, Bowlin GL. Nanofiber technology: designing the next generation of tissue engineering scaffolds. Adv Drug Delivery Rev 2007; 59: 1413-1433.
2. Berthet C, Lei H, Thevenet J, Gruetter R, Magistretti PJ, Hirt L. Neuroprotective role of lactate after cerebral ischemia. J Cereb Blood Flow Metab 2009; 29: 1780-1789.
3. Bretcanu O, Misra SK, Yunos DM, Boccaccini AR, Roy I, Kowalczyk T, Błoński S, Kowalewski TA. Electrospun nanofibrous biodegradable polyester coatings on Bioglass®-based glass-ceramics for tissue engineering. Mater Chem Phys 2009; 118: 420-426.
4. Bruns JR, Hauser WA. The epidemiology of traumatic brain injury: a review. Epilepsia 2003; 44 (Suppl 10): 2-10.
5. Cole TB. Global road safety crisis remedy sought: 1.2 milion killed, 50 milion injured annually. JAMA 2004; 291: 2531-2532.
6. Cruchten S, van den Broeck W. Morphological and biochemical aspects of apoptosis, oncosis and necrosis. Anat Histol Embryol 2002; 31: 214-223.
7. Frontczak-Baniewicz M, Chrapusta SJ, Sulejczak D. Long-term consequences of surgical brain injury – characteristics of the neurovascular unit and formation and demise of the glial scar in a rat model. Folia Neuropathol 2011; 49: 204-218.
8. Frontczak-Baniewicz M, Walski M. New vessel formation after surgical brain injury in the rat's cerebral cortex. I. Formation of the blood vessels proximally to the surgical injury. Acta Neurobiol Exp 2003; 63: 65-75.
9. Frontczak-Baniewicz M, Walski M. Glial scar instability after brain injury. J Physiol Pharmacol 2006; 57 (Suppl 4): 97-102.
10. Frontczak-Baniewicz M, Sulejczak D, Andrychowski J, Gewartowska M, Laure-Kamionowska M, Kozłowski W. Morphological evidence of the beneficial role of immune system cells in a rat model of surgical brain injury. Folia Neuropathol 2013; 5: 324-332.
11. Fryczkowski R, Kowalczyk T. Nanofibres from polyaniline/polyhydroxybutyrate blends. Synth Met 2009; 159: 2266-2268.
12. Geissmann F, Manz MG, Jung S, Sieweke MH, Merad M, Ley K. Development of monocytes, macrophages, and dendritic cells. Science 2010; 327: 656-661.
13. Giunta B, Obregon D, Velisetty R, Sanberg PR, Borlongan CV, Tan J. The immunology of traumatic brain injury: a prime target for Alzheimer's disease prevention. J Neuroinflammation 2012; 9: 185.
14. Hillier SL, Hiller JE, Metzer J. Epidemiology of traumatic brain injury in South Australia. Brain Inj 1997; 11: 649-659.
15. Jablonska A, Lukomska B. Stroke induced brain changes: implications for stem cell transplantation. Acta Neurobiol Exp 2011; 71: 74-85.
16. Kamel H, Iadecola C. Brain-immune interactions and ischemic stroke: clinical implications. Arch Neurol 2012; 69: 576-581.
17. Kiraly MA, Kiraly SJ. Traumatic brain injury and delayed sequelae: a review-traumatic brain injury and mild traumatic brain injury (concussion) are precursors to later-onset brain disorders, including early-onset dementia. Scientific World Journal 2007; 7: 1768-1776.
18. Koskinen S, Alaranta H. Traumatic brain injury on Finland 1991-2005; a nationwide registered study of hospitalized and fatal TBI. Brain Inj 2008; 22: 205-214.
19. Kowalczyk T, Nowicka A, Elbaum D, Kowalewski TA. Electrospinning of bovine serum albumin. Optimization and the use for production of biosensors. Biomacromolecules 2008; 9: 2087-2090.
20. Kowalewski TA, Barral S, Kowalczyk T. Modeling electrospinning of nanofibers. In: Pyrz R, Rauhe JC (eds.). IUTAM Symposium on modeling nanomaterials and nanosystems. Springer 2009; 13: 279-292.
21. Langlois JA, Sattin RW. Traumatic brain injury in the United States: research and programs of the Centers for Disease Control and Prevention (CDC). J Head Trauma Rehabil 2005; 20: 187-188.
22. Lee JB, Jeong SI, Bae MS, Yang DH, Heo DN, Kim CH, Alsberg E, Kwon IK. Highly porous electrospun nanofibers enhanced by ultrasonication for improved cellular infiltration. Tissue Eng Part A 2011; 17: 2695-2702.
23. Li H, McDonald W, Parada I, Faria L, Graber K, Takahashi DK, Ma Y, Prince D. Targets for preventing epilepsy following cortical injury. Neurosci Lett 2011; 497: 172-176.
24. McKee AC, Cantu RC, Nowinski CJ, Hedley-Whyte ET, Gavett BE, Budson AE, Santini VE, Lee HS, Kubilus CA, Stern RA. Chronic traumatic encephalopathy in athletes: progressive tauopathy after repetitive head injury. J Neuropathol Exp Neurol 2009; 68: 709-735.
25. Reneker DH, Yarin AL, Zussman E, Xu H. Electrospinning of nanofibers from polymer solutions and melts. In: Aref H, VanDerGiessen E (eds.). Advances in Applied Mechanics 2007; 41: 43-195.
26. Rokicki G, Kowalczyk T. Cyclic carbonates and spiro-orthocarbonates - perspective monomers in the polymer chemistry of polymers. Polimery 1998; 43: 407-415.
27. Rokicki G, Kowalczyk T. Synthesis of oligocarbonate diols and their characterization by MALDI-TOF spectrometry. Polymer 2000; 41: 9013-9031.
28. Rokicki G, Kowalczyk T, Glinski M. Synthesis of six-membered cyclic carbonate monomers by disproportionation of 1,3-bis (alkoxycarbonyloxy) propanes and their polymerization. Polym J 2000; 32: 381-390.
29. Rokicki G, Piotrowska A, Kowalczyk T. Cyclic carbonates used in the synthesis of oligocarbonate diols involving step growth polymerization. Polimery 2001; 46: 483-493.
30. Rolls A, Shechter R, Schwartz M. The bright side of the glialscar in CNS repair. Nat Rev Neurosci 2009; 10: 235-241.
31. Shively S, Scher AI, Perl DP, Diaz-Arrastia R. Dementia resulting from traumatic brain injury. What is the patology? Arch Neurol 2012; 9: 1-7.

32. Sulejczak D, Grieb P, Walski M, Frontczak-Baniewicz M. Apoptotic death of cortical neurons following the surgical brain injury. Folia Neuropathol 2008; 46: 213-219.
33. Tomkins O, Feintuch A, Benifla M, Cohen A, Friedman A, Shelef I. Blood-brain barrier breakdown following traumatic brain injury: a possible role in posttraumatic epilepsy. Cardiovasc Psychiatry Neurol 2011; 2011: 765923; doi: 10.1155/2011/765923.
34. Willmore LJ. Posttraumatic epilepsy: What's contusion got to do with it? Epilepsy Curr 2012; 12: 87-91.
35. Ziemka-Nalecz M, Zalewska T. Endogenous neurogenesis induced by ischemic brain injury or neurodegenerative diseases in adults. Acta Neurobiol Exp (Wars) 2012; 72: 309-324.

Original article

Folia Neuropathologica

Sphingosine kinases modulate the secretion of amyloid β precursor protein from SH-SY5Y neuroblastoma cells: the role of α-synuclein

Henryk Jesko[1], Taro Okada[2], Robert P. Strosznajder[3], Shun-ichi Nakamura[2]

[1]Department of Cellular Signalling, Mossakowski Medical Research Centre, Polish Academy of Sciences, Warsaw, Poland,
[2]Division of Biochemistry, Department of Molecular and Cellular Biology, Kobe University Graduate School of Medicine, Kobe, Japan,
[3]Laboratory of Preclinical Research and Environmental Agents, Department of Neurosurgery, Mossakowski Medical Research Centre, Polish Academy of Sciences, Warsaw, Poland

Folia Neuropathol 2014; 52 (1): 70-78 DOI: 10.5114/fn.2014.41745

Abstract

Sphingosine kinases (SphK 1&2) are involved in the regulation of cell survival, differentiation and neurotransmitter secretion. Current data suggest potential links between sphingolipid signalling, α-synuclein (ASN) and Alzheimer's disease (AD). Our aim was to investigate the possible role of SphKs and ASN in the regulation of the production and secretion of the amyloid β precursor protein (APP). We have previously shown that ASN intensified the secretion and toxicity of amyloid β (Aβ) to the point where it caused cell death. Our current results show that APP, the precursor protein for Aβ, is also influenced by ASN. The stable overexpression of wtASN in SH-SY5Y cells caused a three-fold, significant increase of the cellular APP level. This suggests that the influence of ASN on Aβ metabolism may actually occur at the level of APP protein rather than only through the changes of its cleavage into Aβ. To elucidate the mechanisms of APP modulation the cells were exposed to S1P and an SphK inhibitor (SKI). 72 h S1P treatment at 5 μM caused a nearly 50% reduction of the cellular APP signal. S1P also caused a tendency towards higher APP secretion, though the results were insignificant. The inhibition of SphKs decreased medium APP levels in a dose-dependent manner, reaching significance at 5 μM SKI with a correspondingly elevated intracellular level. Thus, it is reasonable to expect that in fact the influence of SphK activity on APP might be pro-secretory. This would also be in agreement with numerous articles on SphK-dependent secretion in the literature. The chronic nature of AD further suggests that subtle alterations in APP metabolism could have the potential to drive important changes in brain condition.

Key words: *sphingosine kinase, S1P, SH-SY5Y, Aβ, α-synuclein, neurodegeneration, AD.*

Introduction

Sphingosine kinases (SphK1&2) and their signalling pathways are key regulators of cell survival, proliferation and differentiation. Moreover, SphKs influence crucial functions of neurons such as the secretion of neurotransmitters or neurite shape. The SphK product sphingosine-1-phosphate (S1P) may play the role

Communicating author:
Robert P. Strosznajder, Laboratory of Preclinical Research and Environmental Agents, Department of Neurosurgery, Mossakowski Medical Research Centre, Polish Academy of Sciences, 5 Pawińskiego Str., 02-106 Warsaw, Poland, phone: +48 22 608 64 11, e-mail: rstrosznajder@yahoo.com

of an intracellular second messenger or act through cell surface receptors. The extracellular presence of S1P is dependent on the translocation of SphK1 to the plasma membrane; SphK2 can also undergo intracellular translocation, but the compartment and targets of S1P produced in such cases are different.

Accumulating evidence suggests the involvement of sphingosine kinases in a number of pathological conditions. Ageing is the crucial risk factor for Alzheimer's and Parkinson's diseases (AD and PD, respectively). The enhanced neuronal vulnerability to oxidative stress in ageing may be a result of the dysregulation of membrane lipids including sphingolipids [15]. Disturbed S1P levels could also potentially facilitate neurodegeneration-linked events such as ischaemic brain damage. S1P and especially its precursor, sphingosine, have already been found to possess some protective effects in the ischaemic heart model; it is tempting to speculate that it could be of interest in the brain ischaemia as well [36]. However, the results are highly unclear as S1P can be both cytoprotective [36] and sensitise the cells to oxidative stress-induced calcium dysregulation [5]; its changes in various organs seem to take different courses. The role of S1P in glutamatergic neurotransmission constitutes another important aspect of its potential influence of neuronal survival. The ischaemic damage is largely linked to a wave of uncontrolled neurotransmitter secretion. S1P takes part in the regulation of neuronal excitability and learning and memory phenomena [19]. It has been shown to trigger glutamate release and, importantly, to enhance depolarisation-induced secretion of the neurotransmitter [16].

It remains to be explained if conditions such as AD or PD can be affected by the age-related disturbances of sphingosine signalling and if these changes could create vulnerable background for the development of such diseases. Some results indeed point to the possible role of SphKs in AD. Sphingolipid signalling influences amyloid beta (Aβ)-induced inflammation [18]. Moreover, Aβ inhibits SphK1 activity in SH-SY5Y neuroblastoma [10] and selectively modulates the expression of some S1P receptor subtypes in monocytes [18]. Disturbances in sphingolipid metabolism are noted in AD starting from the earliest stages [20] with the levels of pro-apoptotic ceramide increased and activated catabolism of the usually pro-survival compound S1P. Importantly, changes observed correlate with cognitive decline. This phenomenon may potentially constitute a crucial factor of neuronal death and the resulting dementia. The levels of ceramides (Cer16, Cer18, Cer20, and Cer24) are changed in AD brains [8] and serum d18:1-C16:0 and d18:1-C24:0 ceramides are associated with an increased AD risk [25]. SphK overexpression reduces the toxic effect of Aβ [10]. Inhibitors of selected enzymes involved in sphingolipid metabolism may be extremely promising tools in AD research. Moreover, ceramide stabilises beta-secretase and boosts Aβ levels while glycosphingolipid depletion inhibits APP maturation and transport [29,34]. Thus, the ceramide-S1P 'biostat' shows vast potential as a possible important point of AD-related pathology.

Amyloid β and its precursor protein (APP) have long been viewed among the central elements of neuronal survival and death. However, more recent research has suggested that α-synuclein (ASN) may also be a factor of AD pathology. ASN is a small peptide of up to 140 amino acids; β- and γ-synucleins have also been identified. All synucleins are enriched in the central nervous system, particularly in the structures affected by AD: the neocortex, hippocampus and substantia nigra.

Despite classically being viewed as an intracellular protein, ASN has recently been found to undergo secretion [11] and uptake to the surrounding cells [22]. ASN is found in intracellular Lewy bodies present in Parkinson's disease and in ca. 60% of Alzheimer's disease (AD) cases. Moreover, a fragment of α-synuclein dubbed non-Aβ component of AD amyloid (NAC) is found in Aβ plaques in Alzheimer's and other diseases [35]. The immunoreactivity of ASN it self was also found in mature core amyloid plaques [3]. α-synuclein enhances amyloid β secretion from cells in culture twofold [21]. ASN also potentiates Aβ toxicity; this leads to mitochondrial damage and programmed cell death in a mode probably dependent on the Aβ load [21]. ASN could facilitate Aβ aggregation [24], though ASN-deficient models can also show accelerated Aβ aggregation [17]. The ASN level is increased in AD [3]. Finally, membrane-bound ASN physically interacts with amyloid β [24], though its mechanism and exact significance are highly unclear.

The currently available data suggest potential links between sphingolipid signalling and α-synuclein. Moreover, ASN may be engaged in Alzheimer's disease and modify the metabolism and fate of amyloid β precursor protein. The aim of our work was

to investigate the possible link between sphingosine kinase signalling, ASN and the production and secretion of APP.

Material and methods

Dulbecco's modified Eagle's medium (DMEM)/F12 and other cell media as well as inorganic reagents were from Wako. All-*trans* retinoic acid was from Sigma-Aldrich. Anti-APP (clone# 22C11) antibody was purchased from Millipore. SphK inhibitors were from Calbiochem; S1P from Biomol.

The human SH-SY5Y neuroblastoma cell line is known to be able to both proliferate and differentiate in culture and is able to express a number of neuronal features including beta dopamine hydroxylase activity and cholinergic and glutamatergic phenotypes. Low-passage (< 16), stably transfected wtASN-expressing SH-SY5Y cells were used for quantitative studies of S1P and SKI influence. As α-synuclein undergoes proteolytic degradation in certain cell states and all-*trans* retinoic acid (ATRA)-induced cell differentiation inhibits this phenomenon [30], we treated the cultures for five days with 10 μM ATRA. ATRA induced morphological changes towards a more arborised phenotype as shown in Fig. 1A. The survival of the differentiated cell line was found to be unaffected by the concentrations of S1P or SKI used, which differs somewhat from the situation in non-differentiated cells.

As the endogenous ASN levels were still very low (data not shown), a stably transfected cell line was prepared for use in the ASN quantification experiments. Standard molecular biology methods were employed. A full-length human ASN sequence was cloned from total RNA using proofreading RT-PCR

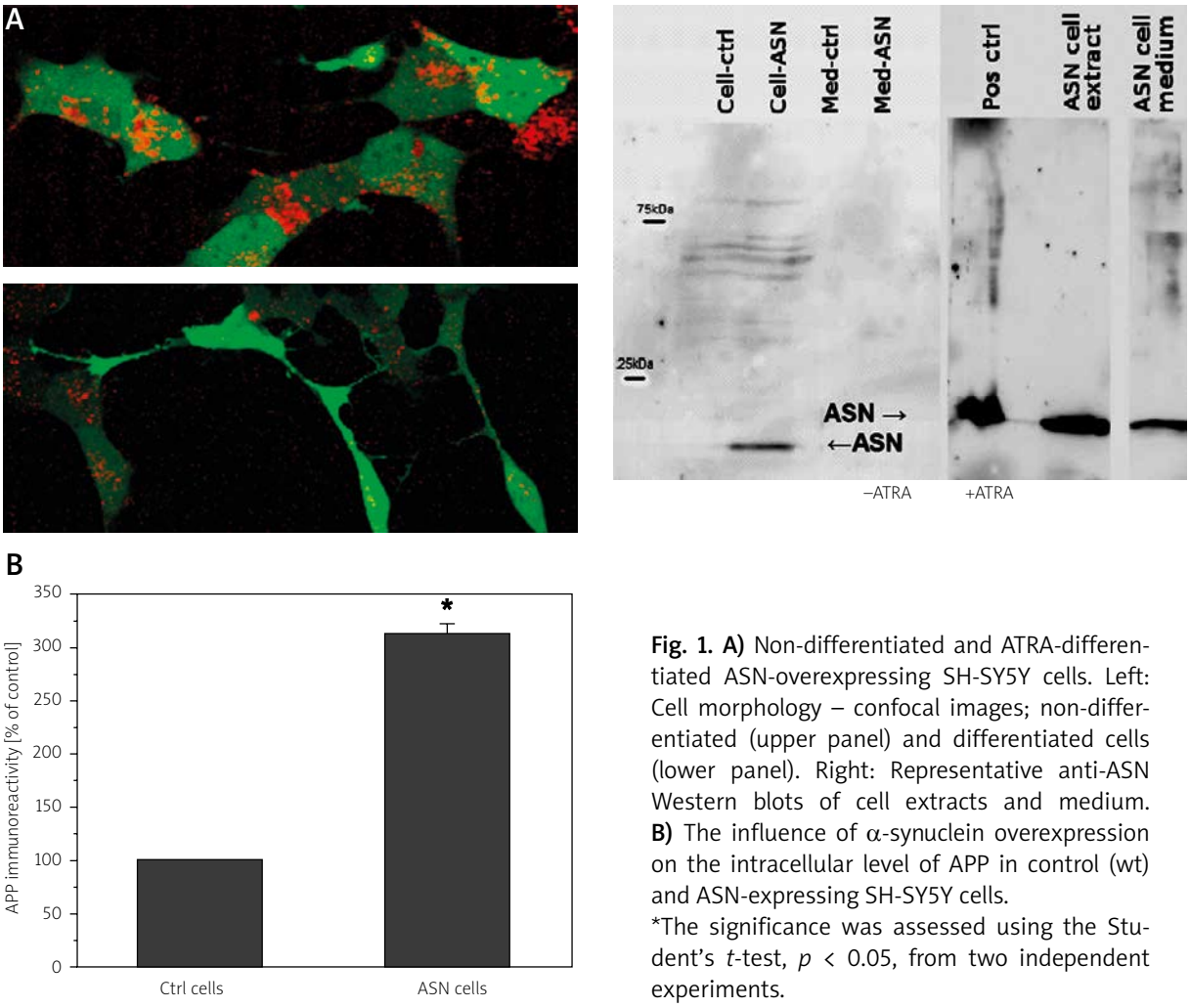

Fig. 1. A) Non-differentiated and ATRA-differentiated ASN-overexpressing SH-SY5Y cells. Left: Cell morphology – confocal images; non-differentiated (upper panel) and differentiated cells (lower panel). Right: Representative anti-ASN Western blots of cell extracts and medium. **B)** The influence of α-synuclein overexpression on the intracellular level of APP in control (wt) and ASN-expressing SH-SY5Y cells.
*The significance was assessed using the Student's *t*-test, $p < 0.05$, from two independent experiments.

(Roche Transcriptor Hi-Fi cDNA Synthesis & KODplus Neo kits) with primers:

5'-cgaggtaccatggatgtattcatgaaagg-3' (sense);

5'-cagggtaccttaggcttcaggttcgtagtc-3' (antisense),

purified using Promega Wizard SV Gel and PCR Clean-Up System according to the manufacturer's protocol, then inserted into a pCMV5 vector. The vector was ligated and amplified in commercially obtained competent DH5α bacteria from TaKaRa, PCR-checked using EmeraldAmp MasterMix (TaKaRa) and isolated with the Promega Wizard Plus miniprep kit. The insert was verified through sequencing using the BigDye® Terminator v3.1 kit from Applied Biosystems. The vector was co-transfected into SH-SY5Y cells with a pSV2 vector using the FuGene 6 reagent (Promega). Stably transfected SH-SY5Y clones were selected with 5 µg/ml blasticidin and used for the experiments.

The SphK product, sphingosine-1-phosphate (S1P), and the potent, selective sphingosine kinase inhibitor (SKI) were both used at concentrations of 0.1, 1.0 and 5.0 µM, respectively.

For the measurements of intracellular and secreted APP low-passage, wtASN-expressing cells were seeded at 0.8 × 10^5/well onto six-well dishes and cultured overnight in DMEM/F12 with 10% foetal calf serum, penicillin + streptomycin and 5 µg/ml blasticidin to achieve ~10% confluence. 10 µM ATRA was then added fresh every day for 120 h. After differentiation the cells were switched to serum-free DMEM/F12 medium and APP was collected for three days. The medium was centrifuged and denatured in a Laemmli sample buffer. The cells were washed twice with phosphate-buffered saline (PBS), scraped in 0.9 ml of PBS, centrifuged and lysed for 30 minutes at 4°C in 0.25 ml of 50 mM Tris-HCl pH 7.5 containing 150 mM NaCl, 0.5% Nonidet P-40. 5 mM EDTA and Complete™ protease inhibitors. The lysates were cleared by centrifugation and denatured. After measurements of protein contents the denatured medium and cell extracts were resolved using sodium dodecyl sulphate-polyacrylamide gel electrophoresis (SDS-PAGE) together with Bio-Rad Precision Plus Protein WesternC standards. After transfer to nitrocellulose membranes, the non-specific binding was blocked with 5% skim milk for two hours at room temperature and western-blots were performed using 1 : 100 "22C11" anti-APP antibody in Tween-20-containing Tris-buffered saline (TTBS) and after washes with 1 : 10 000 anti-mouse horseradish peroxidase (HRP)-linked secondary IgG together with 1 : 10 000 Streptactin-HRP conjugate in 0.5% milk/TTBS for 1 h. The chemiluminescent (ECL) signal was measured with a LAS-1000 apparatus (Fuji) and quantitated using ImageJ software. The statistical significance of the obtained results was assessed using Student's *t*-test.

Results

The endogenous level of APP was detectable in the SH-SY5Y cell line; it was possible to quantitate the secretion of APP protein after three days of incubation in control conditions. The expression of wtASN (Fig. 1A) caused an increase of the cell extract APP signal in non-differentiated SH-SY5Y cells to 313% of the values observed in non-transfected cells (Fig. 1B). Moreover, preliminary results suggest that a similar change could occur also in secreted APP (data not shown).

To characterise the molecular mechanisms of APP modulation we used the sphingosine kinase product S1P and an inhibitor of both SphK isoforms termed SKI. The 72 h treatment with 5 µM S1P caused a reduction of APP signal in the extracts of differentiated SH-SY5Y cells to 51% of the control ($p < 0.05$; Fig. 2A) with an insignificant increase in secretion (Fig. 2B). The effect of S1P on the APP level in the extract was nearly identical (46% of the appropriate control, not shown in the figures) when non-ASN transfected cells were used.

5 µM SKI administered to the differentiated ASN-transfected cells in the same conditions caused a significant increase of the cellular APP level (5 µM: 121%; $p < 0.01$; Fig. 3A). Correspondingly, the APP signal in the medium was reduced (54% of control; $p < 0.02$; Fig. 3B) while lower concentrations did not induce significant changes (APP secretion at 98% of the control level for 0.1 µM SKI and 80% for 1 µM SKI).

Discussion

The dysregulation of membrane lipids takes place in ageing, which is the most important risk factor for neurodegenerative disorders [15]. Disturbed sphingolipid metabolism could also directly affect age-related neurodegenerative diseases such as AD, PD or cerebral ischaemia. This could take place e.g. through the numerous functions of S1P in neuron generation, survival, neurite retraction/extension, neurotransmitter release [1,28], and its ambiguous role in oxidative

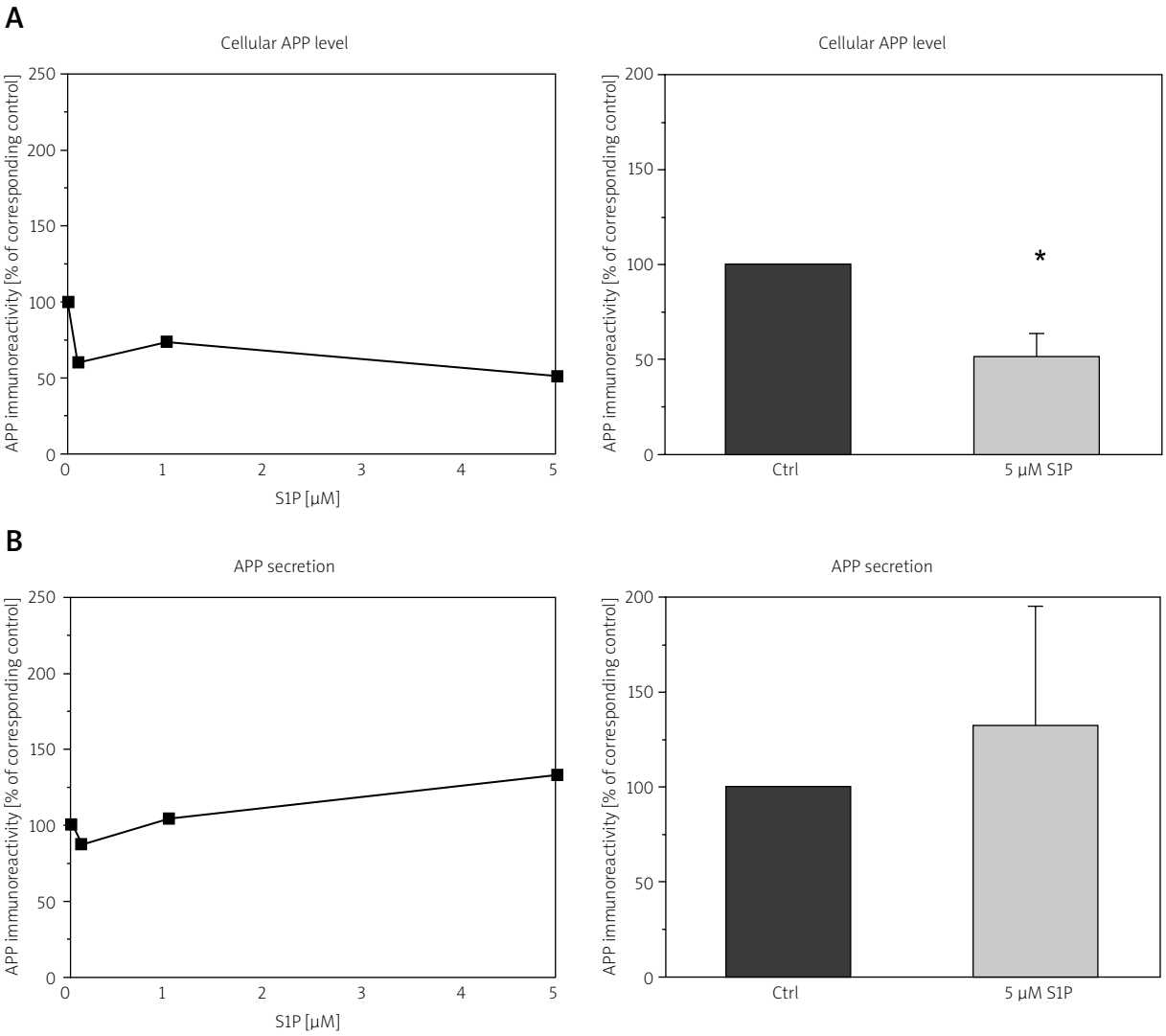

Fig. 2. The intracellular level (cell extract, **A**) and secretion (medium, **B**) of amyloid precursor protein in retinoic acid (ATRA)-differentiated, ASN-transfected SH-SY5Y cells treated with various concentrations of SKI vs. untreated cells.
*$p < 0.05$, Student's *t*-test, 3-4 independent experiments.

stress-linked events (glutathione depletion leading to H_2O_2 sensitivity in PC12 cells vs. heart protection against ischaemia/reperfusion injury) [5,36]. In the current work, we assessed the role of S1P in the ASN-dependent expression and secretion of APP in SH-SY5Y neuroblastoma cells.

ASN is enriched in the central nervous system (CNS) structures particularly affected by AD. Our previous work suggested a link between ASN and Aβ. ASN was able to increase the Aβ secretion and toxicity to a point where it caused cell death [21]. Other results suggest that ASN could influence Aβ aggregation, though the results are far from clear [17,24]. The two proteins can also physically bind each other [24]. Our current work shows that the precursor protein for Aβ is also influenced by ASN. The expression of wt α-synuclein has led to a significant increase of endogenous APP in SH-SY5Y cells. This suggests that APP level and/or secretion might be positively dependent on the intracellular level of ASN. In the study by Kazmierczak *et al*. [21], ASN was added externally and it was possible that its action could have been mediated by cell surface structures or even occurred outside the cell [21]. Our current results suggest that

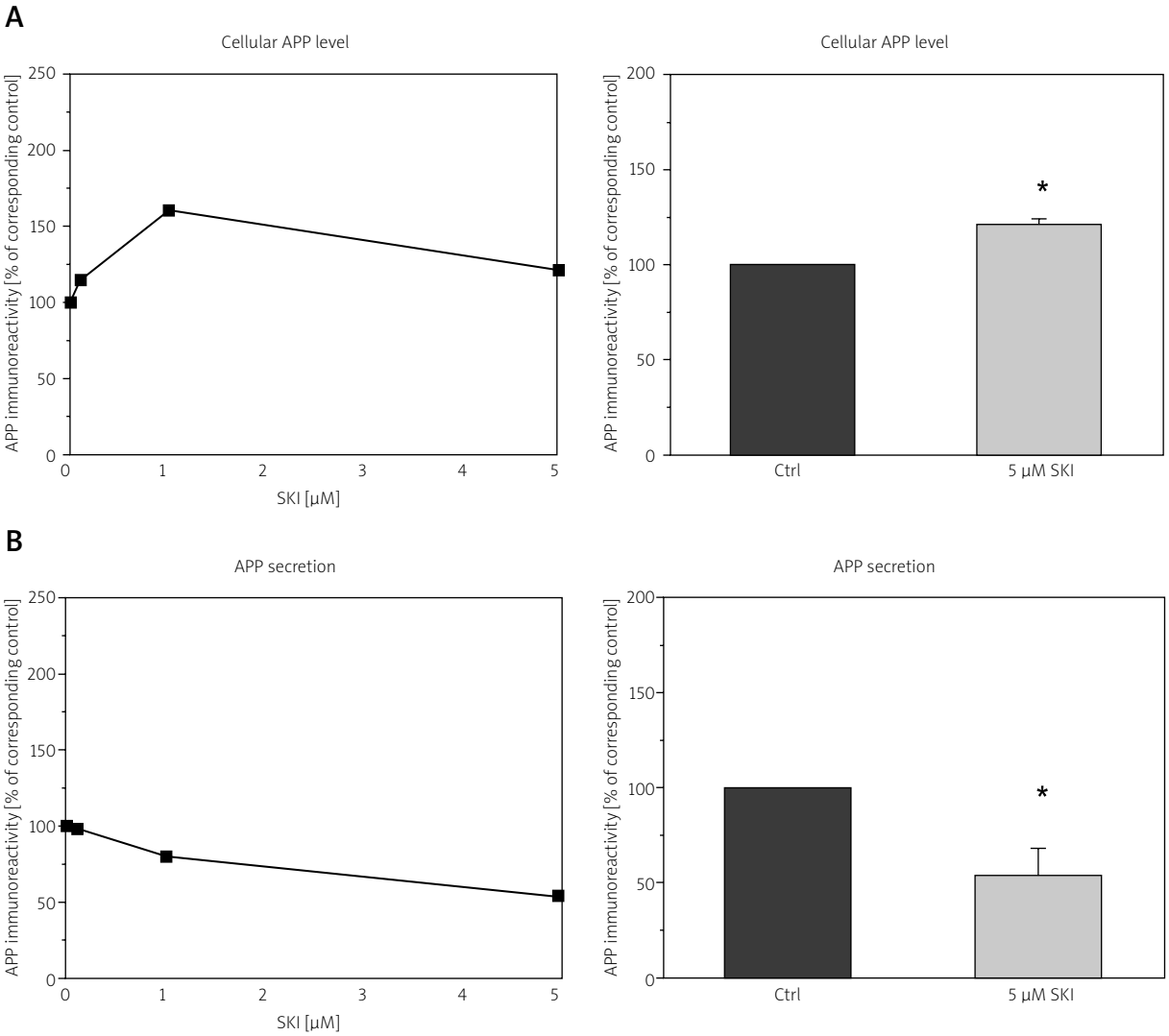

Fig. 3. The intracellular level (cell extract, **A**) and secretion (medium, **B**) of amyloid precursor protein in retinoic acid (ATRA)-differentiated, ASN-transfected SH-SY5Y cells treated with various concentrations of S1P vs. untreated cells.
*$p < 0.05$, Student's *t*-test, three independent experiments.

the phenomenon should be linked to the metabolism of Aβ precursor protein rather than occurring (only) at the level of APP cleavage/Aβ.

Sphingosine kinases undergo precise regulation through post-translational modifications [6], differential subcellular translocation [6,14], binding partners [9,12], and have partially different targets [14,27,28]. Each may be an important factor of AD albeit in different ways. Sphingolipid signalling may influence Aβ production [29,32,34] and siRNA/inhibition of SphK1/SphK2 reduces β-cleavage of APP leading to lower the secretion of Aβ and sAPPβ [33]. SphKs and sphingolipids may also modulate Aβ toxicity [7,10] and the inflammation it causes [18] as well as the resulting brain tissue damage [2]. In turn, Aβ inhibits S1P production [10] and modulates S1P receptors [18]. A correlation of sphingolipid disturbances with cognitive decline was observed in AD [20] and the protective influence of SphKs in Aβ toxicity has been reported [10].

We found that the SphK product S1P lowered the cellular level of APP. The influence of S1P on the secretion of APP showed a tendency towards activation, though the results were insignificant. SKI caused a dose-dependent decrease of medium APP levels, reaching a statistical significance at 5 μM.

The cellular level of APP was significantly elevated. Based on these results it is reasonable to suggest that in fact the influence of S1P on APP might be pro-secretory. Such a conclusion would be consistent with the ubiquitous [4,16,26] and physiologically relevant [19] pro-secretory influence of S1P [28]. Results suggesting the influence of the ceramide/sphingolipid signalling on the processing of APP have been published [23]. It is thus reasonable to expect that its actual influence on APP secretion will follow the general trend despite the fact that the various examples seem to employ an array of somewhat different mechanisms. S1P has been found to directly bind (probably the transmembrane and intracellular domains) and modulate the activity of BACE1, the rate-limiting enzyme for Aβ production [33]. The tendency towards higher APP levels in the medium and the reduction of its cellular content in the SH-SY5Y line strongly suggest that the secretion of whole APP probably masks the reduction that would stem from the mentioned increased cleavage. This is analogous to some degree to the situation in hamster ovary cells where the secretion of $A\beta_{1-42}$ follows the profile of APP secretion [31]. In these cells the influence of sphingolipids seemed to be different from its role in neuroblastoma (and probably the brain). Sphingolipid deficiency enhanced the secretion of the products of non-amyloidogenic α-cleavage of overexpressed human APP75 (with amyloidogenic cleavage products unchanged or reduced), an effect mediated by the MAPK/ERK pathway and rescued by sphingosine treatment [31]. This suggests that the various steps of the sphingolipid pathway may influence different aspects of APP/Aβ metabolism in opposite ways; moreover, sphingolipid action may differ significantly between the CNS and the periphery. The chronic nature of AD and the extremely elongated period of changes preceding its clinical manifestation further suggest that even very subtle changes in APP metabolism could have tremendous effects on the state of CNS either taken alone or in combination with simultaneously occurring pathological changes.

Although both ASN and APP undergo regulation by the SphK pathway, APP does not appear to follow the S1P metabolism-induced changes of ASN. We observed rather unexpected results regarding the influence of the S1P pathway on ASN secretion. Both S1P and SKI elevated the ASN signal in the medium without affecting the cellular level significantly (unpublished own results). Somewhat analogous results were obtained by Takasugi *et al*. [33] in a study on APP cleavage suggesting differential roles of cellular vs. exogenous S1P in these processes. It is possible that the influence of sphingolipid metabolism on ASN (which is limited to its secretion) does not modify the production of APP, which could be dependent mainly on the intracellular ASN level. Another explanation is that APP might undergo an additional level of SphK-related regulation working between ASN and APP production, as suggested by the different types of effects of SKI and S1P on APP vs. ASN.

Our results suggest a potentially important link between ASN and APP/Aβ. The interactions between these proteins may open new views on the devastating pathologies and possibly lead to a more comprehensive understanding of these processes.

Acknowledgements

This work was supported in part by the Statutory Budget of the M. Mossakowski Medical Research Centre, Polish Academy of Sciences (theme no. 1 and 17), NCN grant no. 5870/B/P01/2011/40 and research fellowships from the Japan Society for the Promotion of Science (H.J., R.P.S.).

References

1. Agudo-López A, Miguel BG, Fernández I, Martínez AM. Involvement of mitochondria on neuroprotective effect of sphingosine-1-phosphate in cell death in an in vitro model of brain ischemia. Neurosci Lett 2010; 470: 130-133.
2. Asle-Rousta M, Kolahdooz Z, Oryan S, Ahmadiani A, Dargahi L. FTY720 (fingolimod) attenuates beta-amyloid peptide (Aβ42)-induced impairment of spatial learning and memory in rats. J Mol Neurosci 2013; 50: 524-532.
3. Broe M, Shepherd CE, Mann DMA, Milward EA, Gai W-P, Thiel E, Halliday GM. Insoluble alpha-synuclein in Alzheimer's disease without Lewy body formation. Neurotox Res 2005; 7: 69-76.
4. Cantrell Stanford J, Morris AJ, Sunkara M, Popa GJ, Larson KL, Özcan S. Sphingosine 1-phosphate (s1p) regulates glucose-stimulated insulin secretion in pancreatic beta cells. J Biol Chem 2012; 287: 13457-13464.
5. Denisova NA, Fisher D, Provost M, Joseph JA. The role of glutathione, membrane sphingomyelin, and its metabolites in oxidative stress-induced calcium "dysregulation" in PC12 cells. Free Radic Biol Med 1999; 27: 1292-1301.
6. Ding G, Sonoda H, Yu H, Kajimoto T, Goparaju SK, Jahangeer S, Okada T, Nakamura S. Protein kinase D-mediated phosphorylation and nuclear export of sphingosine kinase 2. J Biol Chem 2007; 282: 27493-27502.
7. Doi Y, Takeuchi H, Horiuchi H, Hanyu T, Kawanokuchi J, Jin S, Parajuli B, Sonobe Y, Mizuno T, Suzumura A. Fingolimod phosphate attenuates oligomeric amyloid β-induced neurotoxicity

via increased brain-derived neurotrophic factor expression in neurons. PLoS One 2013; 8: e61988.
8. Filippov V, Song MA, Zhang K, Vinters HV, Tung S, Kirsch WM, Yang J, Duerksen-Hughes PJ. Increased ceramide in brains with Alzheimer's and other neurodegenerative diseases. J Alzheimers Dis 2012; 29: 537-547.
9. Fujita T, Okada T, Hayashi S, Jahangeer S, Miwa N, Nakamura S. Delta-catenin/NPRAP (neural plakophilin-related armadillo repeat protein) interacts with and activates sphingosine kinase 1. Biochem J 2004; 382: 717-723.
10. Gomez-Brouchet A, Pchejetski D, Brizuela L, Garcia V, Altié M-F, Maddelein M-L, Delisle M-B, Cuvillier O. Critical role for sphingosine kinase-1 in regulating survival of neuroblastoma cells exposed to amyloid-beta peptide. Mol Pharmacol 2007; 72: 341-349.
11. Hasegawa T, Konno M, Baba T, Sugeno N, Kikuchi A, Kobayashi M, Miura E, Tanaka N, Tamai K, Furukawa K, Arai H, Mori F, Wakabayashi K, Aoki M, Itoyama Y, Takeda A. The AAA-ATPase VPS4 regulates extracellular secretion and lysosomal targeting of α-synuclein. PLoS One 2011; 6: e29460.
12. Hayashi S, Okada T, Igarashi N, Fujita T, Jahangeer S, Nakamura S-I. Identification and characterization of RPK118, a novel sphingosine kinase-1-binding protein. J Biol Chem 2002; 277: 33319-33324.
13. He X, Huang Y, Li B, Gong C-X, Schuchman EH. Deregulation of sphingolipid metabolism in Alzheimer's disease. Neurobiol Aging 2010; 31: 398-408.
14. Igarashi N, Okada T, Hayashi S, Fujita T, Jahangeer S, Nakamura S. Sphingosine kinase 2 is a nuclear protein and inhibits DNA synthesis. J Biol Chem 2003; 278: 46832-46839.
15. Joseph JA, Denisova NA, Bielinski D, Fisher DR, Shukitt-Hale B. Oxidative stress protection and vulnerability in aging: putative nutritional implications for intervention. Mech Ageing Dev 2000; 116: 141-153.
16. Kajimoto T, Okada T, Yu H, Goparaju SK, Jahangeer S, Nakamura S. Involvement of sphingosine-1-phosphate in glutamate secretion in hippocampal neurons. Mol Cell Biol 2007; 27: 3429-3440.
17. Kallhoff V, Peethumnongsin E, Zheng H. Lack of alpha-synuclein increases amyloid plaque accumulation in a transgenic mouse model of Alzheimer's disease. Mol Neurodegener 2007; 2: 6.
18. Kaneider NC, Lindner J, Feistritzer C, Sturn DH, Mosheimer BA, Djanani AM, Wiedermann CJ. The immune modulator FTY720 targets sphingosine-kinase-dependent migration of human monocytes in response to amyloid beta-protein and its precursor. FASEB J 2004; 18: 1309-1311.
19. Kanno T, Nishizaki T, Proia RL, Kajimoto T, Jahangeer S, Okada T, Nakamura S. Regulation of synaptic strength by sphingosine 1-phosphate in the hippocampus. Neuroscience 2010; 171: 973-980.
20. Katsel P, Li C, Haroutunian V. Gene expression alterations in the sphingolipid metabolism pathways during progression of dementia and Alzheimer's disease: a shift toward ceramide accumulation at the earliest recognizable stages of Alzheimer's disease? Neurochem Res 2007; 32: 845-856.
21. Kazmierczak A, Strosznajder JB, Adamczyk A. alpha-Synuclein enhances secretion and toxicity of amyloid beta peptides in PC12 cells. Neurochem Int 2008; 53: 263-269.
22. Lee H-J, Suk J-E, Bae E-J, Lee S-J. Clearance and deposition of extracellular alpha-synuclein aggregates in microglia. Biochem Biophys Res Commun 2008; 372: 423-428.
23. Li H, Kim WS, Guillemin GJ, Hill AF, Evin G, Garner B. Modulation of amyloid precursor protein processing by synthetic ceramide analogues. Biochim Biophys Acta 2010; 1801: 887-895.
24. Mandal PK, Pettegrew JW, Masliah E, Hamilton RL, Mandal R. Interaction between Abeta peptide and alpha synuclein: molecular mechanisms in overlapping pathology of Alzheimer's and Parkinson's in dementia with Lewy body disease. Neurochem Res 2006; 31: 1153-1162.
25. Mielke MM, Bandaru VVR, Haughey NJ, Xia J, Fried LP, Yasar S, Albert M, Varma V, Harris G, Schneider EB, Rabins PV, Bandeen-Roche K, Lyketsos CG, Carlson MC. Serum ceramides increase the risk of Alzheimer disease: the Women's Health and Aging Study II. Neurology 2012; 79: 633-641.
26. Milara J, Mata M, Mauricio MD, Donet E, Morcillo EJ, Cortijo J. Sphingosine-1-phosphate increases human alveolar epithelial IL-8 secretion, proliferation and neutrophil chemotaxis. Eur J Pharmacol 2009; 609: 132-139.
27. Okada T, Ding G, Sonoda H, Kajimoto T, Haga Y, Khosrowbeygi A, Gao S, Miwa N, Jahangeer S, Nakamura S-I. Involvement of N-terminal-extended form of sphingosine kinase 2 in serum-dependent regulation of cell proliferation and apoptosis. J Biol Chem 2005; 280: 36318-36325.
28. Okada T, Kajimoto T, Jahangeer S, Nakamura S. Sphingosine kinase/sphingosine 1-phosphate signalling in central nervous system. Cell Signal 2009; 21: 7-13.
29. Puglielli L, Ellis BC, Saunders AJ, Kovacs DM. Ceramide stabilizes beta-site amyloid precursor protein-cleaving enzyme 1 and promotes amyloid beta-peptide biogenesis. J Biol Chem 2003; 278: 19777-19783.
30. Satoh JI, Kuroda Y. Ubiquitin C-terminal hydrolase-L1 (PGP9.5) expression in human neural cell lines following induction of neuronal differentiation and exposure to cytokines, neurotrophic factors or heat stress. Neuropathol Appl Neurobiol 2001; 27: 95-104.
31. Sawamura N, Ko M, Yu W, Zou K, Hanada K, Suzuki T, Gong J-S, Yanagisawa K, Michikawa M. Modulation of amyloid precursor protein cleavage by cellular sphingolipids. J Biol Chem 2004; 279: 11984-11991.
32. Takasugi N, Sasaki T, Ebinuma I, Osawa S, Isshiki H, Takeo K, Tomita T, Iwatsubo T. FTY720/fingolimod, a sphingosine analogue, reduces amyloid-β production in neurons. PLoS One 2013; 8: e64050.
33. Takasugi N, Sasaki T, Suzuki K, Osawa S, Isshiki H, Hori Y, Shimada N, Higo T, Yokoshima S, Fukuyama T, Lee VM-Y, Trojanowski JQ, Tomita T, Iwatsubo T. BACE1 activity is modulated by cell-associated sphingosine-1-phosphate. J Neurosci 2011; 31: 6850-6857.
34. Tamboli IY, Prager K, Barth E, Heneka M, Sandhoff K, Walter J. Inhibition of glycosphingolipid biosynthesis reduces secretion of the beta-amyloid precursor protein and amyloid beta-peptide. J Biol Chem 2005; 280: 28110-28117.

35. Uéda K, Fukushima H, Masliah E, Xia Y, Iwai A, Yoshimoto M, Otero DA, Kondo J, Ihara Y, Saitoh T. Molecular cloning of cDNA encoding an unrecognized component of amyloid in Alzheimer disease. Proc Natl Acad Sci U S A 1993; 90: 11282-11286.
36. Vessey DA, Kelley M, Li L, Huang Y. Sphingosine protects aging hearts from ischemia/reperfusion injury: Superiority to sphingosine 1-phosphate and ischemic pre- and post-conditioning. Oxid Med Cell Longev 2009; 2: 146-151.

Original article

Folia Neuropathologica

Differential expression of microRNA-210 in gliomas of variable cell origin and correlation between increased expression levels and disease progression in astrocytic tumours

Niansheng Lai[1,2], Hao Zhu[3], Yijun Chen[3], Shuai Zhang[1], Xudong Zhao[1], Yuchang Lin[1]

[1]Department of Neurosurgery, Wuxi Second Hospital Affliated to Nanjing Medical University, Wuxi, Jiangsu Province, [2]Department of Neurosurgery, Wuhu Second People's Hospital Affliated to Wannan Medical College, Wuhu, Anhui Province, [3]Department of Neurosurgery, Nanjing Brain Hospital Affliated to Nanjing Medical University, Nanjing, Jiangsu Province, China

Folia Neuropathol 2014; 52 (1): 79-85

DOI: 10.5114/fn.2014.41746

Abstract

Introduction: *The microRNA, miR-210, is frequently associated with hypoxia induction, and an increase in its levels is often correlated with poor prognosis in many solid tumours. The present study examines the levels of miR-210 in glioma tumours of multiple origins to determine if an association can be established with disease progression.*

Material and methods: *Tissue samples were acquired from normal brain tissue, oligodendroglial tumours and astrocytic tumours. The astrocytic tumours were further divided by grade: diffuse astrocytomas (WHO grade II), anaplastic astrocytomas (WHO grade III), and glioblastoma (WHO grade IV). The expression of miR-210 was examined by real-time quantitative RT-PCR. The correlation of the expression of miR-210 and astrocytic tumour grade was analyzed by the Spearman correlation test.*

Results: *MiR-210 presents a differential expression depending on the origin of the glioma. Oligodendroglial tumours exhibit a significantly reduced level of miR-210 as compared with normal brain tissue. In contrast, astrocytic tumours demonstrate significantly increased levels of miR-210. Furthermore, the expression of miR-210 is positively correlated with the grade of astrocytic tumour, in the following order: grade IV > grade III > grade II > normal brain tissue ($p < 0.05$).*

Conclusions: *MiR-210 levels can be potentially established as a biomarker for pathological diagnosis of malignant astrocytic tumour progression. In addition, the expression of miR-210 can be utilized as an additional identification measure of glioma tumour origin.*

Key words: *astrocytic tumour, oligodendroglial tumour, miR-210, glioma, real-time quantitative RT-PCR.*

Introduction

Gliomas are tumours that start in the brain or spine and arise from glial cells. They are characterized by the cell type (ependymal cells, astrocytes, oligodendrocytes, or mixed cells), grade (I-IV), and location (cerebrum or cerebellum). Malignant gliomas account for approximately 70% of the 22 500 malignant primary brain tumours diagnosed each year. Of the malignant gliomas, 60-70% are glioblastomas [37]. Gliomas are characterized by high invasiveness, high recurrence, poor clinical prognosis, and are associated

Communicating author:

Yuchang Lin, Department of Neurosurgery, Wuxi Second Hospital Affiliated to Nanjing Medical University, Wuxi 214002, Jiangsu Province, China, e-mail: yuchanglin123@126.com

with a disproportionately high morbidity and mortality [40,46]. According to the World Health Organization (WHO) classification scheme established in 2007 [18], astrocytic tumours are further sub-divided into grades: pilocytic astrocytoma (WHO grade I), diffuse astrocytoma (WHO grade II), anaplastic astrocytoma (WHO grade III), and glioblastoma (WHO grade IV). Oligodendroglial tumours are divided into oligodendroglioma and anaplastic oligodendroglioma.

MicroRNAs (miRNAs) are small (17-24 nucleotides) non-coding single-stranded RNAs, which regulate the expression of multiple target genes either by degrading specific mRNA or inhibiting translation [20]. To date, more than 2000 human miRNAs have been identified (http://www.mirbase.org/). They are involved in the regulation of multiple cellular and developmental processes, including cell proliferation, cell differentiation, cell cycle regulation, and epithelial-mesenchymal transition. miRNAs also play a role in the molecular pathology of cancer, including tumorigenesis, differentiation, proliferation, cell cycle regulation, angiogenesis, adhesion, migration, invasion and apoptosis of tumour cells [11]. miRNAs are often regarded as highly stable molecules but can undergo accelerated decay under certain environmental conditions allowing for maintenance of homeostasis through both biosynthetic and decay processes. Mitotically active cells, cells exposed to growth factors, and increases in neuronal activity are physiologic triggers known to induce a rapid decay of associated miRNA molecules. For example, the half-life of miR-29b is 4 hours in cycling cells but > 12 hours in mitotically arrested cells. Rapid degradation only affects certain subsets of miRNAs but appears to be a prevalent characteristic of miRNAs involved in neuronal activity [30]. Five different miRNAs tested in primary human neuron cultures were observed to all have half-lives less than 3.5 hours [3,30,32]. In multiple studies, miRNA expression levels have been analyzed as potential biomarkers for specific diagnosis and disease progression [17,36].

The miRNA, miR-210, is consistently identified in hypoxic events in both normal and transformed cells [5]. It was originally identified in cardiac cells undergoing a cardiac infarction. MiR-210 is up-regulated under hypoxia, which has been observed to increase angiogenesis and inhibit apoptosis [5]. MiR-210 has also been observed to be up-regulated in tumours. Hypoxia is a predominant feature of the tumour microenvironment of gliomas with more aggressive tumours leading to an increase in hypoxia. It has been demonstrated that miR-210 plays an important role in regulation of cell growth, angiogenesis, invasion and apoptosis in different human tumour models [5,11]. MiR-210 expression is frequently up-regulated in a variety of solid tumours, including breast cancer [12], non-small cell lung cancer [29], head and neck cancer [8], pancreatic cancer [4], oral tumours [31], hepatocellular cancer (HCC) [42], adrenocortical carcinoma (ACC) [23], glioblastoma [26], colon cancer [24], ovarian cancer [9], malignant melanoma [22] and renal cell cancer [27]. The expression of miR-210 is found to be down-regulated in human esophageal squamous cell carcinoma (ESCC) tissues and derived cell lines [34]. Because of the consistency of the presence of miR-210 in hypoxic environments, it is often utilized as a biomarker for glioma detection [16,21,41]. The aim of this study was to determine if there is a correlation between the grade of astrocytoma and miR-210 expression and if the origin of the glioma affects miR-210 expression.

Material and methods

Clinical samples

This study complied with the requirements of the Research Ethics Committee of Nanjing Medical University, P.R. China.

Eighty-one glioma samples were obtained from February 2010 to January 2013 in the Department of Neurosurgery of Wuxi Second People's Hospital. The diagnosis of primary gliomas was re-reviewed histologically by the experimental neuropathologist. Each sample was classified and scored based on the WHO standard for tumour classification [18] by two neuropathologists to ensure accuracy, with differences resolved by careful discussion. Fifty-eight of the 81 gliomas were classified as astrocytic tumours [10 diffuse astrocytomas (WHO grade II), 17 anaplastic astrocytomas (WHO grade III), and 31 glioblastomas (WHO grade IV)]. Twenty-three of 81 gliomas were classified as oligodendroglial tumours.

Glioma types were further confirmed through hematoxylin and eosin staining-based microscopic investigations after the surgery. Tissue samples were quickly resected, immediately snap-frozen in liquid nitrogen and stored at –80°C until RNA extraction. The study group of patients consisted of 37 women and 44 men, and the median age was 47 (15-77

years). None of the patients had received chemotherapy or radiotherapy prior to surgery. Ten snap-frozen samples of normal brain tissue were obtained from internal decompression of patients who underwent neurosurgery due to cerebral injury and cerebral haemorrhage. Informed consent was obtained before the surgery.

Isolation of RNA

Total RNA was extracted from frozen tissue with Trizol reagent (Invitrogen, Carlsbad, CA, USA), according to manufacturer's protocol. The RNA quantity and quality were measured by NanoDrop 2000 spectrophotometer (NanoDrop Technologies, Houston, TX, USA). Only samples with an OD A260/A280 ratio between 1.8 and 2.0 were utilized for further analysis by RT-PCR.

cDNA synthesis

The miR-210 and U6B (as an internal control)-specific cDNA was synthesized from 3-4 µg of total RNA with a mixture of miR-210-RT primers/U6B-RT primers (Genepharma, Shanghai, China) and M-MLV reverse transcriptase.

Real-time quantitative reverse transcription-PCR

Analysis of gene expression was performed by real time quantitative PCR (RT-PCR). RT-PCR was performed using the miR-210 primer set with the RT-PCR Master Mix and analyzed with the DNA Engine Opticon 2 Real-Time Cycler (MJ Research, Inc., Waltham, MA, USA) according to the manufacturer's instructions. Each reaction included 0.8 µl of miR-210 primer set (5 µM) (Genepharma), 20 µl of RT-PCR master mix (Genepharma), 0.2 µl of Taq DNA polymerase (5 U/µl) (Genepharma) and 4 µl of RT products. The quantitative analysis of the change in expression levels was calculated in triplicate using the comparative cycle threshold (CT) method. The raw data of target miRNA were normalized to U6B which served as an internal control.

Statistical analysis

All data were analyzed using IBM SPSS Statistics 13.0 for Windows (SPSS Inc., Chicago, IL, USA). The independent sample *t*-test was utilized to determine the statistical differences among the groups between glioma tissues and normal brain tissues. To determine the correlation between expression levels of miR-210 and histologic grade, the Spearman rank correlation test was applied. Differences were considered statistically significant when $p < 0.05$.

Results

MiR-210 expression in astrocytic tumours

The expression of miR-210 was detected in 58 astrocytic tumours and 10 normal brain tissues normalized to U6B by quantitative RT-PCR. As shown in Fig. 1, astrocytic tumours demonstrated a significant increase in miR-210 transcript levels compared with the mean expression levels observed in normal brain tissues (mean ± SD 6.91 ± 1.3 vs. 4.84 ± 0.35; $p < 0.001$). Expression levels of miR-210 in diffuse astrocytomas (WHO grade II; mean ± SD 5.69 ± 0.67; $p = 0.004$), anaplastic astrocytomas (WHO grade III; mean ± SD 6.46 ± 0.90; $p < 0.001$), and glioblastomas (WHO grade IV; mean ± SD 7.62 ± 1.12; $p < 0.001$) were significantly higher than those found in normal brain tissues.

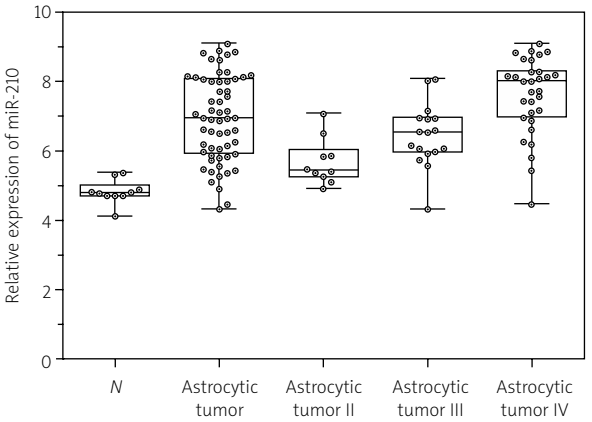

Fig. 1. MiR-210 expression in 58 astrocytic tumours and 10 normal brain tissues detected by real-time quantitative RT-PCR. Astrocytic tumours demonstrated a significant increase in miR-210 transcript levels compared with the mean expression levels observed in normal brain tissues (mean ± SD 6.91 ± 1.3 vs. 4.84 ± 0.35; $p < 0.001$). Expression levels of miR-210 in diffuse astrocytomas (WHO grade II; mean ± SD 5.69 ± 0.67; $p = 0.004$), anaplastic astrocytomas (WHO grade III; mean ± SD 6.46 ± 0.90; $p < 0.001$), and glioblastomas (WHO grade IV; mean ± SD 7.62 ± 1.12; $p < 0.001$) were significantly higher than those found in normal brains tissues.

Increase in miR-210 expression is directly correlated with the histopathological grade of the astrocytic tumour

Once it was determined that astrocytic tumours expressed a significantly higher level of miR-210 than normal brain tissue, we wanted to determine if there was a statistically significant correlation between the histopathological grade of the tumour and level of miR-210 transcript. There was a significant increase in miR-210 expression in glioblastomas compared with anaplastic astrocytomas ($p < 0.001$), glioblastomas compared with diffuse astrocytomas ($p < 0.001$), and anaplastic astrocytomas compared with diffuse astrocytomas ($p < 0.05$) (Fig. 1). According to the Spearman rank correlation test, increasing levels of miR-210 expression could be directly correlated with a higher pathological grade. In other words, there was a positive correlation between miR-210 expression and pathological grade ($r = 0.646$, $p < 0.001$). No statistically significant association between miR-210 expression and age at diagnosis, size of tumours, gender of patients, or KPS score could be identified ($p > 0.05$, Table I).

Table I. Association between miR-210 expression and different clinicopathological features of astrocytic tumours

Clinicopathological parameters	No. of cases	miR-210 expression	*p* value
Sex			
Male	32	6.86 ± 1.27	0.55
Female	26	7.06 ± 1.23	
Age			
< 55	28	6.93 ± 1.21	0.912
≥ 55	30	6.97 ± 1.30	
WHO grade			
II	10	5.69 ± 0.67	< 0.001
III	17	6.46 ± 0.90	
IV	31	7.62 ± 1.12	
Tumour size			
≥ 5 cm	23	6.84 ± 1.21	0.58
< 5 cm	35	7.02 ± 1.28	
KPS			
< 90	25	6.90 ± 1.15	0.80
≥ 90	33	6.99 ± 1.33	

MiR-210 expression in oligodendroglial tumours

To determine if miR-210 expression was increased in gliomas of different origins, the expression level of miR-210 was analyzed in 23 oligodendroglial tumours and compared to levels in 10 normal brain tissues normalized to U6B. The results demonstrated that the expression of miR-210 was significantly reduced in oligodendroglial tumours, compared with the mean expression levels observed in normal brain tissues (Fig. 2; mean ± SD 3.78 ± 0.76; $p < 0.01$).

Discussion

Altered expression levels of miRNAs have been observed in gliomas, appearing to have both an oncogenic role as well as a tumour suppressor role. More than 1000 studies in cancer and more than 100 studies in gliomas on associated miRNAs have been published to date [44]. Most of these studies examine the expression levels, targets and functional effects of selected miRNAs in glioma cells and tissues. Some miRNAs that are highly expressed in glioma tumours have been implicated in up-regulating cell processes such as cell growth and proliferation, migration, invasion, angiogenesis and cell transformation and down-regulating apoptosis. Examples of these miRNA include: miR-21, miR-221/222, miR-

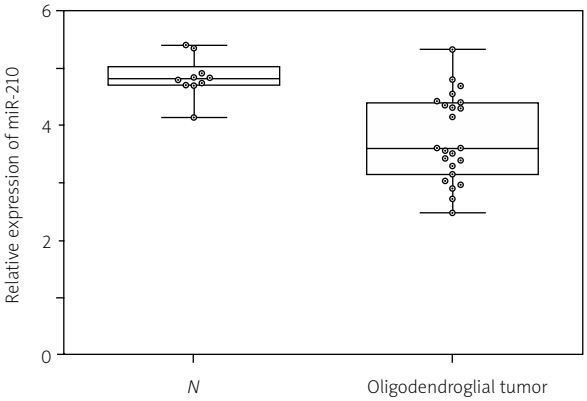

Fig. 2. MiR-210 expression in 23 oligodendroglial tumours and 10 normal brain tissues detected by real-time quantitative RT-PCR. Oligodendroglial tumours demonstrated a significant decrease in miR-210 transcript levels compared with the mean expression levels observed in normal brain tissues (mean ± SD 3.78 ± 0.76 vs. 4.84 ± 0.35; $p < 0.01$).

210, miR-9, miR-10(a,b), miR-15(a,b) and miR-26a. MiRNA expression can also be reduced in gliomas, acting as tumour repressors, decreasing cell growth and proliferation, migration and invasion and increasing apoptosis, such as seen with miR-181(a,b,c), miR-128, miR-451, miR-7, miR-34a, miR-124, miR-218 and miR-326 [1,14,27,33,38,44]. There have also been studies profiling miRNA levels in gliomas in order to compare and determine potential differences between tumour grades. Currently there is an assay to analyze a 23-miRNA signature that differentiates between glioblastomas and anaplastic astrocytomas with 95% accuracy [44]. Changes in miRNA expression patterns can serve as informative biomarkers indicating the functional status of a normal brain as well as disease progression and prognosis of brain tumours [13,35].

By combining miRNA expression profiles with conventional radio/chemotherapy, treatment efficiency could be improved leading to a reduction in tumour recurrence after surgical resection [20]. Recently, a therapeutic scheme involving incorporation of artificial miRNAs in an oncolytic herpes simplex virus achieved successful silencing of specific targets in patients with melanoma and provides a new method for using miRNA as a potential therapeutic target [1]. In gliomas, down-regulation of miR-21 increases glioma apoptosis, represses cell growth, and induces cell cycle arrest. Anti-sense miR-21 was utilized in combination with 5-fluorouracil to target the human glioma cell line U251, significantly increasing apoptosis and decreasing cell migration [28].

MiR-210 is consistently induced under conditions of hypoxia [5], and plays an important role in many tumorigenic processes, such as cell proliferation [10], metabolism [39], cell migration and angiogenesis [6]. A number of targets of miR-210 have been reported, such as vacuole membrane protein 1 (VMP1), enzyme glycerol-3-phosphate dehydrogenase 1-like (GPD1L), iron-sulfur cluster scaffold homolog (ISCU), succinate dehydrogenase complex subunit D (SDHD) and MNT [15,19,25,42,45].

MiR-210, under hypoxic conditions, is frequently increased in HCC and is involved in hypoxia-induced HCC metastasis. VMP1, a putative metastasis suppressor in HCC, is identified as a direct and functional target of miR-210. Down-regulation of VMP1 by miR-210 mediates hypoxia-induced HCC migration and invasion [42].

A hypoxia-induced positive feedback loop promotes hypoxia-inducible factor 1α (HIF-1α) stability through miR-210 suppression of GPD1L [15]. Preventing degradation of HIF-1α leads to induction of a wide variety of genes including those involved in energy metabolism, angiogenesis, cell proliferation and survival [15]. In addition, HIF-1α stability leads to further up-regulation of miR-210 [15,19].

In renal tumours, miR-210 expression is increased under hypoxia by HIF-1/2. ISCU is repressed in the presence of miR-210 leading to a decrease in Krebs cycle enzyme activity and mitochondrial function, providing a mechanism for handling increases in free radical production and a switch to glycolysis affecting cell growth and survival under hypoxic conditions. A decrease in ISCU in cancer patients has been associated with a worse prognosis and is therefore important as a clinicopathological prognostic factor [7,19]. MiR-210's induction of mitochondrial dysfunction under hypoxia is further supported by down-regulation of SDHD in the presence of miR-210, which leads to an increase in HIF-1 stability in lung tumour cells, A549 [25].

MiR-210 constitutes a negative feedback of the HIF hypoxic response by reducing MNT and thereby increasing MYC transcription factor activity, which is known to enhance cell proliferation. An increase in miR-210 and therefore a sustained increase in MYC activity can be correlated with metastatic behaviour in tumours [45]. These examples demonstrate that miR-210 plays a key role in tumour progression and provides vital information about the tumour microenvironment. In addition to being a consistent biomarker, miR-210 could also be an excellent therapeutic target.

The expression of miR-210 has been shown to be correlated with a poor outcome in a variety of solid tumours, such as breast cancer [12], head and neck cancer [8], renal cancer [19], paediatric osteosarcoma [2] and acute ischemic stroke [43]. Meta-analysis has found that a high expression of miR-210 was an independent factor indicating a poor prognosis in 511 cases of breast cancer [12]. MiR-210 up-regulation showed a strong correlation with tumour aggressiveness in paediatric osteosarcoma, with a significant reduction in both overall survival and progression-free survival [2].

Results of the current study indicate that miR-210 will also be an appropriate biomarker and disease progression indicator for glioma tumours. We had

the opportunity to perform a large retrospective study to determine if there is a correlation between miR-210 expression and pathologic features and the clinical outcome of patients with different gliomas. By analyzing 81 clinical primary glioma tissues and 10 non-neoplastic brain tissues, we demonstrated that the expression of miR-210 is variable depending on the origin of the glioma. MiR-210 was found to be over-expressed in astrocytic tumour, whereas expression was down-regulated in the oligodendroglial tumours. We do not currently understand the biological relevance of the differential regulation between these two types of gliomas. Oligodendroglial tumours do possess different upstream regulatory genes and proteins and miR-210 may have simply evolved alternative regulatory targets. Additional research will be necessary to determine if miR-210 is a relevant biomarker for oligodendroglial tumours and what its potential role in tumour progression is. Moreover, the expression of miR-210 increased as the grade of astrocytic tumour increased.

In conclusion, miR-210 can be used as an auxiliary identification method for pathological identification of glioma origin, as well as a biomarker for malignant progression of astrocytic tumours. In future studies we hope to determine if miR-210 plays a regulatory role in tumour progression and evaluate its potential as a therapeutic target.

References

1. Anesti AM, Simpson GR, Price T, Pandha HS, Coffin RS. Expression of RNA interference triggers from an oncolytic herpes simplex virus results in specific silencing in tumor cells in vitro and tumors in vivo. BMC Cancer 2010; 10: 1471-2407.
2. Cai H, Lin L, Tang M, Wang Z. Prognostic evaluation of microRNA-210 expression in pediatric osteosarcoma. Med Oncol 2013; 30: 499.
3. Chen AJ, Paik JH, Zhang H, Shukla SA, Mortensen R, Hu J, Ying H, Hu B, Hurt J, Farny N, Dong C, Xiao Y, Wang YA, Silver PA, Chin L,Vasudevan S, Depinho RA. STAR RNA-binding protein Quaking suppresses cancer via stabilization of specific miRNA. Genes Dev 2012; 26: 1459-1472.
4. Chen WY, Liu WJ, Zhao YP, Zhou L, Zhang TP, Chen G, Shu H. Induction, modulation and potential targets of miR-210 in pancreatic cancer cells. Hepatobiliary Pancreat Dis Int 2012; 11: 319-324.
5. Cicchillitti L, Di Stefano V, Isaia E, Crimaldi L, Fasanaro P, Ambrosino V, Antonini A, Capogrossi MC, Gaetano C, Piaggio G, Martelli F. Hypoxia- inducible factor 1-alpha induces miR-210 in normoxic differentiating myoblasts. J Biol Chem 2012; 287: 44761-44771.
6. Fasanaro P, Greco S, Lorenzi M, Pescatori M, Brioschi M, Kulshreshtha R, Banfi C, Stubbs A, Calin GA, Ivan M, Capogrossi MC, Martelli F. An integrated approach for experimental target identification of hypoxia-induced miR-210. J Biol Chem 2009; 284: 35134-35143.
7. Favaro E, Ramachandran A, McCormick R, Gee H, Blancher C, Crosby M, Devlin C, Blick C, Buffa F, Li J, Vojnovic B, Pires das Neves R, Glazer P, Iborra F, Ivan M, Ragoussis J, Harris AL. MicroRNA-210 regulates mitochondrial free radical response to hypoxia and Krebs cycle in cancer cells by targeting iron sulfur cluster protein ISCU. PlosOne 2010; 5: 1-11.
8. Gee HE, Camps C, Buffa FM, Patiar S, Winter SC, Betts G, Homer J, Corbridge R, Cox G, West CM, Ragoussis J, Harris AL. hsa-mir-210 is a marker of tumor hypoxia and a prognostic factor in head and neck cancer. Cancer 2010; 116: 2148-2158.
9. Giannakakis A, Sandaltzopoulos R, Greshock J, Liang S, Huang J, Hasegawa K, Li C, O'Brien-Jenkins A, Katsaros D, Weber BL, Simon C, Coukos G, Zhang L. miR-210 links hypoxia with cell cycle regulation and is deleted in human epithelial ovarian cancer. Cancer Biol Ther 2008; 7: 255-264.
10. He J, Wu J, Xu N, Xie W, Li M, Li J, Jiang Y, Yang BB, Zhang Y. MiR-210 disturbs mitotic progression through regulating a group of mitosis-related genes. Nucleic Acids Res 2013; 41: 498-508.
11. Hong L, Han Y, Zhang H, Zhao Q, Qiao Y. miR-210: a therapeutic target in cancer. Expert Opin Ther Targets 2013; 17: 21-28.
12. Hong L, Yang J, Han Y, Lu Q, Cao J, Syed L. High expression of miR-210 predicts poor survival in patients with breast cancer: a meta-analysis. Gene 2012; 507: 135-138.
13. Huang Y, Yang S, Zhang J, Tan L, Jiang F, Li N, Cheng J, Lu Y, Dai Y. MicroRNAs as promising biomarkers for diagnosing human cancer. Cancer Invest 2010; 28: 670-671.
14. Karsy M, Arslan E, Moy F. Current Progress on Understanding MicroRNAs in Glioblastoma Multiforme. Genes Cancer 2012; 3: 3-15.
15. Kelly TJ, Souza AL, Clish CB, Puigserver P. A hypoxia-induced positive feedback loop promotes hypoxia-inducible factor 1alpha stability through miR-210 suppression of glycerol-3-phosphate dehydrogenase 1-like. Mol Cell Biol 2011; 31: 2696-2706.
16. Kucharzewska P, Christianson HC, Welch JE, Svensson KJ, Fredlund E, Ringner M, Morgelin M, Bourseau-Guilmain E, Bengzon J, Belting M. Exosomes reflect the hypoxic status of glioma cells and mediate hypoxia-dependent activation of vascular cells during tumor development. Proc Natl Acad Sci U S A 2013; 15: 15.
17. Li G, Zhang Z, Tu Y, Jin T, Liang H, Cui G, He S, Gao G. Correlation of microRNA-372 upregulation with poor prognosis in human glioma. Diagn Pathol 2013; 8: 1.
18. Louis DN, Ohgaki H, Wiestler OD, Cavenee WK, Burger PC, Jouvet A, Scheithauer BW, Kleihues P. The 2007 WHO classification of tumours of the central nervous system. Acta Neuropathol 2007; 114: 97-109.
19. McCormick RI, Blick C, Ragoussis J, Schoedel J, Mole DR, Young AC, Selby PJ, Banks RE, Harris AL. miR-210 is a target of hypoxia-inducible factors 1 and 2 in renal cancer, regulates ISCU and correlates with good prognosis. Br J Cancer 2013; 108: 1133-1142.
20. Nikaki A, Piperi C, Papavassiliou AG. Role of microRNAs in gliomagenesis: targeting miRNAs in glioblastoma multiforme therapy. Expert Opin Investig Drugs 2012; 21: 1475-1488.

21. Nissou MF, El Atifi M, Guttin A, Godfraind C, Salon C, Garcion E, van der Sanden B, Issartel JP, Berger F, Wion D. Hypoxia-induced expression of VE-cadherin and filamin B in glioma cell cultures and pseudopalisade structures. J Neurooncol 2013; 31: 31.
22. Noman MZ, Buart S, Romero P, Ketari S, Janji B, Mari B, Mami-Chouaib F, Chouaib S. Hypoxia-inducible miR-210 regulates the susceptibility of tumor cells to lysis by cytotoxic T cells. Cancer Res 2012; 72: 4629-4641.
23. Ozata DM, Caramuta S, Velazquez-Fernandez D, Akcakaya P, Xie H, Hoog A, Zedenius J, Backdahl M, Larsson C, Lui WO. The role of microRNA deregulation in the pathogenesis of adrenocortical carcinoma. Endocr Relat Cancer 2011; 18: 643-655.
24. Price KJ, Tsykin A, Giles KM, Sladic RT, Epis MR, Ganss R, Goodall GJ, Leedman PJ. Matrigel basement membrane matrix influences expression of microRNAs in cancer cell lines. Biochem Biophys Res Commun 2012; 427: 343-348.
25. Puissegur MP, Mazure NM, Bertero T, Pradelli L, Grosso S, Robbe-Sermesant K, Maurin T, Lebrigand K, Cardinaud B, Hofman V, Fourre S, Magnone V, Pouyssegur J, Gounon P, Hofman P, Barbry P, Mari B. miR-210 is overexpressed in late stages of lung cancer and mediates mitochondrial alterations associated with modulation of HIF-1 activity. Cell Death Differ 2011; 18: 465-478.
26. Qiu S, Lin S, Hu D, Feng Y, Tan Y, Peng Y. Interactions of miR-323/miR-326/miR-329 and miR-130a/miR-155/miR-210 as prognostic indicators for clinical outcome of glioblastoma patients. J Transl Med 2013; 11: 1479-5876.
27. Redova M, Poprach A, Besse A, Iliev R, Nekvindova J, Lakomy R, Radova L, Svoboda M, Dolezel J, Vyzula R, Slaby O. MiR-210 expression in tumor tissue and in vitro effects of its silencing in renal cell carcinoma. Tumour Biol 2012; 13: 13.
28. Ren Y, Kang CS, Yuan XB, Zhou X, Xu P, Han L, Wang GX, Jia Z, Zhong Y, Yu S, Sheng J, Pu PY. Co-delivery of as-miR-21 and 5-FU by poly (amidoamine) dendrimer attenuates human glioma cell growth in vitro. J Biomater Sci Polym Ed 2010; 21: 303-314.
29. Roa WH, Kim JO, Razzak R, Du H, Guo L, Singh R, Gazala S, Ghosh S, Wong E, Joy AA, Xing JZ, Bedard EL. Sputum microRNA profiling: a novel approach for the early detection of non-small cell lung cancer. Clin Invest Med 2012; 35: E271.
30. Rüegger S, Großhans H. MicroRNA turnover: when, how, and why. Trends Biochem Sci 2012; 37: 436-446.
31. Scapoli L, Palmieri A, Lo Muzio L, Pezzetti F, Rubini C, Girardi A, Farinella F, Mazzotta M, Carinci F. MicroRNA expression profiling of oral carcinoma identifies new markers of tumor progression. Int J Immunopathol Pharmacol 2010; 23: 1229-1234.
32. Sethi P, Lukiw WJ. Micro-RNA abundance and stability in human brain: specific alterations in Alzheimer's disease temporal lobe neocortex. Neurosci Lett 2009; 459: 100-104.
33. Skalsky RL, Cullen BR. Reduced expression of brain-enriched microRNAs in glioblastomas permits targeted regulation of a cell death gene. PLoS One 2011; 6: e24248.
34. Tsuchiya S, Fujiwara T, Sato F, Shimada Y, Tanaka E, Sakai Y, Shimizu K, Tsujimoto G. MicroRNA-210 regulates cancer cell proliferation through targeting fibroblast growth factor receptor-like 1 (FGFRL1). J Biol Chem 2011; 286: 420-428.
35. Wang H, Yuan X, Zhou Z, Hu J, Zhang T, Hu S, Luo J, Li X. MicroRNAs might be promising biomarkers of human gliomas. Asian Pac J Cancer Prev 2011; 12: 833-835.
36. Wang S, Lu S, Geng S, Ma S, Liang Z, Jiao B. Expression and clinical significance of microRNA-326 in human glioma miR-326 expression in glioma. Med Oncol 2013; 30: 373.
37. Wen PY, Kesari S. Malignant gliomas in adults. N Engl J Med 2008; 359: 492-507.
38. Wuchty S, Arjona D, Li A, Kotliarov Y, Walling J, Ahn S, Zhang A, Maric D, Anolik R, Zenklusen JC, Fine HA. Prediction of Associations between microRNAs and Gene Expression in Glioma Biology. PLoS One 2011; 6: e14681.
39. Xiong L, Wang F, Huang X, Liu ZH, Zhao T, Wu LY, Wu K, Ding X, Liu S, Wu Y, Zhao Y, Zhu LL, Fan M. DNA demethylation regulates the expression of miR-210 in neural progenitor cells subjected to hypoxia. FEBS J 2012; 279: 4318-4326.
40. Yan W, Zhang W, Sun L, Liu Y, You G, Wang Y, Kang C, You Y, Jiang T. Identification of MMP-9 specific microRNA expression profile as potential targets of anti-invasion therapy in glioblastoma multiforme. Brain Res 2011; 1411: 108-115.
41. Yang L, Lin C, Wang L, Guo H, Wang X. Hypoxia and hypoxia-inducible factors in glioblastoma multiforme progression and therapeutic implications. Exp Cell Res 2012; 318: 2417-2426.
42. Ying Q, Liang L, Guo W, Zha R, Tian Q, Huang S, Yao J, Ding J, Bao M, Ge C, Yao M, Li J, He X. Hypoxia-inducible microRNA-210 augments the metastatic potential of tumor cells by targeting vacuole membrane protein 1 in hepatocellular carcinoma. Hepatology 2011; 54: 2064-2075.
43. Zeng L, Liu J, Wang Y, Wang L, Weng S, Chen S, Yang GY. Cocktail blood biomarkers: prediction of clinical outcomes in patients with acute ischemic stroke. Eur Neurol 2013; 69: 68-75.
44. Zhang Y, Dutta A, Abounader R. The role of microRNAs in glioma initiation and progression. Front Biosci 2012; 17: 700-712.
45. Zhang Z, Sun H, Dai H, Walsh RM, Imakura M, Schelter J, Burchard J, Dai X, Chang AN, Diaz RL, Marszalek JR, Bartz SR, Carleton M, Cleary MA, Linsley PS, Grandori C. MicroRNA miR-210 modulates cellular response to hypoxia through the MYC antagonist MNT. Cell Cycle 2009; 8: 2756-2768.
46. Zhao WJ, Zhang W, Li GL, Cui Y, Shi ZF, Yuan F. Differential expression of MMP-9 and AQP4 in human glioma samples. Folia Neuropathol 2012; 50: 176-186.

Original article

Folia Neuropathologica

Complex immune-mediated mechanisms of vasculitis in cerebral toxoplasmosis in AIDS patients

Dorota Dziewulska[1,2], Janina Rafałowska[1]

[1]Department of Experimental and Clinical Neuropathology, Mossakowski Medical Research Centre, Polish Academy of Sciences, Warsaw, [2]Department of Neurology, Medical University of Warsaw, Poland

Folia Neuropathol 2014; 52 (1): 86-91 DOI: 10.5114/fn.2013.39721

Abstract

The increasing population of patients treated with immunosuppressive and immunomodulatory drugs, as well as growing resistance to anti-retroviral therapy, has caused the reemergence of cerebral toxoplasmosis as a clinical problem. Encephalitis caused by Toxoplasma gondii (Tg) is the most common opportunistic infection in patients with acquired immunodeficiency syndrome (AIDS). The scarcity of data concerning vessel involvement in cerebral toxoplasmosis in AIDS impelled us to examine this process.

In 15 of 178 cases with AIDS cerebral toxoplasmosis was the only opportunistic infection. In these patients routine histological stains and immunohistochemical reactions against T and B lymphocytes, immunoglobulins IgG and IgM, and factors C4β and B, involved respectively in classical and alternative pathways of complement activation, were performed. Apart from morphological changes typical for cerebral toxoplasmosis, eosinophilic necrosis of the vascular media, and vascular inflammatory infiltrates containing T and B lymphocytes were seen. In some arterial vessels intramural deposits of immunoglobulin IgG and IgM, and complement factors C4β and B were found.

Presence of polyarteritis nodosa-like changes, deposits of immunoglobulins and complement factors in the vessel wall, as well as inflammatory infiltrates containing B lymphocytes indicate that vasculitis in cerebral toxoplasmosis in AIDS has a very complex pathomechanism involving not only cell-mediated but also humoral-mediated immunological reactions.

Key words: *AIDS, complement, HIV, toxoplasmosis, vasculitis.*

To the memory of Prof. Mirosław M. Mossakowski, who, together with Prof. Irmina Zelman, gathered a significant AIDS Brain Collection in the Mossakowski Medical Research Centre.

Introduction

Toxoplasma gondii (Tg) infection in immunocompetent humans is generally rare and latent. But persistent cyst containing latent forms of Tg may be responsible for reactivation of the toxoplasmic infection. Although the process of Tg reactivation is poorly understood, it is known that Tg cysts are controlled by the intact immune system, and only in the case of immune suppression CD4+ T cells are unable to suppress this latent infection. That dysfunction leads to the release of bradyzoites from cysts, their conver-

Communicating author:

Dorota Dziewulska, MD, PhD, Department of Neurology, Medical University of Warsaw, Banacha 1 A, 02-097 Warsaw, Poland, phone: +48 22 599 28 75, fax: +48 22 599 18 57, e-mail: dorota.dziewulska@wum.edu.pl

sion to tachyzoites and toxoplasmosis reactivation. Some studies suggest that dendritic cells may act as Trojan horses to spread the infection [4,13]. An alternative hypothesis assumes that cyst rupture and re-formation of a new cyst is a constant process even in immunocompetent individuals, and the role of the immune system is limited to the control of the tachyzoites [7].

Apart from brain damage, a very common result of Tg invasion is ocular involvement. The infection affecting various parts of the eyes was described both in humans [1,16,17,20] and in experimental animals [21,22]. While in immunocompetent individuals Tg infection is frequently asymptomatic, in immunocompromised patients toxoplasmic encephalitis, retinochoroiditis, and uveitis are frequent [16]. Encephalitis caused by Tg is the most common opportunistic infection in patients with acquired immunodeficiency syndrome (AIDS) and has been well characterized in the literature. But cerebral vasculitis in patients with toxoplasmosis and AIDS was described only occasionally and mainly in case reports from the 1980s [3,10].

Many components of the host immune response to Tg such as production of gamma interferon, cell-mediated immunity, and control of Tg replication by macrophages participate in development of toxoplasmic encephalitis but the exact pathomechanism of Tg neuroinfection in AIDS patients is poorly understood, especially the pathomechanism of vasculitis. But not only the scarcity of data concerning vessel involvement in Tg infection in AIDS impelled us to examine this process. Growing drug resistance to anti-retroviral therapy and the increasing population of patients treated with immunosuppressive or immunomodulatory drugs caused the reemergence of cerebral toxoplasmosis as a clinical problem.

Material and methods

In the AIDS Brain Collection of the Mossakowski Medical Research Centre 178 brains from AIDS patients were collected. Among them cerebral toxoplasmosis was diagnosed in 32 cases (18%) [16]. In 15/32 cases cerebral toxoplasmosis was the only opportunistic infection and these brains were selected for further investigations. These patients died at the age of 30-40 years and one at the age of 52 years. The investigated material was collected between 1992 and 1998 and in none of the patients highly active antiretroviral therapy (HAART) or immunomodulatory management was applied.

On formalin-fixed and paraffin-embedded tissue samples from cerebral hemispheres routine histological stains (hematoxylin and eosin [H&E], Klüver-Barrera method), and immune reactions were applied. Immunohistochemistry was performed using routine microwave antigen retrieval and avidin-biotin-peroxidase methods with antibodies against: *Toxoplasma gondii* (Novocastra, NCL-TG, 1 : 15), fibronectin (Santa Cruz Biotechnology, sc-69681, 1 : 100), IgG (DAKO, A0423, 1 : 500), IgM (DAKO, A0425, 1 : 500), B lymphocyte marker (Novocastra, NCL-MB2, 1 : 50), and T lymphocytes: CD3 (Novocastra, NCL-CD3-PS1 1 : 100), and CD8 (Novocastra, NCL-CD8-295, 1 : 20). To define involvement of the complement system in vasculitis we performed immunohistochemical reactions with antibodies against factor C4β (Santa Cruz Biotechnology, sc-25816, 1 : 250) participating in the classical pathway of complement activation and factor B (Santa Cruz Biotechnology, sc-67141, 1 : 500) involved in the alternate pathway.

Results

In all examined brains Tg cysts or tachyzoites were found. They were visible in brain parenchyma (Fig. 1A), vessel lumen (Fig. 1B) or vessel wall. Apart from different forms of the parasite, numerous foci of coagulative necrosis ("toxoplasmic abscesses") of different size and location were observed. Within the necrotic foci, vessels with the lumen occluded by thrombosis were often visible. Some of the necrotic foci revealed an advanced stage of the breakdown process and they were surrounded by inflammatory infiltrates (granulomatous ridge) composed of leukocytes, lymphocytes, phagocytic cells, histiocytes, and infrequent plasmatic cells. In granulomatous ridge and nearby parenchyma, inflammatory infiltrates were visible both in the perivascular space and within the walls of arteries (Fig. 1C) and veins (Fig. 1D). Distinct inflammation was also found in tissue distant from the necrotic lesions but in such areas inflammatory infiltrates were visible only in precapillary and capillary blood vessels (Fig. 1E). In routine histopathological assessment, vessel inflammation did not demonstrate any characteristic features distinct from vasculitides observed in other neuroinfections.

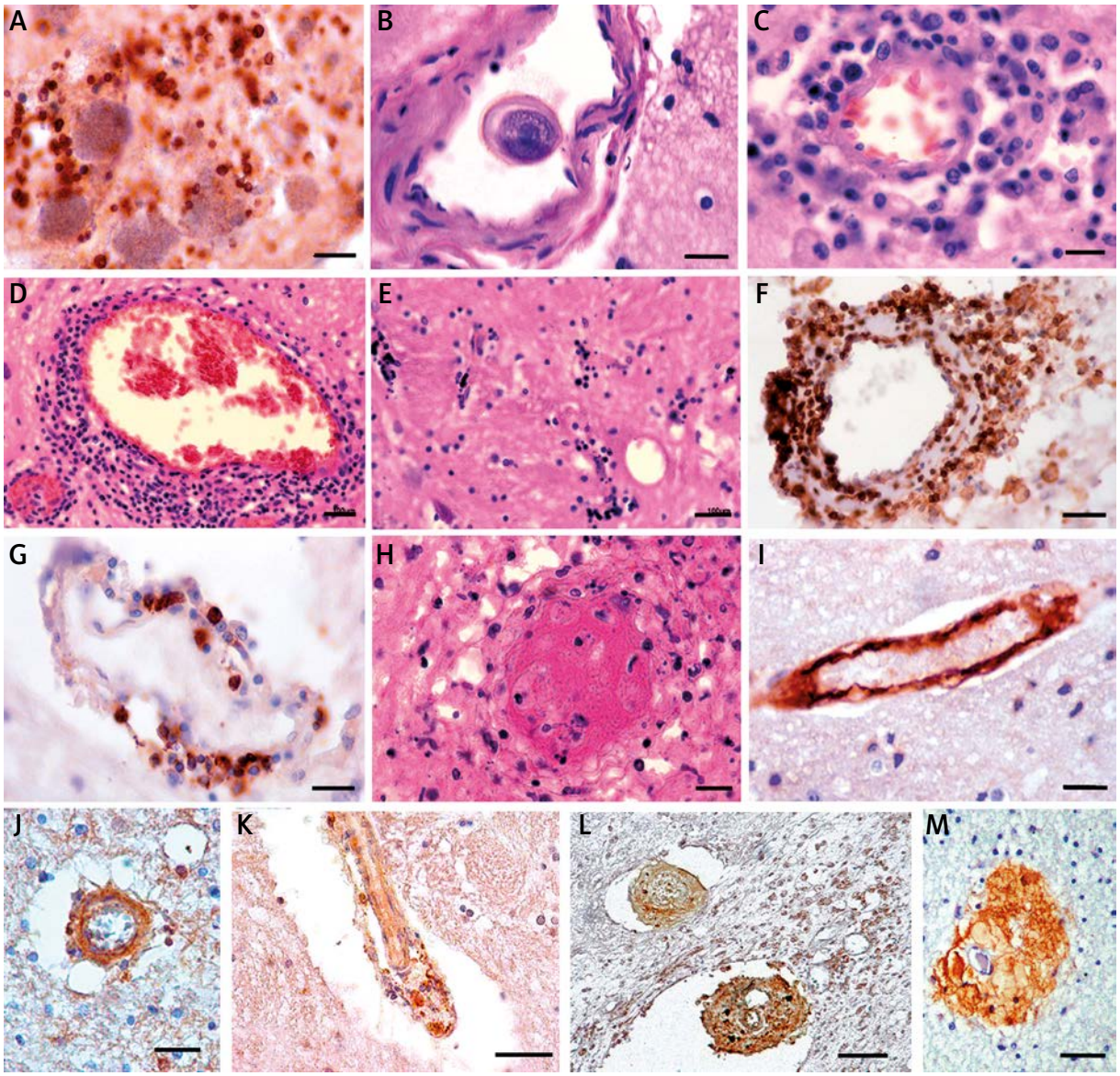

Fig. 1. A) Tachyzoites in brain parenchyma, anti-Tg, bar – 100 µm. **B)** Toxoplasmic cyst in vessel lumen, H&E, bar – 100 µm. **C)** Small cerebral artery infiltrated by mononuclear cells, H&E, bar – 100 µm. **D)** Small cerebral vein with inflammatory infiltrates, H&E, bar – 200 µm. **E)** Infiltrates around precapillary and capillary blood vessels, H&E, bar – 200 µm. **F)** Numerous CD3+ T lymphocytes in vessel wall infiltrates, anti-CD3, bar – 100 µm. **G)** Non-numerous B lymphocytes in vessel wall infiltrates, anti-B lymphocyte marker, bar – 100 µm. **H)** Eosinophilic fibrinoid necrosis of the vascular media with occlusion of the vessel lumen, H&E, bar – 100 µm. **I)** Strong positive immune reaction to IgG in wall of small cerebral artery, anti-IgG, bar – 100 µm. **J)** Moderately positive immune reaction to IgM in vessel wall, anti-IgM, bar – 100 µm. **K)** Intramural deposits of factor C4β in wall of the white matter artery; anti-C4β, bar – 200 µm. **L)** Granular immunolabel for complement factor B in wall of small arterial vessels; visible moderately positive cytoplasmic reaction in parenchymal macrophages; anti-factor B, bar – 250 µm. **M)** Immunolabel for fibronectin around small vessel in the cerebral white matter, anti-fibronectin, bar – 200 µm.

Immunohistochemical reactions revealed predominance of CD3+ T lymphocytes in inflammatory infiltrates localized both in granulomatous ridge and in vessel wall (Fig. 1F) while CD8+ T lymphocytes and B lymphocytes were found infrequently and only within vessel wall (Fig. 1G). In five cases, apart from intramural inflammatory infiltrates, eosinophilic fibrinoid necrosis of the vascular media was observed (Fig. 1H). In some of the cerebral blood vessels immunopositive reactions to IgG (Fig. 1I) and IgM (Fig. 1J) were observed. Deposits of the immunoglobulins were observed in the walls of medium- and small-sized arterial vessels but not in veins and capillaries. The immune reactions for compounds of the complement system had a granular character and they were moderately positive for factor C4β (Fig. 1K) and strongly for factor B (Fig. 1L). Positive immunolabel for C4β was observed only in some of the parenchymal small arteries while a pronounced immune reaction for factor B was seen in numerous vessels of different types. Immunoreactivity for both complement factors was also noted in macrophages. In some cases with coagulative necrosis increased perivascular immunolabel for both complement compounds and fibronectin (Fig. 1M) was found.

The vascular changes revealed in immunohistochemical reactions and described above were observed in vessels not only localized within foci of coagulative necrosis and granulomatous ridge but also in nearby parenchyma but not in distant precapillaries or capillaries with inflammatory infiltrates.

Discussion

Our investigation on cerebral toxoplasmosis in AIDS patients showed, typically for the disease, morphological foci of coagulative necrosis and inflammation involving cerebral vessels.

In ischemic vascular diseases coagulative necrosis due to stenosis or occlusion of the vessel lumen is rarely observed because this stage of necrosis is usually transient. Normally, after the onset of ischemia, damage to the blood-brain barrier (BBB) leads to increased permeability of the vessel wall and afflux of leukocytes, lymphocytes and monocytes/macrophages. That phenomenon results in tissue breakdown and development of colliquative necrosis. In AIDS and other immunocompromised patients, severe dysfunction of the immune system can delay tissue breakdown and maintenance of the coagulative changes.

Although in HIV encephalitis perivascular infiltrates disseminated in brain parenchyma are common, involvement of the vessel wall is very rare with an incidence of less than 1% [9]. In our material intramural inflammatory infiltrates were observed in vessels of different type and size localized not only within foci of coagulative necrosis but also in adjacent and distant parenchyma. The affected vessels sometimes revealed perivascular immunoexpression of fibronectin and complement factor C4β. Since complement factor C4β and a fraction of fibronectin exist in a soluble form in serum, their perivascular occurrence indicates increased permeability of the vessel wall. This phenomenon characteristic for disturbed BBB may play a key role in Tg spread in the CNS [7,12].

Apart from intramural inflammatory infiltrates, some cerebral vessels also revealed eosinophilic necrosis of the muscular layer. Eosinophilic necrosis in cerebral vessels has been observed in many different diseases from idiopathic arterial hypertension to amyloid angiopathy. However, in such patients the vessel wall was usually devoid of inflammatory infiltrates.

It is still unknown what factor(s) is directly responsible for development of vasculitis in cerebral toxoplasmosis in AIDS. It is known that in ischemic vascular diseases presence of coagulative or colliquative necrosis does not lead to vasculitis. Therefore other factors have to be responsible for vessel inflammation. There are two major mechanisms by which infection can induce vasculitis: (1) direct invasion of the microorganism due to damage to the vessel wall, and (2) immune-mediated injury.

In cerebral toxoplasmosis both HIV and Tg can give rise to development of vasculitis. In HIV positive individuals without co-infections with other pathogens, a wide spectrum of vasculitides has been found [9]. But presence of Tg cysts in vessel lumen and tachyzoites in vascular wall can also cause vessel damage, particularly damage to endothelial cells, and triggers not only thrombotic cascade [10] but also inflammatory and immune reactions. Results of recent investigations confirmed that Tg can modulate gene expression of cerebral endothelial cells to promote its own migration through the BBB [12]. Among these modulatory changes, prominent upregulation of the cell adhesion molecule ICAM-1, activated leukocyte cell adhesion molecule (ALCAM), and vascular cell adhesion molecule 1 (VCAM-1) was

found [19]. Expression of different classes of adhesion molecules observed both in acute and chronic toxoplasmic encephalitis [5] not only facilitates Tg migration but also supports infiltration of the vessel wall by circulating blood cells and development of inflammation.

Another pathomechanism implicated in the induction of vasculitis is immune-mediated inflammation in which vessel damage may be caused by cell-mediated, immune complex-mediated and autoantibody-mediated reactions.

T cell-mediated vascular injury has been demonstrated in several types of vasculitides including PAN and AIDS. It is known that in HIV infection there is an oligoclonal expansion of T cells, especially CD8 + cells [8]. But our and some other authors' immunohistochemical studies revealed that lymphocytes seen in the vessel wall and perivascular space are not exclusively of the T but also of B cell lineage.

In our material some of the arterial vessels showed intramural deposits of IgG and IgM. Although immunoglobulin deposits in the vessel wall have been described in many disorders, even in some genetically determined vascular diseases such as CADASIL (cerebral autosomal dominant arteriopathy with subcortical infarcts and leukoencephalopathy) [18], they are highly indicative for the immune complex-mediated pathomechanism of vasculitis. In patients with Tg infection, specific IgM, IgG, IgA, and even IgE antibodies were found [6,15]. In immunocompetent individuals with latent Tg infection, the parasites inside the brain may be protected from circulating antibodies by intact BBB [14]. But in immunodepressed patients with toxoplasmosis reactivation, damage to the BBB may promote antibody accumulation in the vessel wall leading to development of vasculitis.

Vasculitis induced by the immune complexes is identified by the presence of immunoglobulin and complement deposits in the vessel wall [11]. In our material not only deposits of IgG and IgM were found but also complement factors C4β and B.

Complement is activated by three pathways: the classical, the alternative and the lectin pathway. Factor C4β is a potent anaphylatoxin that is released during the classical pathway of complement activation while factor B is involved in the alternative pathway. It is known that in the classical pathway, the initiator complex is activated by a wide range of targets, including apoptotic cells, some viruses and bacteria, and antibody-antigen complexes containing immunoglobulin IgG or IgM [2]. The initiation of the alternative pathway does not require presence of the immune complexes but starts with spontaneous hydrolysis of the C3 component or by its binding to specific targets on microorganism and eukaryotic cells. The lectin pathway is also independent of the immune complexes and is initiated by lectin binding to moieties localized on the surface of microorganisms or dying cells. The intramural deposits of immunoglobulins and complement factor C4β in vessels observed by us suggest that complement activation via the classical pathway is involved in development of vasculitis. But the positive immune reaction for factor B in some vessels indicates that complement may also be activated via the alternative pathway which is less specific but more autoaggressive than the classical one.

Vasculitis in AIDS patients with cerebral toxoplasmosis is a very complex system where many factors are unbalanced. Although it is difficult to establish certainly whether toxoplasmosis itself leads to the above-described vascular changes, in the presented study we demonstrated that several distinct immune-mediated mechanisms may coexist in the vasculitis and therefore finding an efficient therapy is still a challenge.

References

1. Antoniazzi E, Guagliano R, Meroni V, Pezzotta S, Bianchi PE. Ocular impairment of toxoplasmosis. Parassitologia 2008; 50: 35-36.
2. Carroll MC. The complement system in regulation of adaptive immunity. Nat Immunol 2004; 5: 981-986.
3. Chaudhari AB, Singh A, Jindal S, Poon TP. Haemorrhage in cerebral toxoplasmosis. A report on a patient with the acquired immunodeficiency syndrome. S Afr Med J 1989; 76: 272-274.
4. Courret N, Darche S, Sonigo P, Milon G, Buzoni-Gâtel D, Tardieux I. CD11c- and CD11b-expressing mouse leukocytes transport single Toxoplasma gondii tachyzoites to the brain. Blood 2006; 107: 309-316.
5. Deckert-Schlüter M, Schluter D, Hof H, Wiestler OD, Lassmann H. Differential expression of ICAM-1, VCAM-1 and their ligands LFA-1, Mac-1, CD43, VLA-4, and MHC class II antigens in murine Toxoplasma encephalitis: a light microscopic and ultrastructural immunohistochemical study. J Neuropathol Exp Neurol 1994; 53: 457-468.
6. Dziubek Z, Zarnowska H, Basiak W, Gorski A, Kajfasz P. Some aspects of immune response in toxoplasmosis. Przegl Epidemiol 2001; 55: 495-502.
7. Feustel SB, Meissner M, Liesenfeld O. Toxoplasma gondii and the blood-brain barrier. Virulence 2012; 3: 182-192.

8. Gisselbrecht M, Cohen P, Lortholary O, Jarrousse B, Gayraud M, Lecompte I, Ruel M, Ghérardi R, Guillevin L. Human immunodeficiency virus-related vasculitis. Clinical presentation of and therapeutic approach to eight cases. Ann Med Interne (Paris) 1998; 149: 398-405.
9. Guillevin L. Vasculitides in the context of HIV infection. AIDS 2008; 22 Suppl 3: S27-33.
10. Huang TE, Chou SM. Occlusive hypertrophic arteritis as the cause of discrete necrosis in CNS toxoplasmosis in the acquired immunodeficiency syndrome. Hum Pathol 1988; 19: 1210-1214.
11. Jennette JCh. Implications for pathogenesis of patterns of injury in small- and medium-sized-vessel vasculitis. Cleve Clin J Med 2002; 69 Suppl 2: SII33-38.
12. Lachenmaier SM, Deli MA, Meissner M, Liesenfeld O. Intracellular transport of Toxoplasma gondii through the blood-brain barrier. J Neuroimmunol 2011; 232: 119-130.
13. Lambert H, Hitziger N, Dellacasa I, Svensson M, Barragan A. Induction of dendritic cell migration upon Toxoplasma gondii infection potentiates parasite dissemination. Cell Microbiol 2006; 8: 1611-1623.
14. Masocha W, Kristensson K. Passage of parasites across the blood-brain barrier: Virulence 2012; 3: 202-212.
15. Matowicka-Karna J, Dymicka-Piekarska V, Kemona H. Does Toxoplasma gondii infection affect the levels of IgE and cytokines (IL-5, IL-6, IL-10, IL-12, and TNF-alpha)? Clin Dev Immunol 2009; 2009: 374696; doi: 10.1155/2009/374696.
16. Mossakowski MJ, Zelman IB. Neuropathological syndromes in the course of full blown acquired immune deficiency syndrome (AIDS) in adults in Poland (1987-1995). Folia Neuropathol 1997; 35: 133-143.
17. Pleyer U, Torun N, Liesenfeld O. Ocular toxoplasmosis. Ophthalmologe 2007; 104: 603-615.
18. Rafałowska J, Fidzianska A, Dziewulska D, Podlecka A, Szpak GM, Kwiecinski H. CADASIL: new cases and new questions. Acta Neuropathol 2003; 106: 569-574.
19. Silva NM, Manzan RM, Carneiro WP, Milanezi CM, Silva JS, Ferro EA, Minor JR. Toxoplasma gondii: the severity of toxoplasmic encephalitis in C57BL/6 mice is associated with increased ALCAM and VCAM-1 expression in the central nervous system and higher blood-brain barrier permeability. Exp Parasitol 2010; 126: 167-177.
20. Smith JR, Cunningham ET Jr. Atypical presentations of ocular toxoplasmosis. Curr Opin Ophthalmol 2002; 13: 387-392.
21. Stahl W, Turek G. Chronic murine toxoplasmosis: clinicopathologic characterization of a progressive wasting syndrome. Ann Trop Parasitol 1988; 82: 35-48.
22. Webb RM, Tabbara KF, O'Connor GR. Retinal vasculitis in ocular toxoplasmosis in nonhuman primates. Retina 1984; 4: 182-188.

Original article

Folia Neuropathologica

Clinical and neuroimaging correlation of movement disorders in multiple sclerosis: case series and review of the literature

Anna Potulska-Chromik[1], Monika Rudzinska[2], Monika Nojszewska[1], Aleksandra Podlecka-Piętowska[1], Andrzej Szczudlik[2], Beata Zakrzewska-Pniewska[1], Marek Gołębiowski[3]

[1]Department of Neurology, Medical University of Warsaw, Warsaw, [2]Department of Neurology, *Collegium Medicum* Jagiellonian University, Krakow, [3]1st Department of Clinical Radiology, Medical University of Warsaw, Warsaw, Poland

Folia Neuropathol 2014; 52 (1): 92-100 DOI: 10.5114/fn.2014.41747

Abstract

Multiple sclerosis (MS) is a chronic inflammatory demyelinating disease of the central nervous system, in which movement disorders (MD) have been reported very rarely. Anatomopathological studies of MS indicate two main processes: inflammation and neurodegeneration. The occurrence of the movement disorders symptoms in MS revises the question of aetiology of these two diseases. During the 10 years of observation in our out-patient clinic and MS units we examined about 2500 patients with clinically definite MS diagnosed according to the revised McDonald's criteria. Only in 10 cases we found coexistence of MS and MD signs. Below we present rare cases of patients with coexistence of MS and chorea, pseudoathetosis, dystonia and parkinsonism. Searching for the strategic focal lesion in our case series showed demyelinating plaques placed in the thalamus most often. Detailed analysis of the clinical, pharmacological and neuroimaging correlations may help to explain the character of movement disorders in MS.

Key words: *multiple sclerosis, movement disorders, dystonia, parkinsonism, chorea, pseudoathetosis.*

Introduction

The multiple sclerosis (MS) is an autoimmune disorder associated with several pathophysiological mechanisms such as inflammation, demyelination, axonal/neuronal damage, gliosis, remyelination and repair mechanisms, oxidative injury and excitotoxicity. Heterogeneity in the phenotypic expression of MS is related to these processes, which are not uniformly represented in patient population, even at the same stage of the disease [14].

The clinical symptomatology presenting as transient pyramidal, sensory, cerebellar signs, usually is very characteristic in most cases of MS. In this study we present rare cases of MS with coexistence of a wide spectrum of movement disorders (MD), including MD occurring as a presenting symptom of MS. The occurrence of the movement disorders symptoms in multiple sclerosis revises the question of aetiology of these two disorders. After detailed clinical and neuroimaging analyses of our patients we proposed an algorithm, which can help to find

Communicating author:
Prof. Marek Gołębiowski, 1st Department of Clinical Radiology, Medical University of Warsaw, 5 Chałubińskiego Str., 02-004 Warsaw, Poland, e-mail: marek.golebiowski@wum.edu.pl

the association between inflammatory or/and neurodegenerative damage occurring in MS and MD.

Material and methods

During the 10 years of observation in our out-patient clinic and MS units we examined about 2500 patients with clinically definite MS diagnosed according to the revised McDonald's criteria [10]. Only in 10 cases we found coexistence of MS and MD signs. In all presented patients, the past medical history including exposure to neuroleptics, neurotoxin or head trauma was negative. Wilson's disease, neuroacanthocytosis, thyroid dysfunction and neuroborreliosis were also excluded. Below we present the clinical picture of our patients.

Movement disorders as a presenting symptom of multiple sclerosis

Case 1

A 45-year-old man complained of involuntary movements which appeared in the upper limbs and then progressed to the head, trunk and lower limbs, irritability and memory problems, which started insidiously. His brother revealed a 24-year-history of MS with relapsing/remitting episodes of cerebellar symptoms and lower limb paresis.

Neurological examination revealed increased mood, uninhibited behaviour, choreic movement of the face, trunk and limbs more remarkable in upper limbs, motor tics of the face and arms, bilaterally decreased muscle tone and brisk deep tendon reflexes, lower limbs ataxia, impaired tandem gait. The choreic movement exacerbated during walking or other voluntary movements and under stress.

Genetic tests for Huntington disease and tests for metachromatic leucodystrophy and lupus erythematosus were negative. The activity of protein C and antithrombin III and concentration of protein S were within normal limits. Neuropsychological examination showed an early stage of dementia, with frontal and subcortical dysfunctions. Finally, the patient was diagnosed with a familial, primary progressive multiple sclerosis of unusual symptomatology: involuntary movements, cognitive impairment (dementia) and mood disorder (Fig. 1).

Case 2

A 33-year-old man was being examined at a neurological department because of persistent involuntary rotation of the head to the right side and head tremor. These symptoms began five years before admission and the disease was slowly progressive. The symptoms reminded a focal cervical dystonia (torticollis).

The neurological examination revealed also lack of left abdominal reflexes and bilaterally absent plantar responses.

Finally, after 2 relapses of the disease he was diagnosed according to the McDonald's criteria with relapsing-remitting MS with cervical dystonia as a presenting symptom (Fig. 2).

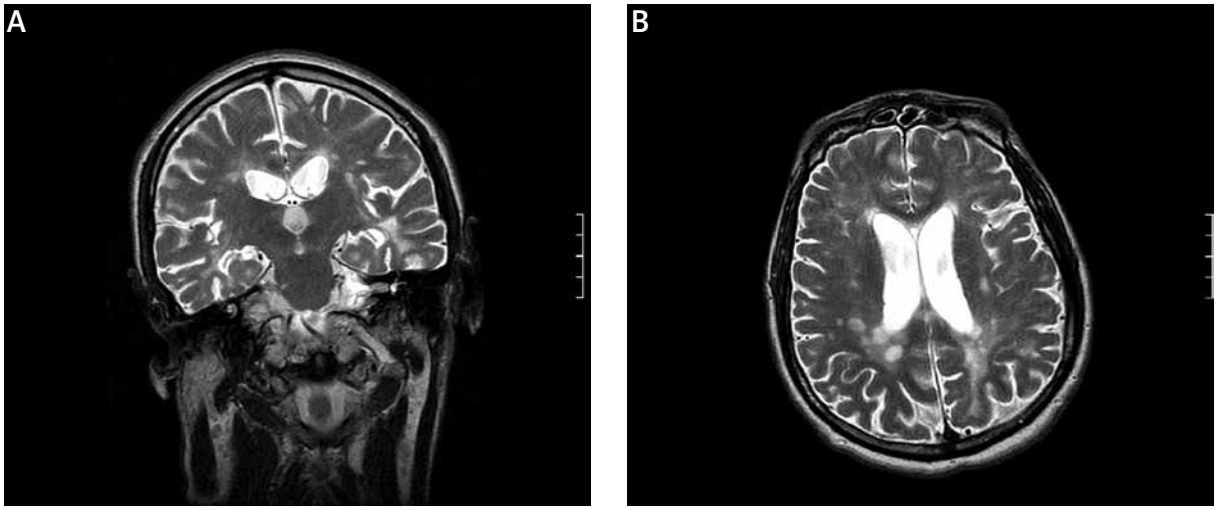

Fig. 1. Case 1. **A)** Coronal and **B)** axial T2 MR images show multiple focal periventricular/subcortical hyperintense lesions compatible with demyelinating plaques.

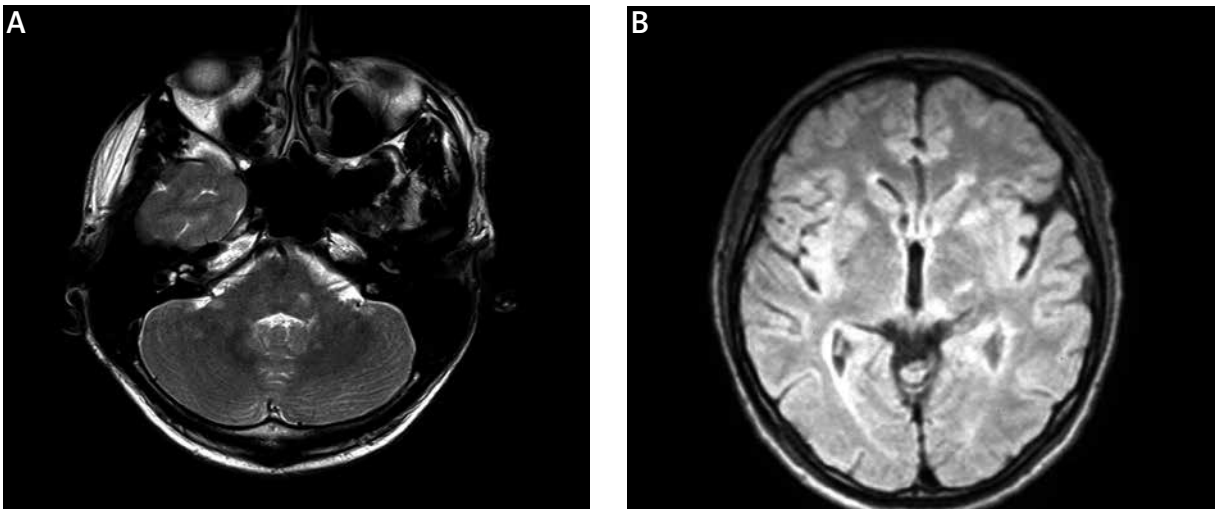

Fig. 2. Case 2. **A)** Axial FLAIR and **B)** T2 MR images demonstrate demyelinating lesions in the cerebellum, left thalamus and periventricular area.

Case 3

A 32-year-old man complained of involuntary movements of the left upper and lower limbs accompanied by severe pain, lasting for 3 weeks. Symptoms started insidiously, lasted 5-10 seconds, usually occurred several times a day initiated by fatigue or voluntary movements of the limbs. On neurological examination the patient presented with mild left side paresis, brisk tendon reflexes in the left lower limb, bilateral flexor plantar reflex. Movements first appeared in the arm, then slowly progressed to the forearm and hand causing painful dystonic posture and spread to the left side of the trunk and to the left lower limb proximally (the thigh).

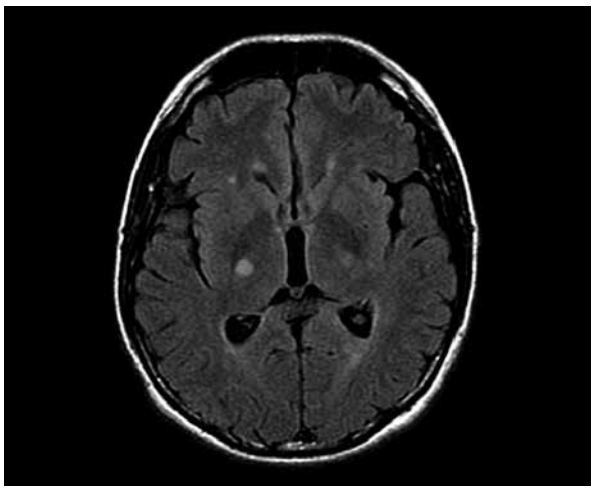

Fig. 3. Case 3. Axial FLAIR MR image shows some bilateral, periventricular focal T2 hyperintensities localized also in the right thalamus and subinsular area.

We diagnosed MS of an unusual symptomatology: involuntary movements similar to muscle spasms accompanied by dystonia. The diagnosis was confirmed by MRI with gadolinium and CSF study (Fig. 3).

Case 4

A 39-year-old woman was being diagnosed in our out-patient clinic because of a 5-year history of the voice and head tremor. She also noticed excessive blinking of the eyes, tendency to the neck rotation to the left side and general fatigability. Neurological examination showed mild cervical dystonia with rotation of 20 degrees to the left side (torticollis), slight dysmetria in the left upper limb, lack of the plantar and all abdominal reflexes bilaterally. Over the subsequent year she experienced 3 relapses of the disease with cerebellar and motor signs. She was qualified to the interferon therapy with marked improvement (no relapses during 1-year therapy were observed), however 3 months after finishing this treatment the patient noticed progression of cervical dystonia.

Movement disorders in the course of the multiple sclerosis

Case 5

A 37-year-old woman with a 5-year history of MS complained of tremor and disability of the right hand, which had started insidiously and slowly progressed.

On neurological examination the patient presented with stiffness, slowness and rest tremor on the right side of the body, deep tendon reflexes were very brisk, exaggerated on the left side, Babinski sign was observed bilaterally.

Genetic tests for early-onset Parkinson's disease (PARK2, DJ-1, PINK) were negative.

She observed improvement after ropnirole 4 mg/day. After 2 months she stopped the therapy by mistake without any consequences. Tremor reappeared during the next relapse of the disease. She responded very well to corticosteroid therapy (Fig. 4).

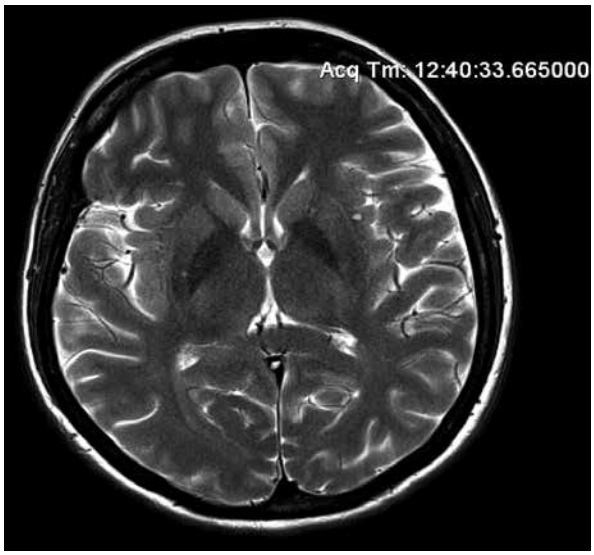

Fig. 4. Case 5. Axial T2 image shows two small demyelinating lesions in the putamen of the right lentiform nucleus and left subinsular area.

Case 6

A 43-year-old woman was diagnosed with multiple sclerosis in 2006 after an episode of the left retrobulbar optic neuritis. In May 2010, she had sudden onset of involuntary movements in the right hand coexisting with pain of the forearm. On her physical examination, there was reduced deep sensation in the right hand with associated pseudoathetotic movements (Fig. 5).

Case 7

A 51-year-old woman with a 28-year history of MS presented to our unit with dystonia of the left hand. She had relapsing-remitting MS with sensory, motor and visual symptoms and signs.

In 2003, she observed involuntary movements and cramp of her left hand, which was diagnosed as symptomatic focal dystonia (Fig. 6).

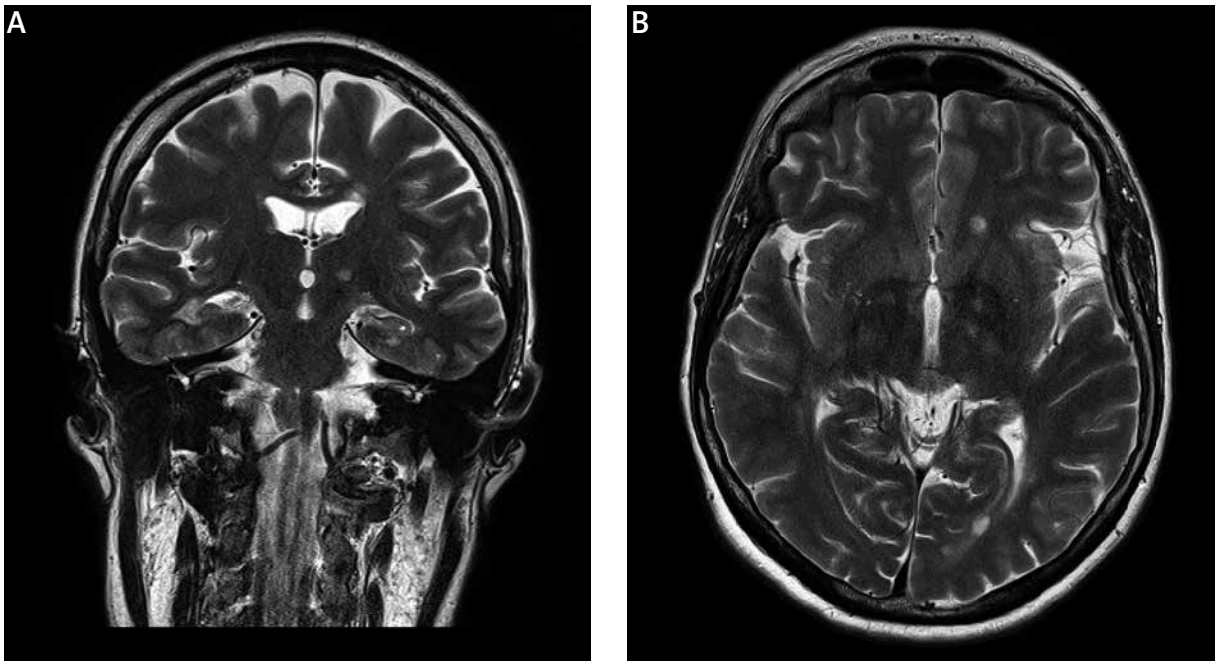

Fig. 5. Case 6. **A)** Coronal and **B)** axial MRI T2 images show demyelinating lesions in both thalami, periventricular and cortico-subcortical area.

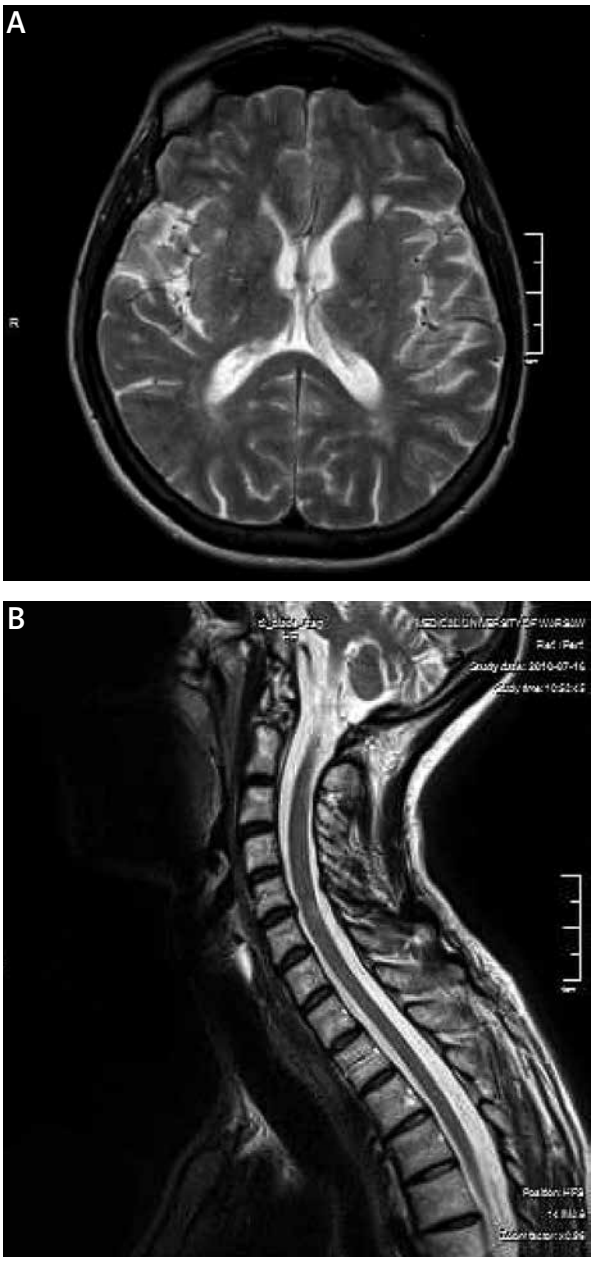

Fig. 6. Case 7. **A)** Axial T2 MR image shows multiple foci of hyperintense signal in both thalami and periventricular/subcortical white matter; **B)** Cervical MRI revealed few intramedullary demyelinating plaques and discopathy at the C4/C5 level.

Case 8

A 66-year-old woman with a 30-year history of MS presented with blepharospasm. Treatment with botulinum toxin has been effective with a significant long-lasting improvement after transient right ptosis 5 days after treatment. Currently, the patient experiences only excessive blinking and she does not need any additional treatment.

Case 9

A 58-year-old woman with a 27-year history of MS experienced excessive blinking and involuntary spasm of both orbicularis eye muscles, diagnosed as a blepharospasm. Treatment of blepharospasm with botulinum toxin repeated every 5 months was slightly effective.

Case 10

A 57-year-old woman with an 18-year history of a very benign course of relapsing-remitting MS presented with dystonic tremor of the head with slight rotation to the left side and right hand dystonia resembling writer's cramp (Fig. 7).

Results

All details, i.e. MS course, type of MD, MRI findings as well as response to the therapy are summarized in Table I.

Discussion

Movement disorders symptomatology is rare in MS. In some cases, even very experienced physicians are diverted from the diagnosis of MS by the presence of unusual symptoms derived from basal ganglia or autonomic nervous system lesions [11], although occasional involvement of the basal ganglia was reported [8-10,18].

Moreover, these unusual findings are still very challenging in looking for neuropathological basis for dystonia, chorea and parkinsonism. In the literature, causal or coincidental association of these two disorders was discussed. To the best of our knowledge, chorea has been reported in only few cases, almost always during the course of the diagnosed MS. Demyelinating lesions were usually situated in the basal ganglia (striatum). In our case 1 with chorea as a presenting symptom of MS, neuroimaging revealed typical demyelinating changes in the periventricular white matter, most remarkable in the frontal and parietal lobes and in the left cerebellar hemisphere without any significant correlation with the extrapyramidal tract. Although chorea and ticks did not respond to neuroleptic treatment, their severity was

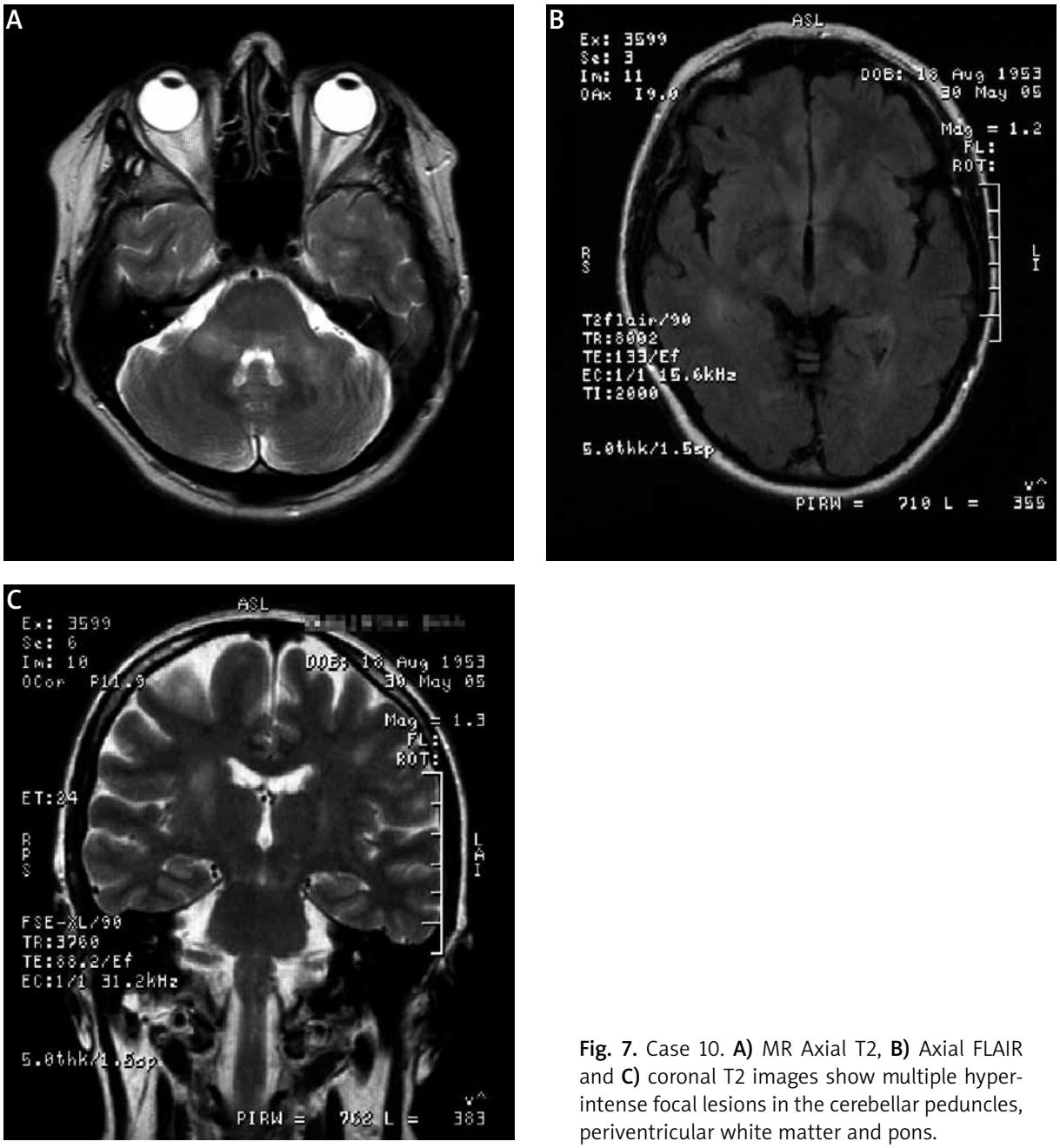

Fig. 7. Case 10. **A)** MR Axial T2, **B)** Axial FLAIR and **C)** coronal T2 images show multiple hyperintense focal lesions in the cerebellar peduncles, periventricular white matter and pons.

slightly temporarily diminished on corticosteroid therapy. The positive response to this treatment does not allow to exclude causal relationship between chorea and MS.

Paroxysmal symptoms (dysarthria, ataxia, paresthesia, pain, itching, pain, hemiparesis) as presenting symptoms were also described in MS. Tuzun *et al.* [19] reported that clusters of paroxysmal symptoms usually tend to occur early in the course of the disease. Espir and Millac [2] postulated that "paroxysms result from a degree of demyelination insufficient to give persistent deficit, but rendering axons hypersensitive to minor stresses". Paroxysmal symptoms, especially the spasm, probably result from ephaptic transmission between a sensory pathway and the corticospinal tract. Response to the corticosteroids observed in our case 3 indicates the inflammatory/demyelinating mechanism of this disorder.

Cervical dystonia as a presenting symptom of MS has been also reported very rarely [13], however spas-

Table I. Clinical signs, MRI features and response to specific therapy in our group of patients

Patients	MS course	Type of movement disorder	Localization of hyperintense focal lesions in MRI possibly related to the movement disorders*	MRI findings reported in the literature	Positive response to MS therapy (corticosteroids/ interferon)	Positive response to movement disorders therapy
Case 1	primary progressive	chorea	only typical for MS	thalamus, lentiform nucleus [12] caudate nucleus [5]	yes/not available	neuroleptics – no
Case 2	relapsing-remitting	dystonia	thalamus, cerebellar peduncles	caudate nucleus, putamen [17], pallidum [18], midbrain [9], pontomesencephalic junction [17], cervical spinal cord [3]	yes/yes	botulinum toxin – no (side effects)
Case 3	relapsing-remitting	paroxysmal dystonia of the limb	the right thalamus, brainstem, midbrain, pons, cerebellar peduncle	thalamus, lentiform nuclei [18], cervical spinal cord [20]	yes/yes	baclofen – no
Case 4	relapsing-remitting	dystonia	cervical spinal cord at the level C1/C2	as in case 2	no/yes	botulinum toxin – yes
Case 5	relapsing-remitting	parkinsonism on the right side	the right nucleus lentiformis	centrum semiovale, cerebellum, pons, internal capsule, thalamus, bilateral pallidum, substantia nigra, red nucleus [18]	yes	ropinirole – yes
Case 6	relapsing-remitting	pseudoathetosis	thalamus, nucleus lentiformis, medulla oblongata	C2-C5 spinal cord segments [4, 6] internal capsule, pallidum, mesencephalus, pons [16]	no	not available
Case 7	relapsing-remitting	hand dystonia	thalamus, cervical spinal cord C4-C5	thalamus and lentiform nuclei [17], cervical spinal cord [3]	no	botulinum toxin – yes
Case 8	secondary progressive	dystonia – blepharospasm	only typical for MS	parietal lobe [8]	no	botulinum toxin – yes
Case 9	secondary progressive	dystonia – blepharospasm	only typical for MS	parietal lobe [8]	the patient did not consent to the mitoxantrone therapy	botulinum toxin – yes
Case 10	relapsing-remitting	segmental dystonia (dystonic tremor of the head and task specific dystonia resembling writer's cramp of the right hand)	pons, cerebellar peduncles	as in case 2 and 7	no	not estimated

**All patients fulfil radiological criteria of MS diagnosis (periventricular, juxtacortical and infratentorial lesions)*

modic torticollis expressed during the course of the definite MS is found more frequently [5,17,18]. Subcortical grey matter contains myelinated fibers and plaques causing movement disorders can be found in the striatum, pallidum, thalamus and most commonly the brainstem. However, in the majority of reported cases, a relationship between plaque's location and movement disorders including dystonia was not stated [18]. In our group of patients, a possible association between location of the lesion and dystonia was found in case 2, 4, 7 and 10. In case 8 and 9 only diffuse periventricular lesions were found, probably not related to the blepharospasm, however clinical observation with long-lasting improvement in case 8 may suggest an autoimmune inflammatory origin. Brain MRI of patients 7 and 10 with dystonia of the upper limb showed lesions located in the periventricular white matter as well as in thalamus and pons. A hyperintensive focus in the cervical spinal cord was found in case 4 (cervical dystonia and voice tremor) and 7 (hand dystonia). Magnetic resonance imaging of the cervical spinal cord in case 10 revealed only discopathy at the level of C4/C5 and C5/C6 presumably not related to the movement disorders.

Pseudoathetosis is also a very rare symptom in MS. In our patient, transient involuntary movements of the right hand with coexisting loss of proprioception, clinically indistinguishable from athetosis were diagnosed as pseudoathetosis. Sharp *et al.* [15] postulated that this symptom is usually due to lesion of the proprioception pathway resulting in the dysfunction of the integration of the deep sensation with motor function with location in the striatum. Magnetic resonance imaging scan of our patient 6 revealed multiple foci in the basal ganglia, and thalamus. Location as well as resembling of the symptoms after 3 months may suggest its autoimmune origin.

There are several reports found in historic neurologic literature of parkinsonian tremor in the course of MS. In two cases reported by Mao *et al.*, no correlations between location of demyelinating lesion and parkinsonism were observed [5]. Remitting parkinsonism presented with focal hypersignal in immediate vicinity of the extrapyramidal tract strongly suggest possibility of a relationship between these two disorders. In our case, a suspected lesion was located in the right nucleus lentiformis. Response to a dopaminergic agonist was very satisfactory in this patient but treatment with corticosteroids during relapse brought to light complete resolution of parkinsonian tremor. It could be explained by hypothesis that PD symptoms may be aggravated by MS plaques, thus explaining the good response to corticosteroids in reported patients.

Next postulated association between parkinsonism and MS suggested that repeated perivenous demyelination in pigmented neurons may provoke chromatolysis and myelinoclastic process in substantia nigra causing PD [7].

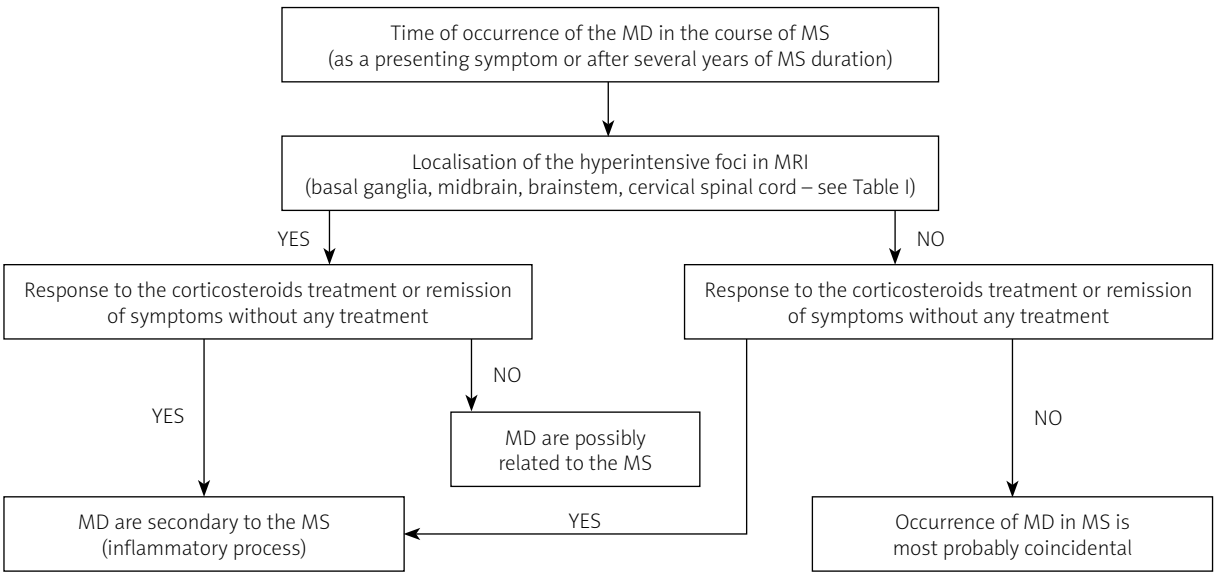

Fig. 8. Algorithm of searching for a causal relationship between movement disorders and multiple sclerosis.

A recently reported case of dystonia/parkinsonism as a presenting symptom of primary progressive MS syndrome showed one more explanation of the association between MD and MS [1,7]. In primary progressive MS both autoimmunological/inflammatory as well as neurodegenerative pathomechanisms are considered. Delgado *et al.* [1] found human anti basal ganglia antibodies in their reported case. This observation confirmed a possible causal relationship between MD and MS. Moreover, during the course of MS, the risk of MD occurrence may increase because neurodegeneration known to be responsible for movement disorders start to be much more pronounced comparing to the inflammatory process. On the other hand, demyelinating lesions are diffuse in time and space and progression of the disease is a risk factor for the new plaques and new, even atypical, symptoms.

In conclusion, searching for the strategic focal lesion in patients with MD and MS might be difficult because of the limitation of the neuroimaging methods. Our case series showed demyelinating plaques placed in the thalamus most often. In the future more accurate methods of magnetic resonance imaging may help find even small lesions in the extrapyramidal tract. Another interesting explanation of the association between MD and MS is response to the treatment. Below we present an algorithm which may help to explain the causal relationship and origin of the symptoms (Fig. 8).

In our opinion, MD are very often secondary to the demyelinating or neurodegenerative process occurring in MS. We suggest that this association should be considered in each case individually. Patients presented in this paper and cases reported in the literature show that MD in MS may have heterogeneous mechanisms and course.

References

1. Delgado S, Baez S, Singer C, Sengun C, Sheremata WA, Papapetropoulos S. Parkinsonism/dystonia syndrome secondary to multiple sclerosis with anti-basal-ganglia antibodies. Mov Disord 2009; 24: 309-311.
2. Espir M, Millac P. Paroxysmal brain stem dysfunction in multiple sclerosis. Br Med J 1972; 18: 1503.
3. Klostermann W, Vieregge P, Kömpf D. Spasmodic torticollis in multiple sclerosis: significance of an upper cervical spinal cord lesion. Mov Disord 1993; 8: 234-236.
4. Lu CS, Tsai CH, Chiu HC, Yip PK. Pseudoathetosis as a presenting symptom of spinal multiple sclerosis. J Formos Med Assoc 1992; 91: 106-109.
5. Mao CC, Gancher ST, Herndon RM. Movement disorders in multiple sclerosis. Mov Disord 1988; 3: 109-116.
6. Nagano T, Mizoi R, Watanabe I, Tomi H, Sunohara N. A case of multiple sclerosis manifesting piano playing movement. Rinsho Shinkeigaku 1993; 33: 442-445 (abstract).
7. Nelson DA, Paulson GW. Idiopathic Parkinson's disease(s) may follow subclinical episodes of perivenous demyelination. Med Hypotheses 2002; 59: 762-769.
8. Nociti V, Bentivoglio AR, Frisullo G, Fasano A, Soleti F, Iorio R, Loria G, Patanella AK, Marti A, Tartaglione T, Tonali PA, Batocchi AP. Movement disorders in multiple sclerosis: Causal or coincidental association? Mult Scler 2009; 14: 1284-1287.
9. Plant GT, Kermode AG, du Boulay EP, McDonald WI. Spasmodic torticollis due to a midbrain lesion in a case of multiple sclerosis. Mov Disord 1989; 4: 359-362.
10. Polman CH, Reingold SC, Banwell B, Clanet M, Cohen JA, Filippi M, Fujihara K, Havrdova E, Hutchinson M, Kappos L, Lublin FD, Montalban X, O'Connor P, Sandberg-Wollheim M, Thompson AJ, Waubant E, Weinshenker B, Wolinsky JS. Diagnostic criteria for multiple sclerosis: 2010 revisions to the 'McDonald Criteria'. Ann Neurol 2011; 69: 292-302.
11. Poser CM, Brinar BB Diagnostic criteria for multiple sclerosis: Clin Neurol Neurosur 2001; 103: 1-11.
12. Roos RA, Wintzen AR, Vielvoye G, Polder TW. Paroxysmal kinesigenic choreoathetosis as presenting symptom of multiple sclerosis. J Neurol Neurosurg Psychiatry 1991; 54: 657-658.
13. Rüegg SJ, Bühlmann M, Renaud S, Steck AJ, Kappos L, Fuhr P. Cervical dystonia as first manifestation of multiple sclerosis. J Neurol 2004; 251: 1408-1410.
14. Seven A, Aslan M, Incir S, Altıntaş A. Evaluation of oxidative and nitrosative stress in relapsing remitting multiple sclerosis: effect of corticosteroid therapy. Folia Neuropathol 2013; 51: 56-64.
15. Sharp FR, Rando TA, Greenberg SA, Brown L, Sagar SM. Pseudochoreoathetosis: movement associated with loss of proprioception. Arch Neurol 1994; 51: 1103-1109.
16. Spitz M, Costa Machado AA, Carvalho Rdo C, Maia FM, Haddad MS, Calegaro D, Scaff M, Reis Barbosa E. Pseudoathetosis: report of three patients. Mov Disord 2006; 21: 1520-1522.
17. Svetel M, Ivanović N, Marinković J, Jović J, Dragasević N, Kostić VS. Characteristics of dystonic movements in primary and symptomatic dystonias. J Neurol Neurosurg Psychiatry 2004; 75: 329-330.
18. Tranchant C, Bhatia KP, Marsden CD. Movement disorders in multiple sclerosis. Mov Disord 1995; 10: 418-423.
19. Tüzün E, Akman-Demir G, Eraksoy M. Paroxysmal attacks in multiple sclerosis. Mult Scler 2001; 7: 40-43.
20. Uncini A, Di Muzio A, Thomas A, Lugaresi A, Gambi D. Hand dystonia secondary to cervical demyelinating lesion. Acta Neurol Scand 1994; 90: 51-55.

Folia Neuropathologica

Does "cerebellar liponeurocytoma" always reflect an expected site? An unusual case with a review of the literature

Pinar Karabagli[1], Aydin Sav[2], Necmettin Pamir[3]

[1]Department of Pathology, School of Medicine, Selcuk University, Konya, [2]Department of Pathology, School of Medicine, Acibadem University, İstanbul, [3]Department of Neurosurgery, School of Medicine, Acibadem University, İstanbul, Turkey

Folia Neuropathol 2014; 52 (1): 101-105 DOI: 10.5114/fn.2014.41749

Abstract

A rare tumour, cerebellar liponeurocytoma, is classified into glioneuronal tumours under the 2000 World Health Organization (WHO) classification of tumours of the central nervous system. The current 2007 WHO classification, therefore, assigns grade II to the cerebellar liponeurocytoma. Tumours are predominantly localized in cerebellar hemispheres, and the second most common location is the vermis. To date, approximately 40 reported cases of cerebellar and 10 cases of supratentorial intraventricular liponeurocytoma have been reported. In this report, an unusual case of cerebellar liponeurocytoma was presented with extracerebellar location. In the future tumour classification, it should be considered that liponeurocytomas are not restricted only to the cerebellum, but they are located in supratentorial areas as well.

Key words: *liponeurocytoma, cerebellar, supratentorial, intraventricular.*

Introduction

Cerebellar liponeurocytomas have been included in the 2000 World Health Organization (WHO) classification of tumours of the central nervous system, under the heading of glioneuronal tumours. It is a rare cerebellar neoplasm of adults with consistent neuronal, variable astrocytic and focal lipomatous differentiation, and with low proliferative potential. The current 2007 WHO classification therefore assigns cerebellar liponeurocytoma to WHO grade II [10,11].

In 1978, Bechtel *et al*. reported a case of lipomatous medulloblastoma in a 44-year-old man. The terms neurolipocytoma, medullocytoma, lipomatous glioneurocytoma, lipidized mature neuroectodermal tumour have also been proposed [4,10]. As a term, cerebellar liponeurocytoma is now largely accepted and is supported by genetic analyses that indicate that this lesion is not a variant of medulloblastoma [7,10].

Tumours are predominantly located in cerebellar hemispheres, followed by a more central location in the vermis [10]. Tumours with features of liponeurocytoma have also been observed in supratentorial locations. There have been approximately 40 reported cases of cerebellar and 10 cases of supratentorial liponeurocytoma in the literature [2,4-6,9,11,13,15]. The tumour usually has a favourable clinical prognosis, although recurrences are frequent [3,8].

We report a case of this tumour with supratentorial location. Characteristic features of these tumours are discussed in the light of pertinent literature.

Communicating author:

Pinar Karabagli, Department of Pathology, School of Medicine, Selcuk University, Selcuklu, 42075, Konya, Turkey, phone: +90 332 241 50 00, fax: +90 332 241 60 65, e-mail: pinarkarabagli@yahoo.com

Case report

A 34-year-old previously healthy man developed a progressive headache. The neurological examination was normal. Magnetic resonance imaging (MRI) scan showed a large partly cystic, 4 × 5 cm mass in the third ventricle (Fig. 1A). Enhancement with gadolinium was heterogeneous (Fig. 1B). The patient underwent an occipital craniotomy and gross total excision of the tumour. His postoperative period was uneventful.

The hematoxylin and eosin (H&E) stained paraffin sections showed a moderately cellular tumour showing uniform, round oligodendroglia like cells containing round, "salt-pepper" nuclei and clear cytoplasm, and focal lipidized cells that comprised almost 10-15% of the tumour area. Upon detailed microscopic evaluation, these lipidized cells share some morphological consistencies with lipidized medulloblastoma and clear cell ependymoma (Fig. 2A). Only few mitoses and minute foci of micronecrosis were observed in the neuronal component. In immunohistochemical analysis neuron-specific enolase (NSE) (Fig. 2B) and synaptophysin (Fig. 2C) and MAP-2 immunopositivity were detected. Glial fibrillary acidic protein (GFAP), S-100, neurofilament (NF), vimentin, chromogranin, p53, EMA and desmin were immunonegative. Ki-67/MIB 1 antibody immunolabeling index was 1.5% (Fig. 2D). No neuroradiologic or clinical neurologic evidence of recurrence and/or residual tumour was noticed during a 2-year period of follow-up.

Discussion

Liponeurocytomas are rare cerebellar neoplasms with benign histological features and a favourable clinical prognosis. However, the current clinical opinion is based on a total of approximately 40 published cases [8,10,14]. Linking the concept of liponeurocytoma to its occurrence in the cerebellum unnecessarily obscures the existence of similar neoplasms at other sites. Indeed ten such cases have been reported in the English literature (Table I) [2,4-6,9,11,13,15]. We herein present the eleventh example of supratentorial intraventricular liponeurocytoma (Table I).

Liponeurocytomas are characterized by presence of various lipidized cells in clusters or scattered between small neoplastic cells. Immunohistochemical staining demonstrated both neuronal and glial differentiation. Histologically mitotic activity and proliferation rate are generally low in these lesions [2,10,14,16].

The immunostaining profile of previously published cases of supratentorial liponeurocytomas demonstrates uniform reactivity for neuronal markers like synaptophysin, and/or NSE as was seen in the present case [2,4-6,9,11,13,15]. Expression of GFAP and S-100 is limited to scattered reactive astrocytes [4,9,15], and a few tumour cells [2,5,11,13]. The tumour cells are negative for NF [2,4,5,9,11,15]. MIB-1 labelling index was < 1% [2], 4% [11], 5.8% [4] and 15% and increased to 30% in the recurrent tumour [9]. It was 1.5% in the present case and no

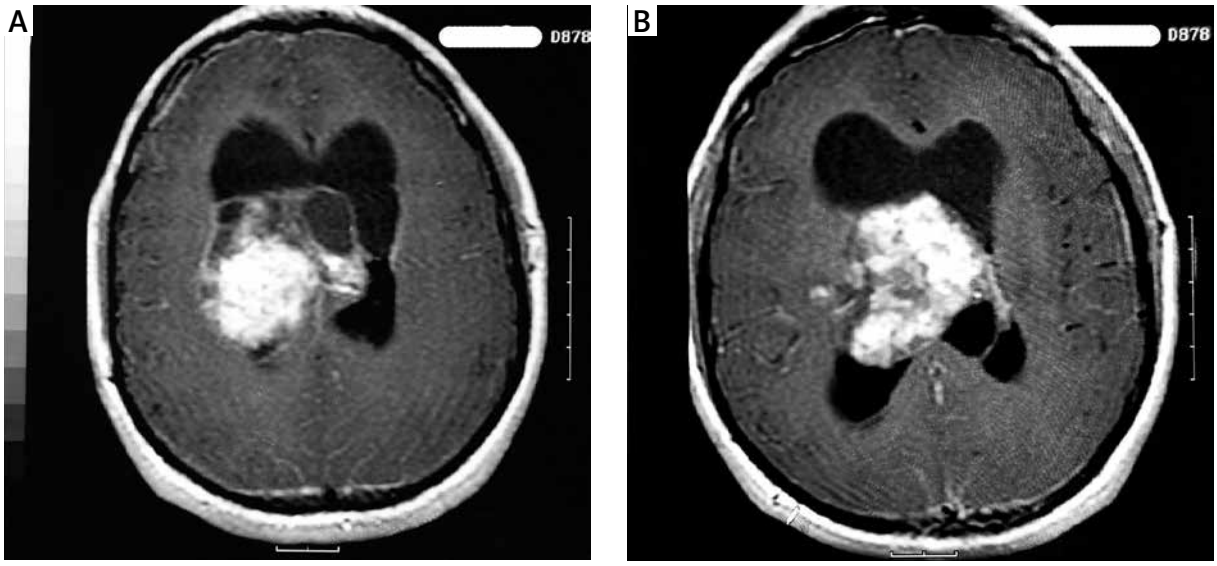

Fig. 1. On T1-weighted MRI showed a large, partly cystic, 4 × 5 cm mass in the third ventricle with heterogeneous enhancement with gadolinium.

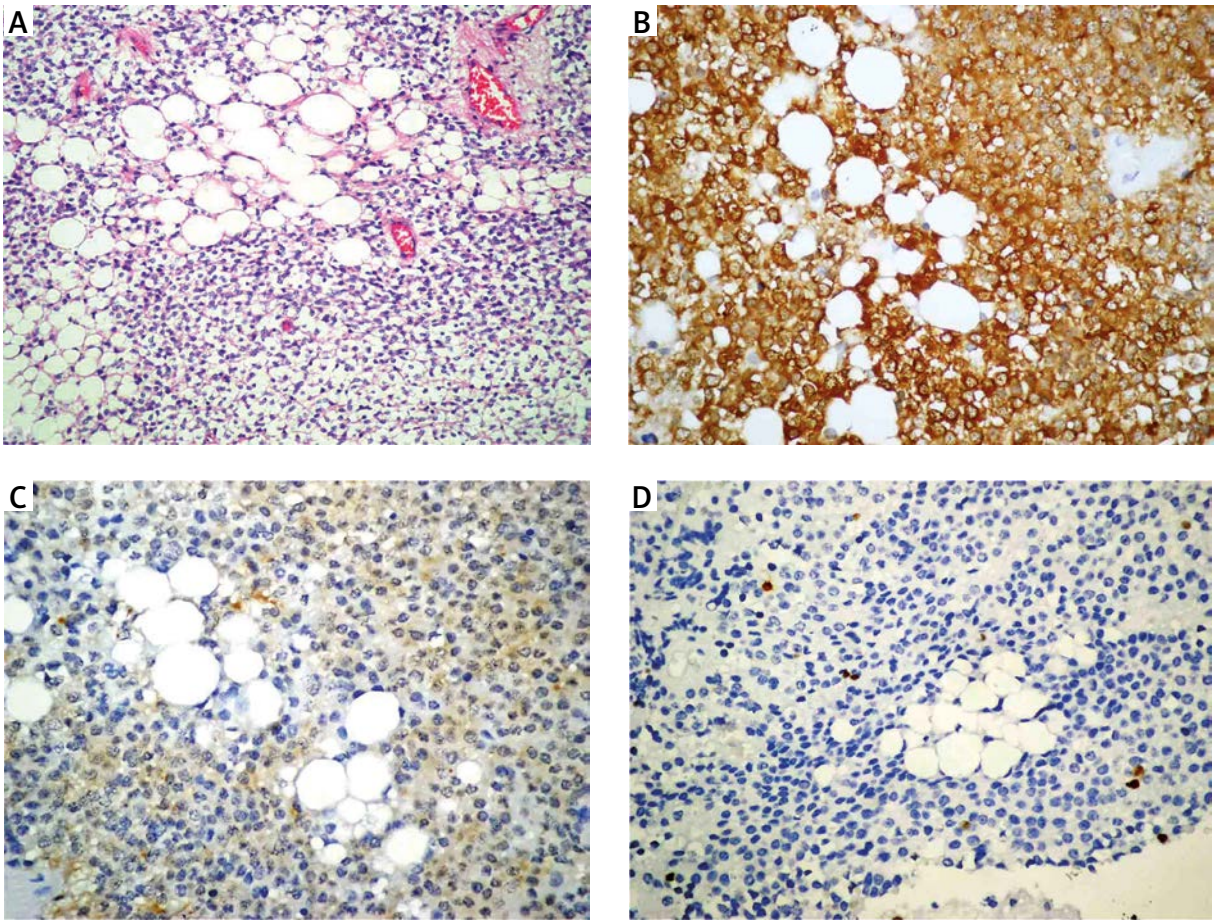

Fig. 2. A) Monotonous tumour cell proliferation with focal lipidized cells (HE ×200). **B)** Tumour cells reacting intensely with NSE (Anti-NSE; streptavidin-biotin complement, ×400 original magnification). **C)** Synaptophysin reactivity is only focal and mild (Anti-synaptophysin; streptavidin-biotin complement, ×400 original magnification). **D)** Ki-67/MIB-1 labelling index is low (1.5%) (MIB-1; streptavidin-biotin complement, ×400 original magnification).

recurrences were noticed during 2 years' follow-up period.

Among the relevant cases in files, only three of them were examined ultrastructurally. This particular consistent evidence provides that lipid vacuoles progressively accumulate and coalesce within cells while retaining their neurocytic features. Thus, these distinctive lesions are a result of tumoral lipidization rather than true adipose metaplasia [4,5,9]. Some authors have interpreted this lipidization as true adipose metaplasia [15]. Unfortunately, no ultrastructural study was applied to the case under investigation.

The immunohistochemical panel showed evidence of neuronal expression. Moreover, no immunoreactivity in lipidized tumour component was seen for synaptophysin, GFAP and S-100. We could not definitively confirm the presence of lipids within the cytoplasm of the tumour cells. Hypothetically, presence of lipid vacuoles most likely suggests the possibility of mesenchymal differentiation in the tumour [12]. The association of mesenchymal phenotypes in the tumour implies the possibility of a common origin from pluripotent cells related to such structures. Conveniently, this tumour may have derived from pluripotential embryonic ectomesenchymal stem cells of neural crest probably persisting in the ventricular matrix and the external granular layer [1,6,12].

Apart from the cerebellar and 10 cases of supratentorial liponeurocytoma, it should be emphasized that the fact about lipidization within the neuroec-

Table I. Summary of the 10 cases of supratentorial liponeurocytoma reported in the literature and our case

Authors, [Ref. No]	Sex/Age (yr)	Tumor location
Horoupian, 1997 [6]	M/30	Left Lat v., 3rd v., CC
George, 2001 [4]	F/59	Anterior horn, Left Lat v.
Rajesh, 2003 [15]	M/30	Frontal horn, Lat v.
Jouvet, 2005 [9]	F/4	4th v.
Kuchelmeister, 2006 [11]	M/35	Left lat v.
Pankaj, 2010 [13]	M/35	Lateral horn, Right Lat v.
Gupta, 2011 [5]	F/45	Trigone of Lat. v.
Chakraborti, 2011 [2]	M/36 M/30 M/32	Bilateral Lat v. Lateral and 3rd v. Bilateral Lat v., central
(present case)	M/34	3rd v.

Lat v. – lateral ventricle, 3rd v. – third ventricle, 4th v. – fourth ventricle, CC – corpus callosum

todermal tumours of the central nervous system includes cerebellar astrocytomas, multiple intraspinal low grade astrocytoma, frequently in pleomorphic xanthoastrocytoma, occasionally in glioblastoma, ependymomas and supratentorial PNET [2].

Cerebellar liponeurocytoma has a relatively benign clinical course and a recurrence may appear after a long period of time [9]. The 5-year survival rate of cerebellar liponeurocytoma is 48% but this should be interpreted with caution because of rarity of this tumour and lack of systemic follow-up [10].

Cluster analysis of the cDNA expression data of 1176 genes grouped cerebellar liponeurocytomas close to central neurocytomas, but distinctive from medulloblastoma. Furthermore, the cDNA expression array data suggest a relationship to central neurocytomas, but presence of TP53 mutations (20%), which are absent in central neurocytomas, suggest that their genetic pathways are different. Horstmann *et al*. reveal TP53 missense mutation with a higher frequency than medulloblastoma. Moreover, isochromosome 17q, a genetic hallmark of cerebellar medulloblastoma was not observed in any of the cases investigated in this study [7,10].

Total resection is considered the best possible treatment. There is no consensus regarding the specific treatment of liponeurocytoma, if only chemo- or radiotherapy is an indispensable part of the postoperative treatment regimen [3,8,10,14].

Conclusions

In conclusion, this study constitutes the 11th case of "cerebellar" liponeurocytoma in an extracerebellar location. The future tumour classification should consider that liponeurocytoma is not restricted to the cerebellum, but may be located in extracerebellar sites as well. Consequently, it may be expected that the prefix 'cerebellar' would be omitted as evidenced by sporadic cases in the pertinent literature.

References

1. Akhaddar A, Zrara I, Gazzaz M, Moustarch d BE, Benomar S, Boucetta M. Cerebellar liponeurocytoma (lipomatous medulloblastoma). J Neuroradiol 2003; 30: 121-126.
2. Chakraborti S, Mahadevan A, Govindan A, Yasha TC, Santosh V, Kovoor JME, Ramamurthi R, Alapatt JP, Hedge T, Shankar SK. Supratentorial and cerebellar liponeurocytomas:report of four cases with review of literature. J Neurooncol 2011; 103: 121-127.
3. Gallina P, Buccoliero AM, Prillo V, Pansini G, Di Lorenzo N. Cerebellar liponeurocytoma: an update follow-up of a case presenting histopathological and clinically aggressive features. Neurol India 2009; 57: 194-196.
4. George DH, Scheithauer BW. Central liponeurocytoma. Am J Surg Pathol 2001; 25: 1551-1555.
5. Gupta K, Salunke P, Kalra I, Vasishta RK. Central liponeurocytoma: case report and review of literature. Clin Neuropathol 2011; 30: 80-85.
6. Horoupian DS, Shuster DL, Kaarsoo-Herrick M, Shuer LM. Central neurocytoma: One associated with a fourth ventricular PNET/Medulloblastoma and the second mixed with adipose tissue. Hum Pathol 1997; 28: 1111-1114.
7. Horstmann S, Perry A, Reifenberger G, Giangaspero F, Huang H, Hara A, Masuoka J, Rainov NG, Bergmann M, Heppner FL, Brandner S, Chimelli L, Montagna N, Jackson T, Davis DG, Markesbery WR, Ellison DW,Weller RO, Taddei GL, Conti R, Del Bigio MR, Gonzale-Campora R, Radhakrishnan W, Soylemezoglu F, Uro-Coste E, Qlan J, Kleihues P, Ohgaki H. Genetic and expression profiles of cerebellar liponeurocytomas. Brain Pathol 2004; 14: 281-289.
8. Jenkinson MD, Bomsa JJ, Du Plessis D, Ohgaki H, Kleihues P, Warnke P, Rainov NG. Cerebellar liponeurocytoma with an unusually aggressive clinical course: case report. Neurosurg 2003; 53: 1425-1427.
9. Jouvet A, Lellouch-Tubiana A, Boddaert N, Zerah M, Champier J, Fevre-Montange M. Fourth ventricle neurocytoma with lipomatous and ependymal differentiation. Acta Neuropathol (Berl) 2005; 109: 346-351.
10. Kleihues P, Chimelli L, Giangaspero F, Ohgakin H. Cerebellar liponeurocytoma. In: Louis DN, Ohgaki H, Wiestler OD, Cavenee WK (eds.).WHO Classification of Tumors of the Central Nervous System. IARC, Lyon 2007; pp. 110-112.
11. Kuchelmeister K, Nestler U, Siekmann R, Schachenmayr W. Liponeurocytoma of the left lateral ventricle-case report and review of the literature. Clin Neuropathol 2006; 25: 86-94.

12. Mena H, Morrison AL, Jones RV, Gyure KA. Central neurocytomas express photoreceptor differentiation. Cancer 2001; 91: 136-143.
13. Pankaj R, Jindal A, Banerjee AK. Liponeurocytoma of lateral ventricle. Neurol India 2010; 58: 805-806.
14. Patel N, Fallah A, Provias J, Jha NK. Cerebellar liponeurocytoma. Can J Surg 2009; 52: E117-E119.
15. Rajesh LS, Vasishta RK, Chhabra R, Banerjee AK. Case report: central liponeurocytoma. Neuropathol Appl Neurobiol 2003; 29: 511-513.
16. Soylemezoglu F, Soffer D, Onol B, Schwechheimer K, Kleihues P. Lipomatous medulloblastoma in adults. A distinct clinicopathological entity. Am J Surg Pathol 1996; 20: 413-418.

Instructions to Authors

This instruction is based upon *Uniform Requirements for Manuscripts Submitted to Biomedical Reviews* (the complete document appears in N Engl J Med 1997; 336, 309-315).

Aims and scope

Folia Neuropathologica is an official journal of the Mossakowski Medical Research Centre Polish Academy of Sciences and the Polish Association of Neuropathologists. The journal publishes original articles and reviews that deal with all aspects of clinical and experimental neuropathology and related fields of neuroscience research. The scope of journal includes surgical and experimental pathomorphology, ultrastructure, immunohistochemistry, biochemistry and molecular biology of the nervous tissue. Papers on surgical neuropathology and neuroimaging are also welcome. The reports in other fields relevant to the understanding of human neuropathology might be considered.

Ethical consideration

Papers describing animal experiments can be accepted for publication only if the experiment conforms to the legal requirements in Poland as well as with the European Communities Council Directive of November 24, 1986 or the National Institute of Health Guide (National Institute of Health Publications No. 80-23, Revised 1978) for the care and use of Laboratory Animals for experimental procedure. Authors must provide a full description of their anesthetics and surgical procedures. Papers describing experiments on human subjects must include a statement that experiments were performed with the understanding and consent of each subject, with the approval of the appropriate local ethics committee.

Submission of manuscripts

Articles should be written in English. **All new manuscripts should be submitted through the online submission at http://panel2.termedia.pl/fn**
For authors unable to submit their manuscript online, please contact with Prof. E. Matyja, Editor-in-Chief of *Folia Neuropathologica*, ematyja@imdik.pan.pl
The Editorial Board reserves the right to reject a paper without reviewers' opinion if the content or the form of the paper does not meet minimum acceptance criteria or if the subject of the paper is beyond the aims and scope of the journal.

Legal aspects

In sending the manuscript the author(s) confirm(s) that (s)he has (they have) not previously submitted it to another journal (except for abstracts of no more than 400 words) or published it elsewhere. The author(s) also agree(s), if and when the manuscript is accepted for publication, to automatic and free transfer of copyright to the Publisher allowing for the publication and distribution of the material submitted in all available forms and fields of exploitation. The author(s) accept(s) that the manuscript will not be published elsewhere in any language without the written consent of the copyright holder, i.e. the Publisher.
All manuscripts submitted should be accompanied by an authors' statement including signed confirmation of the above and confirming that this publication has been approved by all co-authors (if any), as well as by the responsible authorities at the institution where the work has been carried out. The authors' statement should be signed by ALL co-authors. Additionally, the author(s) confirm(s) that (s)he is (they are) familiar with and will observe the "Instruction to Authors" included in *Folia Neuropathologica* and also that all sources of financial support have been fully disclosed. Materials previously published should be accompanied by written consent for reprinting from the relevant Publishers. In the case of photographs of identifiable persons, their written consent should also be provided. Any potential conflict of interest will be dealt with by the local court specific to the Publisher. Legal relations between the Publisher and the author(s) are in accordance with Polish law and with international conventions binding on Poland.
Authors agree to waive their royalties.

Anonymous review

All manuscripts will be subject to a process of anonymous editorial review.

Preparation of manuscripts

Articles must be written in English, with British spelling used consistently throughout. Authors not entirely familiar with English are advised to correct the style by professional language editors or native English speakers.

- The length of original article should not exceed 20 printed pages including text, illustrations, tables, and references.
- Manuscripts should be typed using 12pts.font, double-spaced, and fully corrected. Allow a margin at least 2.5 cm at the top, bottom and left side of the page. Text should not be justified.

- The title page should contain: the author's full names, title of the paper, all authors' affiliations, full name and address of the communicating author (including e-mail address and fax number), running title (not exceed 40 characters including spaces).
- The abstract should not exceed 350 words. A list of 3–10 key words is recommended below the abstract.
- The manuscript body should be organized in a standard form with separate sections: Introduction, Material and Methods, Results, Discussion, and References. Review articles should be divided into sections and subsections as appropriate without numbering.
- Do not underline in the text. Avoid footnotes.
- All dimensions and measurements must be specified in the metric system.
- The source of any drug and special reagent should be identified.
- Particular attention needs to be paid to the selection of appropriate analysis of data and the results of statistical test should be incorporated in the results section.
- The nomenclature used should conform to the current edition of the Nomina Anatomica or Nomina Anatomica Veterinaria.
- Acknowledgements should be made in a separate sheet following Discussion and before References. These should contain a list of dedications, acknowledgements, and funding sources.
- Legends of figures and tables should be typed on separate pages.
- The editor reserves the right to make corrections.

Tables

- Tables numbered in Roman numerals require a brief but descriptive heading.
- The major divisions of the table should be indicated by horizontal rules.
- Explanatory matter should be included in footnotes, indicated in the body of the table in order of their appearance.
- Tables must not duplicate material in the text or in illustration.

Illustrations

All figures should be supplied electronically at resolution 300dpi in all standard formats (tiff, jpg, Adobe Photoshop, Corel Draw, and EPS). Name your figure files with "Fig" and the figure number, e.g., Fig1.tif
- The maximum figure size is 84 mm or 174 mm for use in a single or double column width, respectively.
- When possible, group several illustrations on one block for reproduction. Like all other figures, block should be prepared within a rectangular frame to fit within a single or double column width of 84 and 174 mm, respectively, and a maximum page height of 226 mm.
- Each figure should include scale magnification bar; do not use magnification factors in the figure legends.
- All figures, whether photographs, graphs or diagrams, should be numbered using Arabic numerals and cited in the text in consecutive numerical order
- **Immunohistochemical study requires color illustrations of very good quality. The papers with white and black immunohistochemistry will not be accepted.**
- **The expense of color illustrations must be borne by the authors.** The cost of color print for every successive 8 pages is 200 euro irrespective of the number of color pages, i.e., the price remains the same whether there is one or eight pages.

The Publisher makes out the bill to the communicating Author.

References

The list of references (written on a separate page) should include only those publications that are cited in the text. Avoid citation of academic books, manuals and atlases. References may be arranged alphabetically and numbered consecutively. References should be given in square brackets with no space between the comma and the consecutive number, e.g. [3,4,6-12].
References should be written as follows:
Journal papers: initials and names of all authors, full title of paper, journal abbreviation (according to Index Medicus), year of publication, volume (in Arabic numerals), first and last page (example below):
1. Valverde F. The organization of area 18 in the monkey. Anat Embryol 1978; 154: 305-334.
2. Uray NJ, Gona AG. Calbindin immunoreactivity in the auricular lobe and interauricular granular band of the cerebellum in bullfrogs. Brain Behav Evol 1999; 53: 10-19.

Book and monographs: initials and names of all authors, full title, edition, publisher, place, year (examples below):
1. Pollack RS. Tumor surgery of the head and neck. Karger, Basel 1975.
2. Amaral DG, Price JL, Pitkanen A, Carmichael ST. Anatomical organization of the primate amygdaloid complex. In: Aggleton JP (ed.). The amygdala. Wiley-Liss, New York 1992; pp. 1-66.

Reference to articles that are accepted for publication may be cited as „in press" or Epub.

Proofs

Corrections to the proofs should be restricted to printer's errors only; other alterations will be charged to the authors. In order to maintain rapid publication, proofs should be returned within 48 hours, preferably by e-mail, fax or courier mail. If the Publisher receives no response from the authors after 10 days, it will be assumed that there are no errors to correct and the article will be published.

Subscription information

The journal is published in one volume per year consisting of four numbers. The annual subscription price is 160 PLN for Institutions from Poland and 80 PLN for individual subscribers from Poland and 140 Euro for foreign Institutions and 70 Euro for foreign individual subscribers.
Payment should be made to:
Termedia sp. z o.o., ul. Kleeberga 8, 61-615 Poznań
BZ WBK III O/Poznań PL 61 1090 1359 0000 0000 3505 2645
SWIFT: WBKPPLPP

The publisher must be notified of a cancellation of a subscription not later than two months before the end of the calendar year. After that date the subscription is automatically prolonged for another year.
Publishing, Subscription and Advertising Office:
TERMEDIA Publishing House
ul. Kleeberga 2
61-615 Poznań, Poland
phone/fax +48 61 822 77 81
e-mail: termedia@termedia.pl
http://www.folianeuro.termedia.pl

Folia Neuropathologica

AUTHOR'S STATEMENT

Title of the article

.....

.....

.....

The author(s) hereby confirm(s) that:

☐ The above-mentioned work has not previously been published and that it has not been submitted to the Publishers of any other journal (with the exception of abstracts not exceeding 400 words).

☐ All co-authors named and the relevant authorities of the scientific institutions at which the work has been carried out are familiar with the contents of this work and have agreed to its publication.

☐ In sending the manuscript together with illustrations and tables agree(s) to automatic and free transfer of copyright to the Publisher allowing for the publication and distribution of the material submitted in all available forms and fields of exploitation, without limits of territory or language, provided that the material is accepted for publication. At the same time the author(s) accept(s) that the submitted work will not be published elsewhere and in whatever language without the earlier written permission of the copyright holder, i.e. the Publisher.

☐ (S)he (they) agree to waive his(her)(their) royalties (fees).

☐ (S)he (they) empower(s) the Publisher to make any necessary editorial changes to the submitted manuscript.

☐ All sources of funding of the work have been fully disclosed.

☐ The manuscript has been prepared in accordance with the Publisher's requirements.

☐ (S)he (they) is (are) familiar with the regulations governing the acceptance of works as published in *Folia Neuropathologica* and agree(s) to follow them.

☐ (S)he (they) agree to accept appropriate invoice from the Publisher in case colour illustrations are implemented.

Date *Signatures of* ***all authors***

The covering letter formula can be found at: www.folianeuro.termedia.pl
-The covering letter should be sent to Associate Editor:

Milena Laure-Kamionowska
-Editorial Office of Folia Neuropathologica
Mossakowski Medical Research Centre, Polish Academy of Sciences
Poland Medical Research Centre
ul. Pawińskiego 5
02-106 Warszawa, Poland

CONTENTS